Universiteit
Leiden
The Netherlands

# Coiled-coil mediated liposomal fusion: Asymmetric behaving peptide fusogens

Daudey, G.A.

**Citation**
Daudey, G. A. (2018, December 5). *Coiled-coil mediated liposomal fusion: Asymmetric behaving peptide fusogens*. Retrieved from https://hdl.handle.net/1887/67109

| | |
|---|---|
| Version: | Not Applicable (or Unknown) |
| License: | Licence agreement concerning inclusion of doctoral thesis in the Institutional Repository of the University of Leiden |
| Downloaded from: | https://hdl.handle.net/1887/67109 |

**Note:** To cite this publication please use the final published version (if applicable).

Cover Page

Universiteit Leiden

The handle http://hdl.handle.net/1887/67109 holds various files of this Leiden University dissertation.

**Author**: Daudey, G.A.
**Title**: Coiled-coil mediated liposomal fusion: Asymmetric behaving peptide fusogens
**Issue Date**: 2018-12-05

# COILED-COIL MEDIATED LIPOSOMAL FUSION:

## *ASYMMETRIC BEHAVING PEPTIDE FUSOGENS*

GEERT AREND DAUDEY

# Coiled-coil mediated liposomal fusion: Asymmetric behaving peptide fusogens

Proefschrift

ter verkrijging van
de graad van Doctor aan de Universiteit Leiden,
op gezag van Rector Magnificus prof.mr. C.J.J.M. Stolker,
volgens besluit van het College voor Promoties
te verdedigen op woensdag 5 december 2018
klokke 10.00 uur

door

Geert Arend Daudey
Geboren te Rijssen, 1988

Promotiecommissie

Promotor:

Prof. Dr. A. Kros

Leden:

Prof. Dr. H.S. Overkleeft (vz)

Prof. Dr. M.H.M Noteborn (sec)

| | |
|---|---|
| Prof. Dr. W. Roos | Rijksuniversiteit Groningen |
| Prof. Dr. R. Jerala | National Institute of Chemistry, Slovenia |
| Dr. J.A.A.W. Elemans | Radboud Universiteit |

Geert A. Daudey

Coiled-coil mediated liposomal fusion:

Asymmetric behaving peptide fusogens

164 pages

PhD thesis, Leiden University, Leiden, NL (2018)

ISBN 978-94-6375-215-2

Printing Ridderprint BV | www.ridderprint.nl

Voor Mariëtte

SDG

Thinking from the eye closes understanding,
but thinking from understanding opens the eye.

Emanuel Swedenborg

# TABLE OF CONTENTS


| | | |
|---|---|---|
| **CHAPTER I** | General introduction to membrane fusion | 9 |
| **CHAPTER II** | Membrane-fusogen distance is critical for efficient coiled-coil-peptide mediated liposome fusion | 19 |
| **CHAPTER III** | Influence of membrane-fusogen distance on the secondary structure of coiled-coil peptides | 53 |
| **CHAPTER IV** | Dimers of peptide K: (Super)secondary structures and fusogenic activity | 91 |
| **CHAPTER V** | Liposome fusion with orthogonal coiled-coil peptides as fusogens: Peptide roleplay is critical for efficient fusion | 115 |
| **CHAPTER VI** | Summary and Perspectives | 149 |

# CHAPTER I

## GENERAL INTRODUCTION TO MEMBRANE FUSION

# INTRODUCTION

Membrane fusion, a vital process in all living organisms is triggered by special zipper-like proteins and is key for understanding cellular logistics. These processes include exocytosis, fusion of small enveloped viruses with cells and cell-cell fusion.[1] Whilst the exact mechanism of membrane fusion is still a matter of debate, it is widely accepted that it proceeds in four stages:[2] (Figure 1) opposing membranes are brought into close proximity (I); the membrane is disrupted at the site of contact (II); outer membranes are merged resulting in hemifusion (III/IV); and full fusion is achieved, facilitating content mixing between the two fused compartments via pore formation (V). Since lipid bilayers possess an intrinsic stability against any structural deformations by a powerful hydrophobic effect, membrane remodeling via highly curved intermediates requires energy. This energy barrier prohibits spontaneous and non-targeted vesicle fusion in biological systems[3-4] and specialized proteins are employed to overcome the energy-gap and to guide these processes.[5]

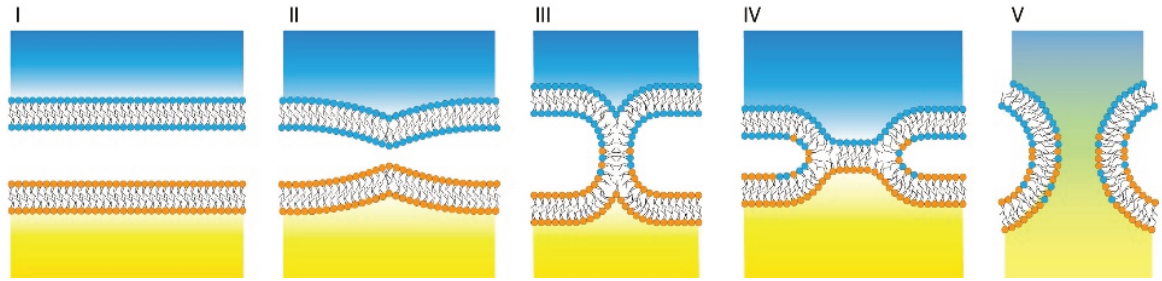


**Figure 1.** *Stages of the fusion cascade. Membranes are brought in close apposition (I) and approach each other in a point-like protrusion (II). A stalk intermediate is formed by merging of the outer membrane layers (III). This intermediate widens (IV) resulting in pore formation and full fusion (V).*

SNARE (soluble N-ethylmaleimide-sensitive factor (NSF) attachment protein receptor) proteins are a well conserved class of fusion proteins, which have been implicated as central in most, if not all, intracellular vesicle trafficking events studied so far.[6-8] SNARE proteins are located on both target membranes and transport vesicles, and zipper into a parallel four-helix bundle,[9-11] bringing the opposing membranes into close contact and guiding the fusion process, as shown in Figure 2.[12-13] Furthermore, several other membrane tethered proteins are known to initiate merging of the membranes via quick and specific $Ca^{2+}$ triggered membrane destabilization.[14-18] Upon fusion, the complex undergoes ATP catalyzed disassembly to recycle the SNAREs for a new fusion

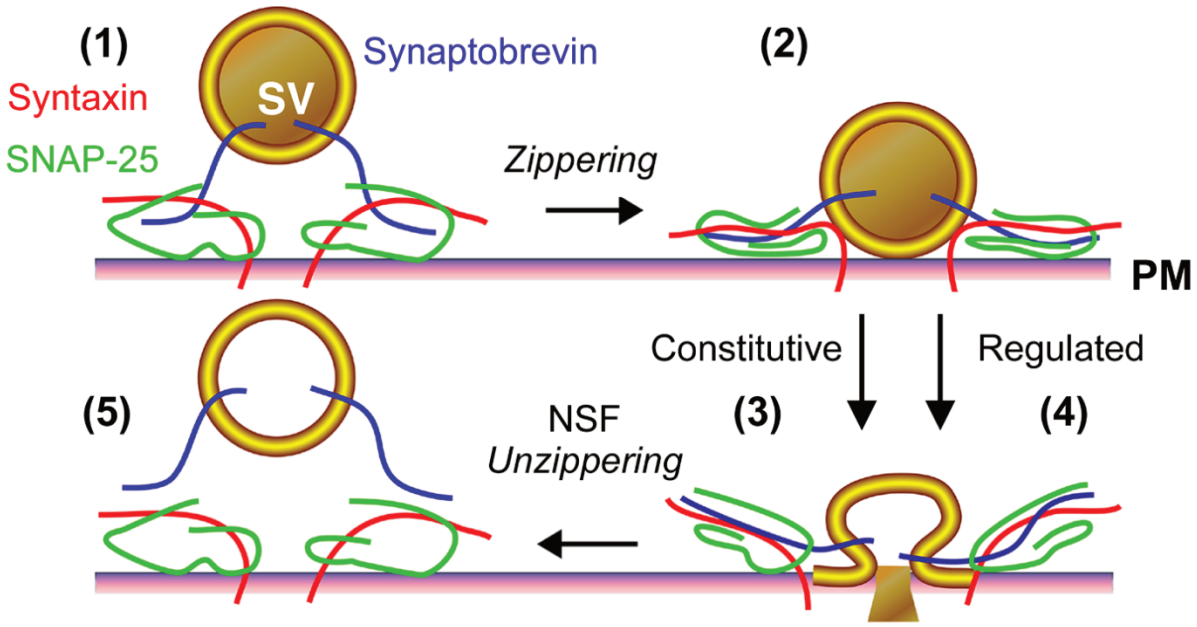


**Figure 2.** *The proposed model of the SNARE mediated synaptic fusion cycle. Synaptobrevin forms a partial complex with Syntaxin and SNAP 25 (1). Full coiled coil formation brings the synaptic vesicle close to the plasma membrane (2) and full fusion occurs either spontaneously (3) or evoked by $Ca^{2+}$ (4). Finally, NSF ATPase catalyzes the disassembly of the SNARE complex and the recycling of the vesicles. Figure adapted from Lagow et al.*[14-15]

event.[16-19] It is commonly accepted that the lower limit to induce membrane fusion involves only 3 SNARE complexes, and even a minimum of only 1 SNARE complex has been reported,[20] indicating the large amount of energy released with the formation of the tetrameric coiled-coil complex. Although the basic principles of SNARE mediated vesicle fusion are identified, many details are still unknown.

## ARTIFICIAL STATE-OF-THE-ART MEMBRANE FUSION

Understanding and mimicking directed membrane fusion, i.e. targeted and leakage-free content mixing between two different enclosed compartments, opens ways to applications in drug delivery and biotechnology, and is thus an interesting target for supramolecular and biomaterials chemists. In recent years, simplified model systems have been reported in which membrane fusion is mediated by designed supramolecular model systems such as carbo-hydrates,[21-22] peptides,[23-27] DNA,[28-29] small molecule recognition,[30-35] and light responsive systems.[36-37] Despite the immense efforts in this field, efficient content mixing of fusogen-functionalized liposomes remains challenging.

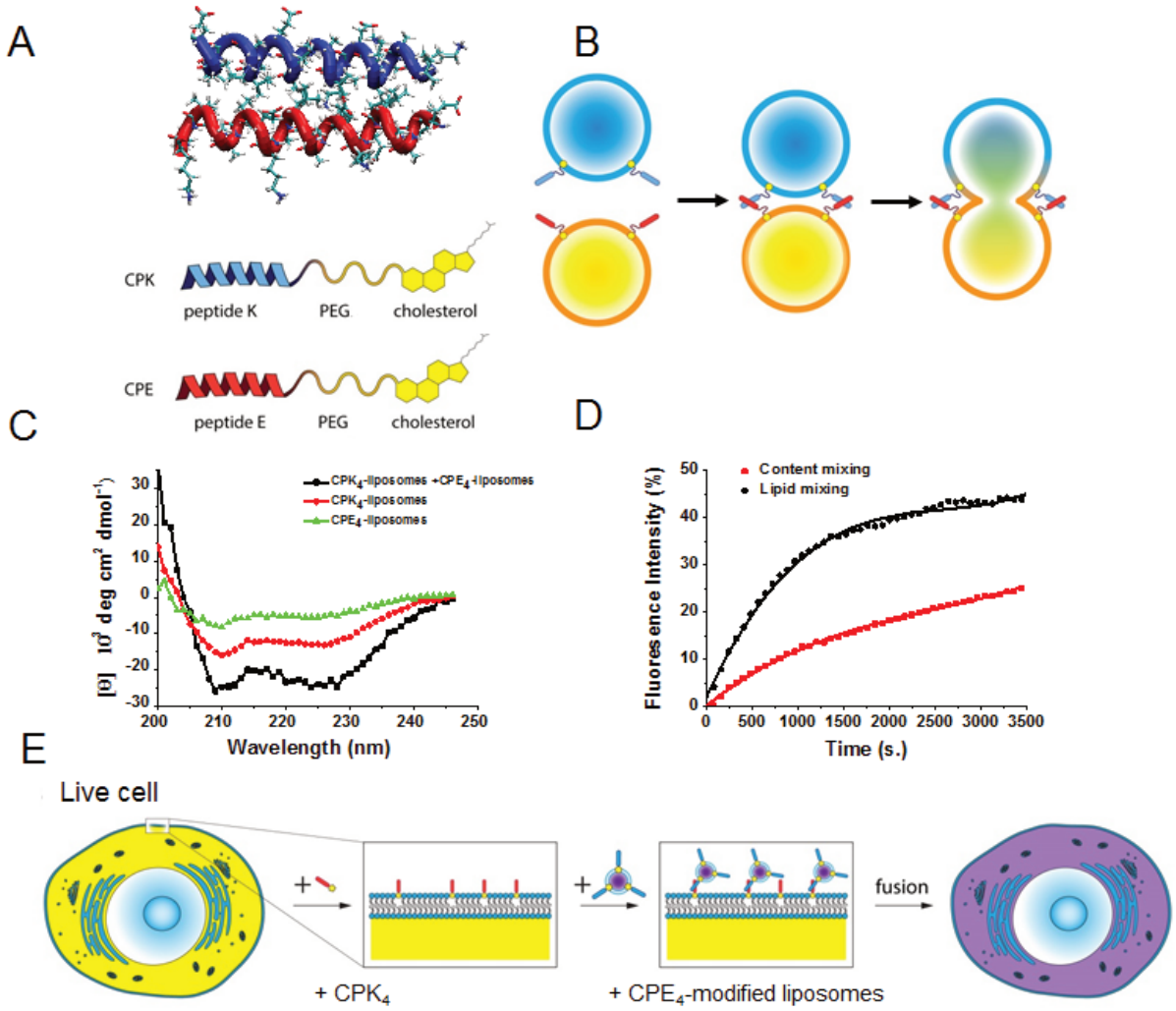


**Figure 3.** *Schematic representation of (A) coiled-coil structure between peptides E and K, (B) targeted liposome fusion mediated by coiled-coil formation between $CPE_4$ modified liposomes and $CPK_4$ modified liposomes, (C) CD spectra of $CPE_4$ modified liposomes, and $CPK_4$ modified liposomes and an equimolar mixture thereof. [Total lipid] = 0.5 mM with 1 mol % lipopeptide in PBS. (D) Lipid mixing and content mixing between $CPE_4$-liposomes and $CPK_4$-liposomes. Fluorescence traces showing lipid mixing between $CPE_4$ and $CPK_4$ decorated liposomes, as measured through an increase in NBD fluorescence. [Total lipid] = 0.1 mM with 1 mol % of lipopeptide, in PBS; and showing content mixing between sulphorhodamine loaded (20 mM), $CPE_4$ decorated liposomes and nonfluorescent, $CPK_4$ decorated liposomes. [Total lipid] = 0.25 mM with 1 mol % lipopeptide in PBS. (E) Scheme of fusion between cell and liposomes. Figure reprinted from Yang et al.*[38]

In our lab, we successfully modified the specific heterodimeric coiled-coil pair E $(EIAALEK)_3$ and K $(KIAALKE)_3$ to mediate the fusion of liposomes, as shown in Figure 3.[39-41] Peptides are tethered to the liposomal membrane by a flexible PEG-linker conjugated to a lipid anchor, usually a membrane constituent.[42] Recently, we reported the targeted and leakage-free delivery of various molecules, including the cytotoxic drug doxorubicin, both *in vitro* and *in vivo* via fusion of small unilamellar liposomes with live cells or zebra fish embryo's.[38, 43] This method allows for quick and efficient delivery of

drugs and (bio)macromolecules without cell damage and is expected to have many applications *in vitro* and *in vivo*.

## COILED-COIL MEDIATED LIPOSOMAL FUSION

However, years of research revealed that the mechanism is less straightforward than initially proposed,[41] and that similarly designed peptides play different roles in the fusion mechanism.[44] Furthermore, study of the relationship between structure and behavior of membrane-tethered peptides and the unambiguous assignment of these factors in the complex and short living fusion machinery is inherently difficult.

The role of the lipopeptides in the fusion process is revealed by studying relationships between rational lipopeptide modifications and their resulting influence on fusion efficiency. The consequences of the anchor type were previously investigated,[42] and it was shown that only DOPE and cholesterol anchors yielded significant fusion, with the latter being the most efficient. Increasing the length of the peptide (which increases coiled-coil binding strength and peptide-membrane interactions) also had a positive effect on fusion efficiency.[41] Conversely, parallel or anti-parallel coiled-coil orientation,[45] and coiled-coil oligomer state,[46] did not influence the rate of fusion.The asymmetric roles of the peptides in the fusion process was recently discovered.[44] Peptide K interacts with the liposomal membrane, resulting in membrane destabilization and the initiation of the fusion process, whereas peptide E facilitates coiled-coil formation, thereby forcing the opposing liposomes in close proximity and concomitant fusion. These different roles lead to competing interactions, resulting in an equilibrium between K – E coiled-coil formation and K – membrane interactions. These results gave us new insights in the fusion mechanism and it is proposed that the membrane immersion of K is of major importance for efficient membrane fusion.

## SCOPE OF THIS THESIS

In all previous studies the $PEG_{12}$ linker between the peptide and the anchor was kept constant. However, the length of this spacer could highly influence the roles of both peptides and a systematic study could reveal the dynamics of the peptides in the fusion mechanism. Therefore, the influence of the PEG-spacer length and the anchor type on the fusion efficiency and on the peptide-membrane interaction was investigated. In this thesis cholesterol anchored peptides were used and compared to previous research conducted with DOPE-anchored peptides. The results of these studies are described in **Chapter II** (liposome fusion) and **Chapter III** (peptide-membrane interaction).

To better understand the role of homo-coiled-coil interaction of peptide K, structure – behavior relationships of K-dimers were investigated via different covalently bound K-K dimers, as described in **Chapter IV**. These peptide-dimers also mediate liposomal fusion between CPE decorated vesicles, demonstrating the versatility of fusion systems with anchored and non-anchored fusogens.

Next, coiled-coil peptide mediated liposome fusion was optimized in terms of fusion efficiency by using a range of coiled-coil peptide pairs. Therefore, a set of orthogonal coiled-coil peptides is introduced in **Chapter V**, and the characteristics of these heterodimeric coiled-coil peptides were studied. Subsequently, cholesterol anchored lipopeptide derivatives were synthesized, and the properties of the peptides when tethered to liposomal membranes was investigated. Furthermore, the ability of these peptides to mediate liposomal fusion is measured and the results are related to the described peptide characteristics. Finally, **Chapter VI** summarizes and interconnects the findings in the present work.

## REFERENCES


1. Jahn, R.; Lang, T.; Sudhof, T. C., Membrane fusion. *Cell* **2003,** *112* (4), 519-533.
2. Chernomordik, L. V.; Kozlov, M. M., Mechanics of membrane fusion. *Nat. Struct. Mol. Biol.* **2008,** *15* (7), 675-683.
3. Jahn, R.; Grubmuller, H., Membrane fusion. *Curr. Opin. Cell Biol.* **2002,** *14* (4), 488-495.
4. Francois-Martin, C.; Rothman, J. E.; Pincet, F., Low energy cost for optimal speed and control of membrane fusion. *Proc. Natl. Acad. Sci. U. S. A.* **2017,** *114* (6), 1238-1241.
5. Bonifacino, J. S.; Glick, B. S., The mechanisms of vesicle budding and fusion. *Cell* **2004,** *116* (2), 153-66.
6. Weber, T.; Zemelman, B. V.; McNew, J. A.; Westermann, B.; Gmachl, M.; Parlati, F.; Sollner, T. H.; Rothman, J. E., SNAREpins: Minimal machinery for membrane fusion. *Cell* **1998,** *92* (6), 759-772.
7. Jahn, R.; Scheller, R. H., SNAREs--engines for membrane fusion. *Nat. Rev. Mol. Cell Biol.* **2006,** *7* (9), 631-43.
8. Han, J.; Pluhackova, K.; Bockmann, R. A., The Multifaceted Role of SNARE Proteins in Membrane Fusion. *Front. Membr. Physiol. Membr. Biophys.* **2017,** *8*, 5.
9. Lou, X.; Shin, Y. K., SNARE zippering. *Biosci. Rep.* **2016,** *36* (3).
10. Zhang, Y., Energetics, kinetics, and pathway of SNARE folding and assembly revealed by optical tweezers. *Protein Sci.* **2017**.
11. Zorman, S.; Rebane, A. A.; Ma, L.; Yang, G.; Molski, M. A.; Coleman, J.; Pincet, F.; Rothman, J. E.; Zhang, Y., Common intermediates and kinetics, but different energetics, in the assembly of SNARE proteins. *Elife* **2014,** *3*, e03348.
12. Risselada, H. J.; Grubmuller, H., How SNARE molecules mediate membrane fusion: recent insights from molecular simulations. *Curr. Opin. Struct. Biol.* **2012,** *22* (2), 187-96.
13. Hong, W.; Lev, S., Tethering the assembly of SNARE complexes. *Trends Cell Biol.* **2014,** *24* (1), 35-43.
14. Lagow, R. D.; Bao, H.; Cohen, E. N.; Daniels, R. W.; Zuzek, A.; Williams, W. H.; Macleod, G. T.; Sutton, R. B.; Zhang, B., Modification of a hydrophobic layer by a point mutation in syntaxin 1A regulates the rate of synaptic vesicle fusion. *Plos Biology* **2007,** *5* (4), 800-817.
15. Lin, R. C.; Scheller, R. H., Structural organization of the synaptic exocytosis core complex. *Neuron* **1997,** *19* (5), 1087-94.
16. Winter, U.; Chen, X.; Fasshauer, D., A conserved membrane attachment site in alpha-SNAP facilitates N-ethylmaleimide-sensitive factor (NSF)-driven SNARE complex disassembly. *J. Biol. Chem.* **2009,** *284* (46), 31817-26.
17. Baker, R. W.; Hughson, F. M., Chaperoning SNARE assembly and disassembly. *Nat. Rev. Mol. Cell Biol.* **2016,** *17* (8), 465-79.
18. Ryu, J. K.; Jahn, R.; Yoon, T. Y., Review: Progresses in understanding N-ethylmaleimide sensitive factor (NSF) mediated disassembly of SNARE complexes. *Biopolymers* **2016,** *105* (8), 518-31.
19. Zhao, M.; Wu, S.; Zhou, Q.; Vivona, S.; Cipriano, D. J.; Cheng, Y.; Brunger, A. T., Mechanistic insights into the recycling machine of the SNARE complex. *Nature* **2015,** *518* (7537), 61-7.
20. van den Bogaart, G.; Holt, M. G.; Bunt, G.; Riedel, D.; Wouters, F. S.; Jahn, R., One SNARE complex is sufficient for membrane fusion. *Nat. Struct. Mol. Biol.* **2010,** *17* (3), 358-64.
21. Kauscher, U.; Ravoo, B. J., Mannose-decorated cyclodextrin vesicles: The interplay of multivalency and surface density in lectin-carbohydrate recognition. *Beilstein J. Org. Chem.* **2012,** *8*, 1543-1551.

22. Voskuhl, J.; Stuart, M. C. A.; Ravoo, B. J., Sugar-Decorated Sugar Vesicles: Lectin-Carbohydrate Recognition at the Surface of Cyclodextrin Vesicles. *Chem. - Eur. J.* **2010,** *16* (9), 2790-2796.
23. Rauschenberg, M.; Bomke, S.; Karst, U.; Ravoo, B. J., Dynamic Peptides as Biomimetic Carbohydrate Receptors. *Angew. Chem., Int. Ed.* **2010,** *49* (40), 7340-7345.
24. Nomura, F.; Inaba, T.; Ishikawa, S.; Nagata, M.; Takahashi, S.; Hotani, H.; Takiguchi, K., Microscopic observations reveal that fusogenic peptides induce liposome shrinkage prior to membrane fusion. *Proc. Natl. Acad. Sci. U. S. A.* **2004,** *101* (10), 3420-5.
25. Kashiwada, A.; Matsuda, K.; Mizuno, T.; Tanaka, T., Construction of a pH-responsive artificial membrane fusion system by using designed coiled-coil polypeptides. *Chem. - Eur. J.* **2008,** *14* (24), 7343-7350.
26. Gong, Y.; Luo, Y.; Bong, D., Membrane activation: selective vesicle fusion via small molecule recognition. *J. Am. Chem. Soc.* **2006,** *128* (45), 14430-14431.
27. Lygina, A. S.; Meyenberg, K.; Jahn, R.; Diederichsen, U., Transmembrane Domain Peptide/Peptide Nucleic Acid Hybrid as a Model of a SNARE Protein in Vesicle Fusion. *Angew. Chem., Int. Ed.* **2011,** *50* (37), 8597-8601.
28. Chan, Y. H.; van Lengerich, B.; Boxer, S. G., Lipid-anchored DNA mediates vesicle fusion as observed by lipid and content mixing. *Biointerphases* **2008,** *3* (2), FA17.
29. Stengel, G.; Simonsson, L.; Campbell, R. A.; Hook, F., Determinants for membrane fusion induced by cholesterol-modified DNA zippers. *J. Phys. Chem. B* **2008,** *112* (28), 8264-8274.
30. Ma, M. M.; Bong, D., Controlled Fusion of Synthetic Lipid Membrane Vesicles. *Acc. Chem. Res.* **2013,** *46* (12), 2988-2997.
31. Kashiwada, A.; Tsuboi, M.; Mizuno, T.; Nagasaki, T.; Matsuda, K., Target-selective vesicle fusion system with pH-selectivity and responsiveness. *Soft Matter* **2009,** *5* (23), 4719-4725.
32. Kashiwada, A.; Tsuboi, M.; Takamura, N.; Brandenburg, E.; Matsuda, K.; Koksch, B., Design and Characterization of Endosomal-pH-Responsive Coiled Coils for Constructing an Artificial Membrane Fusion System. *Chem. - Eur. J.* **2011,** *17* (22), 6179-6186.
33. Marchi-Artzner, V.; Gulik-Krzywicki, T.; Guedeau-Boudeville, M. A.; Gosse, C.; Sanderson, J. M.; Dedieu, J. C.; Lehn, J. M., Selective adhesion, lipid exchange and membrane-fusion processes between vesicles of various sizes bearing complementary molecular recognition groups. *ChemPhysChem* **2001,** *2* (6), 367-376.
34. Richard, A.; Marchi-Artzner, V.; Lalloz, M. N.; Brienne, M. J.; Artzner, F.; Gulik-Krzywicki, T.; Guedeau-Boudeville, M. A.; Lehn, J. M., Fusogenic supramolecular vesicle systems induced by metal ion binding to amphiphilic ligands. *Proc. Natl. Acad. Sci. U. S. A.* **2004,** *101* (43), 15279-15284.
35. Voskuhl, J.; Fenske, T.; Stuart, M. C.; Wibbeling, B.; Schmuck, C.; Ravoo, B. J., Molecular recognition of vesicles: host-guest interactions combined with specific dimerization of zwitterions. *Chemistry* **2010,** *16* (28), 8300-8306.
36. Nalluri, S. K. M.; Ravoo, B. J., Light-Responsive Molecular Recognition and Adhesion of Vesicles. *Angew. Chem., Int. Edit.* **2010,** *49* (31), 5371-5374.
37. Nalluri, S. K. M.; Bultema, J. B.; Boekema, E. J.; Ravoo, B. J., Photoresponsive Molecular Recognition and Adhesion of Vesicles in a Competitive Ternary Supramolecular System. *Chem. - Eur. J.* **2011,** *17* (37), 10297-10303.
38. Yang, J.; Bahreman, A.; Daudey, G.; Bussmann, J.; Olsthoorn, R. C.; Kros, A., Drug Delivery via Cell Membrane Fusion Using Lipopeptide Modified Liposomes. *ACS Cent. Sci.* **2016,** *2* (9), 621-630.
39. Marsden, H. R.; Elbers, N. A.; Bomans, P. H. H.; Sommerdijk, N.; Kros, A., A Reduced SNARE Model for Membrane Fusion. *Angew. Chem., Int. Ed.* **2009,** *48* (13), 2330-2333.

40. Marsden, H. R.; Tomatsu, I.; Kros, A., Model systems for membrane fusion. *Chem. Soc. Rev.* **2011,** *40* (3), 1572-1585.
41. Zheng, T.; Voskuhl, J.; Versluis, F.; Zope, H. R.; Tomatsu, I.; Marsden, H. R.; Kros, A., Controlling the rate of coiled coil driven membrane fusion. *Chem. Commun. (Cambridge, U. K.)* **2013,** *49* (35), 3649-3651.
42. Versluis, F.; Voskuhl, J.; van Kolck, B.; Zope, H.; Bremmer, M.; Albregtse, T.; Kros, A., In situ modification of plain liposomes with lipidated coiled coil forming peptides induces membrane fusion. *J. Am. Chem. Soc.* **2013,** *135* (21), 8057-8062.
43. Yang, J.; Shimada, Y.; Olsthoorn, R. C. L.; Snaar-Jagalska, B. E.; Spaink, H. P.; Kros, A., Application of Coiled Coil Peptides in Liposomal Anticancer Drug Delivery Using a Zebrafish Xenograft Model. *ACS Nano* **2016,** *10* (8), 7428-7435.
44. Rabe, M.; Aisenbrey, C.; Pluhackova, K.; de Wert, V.; Boyle, A. L.; Bruggeman, D. F.; Kirsch, S. A.; Bockmann, R. A.; Kros, A.; Raap, J.; Bechinger, B., A Coiled-Coil Peptide Shaping Lipid Bilayers upon Fusion. *Biophys. J.* **2016,** *111* (10), 2162-2175.
45. Versluis, F.; Dominguez, J.; Voskuhl, J.; Kros, A., Coiled-coil driven membrane fusion: zipper-like vs. non-zipper-like peptide orientation. *Faraday Discuss.* **2013,** *166*, 349-359.
46. Zheng, T. T.; Bulacu, M.; Daudey, G.; Versluis, F.; Voskuhl, J.; Martelli, G.; Raap, J.; Sevink, G. J. A.; Kros, A.; Boyle, A. L., A non-zipper-like tetrameric coiled coil promotes membrane fusion. *RSC Adv.* **2016,** *6* (10), 7990-7998.

# CHAPTER II

## MEMBRANE-FUSOGEN DISTANCE IS CRITICAL FOR EFFICIENT COILED-COIL-PEPTIDE MEDIATED LIPOSOME FUSION

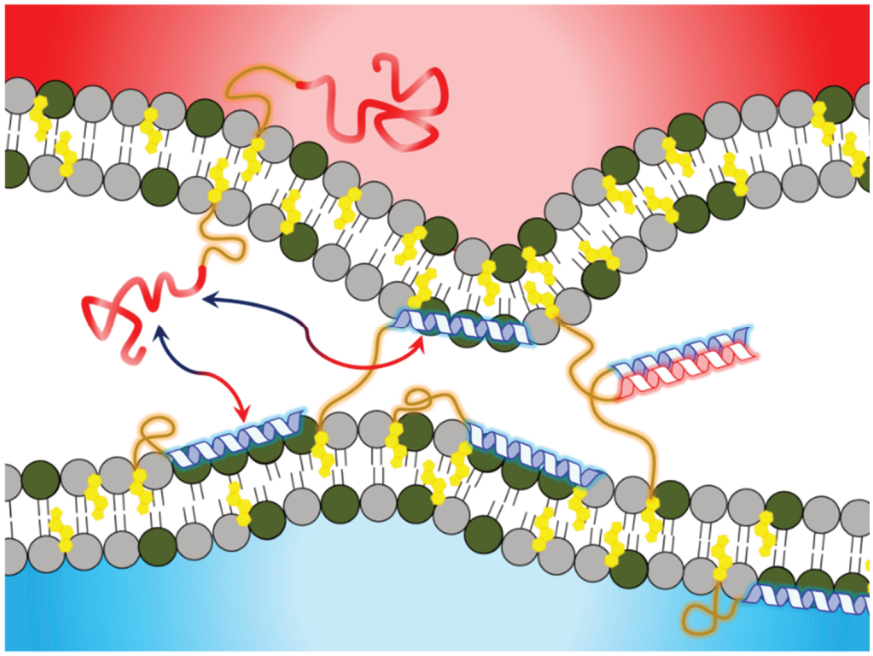

## ABSTRACT

We have developed a model system for membrane fusion that utilizes lipidated derivatives of a heterodimeric coiled-coil pair dubbed E $(EIAALEK)_3$ and K $(KIAALKE)_3$. In this system peptides are conjugated to a lipid anchor via a polyethyleneglycol (PEG) spacer, and this Chapter describes the influence of the PEG-spacer length, coupled with the type of lipid anchor, on liposome-liposome fusion. The effects of these modifications on peptide secondary structure, their interactions with liposomes, and their ability to mediate fusion were studied using a variety of different content mixing experiments and CD spectroscopy. Our results demonstrate the asymmetric role of the peptides in the fusion process, as alterations to the PEG-spacer length affects E and K differently. We conclude that negatively charged E acts as a 'handle' for positively-charged K and facilitates liposome docking, the first stage of the fusion process, through coiled-coil formation. The efficacy of this E handle is enhanced by longer spacer lengths. K directs the fusion process via peptide-membrane interactions, but the length of the PEG-spacer plays two competing roles: a $PEG_4$/$PEG_8$ spacer length is optimal for membrane destabilization, however a $PEG_{12}$ spacer increases fusion efficiency over time by improving the peptide accessibility for successive fusion events. Both anchor type and spacer length affect peptide structure; a cholesterol anchor appears to enhance K-membrane interactions and thus mediates fusion more efficiently.

# INTRODUCTION

SNARE (soluble N-ethylmaleimide-sensitive factor (NSF) attachment protein receptor) proteins are a well conserved class of fusion proteins that are primarily involved in vesicle trafficking and fusion.[1-3] Complementary SNARE protein subunits are located on opposing membranes and, in the first step of the fusion process, they form a tetrameric coiled-coil, which brings the opposing membranes into close proximity. The fusion cascade, initiated by this docking process, consists of 3 more steps[4-5]: (1) disruption of the membrane at the site of contact; (2) merging of outer membranes, i.e. lipid mixing or hemifusion; (3) formation of a fusion pore, facilitating content mixing between the two fused compartments.[6] This SNARE fusion system has been studied extensively using the natural proteins,[7-10] and has served as inspiration for the design of model systems. Such systems are primarily based on phospholipid vesicles functionalized with either DNA,[11-15] peptides,[16-19] or small molecules,[20-24] that act as recognition motifs, but molecular recognition between functionalized cyclodextrin vesicles has also been reported.[25-28] In our lab, a model system for membrane fusion has been developed with the lipidated heterodimeric coiled-coil pair E $(EIAALEK)_3$ and K $(KIAALKE)_3$ as fusogens.[29-30] These peptides are held in lipid membranes by a lipid anchor, either cholesterol (*C*) or 1,2-dioleoyl-*sn*-glycero-3-phosphoethanol-amine (DOPE), (*L*) and this is conjugated to the peptide via a PEG-spacer of variable length (*m*, *n*) to yield C/L$P_m$E and C/L$P_n$K.

The role of these lipopeptide constructs in the fusion process is revealed by studying the relationship between rational lipopeptide modifications and their resulting influence on fusion efficiency. The consequences of the anchor type were previously investigated,[31] and it was shown that only DOPE and cholesterol anchors yielded significant fusion, with the latter being the most efficient. Increasing the length of the peptide (which increases coiled-coil binding strength and peptide-membrane interactions) also had a positive effect on fusion efficiency.[32] Conversely, parallel or anti-parallel coiled-coil orientation,[33] and coiled-coil oligomer state,[34] did not influence the rate of fusion. A recent study has also proposed an asymmetric role for the peptides in the fusion process, as shown in Figure 4 (B).[35] A key function of K is its interaction with the liposome membrane, primarily via its hydrophobic face which comprises leucine and isoleucine

residues but also via the flanking lysine residues in a process known as snorkeling.[35-36] This K-membrane interaction leads to destabilization of the membrane and initiation of the fusion process, whereas E facilitates coiled-coil formation, bringing the membranes into close proximity, allowing fusion to occur. These different roles lead to competing peptide interactions, which provides an equilibrium between K – E coiled-coil formation and K – membrane interactions.

In all these liposomal fusion studies a $PEG_{12}$ spacer was used to tether the fusogenic peptides to their membranes, but it is probable that spacer length is critical for efficient fusion. Indeed, it has been shown that the introduction of a $(GGS)_{1-3}$ spacer in the natural SNARE complex reduced the overall fusogenicity of the system with increasing spacer length,[37] likely due to an increase in distance between the proteins and their membranes. The same relationship between fusion efficiency and spacer length was also reported with DNA-based fusogens,[12] however faster docking kinetics were found with increasing spacer length, which was rationalized with a diffusion-driven collision model. This demonstrates that a spacer has opposing effects at different steps in the fusion cascade, and it indicates that, in our model system, the PEG-spacer length is likely to influence fusion efficiency.

In light of these previous studies, it was decided that the influence of PEG length on fusion efficiency should be studied using our model system. Both cholesterol and DOPE anchors were employed so that separate and cumulative effects of anchor and spacer could be studied as it is likely that the components of this model system (peptides, spacer and anchor) do not act in isolation but have a synergistic effect on fusion. (*Figure 4*) To demonstrate the asymmetry in function of the two complementary peptides the influence of PEG-spacer length for both E and K was measured individually. It was anticipated that this approach would provide further insights as to the fusion mechanism and the roles of the different components, in addition to giving a detailed picture of the functions of the lipopeptides at different stages of the fusion process.

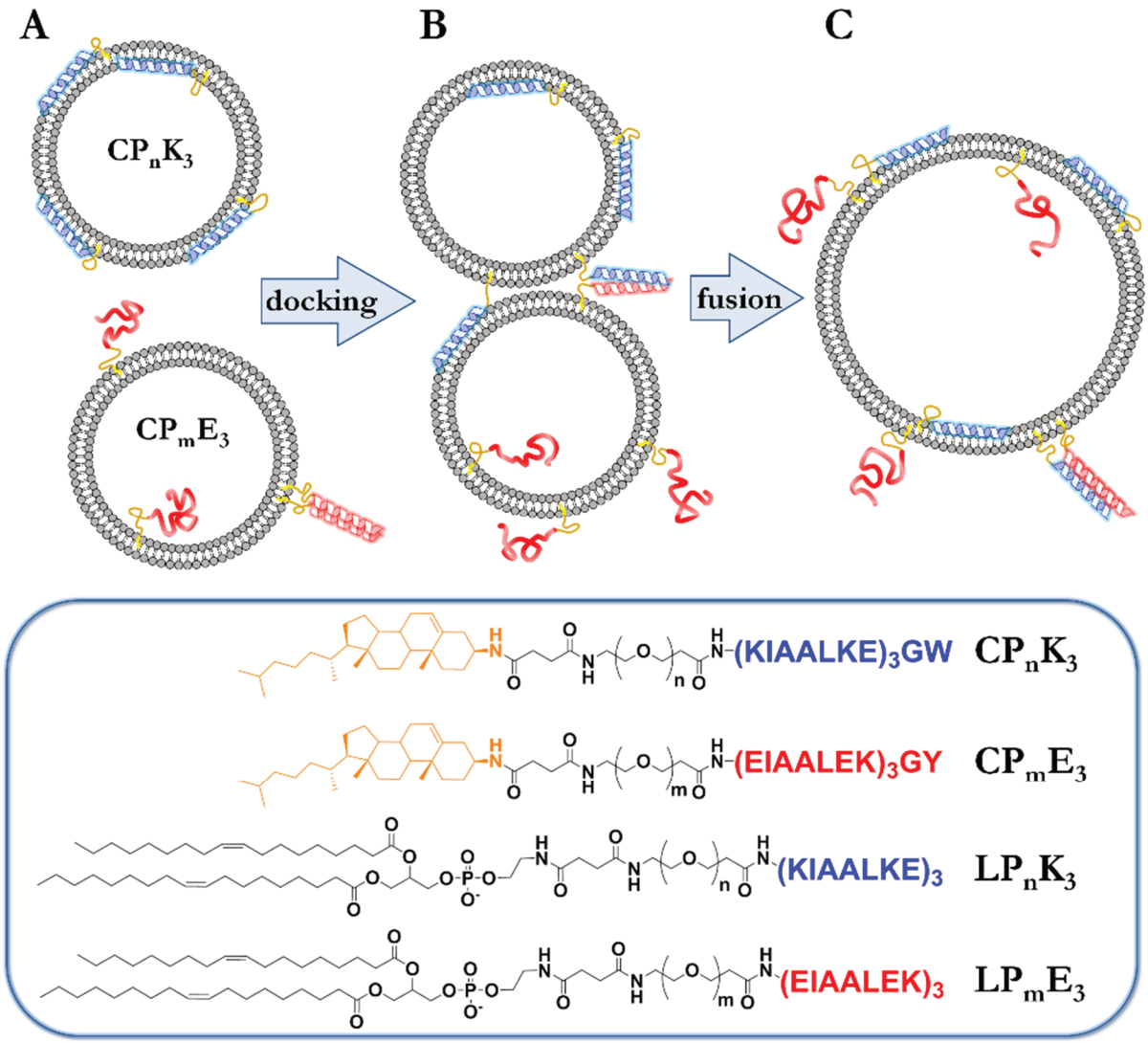


**Figure 4.** *Schematic overview of the process of peptide-mediated liposomal fusion and lipopeptide structures. The peptides are drawn in their appropriate secondary structures at distinct points of the fusion cascade: (A) liposomes functionalized with complementary peptides are initially separated; (B) liposomes dock due to coiled-coil formation, and; (C), liposomes become fully fused. Peptide E (red) can adopt homo-coils, hetero-coils and random coils, while peptide K (blue) adopts only hetero-coils or membrane immersed a-helical structures.*[38] *The lower boxed region shows the structures of the lipopeptide constructs used in this study; succinic anhydride was used to facilitate conjugation of the PEG spacer to the DOPE anchor; the corresponding cholesterol derivative was also employed.*

## DESIGN AND SYNTHESIS

Both DOPE and cholesterol have been demonstrated to be effective anchor moieties and so using both anchors, a PEG series of 0, 4, 8, and 12 repeating units was synthesized initially. During the course of this study, the spacer series was extended to cover a significant range close to the maximum fusion efficiency, and $LP_2E/K$ and $CP_{16}E/K$ derivatives were subsequently synthesized and evaluated. (*Table 1*)

To visualize the influence of the PEG-spacer length, its stretched end-to-end distance was calculated with the software AVOGADRO,[39] and from this value the distance between the peptide and the surface of the membrane was derived and termed $L_{PEG.}$ It should be noted that, for longer linkers this effective distance may be reduced as it is unlikely the PEG will retain a stretched conformation. Since the membrane surface is defined by the polar headgroups, it was assumed that, in the case of a 75% DOPC/DOPE membrane and a lipopeptide DOPE anchor, the PEG length and the peptide-membrane distance are equal. For cholesterol containing DOPC/DOPE membranes, it is known that cholesterol is buried in the membrane,[40] and so to calculate $L_{PEG}$ for cholesterol-anchored peptides, the average thickness of the membrane hydration layer (1.0 nm)[41] was subtracted because cholesterol resides at the glycerol level in the phospholipid membrane.[42]

Designing experiments to obtain insight as to the details of the fusion process is challenging due to complex short-lived intermediate stages and fast dynamics of fusion events. In addition, it is possible that the PEG-spacer will have opposing effects during the fusion process,[30] therefore it is necessary to identify the impact of these effects on the fusion efficiency. The cumulative effect of the combination of PEG-spacer length and anchor type on lipopeptide-mediated membrane fusion was studied using a content mixing assay. Further experiments were then conducted to determine the effects of the PEG-spacer length at different stages of the fusion process. Peptide ratio-dependent fusion provided insights as to the influence of the equilibria between different peptide conformations on the fusion mechanism. Furthermore, an experiment was designed to measure the ability of the lipopeptides to mediate multiple rounds of liposomal fusion.

The influence of membrane-tethering on the peptide structure was measured using circular dichroism (CD) spectroscopy. The results here, supported by previous studies,[35, 38, 43] suggest that the process of membrane fusion is rate–limited by equilibria between different peptide conformations in the initial fusion stages and that PEG-length influences these equilibria and therefore the extent of fusion.

**Table 1.** *Overview of the derivatives of peptides E and K used in this study.*

| Spacer | DOPE anchor | $L_{PEG}$ [3] | Cholesterol anchor | $L_{PEG}$ [3] |
|---|---|---|---|---|
| None [1] | $LP_0E$ / $LP_0K$ | 0.5 | $CP_0E$ / $CP_0K$ | -0.5 |
| $PEG_2$ [2] | $LP_2E$ / $LP_2K$ | 1.6 | n.a. | n.a. |
| $PEG_4$ | $LP_4E$ / $LP_4K$ | 2.3 | $CP_4E$ / $CP_4K$ | 1.3 |
| $PEG_8$ | $LP_8E$ / $LP_8K$ | 3.9 | $CP_8E$ / $CP_8K$ | 2.9 |
| $PEG_{12}$ | $LP_{12}E$ / $LP_{12}K$ | 5.4 | $CP_{12}E$ / $CP_{12}K$ | 4.4 |
| $PEG_{16}$ [2] | n.a. | n.a. | $CP_{16}E$ / $CP_{16}K$ | 5.8 |

*Peptide purities of >95% were confirmed using LC-MS for all constructs. [1]The peptide is connected to the anchor via a succinic di-amide, with a length of 0.5 nm. [2]A $LP_2$ spacer and a $CP_{16}$ spacer were added to the PEG-series to cover a significant range close to the maximum fusion efficiency. [3]$L_{PEG}$ is the distance between the N-terminus of the peptide and the surface of the membrane in nm; for DOPE anchors this is the maximum theoretical chain length of the PEG spacer (nm), as estimated by AVOGADRO,[39] and for cholesterol anchors this is the maximum theoretical chain length - 1.0nm,[40] due to the intrinsic membrane insertion property of cholesterol in DOPC/DOPE membranes.*

### CHOLESTEROL-ANCHOR MODIFICATION

The yield of lipopeptide synthesis is significantly reduced by acidic hydrolysis of the ester bond present in a cholesterolhemisuccinate anchor during cleavage of the synthesized lipopeptides from the resin. Therefore, we designed and synthesized a TFA-stable derivative (**3**), as shown in Scheme 1. Cholesterolazide (**1**)[44] was converted to **2** via a Staudinger reduction, and a subsequent coupling of succinic anhydride yielded the cholesterol anchor **3** which was purified via recrystallization.[45]

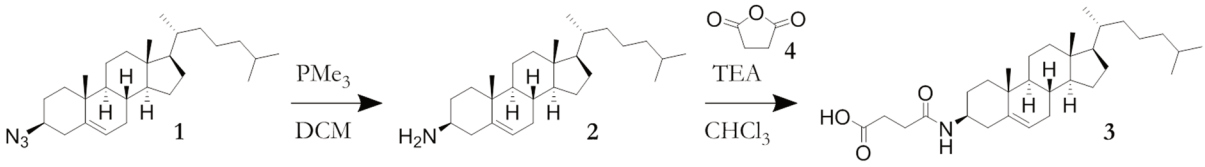


**Scheme 1.** *Synthetic pathway towards cholesterol-amide-hemisuccinate **3**.*

## RESULTS AND DISCUSSION

### CONTENT MIXING ASSAY

The final stage of a full fusion process between two membranes is content mixing. Although efficient and leakage-free content mixing remains a challenge for many fusion model systems, it has been successfully demonstrated using this system in previous studies. To facilitate this process, a quantitative content mixing model was developed by encapsulating the water-soluble dye Sulforhodamine B.[45-50] This dye self-quenches at high

concentrations, but dilution results in relief of self-quenching and an increase in fluorescence. Liposomes incorporating E lipopeptides were loaded with 20 mM Sulforhodamine B in PBS and mixed with K-functionalized buffer-containing liposomes. The effect of anchor type (with a $PEG_{12}$ spacer length) on fusion efficiency was demonstrated previously, resulting in a variable degree of membrane fusion between $LP_{12}E/K$ and $CP_{12}E/K$.[31] Here, the influence of both spacer length and anchor type on content mixing (as a measure for full fusion), was determined, Figure 5, and Figure S1.

It is evident that liposomal fusion with $CP_mE/CP_nK$ is most efficient if both lipopeptide constructs use a $PEG_{12}$ spacer, with fusion being less efficient if shorter, or longer, spacers are employed. For DOPE-anchored peptides, a $PEG_4$ spacer is necessary for the K construct, but the length of the spacer for E appears to be irrelevant. Furthermore, fusion mediated by cholesterol anchored peptides is twice as efficient as DOPE-peptide mediated fusion.

This spacer-dependent trend for DOPE-peptide mediated fusion shows that the $L_{PEG}$ of peptide K highly influences the fusion efficiency, indicating that the K peptide is crucial for efficient fusion and that the linker length strongly influences the efficiency of this process. The observed differences in PEG spacer length preference between cholesterol- and DOPE-anchored peptides can't be explained by differences in $L_{PEG}$, since their various spacers all cover the same distance range (0 - 6 nm), although cholesterol is bound more tightly to the membrane than DOPE.[31] Since liposomal membranes already contain 25 mol% cholesterol, significant influences in general membrane characteristics attributed to cholesterol were not expected.[50-51] However, recent studies on the influence of the lipid anchor on membrane-tethered PEG-spacers showed that a cholesterol anchor increased the flexibility of the spacers,[52] and influenced their function.[53] This reveals that the anchor type does affect the behaviour of the other components (spacer and peptide) in this construct, and it is hypothesized that the cholesterol anchor enhances the membrane-interacting and disrupting role of K in the fusion process, which may explain why increased levels of content-mixing are observed with cholesterol-anchored peptides.

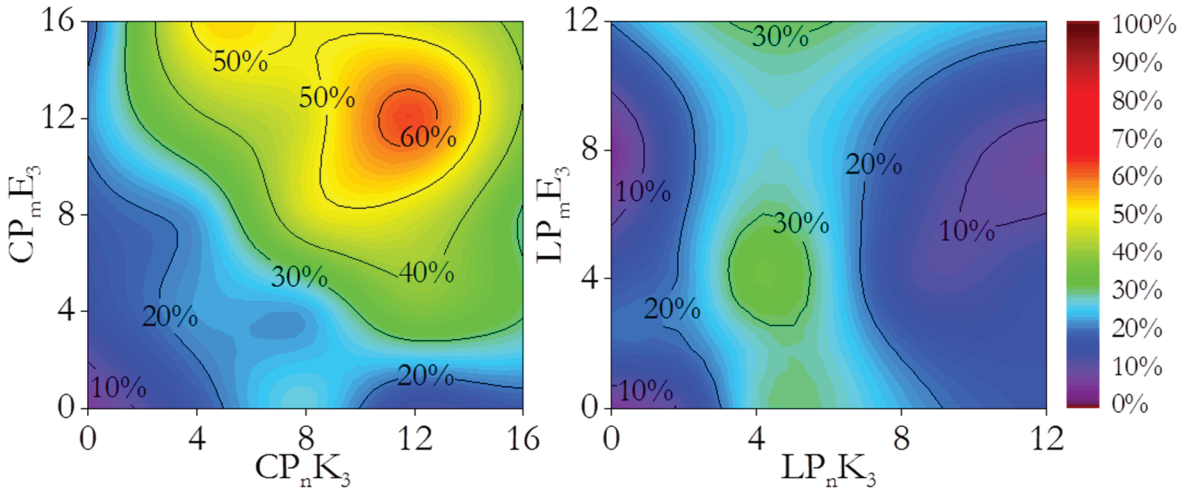


**Figure 5.** *Content mixing between E and K-decorated liposomes as a function of PEG spacer length (m/n) as indicated by an increase in sulforhodamine B emission after 30 min. Left, cholesterol anchored Pm/n-series and, right, DOPE anchored Pm/n-peptides. [Total lipid] = 0.1 mM, with 1 mol% lipopeptide, PBS pH 7.4.*

## CIRCULAR DICHROISM SPECTROSCOPY

Since $LP_{12}E$ and $LP_{12}K$ are known to adopt distinct structures when tethered to lipid membranes,[35, 38] the influence of linker length on peptide secondary structure was examined using circular dichroism (CD) spectroscopy. In addition to exploring these linker effects, both anchors were tested to determine whether these also influence peptide structure. The membrane-tethered peptide constructs were tested in isolation, and when mixed to determine whether heteromeric coiled-coil species were formed. The results are illustrated in Figure 6, and Figure S4. A $\theta_{222}/\theta_{208}$ ratio $\geq 1$ is indicative for coiled-coil formation, however this ratio can be skewed due to inherent scattering properties of liposomes. While $\theta_{222}$ is a measure for helicity, both peptide-membrane interactions and coiled-coil formation contribute to the observed helicity, therefore identifying whether peptides are folded as α-helices or coiled-coils is non-trivial.

It has been demonstrated previously that the α-helical conformation of membrane tethered K is stabilized via spontaneous incorporation into the membrane,[38, 43] and so a correlation between the observed helicity of the peptides and the relative strength of this membrane interaction may be inferred. For $CP_nK$ derivatives, increasing helicity upon decreasing spacer length shows that peptides that are in closer proximity to the membrane experience more stabilization by, and therefore are likely to interact more strongly with, the membrane. The helicity of $LP_n$-anchored K peptides is lower compared

to the $CP_nK$ peptides and does not change significantly with altering PEG-lengths. This indicates that the peptide membrane interaction is less pronounced for $LP_n$ lipopeptides and that the peptide conformation is not significantly affected by varying the spacer length. The decreased fusion efficiency measured when liposomes are decorated with $LP_{m/n}$ anchored peptides is likely a result of this weaker membrane interaction of $LP_nK$, which provides further evidence for a correlation between the strength of the peptide-membrane interaction and the fusion efficiency of peptide decorated liposomes.

To explain this influence of anchor type on peptide-membrane interactions, it is necessary to examine the characteristics of the membrane and the tethered lipopeptides. When peptide K interacts with the membrane, it tends to be surrounded by lipids with smaller headgroups (i.e. DOPE, cholesterol).[35, 54-55] The accumulation of DOPE in the proximity of peptide K destabilizes the membrane, promoting the formation of a protrusion centered at the peptide's position,[35] and supports the highly curved membranes of fusion intermediates.[50, 56] The cholesterol anchor could enhance the membrane insertion of peptide $CP_nK$ due to its relatively small headgroup, and because cholesterol promotes chain-flexibility of conjugated PEG-spacers,[52] these factors could increase the tendency of the conjugated peptides to incorporate in the supporting membrane.

Peptide E adopts structures with relatively low amounts of helicity, supporting previous findings that peptide E does not significantly interact with DOPC/DOPE/ cholesterol membranes, and adopts a mixture of weakly helical homodimers and random coils in solution.[38] Although α-helical peptide stabilization by PEG has been reported,[57] here these PEG-peptide interactions are not likely to be significant due to the short length of the used PEG-spacers.

The structural characteristics of the mixture of E and K decorated liposomes show the ability of the peptides to form a coiled-coil. The helicity measured in a mixture of $LP_mE$ and $LP_nK$ decorated liposomes is, for all $m/n$, higher than the helicity of the separated $LP_mE$ and $LP_nK$ functionalized liposomes and demonstrates coiled-coil formation between peptides tethered to different liposomes. The absence of coiled-coil formation for $CP_0E$ + $CP_0K$ as measured by the $\theta_{222}/\theta_{208}$ ratio supports the previous observation that this lipopeptide-pair does not mediate fusion efficiently, most likely due to the

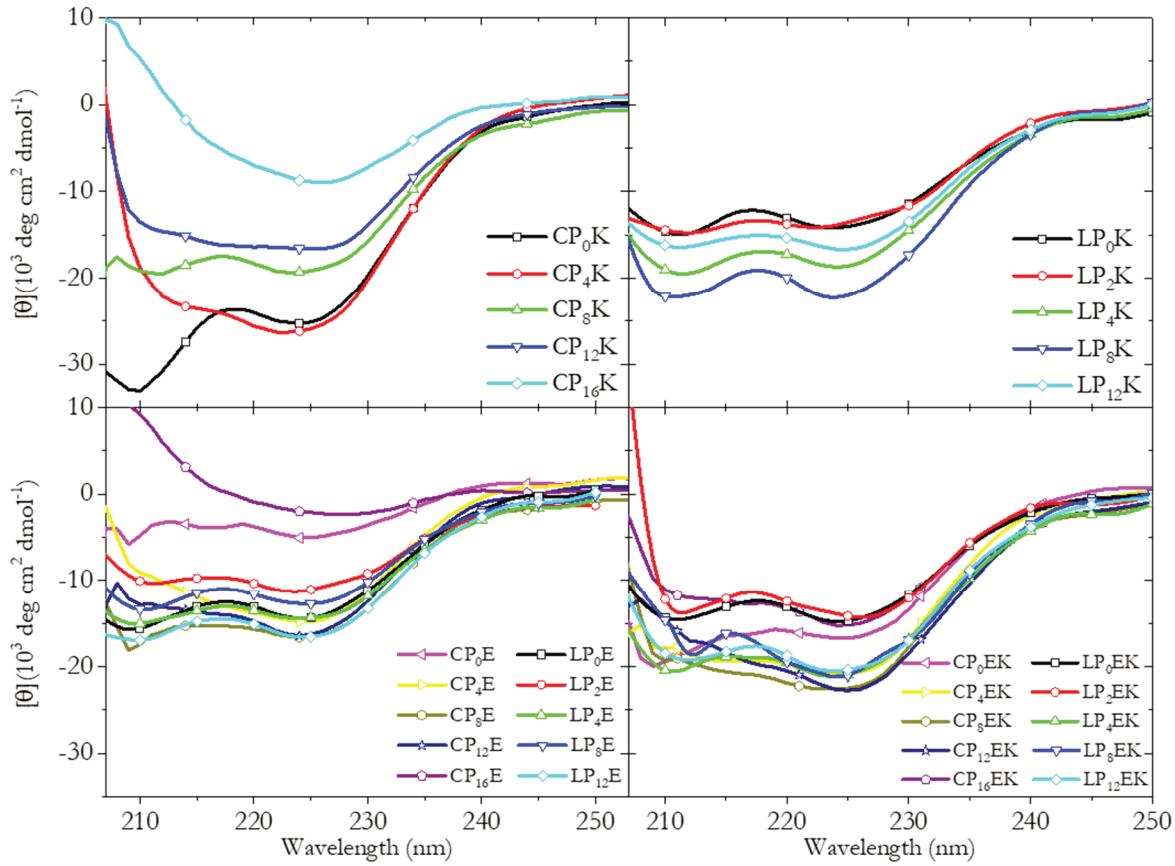


**Figure 6.** *CD spectra of liposome-tethered lipopeptides. [Total lipid] = 0.5 mM, with 1 mol% lipopeptides, PBS pH 7.4.*

**Table 2.** *Degree of peptide helicity as determined by circular dichroism.*

| Anchor + spacer | E | | K | | E + K | |
|---|---|---|---|---|---|---|
| | $\theta_{222}/\theta_{208}$ | %H [1] | $\theta_{222}/\theta_{208}$ | %H [1] | $\theta_{222}/\theta_{208}$ | %H [1] |
| Acyl [2] | 0.4 | 20 | 0.4 | 19 | 1.0 | 60 |
| $CP_0$ | 0.9 | 15 | 0.8 | 72 | 0.8 | 47 |
| $CP_4$ | 1.5 | 42 | 1.2 | 75 | 0.9 | 59 |
| $CP_8$ | 0.9 | 47 | 1.0 | 55 | 1.2 | 65 |
| $CP_{12}$ | 0.6 | 47 | 1.1 | 47 | 1.3 | 65 |
| $CP_{16}$ | n.a. [3] | 6 | n.a. [3] | 26 | 1.3 | 44 |
| $LP_0$ | 1.0 | 37 | 1.0 | 37 | 1.0 | 38 |
| $LP_2$ | 1.1 | 30 | 1.0 | 39 | 1.1 | 36 |
| $LP_4$ | 1.0 | 39 | 1.0 | 49 | 1.0 | 57 |
| $LP_8$ | 0.9 | 34 | 1.0 | 57 | 1.1 | 57 |
| $LP_{12}$ | 1.0 | 44 | 1.0 | 44 | 1.1 | 55 |

*[1]Percentage a-helicity was calculated using the formula $[\theta]_{222}=-39500*(1-2.57/n)$ to obtain a 100% helicity value for an a-helical peptide of n residues.[58] [2]Measurements with acylated peptides, in PBS pH 7.4, without vesicles. [3]Negative ratio due to positive $\boldsymbol{\theta_{208}}$ value caused by a scattering artifact. [Total lipid] = 0.5 mM, with 1 mol% lipopeptides, PBS pH 7.4.*

peptides being held too close to the membrane to be able to form a coiled-coil efficiently, thus preventing liposome docking. For cholesterol anchored peptides with elongated spacers, coiled-coils are formed, which correlates with the efficient fusion observed from the content-mixing experiments.

## TIME RESOLVED RATE OF FUSION

Experiments using model systems incorporating DNA-based fusogens showed that while increasing spacer length decreased fusion efficiency, docking of liposomes (i.e. the initial stage of the fusion process) was accelerated with longer spacers.[12] To separate these influences of time and $L_{PEG}$ on the fusion efficiency of this model system, it is necessary to identify and isolate distinct time periods in the fusion experiment. During the initial minutes of the content-mixing assays, the rate of fusion is linear, and provides a reliable correlation between $L_{PEG}$ and docking/fusion efficiency. This linearity is largely due to the fact that fusion events occur with unfused liposomes randomly dispersed in a well-mixed experimental solution. After a few minutes the experimental mixture becomes increasingly more complex as larger fusion products appear and the available number of unfused liposomes decreases.[30]

Since $CP_mE/CP_nK$ mediated liposomal fusion is significantly more efficient than $LP_mE/LP_nK$ mediated liposomal fusion, fusion efficiency with $CP_mE/CP_nK$ was measured for all possible combinations of $m/n$, continuously for 30 minutes. To compare the different stages in the fusion experiment, the fusion rate was determined after 4 and 30 minutes. (*Figure 7*) Complete datasets, including control experiments which demonstrate a fluorescence increase is only obtained when both peptide-functionalized liposome populations are present, are available in Supporting Information, Figure S1 / S2.

After 4 minutes all fusion events involving the $CP_{12}E$ lipopeptide showed the highest fusion efficiency, regardless of the length of the PEG-spacer in the $CP_nK$ construct, although a $CP_8K/CP_{12}E$ combination gives the highest initial fusion efficiency. Liposomal docking is dependent on the length of $CP_mE$ because peptide K is fully incorporated in the membrane prior to fusion, as evidenced by Infrared Reflection Absorption Spectroscopy (IRRAS) measurements preformed previously.[35, 38] This indicates that the $L_{PEG}$ of E is critical for liposome docking, with longer linkers being

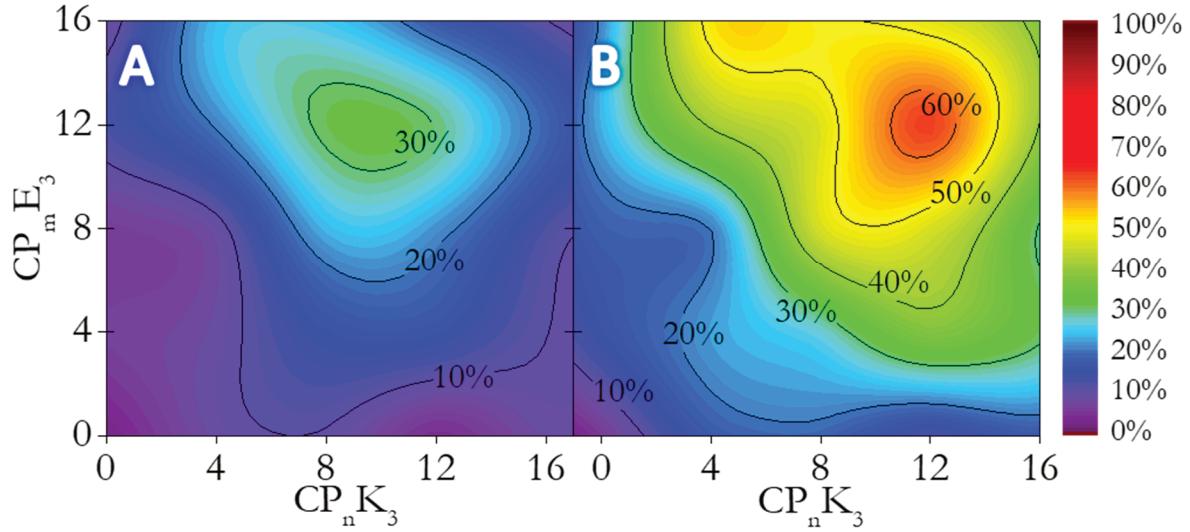


**Figure 7.** *Time resolved rate of fusion (measured using content-mixing assays) with $CP_mE$ and $CP_nK$ decorated liposomes. Data is presented as a function of m/n, indicated by an increase in sulforhodamine B emission after (A) 4 mins, and (B) 30 mins. [Total lipid] = 0.1 mM, with 1 mol% lipopeptide, PBS pH 7.4.*

more efficient. This supports the theory that E acts as a handle for K, searching for a K peptide to form a coiled-coil with, a process resulting in liposome docking. It has been shown that, during liposomal docking, peptide K is in dynamic equilibrium between a heterodimeric coiled-coil structure and a membrane-immersed α-helix; the length of the $CP_nK$ spacer could highly influence this equilibrium. Membrane immersion of multiple K-peptides in both liposomes creates the necessary protrusions to initiate fusion and simultaneously dictates the maximum distance between connected liposomes.[35] Since optimal initial fusion efficiency, with an equimolar ratio of both peptides, is obtained with $CP_8K$ a spacer length of 2.9 nm appears optimal to bring both membranes into close proximity and to overcome the energy barriers in the fusion process.

After 30 minutes, $CP_{12}K$ + $CP_{12}E$ decorated liposomes show the highest overall fusion efficiency. These results oppose a diffusion driven collision model with docking of liposomes as the rate-limiting step,[37] because that implies a linear correlation between observed fusion efficiency and PEG-spacer length. Additionally, fusion with $CP_{16}E$ is less efficient compared to $CP_{12}E$, which also demonstrates that the rate limiting step in this fusion system is not liposomal docking. The shift in fusion efficiency to K peptides functionalized with elongated spacers can be caused by different phenomena: liposomal diffusion, better peptide accessibility and the occurrence of multiple rounds of fusion, all of which can be tested by changing the conditions of the content-mixing experiments (*vide infra*).

Although the fusion process is not driven by diffusion, liposomal diffusion could still have a minor effect on the fusion efficiency, although only over longer time scales when the number of liposomes decreases as a result of fusion. With decreased liposomal concentration, liposomes functionalized with elongated PEG spacers have a higher probability to find unfused liposomes with available coiled-coil binding partners. This is illustrated by data showing that initially, there is no difference between fusion of liposomes functionalized with $CP_4K$ and liposomes bearing $CP_8E$ or $CP_{16}E$, but over time fusion with $CP_{16}E$ decorated liposomes is more efficient.

## INFLUENCE OF CPE / CPK RATIO ON FUSION EFFICIENCY

Liposomal fusion efficiency mediated by $LP_{12}E$ / $LP_{12}K$ is highly dependent on peptide concentration;[30] with concentrations ≥ 0.5 mol%, efficient lipid mixing has been reported. To date, both liposome populations used in the fusion studies were functionalized with $LP_{12}E$ or $LP_{12}K$ in an equimolar ratio. A ratio ≠ 1, should support the asymmetric function of the lipopeptides in the fusion process however, as the roles of both peptides will be affected differently by altering their concentrations.

To test this hypothesis, the concentration of $CP_mE$ was lowered to 0.5 mol% while [$CP_nK$] was maintained at 1 mol%. Here, changes in the fusion efficiency will provide more-detailed insights as to the peptide's roles in the fusion process. Furthermore, lowering the concentration of $CP_mE$ will affect the handle function of E and it is expected that the change in peptide ratio enhances the impact of $L_{PEG}$ of $CP_nK$ on the fusion process. Since the most striking differences in efficiency are found with elongated $CP_mE$ spacers, only liposomal fusion with $CP_{12}E$ and $CP_{16}E$ decorated liposomes was studied. (*Figure 8, Figure S3*)

As is evident from Figure 8, the influence of $CP_nK$ on the fusion process is enhanced by lowering the concentration of $CP_mE$, and the resulting fusion efficiencies reveal that $CP_8K$, with a calculated $L_{PEG}$ of 2.9 nm, is optimal for fusion. Remarkably, initial fusion efficiencies were shifted to elongated spacers with decreasing $CP_mE$ concentration, which supports the handle function of E for liposomal docking, and demonstrates the effect of

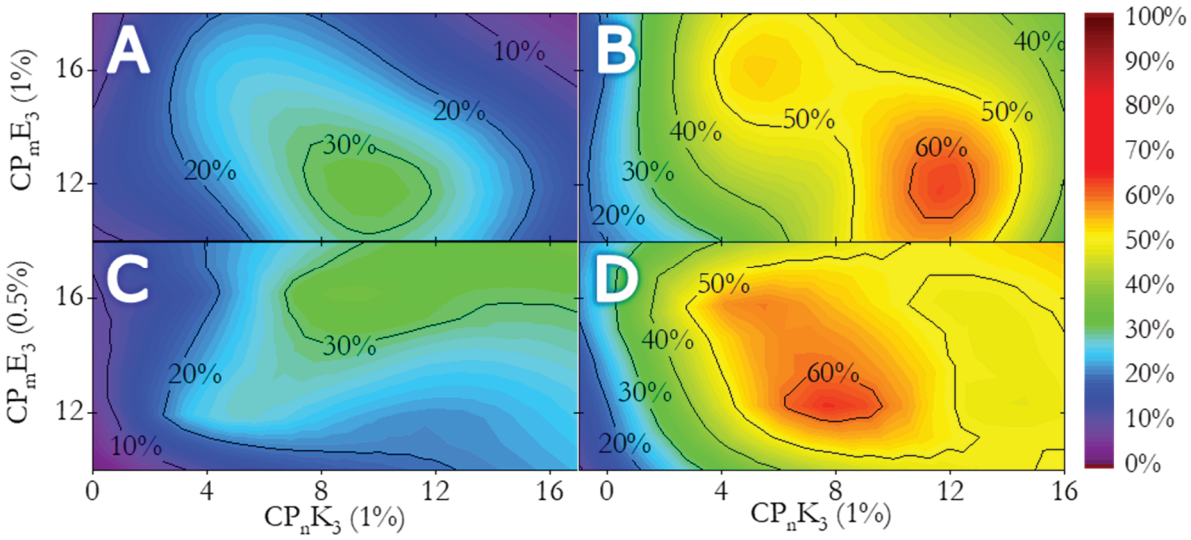


**Figure 8.** *Peptide ratio dependent and time resolved rate of fusion (monitored using a content mixing assay) with $CP_mE$ and $CP_nK$ decorated liposomes as a function of m/n and [peptide], as indicated by an increase in sulforhodamine B emission. Fusion of liposomes decorated with 1 mol% $CP_mE$ and 1 mol% $CP_nK$ is measured after 4 min (A) and 30 min (B) and taken as a reference plot from Figure 2; and fusion of liposomes decorated with 0.5 mol% $CP_mE$ and 1 mol% $CP_nK$ measured after 4 min (C) and 30 min (D). [Total lipid] = 0.1 mM, PBS pH 7.4.*

diffusion driven collision of liposomes. Over time however, no significant difference between $CP_{12}E$ and $CP_{16}E$ was observed indicating a minor role for $L_{PEG}$ of E at these conditions. The impact of $L_{PEG}$ of K is demonstrated by the shift in fusion efficiency to $CP_8K$ decorated liposomes.

In the presence of membrane tethered E, K will either form a coiled-coil with E or insert in the lipid membrane. It has been demonstrated previously that insertion of unbound peptide K in a membrane is favored over coiled-coil formation, and the presence of membrane tethered E highly enhances the speed of this process.[35] This means that, when the concentration of $CP_mE$ is lowered, initial docking of both liposomes via a transient coiled-coil interaction is still efficient, but the equilibrium between coiled-coil formation and membrane insertion of $CP_nK$ (in the opposing liposomal membrane; if not, membrane fusion would be less efficient) shifts to membrane insertion, which in turn results in higher fusion efficiencies for shorter spacers. These results demonstrate that peptide equilibria between different conformations after initial docking highly influences fusion efficiency, and that the interaction between lipopeptide K and the phospholipid membrane is crucial for membrane fusion.

## MULTIPLE ROUNDS OF FUSION ASSAY

Finally, a different content mixing experiment was conducted using $CP_mE/CP_nK$ ($m/n$ = 8, 12, 16) in order to visualise the influence of the PEG-spacer length on the efficiency of multiple rounds of fusion. To measure this parameter, a population of (self-quenched) fluorescent, $CP_mE$ decorated liposomes with an excess of $CP_nK$ decorated plain liposomes which should result in a higher loss of self-quenching, with respect to the standard content mixing assay using an equimolar mixture of fluorescent and non-fluorescent liposomes, upon every round of fusion. Therefore, $CP_nK$ decorated plain liposomes were mixed with sulforhodamine B loaded $CP_mE$ decorated liposomes in 2 ratios (1:1 and 10:1), and fusion efficiencies were determined by measuring the fluorescence increase after 30 minutes, Table 3. Remarkably, the efficiency of multiple-rounds of fusion appears to be dictated by the PEG-spacer length used for peptide K only, and is not affected significantly by $L_{PEG}$ of $CP_mE$, confirming that K controls the fusion process, whilst E serves only to mediate coiled-coil formation which leads to liposome docking. The fluorescence increase measured with fusion of $CP_mE$ decorated liposomes and a 10-fold excess of $CP_8K$ decorated liposomes was as efficient as the fusion experiment with an equimolar mixture of the peptide functionalized liposomes. This shows that the abundant availability of $CP_8K$ decorated liposomes doesn't yield a higher fusion efficiency. For $CP_{12}K$ decorated liposomes, fusion experiments with a 10-fold excess of K decorated liposomes yielded a fluorescence increase of 115±18%, demonstrating the fusion of one $CP_mE$ decorated liposome with multiple $CP_{12}K$ decorated liposomes. For $CP_{16}K$, the multiple round fusion efficiency was 53±7%, indicating the presence of multiple rounds of fusion with this lipopeptide also.

Although it has been shown that $CP_8K$ is most efficient in mediating the early rounds of fusion, it is not able to mediate multiple rounds of fusion in the setting described above. To address this, the behavior of the peptides just before the second fusion event, when both E and K are tethered to the same membrane and are approached by an unfused K decorated liposome have to be considered. E tethered to the membrane of the fluorescent liposome should be accessible to unfused K bearing liposomes, but efficient fusion only occurs when these liposomes are functionalized with $CP_{12}K$ lipopeptides. It is possible that the $L_{PEG}$ distance is again crucial, by shifting peptide equilibria between membrane-incorporated and coiled-coil conformations, and/or by bridging the gap

**Table 3.** *Multiple rounds of fusion assay.*

| $[CP_nK]$/ $[CP_mE]$ [a] | $CP_8K$ + | | | $CP_{12}K$ + | | | $CP_{16}K$ + | | |
|---|---|---|---|---|---|---|---|---|---|
| | $CP_8E$ | $CP_{12}E$ | $CP_{16}E$ | $CP_8E$ | $CP_{12}E$ | $CP_{16}E$ | $CP_8E$ | $CP_{12}E$ | $CP_{16}E$ |
| 1 [b] | 47 | 47 | 51 | 46 | 64 | 48 | 29 | 40 | 38 |
| 10 | 51 | 50 | 55 | 95 | 150 | 97 | 47 | 61 | 55 |
| Δ% [3] | 10% | 7% | 8% | 104% | 135% | 104% | 61% | 53% | 46% |

*[a] Fusion efficiency is indicated by an increase in sulforhodamine B emission after 30 mins, with K decorated liposomes in 1 fold or 10 fold excess with respect to dye loaded E decorated liposomes. [b] Fusion efficiency percentages are normalized to efficiency percentages reported for the equimolar mixture at [total lipid] = 0.1 mmol, shown in Figure 5. [3]Differences in fluorescence increase between both experiments are calculated as a measure for multiple rounds of fusion and the value of the normalized equimolar mixing entry is used as 100%. [Total lipid of $CP_mE$ decorated liposomes] = 0.05 mM, with 1 mol% lipopeptides, PBS pH 7.4.*

between opposite membranes, thus enabling or disabling the next round of liposomal fusion. As a consequence, the mechanism of liposomal fusion is dictated by peptide equilibria affecting the function of peptide K, and a difference of 1 or 2 nm in the length of the spacers employed highly influences the efficiency of the peptides to mediate multiple rounds of fusion.

## IMPLICATIONS FOR THE INITIAL STAGES OF LIPOSOMAL FUSION.

Based on these results the following mechanism for the initial stages of E-K mediated liposomal fusion is proposed: initially, lipopeptide K is fully immersed in the liposomal membrane, while lipopeptide E adopts a largely unfolded state. Interliposomal coiled-coil formation occurs when liposomes collide and lipopeptide E binds transiently with lipopeptide K. K-membrane interactions are favored over coiled-coil formation; therefore peptides are in an equilibrium, switching between the different states. Once folded as a coiled-coil, K is in close proximity to both membranes and hence can interact with either. Immersing itself in the opposite membrane will force both membranes into even closer proximity, destabilizing both membranes by forming protrusions, and will lead to the dehydration of both membrane solvation layers, thus providing the necessary initial conditions for the merging of the membrane bilayers.[35, 55] (*Figure 9*)

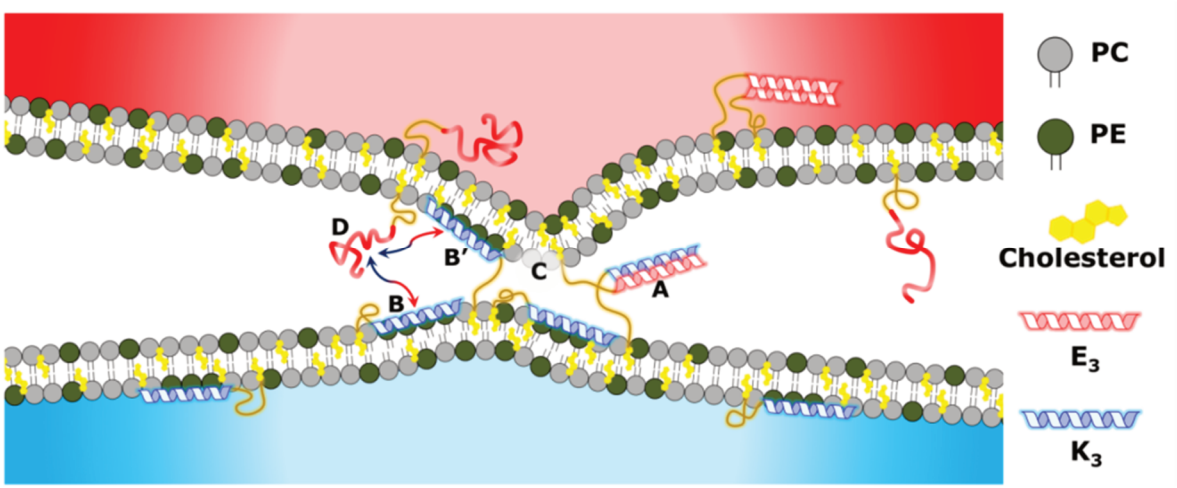


**Figure 9.** *Peptide equilibria prior to fusion. A transient coiled-coil complex (A) forms upon contact of liposomes. From the coiled-coil conformation, peptide K can immerse in both membranes (B – B'); membrane insertion in the opposing membrane will force both membranes in close proximity, destabilize both membranes with protrusions (C), providing the necessary conditions for membrane merging. Equilibria of peptide-interactions between (D) and (B - B') are highly affected by the length of the PEG-spacer used for both E and K.*

## CONCLUSIONS

This study has demonstrated that the membrane interaction propensity of K, a factor crucial for efficient membrane fusion, is dependent on both the anchor and PEG spacer-length employed. When conjugated to a cholesterol anchor, K shows increasing helicity with decreasing PEG-length, indicating a more profound peptide-membrane interaction for shorter spacers. In contrast, the $LP_nK$ derivatives do not affect the peptide structure significantly, and the helical secondary structure of all $LP_nK$ derivatives appears to be less membrane stabilized when compared to $CP_{12}K$ lipopeptides. The influence of the anchor on peptide-membrane interaction is likely caused by altering local membrane characteristics, and is therefore also a factor in the fusion efficiency; cholesterol anchored lipopeptides are more efficient in mediating fusion than DOPE anchored lipopeptides, as evidenced by the content mixing assays.

The intrinsic stability of liposomes prevents coiled-coil formation when peptides are tethered directly to the membrane, (i.e. when a spacer is not used) and lessens the fusion efficiency when very long spacer lengths are applied. Changing the length of the spacer region between E and K independently demonstrated that the peptides clearly have different roles in the fusion process, as shown with the various content-mixing experiments that reflect the initial stages of fusion. It can be concluded that peptide E

acts as a handle for peptide K to enable initial liposomal docking via coiled-coil formation, and, a $CP_{12}E$ or $CP_{16}E$ construct is most efficient.

After coiled-coil formation, peptide K migrates to the lipid membrane,[35] and lowering the concentration of $CP_mE$ at the liposomal surface from 1% to 0.5% revealed the effect of K equilibria between coiled-coil formation and K-membrane interaction on the rate and efficiency of liposomal fusion.[35] This change in $CP_mE/CP_nK$ ratio increased the probability of peptide K immersing itself in the opposing membrane directly after coiled-coil formation, which in turn significantly increased the fusion efficiency for liposomes with shorter spacers, showing the strong influence of $L_{PEG}$ on the rate of membrane fusion. Multiple rounds of liposomal fusion were only observed when liposomes were functionalized with $CP_{12}K$ and $CP_{16}K$, while no apparent influence of $CP_mE$ on the fusion efficiency was measured. Here, the fusion efficiency depends only on the spacer length of lipopeptide K. This pronounced influence of the PEG-spacer illustrates the extreme sensitivity of the fusion system to $L_{PEG}$ and to the dynamics of the involved peptides in the initial stages of fusion.

The differences in the (initial) rate of fusion revealed that lipopeptides $LP_4K$ and $CP_8K$ are most efficient in mediating fusion compared to other $LP_nK$ / $CP_nK$ derivatives which means that a distance of ±2 nm between peptide K and the membrane is most favorable, and this lipopeptide is an ideal candidate for further investigations in similar fusion systems. The length of the spacer highly influences the speed and efficiency of the fusion process and reveals the roles of the peptides in the fusion mechanism.

# EXPERIMENTAL SECTION

## MATERIALS

Fmoc-protected amino acids, rink amide resin, and O-(1H-6-Chloroben-zotriazole-1-yl)-1,1,3,3-tetramethyluronium hexafluorophosphate (HCTU) were purchased from NovaBioChem. Diisopropylethylamine (DIPEA), piperidine, acetic anhydride, N-methylpyrrolidine (NMP), dimethylformamide (DMF), acetonitrile, and trifluoroacetic acid (TFA) were obtained from Biosolve. Dichloromethane (DCM), diethyl ether, triisopropylsilane (TIS), trimethylamine (TEA), cholesterol, trimethylphosphine ($PMe_3$, 1M in toluene) (1H-benzotriazol-1-yloxy)tripyrrolidinophosphoniumhexafluorophosphate (PyBOP), succinic anhydride, and sulforhodamine B were obtained from Sigma Aldrich. 1,2-dioleoyl-sn-glycero-3-phosphatidylcholine (DOPC), and 1,2-dioleoyl-sn-glycero-3-phosphatidylethanolamine (DOPE) were purchased from Avanti polar lipids. The Fmoc–NH–$(PEG)_{2/8/12/16}$–COOH spacers were purchased from Iris Biotech. The $N_3$–$(PEG)_4$–COOH spacer was synthesized according to a literature procedure, as reported previously. [59-60] [59-60] [59-6051-52] Cholesteryl-4-amino-4-oxobutanoic acid (3) was synthesized according to a modified literature procedure,[45] synthesis of the starting compound 3-Azido-5-cholestene (1) is described elsewhere.[44] PBS buffer contains 5 mM $KH_2PO_4$, 15 mM $K_2HPO_4$, 150 mM NaCl, pH 7.4. Data analysis and visualization was performed using OriginPro 9.1.

## SYNTHESIS OF CHOLESTERYL-AMINO-HEMISUCCINATE

**3-Amino-5-cholestene (2):** To a solution of 3-Azido-5-cholestene (1) (15.8 g, 38.4 mmol) in dichloromethane, 4 equivalents of trimethylphosphine (1M solution in THF or toluene) was added and the reaction was stirred overnight. When 3-Azido-5-cholestene was consumed as evidenced by TLC (eluent: hexane, rf = 0.7), the reaction was concentrated *in vacuo* to yield **2** (14.8 g, 100%) as a pure compound. $^1$H NMR (300 MHz, $CDCl_3$) δ = 5.27 (s, 1H), 2.60 (m, 1H), 2.17-0.85 (m, 40H), 0.64 (s, 3H); $^{13}$C NMR (75 MHz, $CDCl_3$) δ 141.8, 120.7, 56.8, 56.2, 52.0, 50.3, 43.4, 42.3, 39.8, 39.5, 38.2, 36.6, 36.2, 35.8, 32.7, 31.9 (× 2), 28.3, 28.0, 24.3, 23.9, 22.8, 22.6, 21.0, 19.5, 18.7, 11.9; IR (film) ν 3354, 3260, 3154, 2936, 2896, 2849, 1464, 1437, 1381 $cm^{-1}$; LRMS ($ESI^+$) $m/z$ 386.4 ($[M+H]^+$, $C_{27}H_{48}N$ calcd. 386.4).

**Cholesteryl- 4-amino-4- oxobutanoic acid (3):** To a solution of **2** (10 g, 26 mmol) in chloroform (150 mL) succinic anhydride (7.8 g, 78 mmol) was added. Triethylamine (8mL, 57 mmol ) was added drop-wise to the solution and the reaction mixture was stirred overnight under nitrogen atmosphere at room temperature, until the starting material was completely consumed as evidenced by TLC (eluent: hexane: ethylacetate 1:1, rf = 0.4). The reaction mixture was transferred to a separatory funnel, and the organic layer was washed with water and brine, was dried with MgSO4 and was concentrated in *vacuo* to afford cholesterol amide acid (10 g) as a yellow solid. The crude cholesterol amide acid was purified by recrystallization in Acetonitrile: MeOH (1:1) at 4°C and was vacuum filtered to afford **3** as an off-white solid (8.7 g, 76%) $^1$H NMR (400MHz, $CDCl_3$) δ = 5.36 (s, 1H), 3.69 (s, 1H), 3.60 (m, 1H) 2.62 (m, 2H), 2.44 (m, 2H), 2.20-1.72 (m, 7H), 1.67-1.03 (m, 20H) 1.01 (s, 3H) 0.92 (d, $J$ = 6.5 Hz, 3H), 0.87 (dd, $J$ = 6.6, 1.7 Hz, 6H), 0.69 (s, 3H). TLC-MS (ESI$^+$) $m/z$ 486.4 ($[M+H]^+$, $C_{31}H_{51}NO_3$ cald. 486.4 g/mol).

## LIPOPEPTIDE SYNTHESIS

**$PEG_n$-peptide synthesis:** Peptide synthesis was performed on a CEM Liberty I on a 100 μmol scale using Rink amide resin of 0.55-0.73 mmol/g substitution. Amino acid activation was achieved using HCTU/DIPEA in DMF. Fmoc deprotection was carried out using 2 cycles of 20% piperidine in DMF. All automated reactions were carried out at 70-80 °C with the use of a microwave. The N-terminal free amine was used to couple the PEG-spacer through standard solid phase chemistry using Py-BOP/DIPEA activation. With the exception of N3-PEG4-COOH containing lipopeptides, Fmoc-deprotection of the PEG component was achieved using 20% piperidine for 20 mins to obtain a free amine at the N-terminus. N3-PEG4-COOH containing lipopeptides were reduced using 2 cycles of PME in dioxane/water (4:1).

**DOPE anchor attachment:** Succinic anhydride was coupled to the N-terminal free amine using a succinic anhydride/TEA (10 eq./10 eq.) mixture in NMP. The reaction was left overnight on a shaker at room temperature. The resin was washed thoroughly with NMP, DCM, and NMP to remove excess reactants. Next, the resin (1 eq.) was activated using PyBOP/DIPEA (3 eq./5 eq.) in DCM:DMF (1:1) for 1hr. DOPE (2 eq.) was dissolved in a minimal volume (2 ml) of DCM: DMF (1:1) and a small amount of TEA (2 eq.) was added to improve solubility. After 1 hr this DOPE solution was added

to the resin, warmed to 50 °C and the reaction was left overnight on a shaker. The resin was washed thoroughly with DMF and DCM to remove excess reactants.

**CHOL anchor attachment:** Cholesteryl- 4-amino-4- oxobutanoic acid (**3**) (1.2 eq.) was activated with PyBOP/DIPEA (3eq/5eq) in DCM:DMF 1:1, added to the peptide-bound resin and the reaction was left for 2 days on a shaker. The resin was washed thoroughly with DMF and DCM to remove excess reactants.

**Cleavage:** The resin bound peptide was cleaved from the resin and deprotected for 2 hours in 4ml of TFA: TIS: Water (95%: 2.5%:2.5%), The cholesterol-anchored peptides were precipitated in cold diethyl ether followed by centrifugation and dried under vacuum, DOPE-anchored peptides were concentrated in vacuo, dissolved in a minimal amount of acetic acid/H2O and subsequently purified.

**Purification:** RP-HPLC was performed with a Shimadzu HPLC system with two LC-8A pumps, and a SPD-10AVP UV-VIS detector. Sample elution was monitored by UV detection at 214 nm and 256 nm. Samples were eluted with a linear gradient from A to B, A being 10 % (v/v) $H_2O$, 0.1 % (v/v) TFA, and B being 90 % (v/v), 0.1 % (v/v) TFA in acetonitrile. Purification of DOPE-lipopeptides was performed on a Vydac C4 reversed phase column (214TP1022, 22 mm diameter, 250 mm length, 10.00 μM particle size) with a flow rate of 20 mL $min^{-1}$. Purification of CHOL-lipopeptides was performed on a Phenomenex C18 reversed phase column (21.2 mm diameter, 150 mm length, 5.00 μM particle size) with a flow rate of 15 mL $min^{-1}$. Collected fractions were tested for >95% purity using LC-MS with Gemini C18 column and further freeze dried to store at -20$^0$C.

## GENERAL METHODS

**Liposome preparation.** A 1 mM stock solution containing DOPC : DOPE : cholesterol (50 : 25 : 25 mol%) lipids in 1 : 1 (v/ v) methanol : chloroform was prepared for all fusion experiments. Lipidated peptides were dissolved in a 1 : 1 (v/v) choloroform : methanol mixture, to a concentration of 50 uM. 1 mol% of these lipidated peptides were mixed with the appropriate liposome solution and the solvent was removed under a stream of air. For content mixing experiments, PBS buffer containing 20 mM sulforhodamine B was added to the dried lipid/peptide mixtures containing lipopeptide E. These solutions were subsequently sonicated for 5-10 minutes at 55 °C to yield 100 nm diameter liposomes[29]. The solutions were used without further purification, except

for the sulforhodamine B containing liposomes, which were purified using a Sephadex column to remove any non-encapsulated sulforhodamine B.

**Fluorescence spectroscopy.** Lipid- and content-mixing experiments were performed on a TECAN Infinite M1000 PRO fluorimeter using a 96-well plate at 25 °C. The percentage of fluorescence increase *%F* was calculated as:

$$\%F = \frac{F(t) - F_0}{F_{max} - F_0} * 100$$

**Content mixing experiments:** Sulphorhodamine B fluorescence intensity *F(t)* at 580 nm was monitored in a continuous fashion for 30 min after mixing non-fluorescent K-liposomes with sulphorhodamine B loaded E-liposomes. $F_0$ was obtained by measuring emission of sulphorhodamine B-loaded E-liposomes to which an equal amount of PBS was added, and $F_{max}$ was obtained by measuring the emission of plain liposomes loaded with 10 mM sulphorhodamine B. [Total lipid] = 0.1 mM, in PBS pH 7.4.

**Multiple round content mixing experiments:** Experimental settings of regular content mixing experiments were used as described above. E decorated, dye loaded, liposomes were prepared with a total lipid concentration of 0.05 mM, in PBS. K decorated liposomes were prepared with a total lipid concentration of 0.5 mM, in PBS. Total experimental mixtures for equimolar fusion experiments contained 100 uL E liposomes, 10 uL K liposomes and 90 uL PBS. Total experimental mixtures for fusion experiments at 10:1 ratio contained 100 uL E liposomes and 100 uL K liposomes.

**Data visualization:** 2D contour graphs were constructed in Origin 9.1, and subjected to a 100pnt smoothing algorithm. Major and minor levels were set at 10% and 1% fluorescence increase respectively. As color scheme, the multicolored and intuitive gradient 'Rainbow' was chosen.

**Dynamic Light Scattering.** Particle size distributions were measured by dynamic light scattering using a Malvern Zetasizer Nano ZS ZEN3500 equipped with a peltier thermostatic cell holder. The laser wavelength was 633 nm and the scattering angle was 173°. The Stokes Einstein relationship

$$D = \frac{k_B T}{3\pi\eta D_h}$$

was used to estimate the hydrodynamic diameter $D_h$. Here, $k_B$ is the Boltzmann constant, $\eta$ is the solvent viscosity, and $T$ was set to 25 °C.

**Circular dichroism spectroscopy.** CD spectra were obtained using a Jasco J-815 spectropolarimeter equipped with a peltier temperature controller. The ellipticity, given as mean residue molar ellipticity, [θ] (deg cm$^2$ dmol$^{-1}$), is calculated using the following equation:

$$[\theta] = \frac{100 * \theta_{obs}}{nlc}$$

where $\theta_{obs}$is the observed ellipticity (mdeg), $n$ is the number of peptide residues, $l$ is the path length of the cuvette (cm) and $c$ is the peptide concentration (mM). Spectra were recorded from 260 nm to 200 nm at 20 °C. Data points were collected with a 1 nm bandwidth at 1 nm intervals, using a scan speed of 1 nm s$^{-1}$. Each spectrum was an average of 5 scans. For analysis, each spectrum had the background spectrum (plain liposomes in PBS) subtracted. Percentage α-helicity was calculated using the predicted value $[\theta]_{222}$=-40000*(1-4.6/n) as 100% value for an α-helical peptide of $n$ residues.[58] [Total lipid] = 0.5 mM, with 1 mol% lipopeptide, in PBS pH 7.4.

## LIPOSOMAL CALCULATIONS

To visualize the peptide density at the surface of a liposome, we calculated the amount of lipid molecules and peptides (N) in an ideal liposome with the following formula[61]:

$$N = 4\pi \frac{r^2 + (r - d_m)^2}{A_{Lipid}}$$

where r = liposomal radius, $d_m$ = membrane thickness and A = surface area of respective lipid headgroups.[62] When $A_{lipid} = \frac{2A_{DOPC}+A_{DOPE}+A_{Chol}}{4} = \frac{2*0.67+0.75+0.34}{4}$ = 0.61 nm$^2$, r = 50 nm, and $d_m$ = 4.6 nm, N is approximately 94400. The number of peptides (1% M/M) exposed at the outer surface of the liposomes is approximately 520 upon assumption of equal preference for inner and outer membrane, with a surface area per peptide of 61 nm$^2$ (square of 7.8nm). At [total lipid] = 0.1 mM, the liposomal concentration is calculated to be 7.5*10$^8$ liposomes uL$^{-1}$.

## LIPOPEPTIDE ANALYSIS

Purity was confirmed using LC-MS analysis equipped with Gemini 3μ C18 column coupled with Finningan LCQ advantage max (Thermo) ESI-MS analyzer and the results are summarized in Table S1. LCMS eluents were A) H2O + 0.1% v/v TFA, B) MeCN + 0.1 v/v TFA, with a flow rate of 1 mL $min^{-1}$. Gradient was applied between 2 and 12 min, from 10% B in A to 90% B in A. Retention time RT is rounded to 2 significant numbers.

**Table S1. Characteristics of synthesized lipopeptides.**

| Peptide | formula | Calc. mass | Found mass | RT (min) |
|---|---|---|---|---|
| $CP_0E$ | $C_{144}H_{236}N_{26}O_{40}$ | 2971.57 | 2972.14, $[M+H]^+$ | 9.0 |
| $CP_0K$ | $C_{149}H_{252}N_{30}O_{33}$ | 2991.78 | 2992.60, $[M+H]^+$ | 7.7 |
| $CP_4E$ | $C_{154}H_{255}N_{27}O_{45}$ | 3204.83 | 3206.63, $[M+H]^+$ | 8.3 |
| $CP_4K$ | $C_{159}H_{271}N_{31}O_{38}$ | 3225.04 | 1611.48, $[M+2H]^{+2}$ | 6.7 |
| $CP_8E$ | $C_{163}H_{273}N_{27}O_{49}$ | 3395.06 | 1696.40, $[M+2H]^{+2}$ | 8.4 |
| $CP_8K$ | $C_{168}H_{289}N_{31}O_{42}$ | 3415.28 | 1706.40, $[M+2H]^{+2}$ | 6.8 |
| $CP_{12}E$ | $C_{171}H_{289}N_{27}O_{53}$ | 3571.27 | 1190.53, $[M+3H]^{+3}$ | 8.5 |
| $CP_{12}K$ | $C_{176}H_{305}N_{31}O_{46}$ | 3591.49 | 1197.07, $[M+3H]^{+3}$ | 7.3 |
| $CP_{16}E$ | $C_{179}H_{305}N_{27}O_{57}$ | 3747.48 | 1249.27, $[M+3H]^{+3}$ | 8.5 |
| $CP_{16}K$ | $C_{184}H_{321}N_{31}O_{50}$ | 3767.70 | 1255.93, $[M+3H]^{+3}$ | 7.4 |
| $LP_0E$ | $C_{147}H_{256}N_{26}O_{43}P^-$ | 3106.78 | 1563.44, $[M+H+NH_4]^{+2}$ | 12 |
| $LP_0K$ | $C_{150}H_{271}N_{29}O_{37}P^-$ | 3103.96 | 1553.01, $[M+2H]^{+2}$ | 10 |
| $LP_2E$ | $C_{153}H_{267}N_{27}O_{46}P^-$ | 3251.94 | 1084.98, $[M+3H]^{+3}$ | 12 |
| $LP_2K$ | $C_{156}H_{282}N_{30}O_{40}P^-$ | 3249.12 | 1084.03, $[M+3H]^{+3}$ | 10 |
| $LP_4E$ | $C_{157}H_{275}N_{27}O_{48}P^-$ | 3340.04 | 1114.33, $[M+3H]^{+3}$ | 12 |
| $LP_4K$ | $C_{160}H_{290}N_{30}O_{42}P^-$ | 3337.22 | 1113.72, $[M+3H]^{+3}$ | 10 |
| $LP_8E$ | $C_{166}H_{293}N_{27}O_{52}P^-$ | 3530.28 | 1178.04, $[M+3H]^{+3}$ | 12 |
| $LP_8K$ | $C_{169}H_{308}N_{30}O_{46}P^-$ | 3527.46 | 1177.09, $[M+3H]^{+3}$ | 10 |
| $LP_{12}E$ | $C_{174}H_{309}N_{27}O_{56}P^-$ | 3706.49 | 1236.74, $[M+3H]^{+3}$ | 12 |
| $LP_{12}K$ | $C_{177}H_{324}N_{30}O_{50}P^-$ | 3703.67 | 1235.79, $[M+3H]^{+3}$ | 10 |

## CD SPECTROSCOPY

Characteristics ($\theta_{222}/\theta_{208}$ and percentage helicity at $\theta_{222}$) of the spectra as summarized in Table 2, are supported with the recorded spectra between 207nm and 250 nm (*Figure S1*). Below 207nm, spectra were too noisy due to scattering of the signal by liposomes.

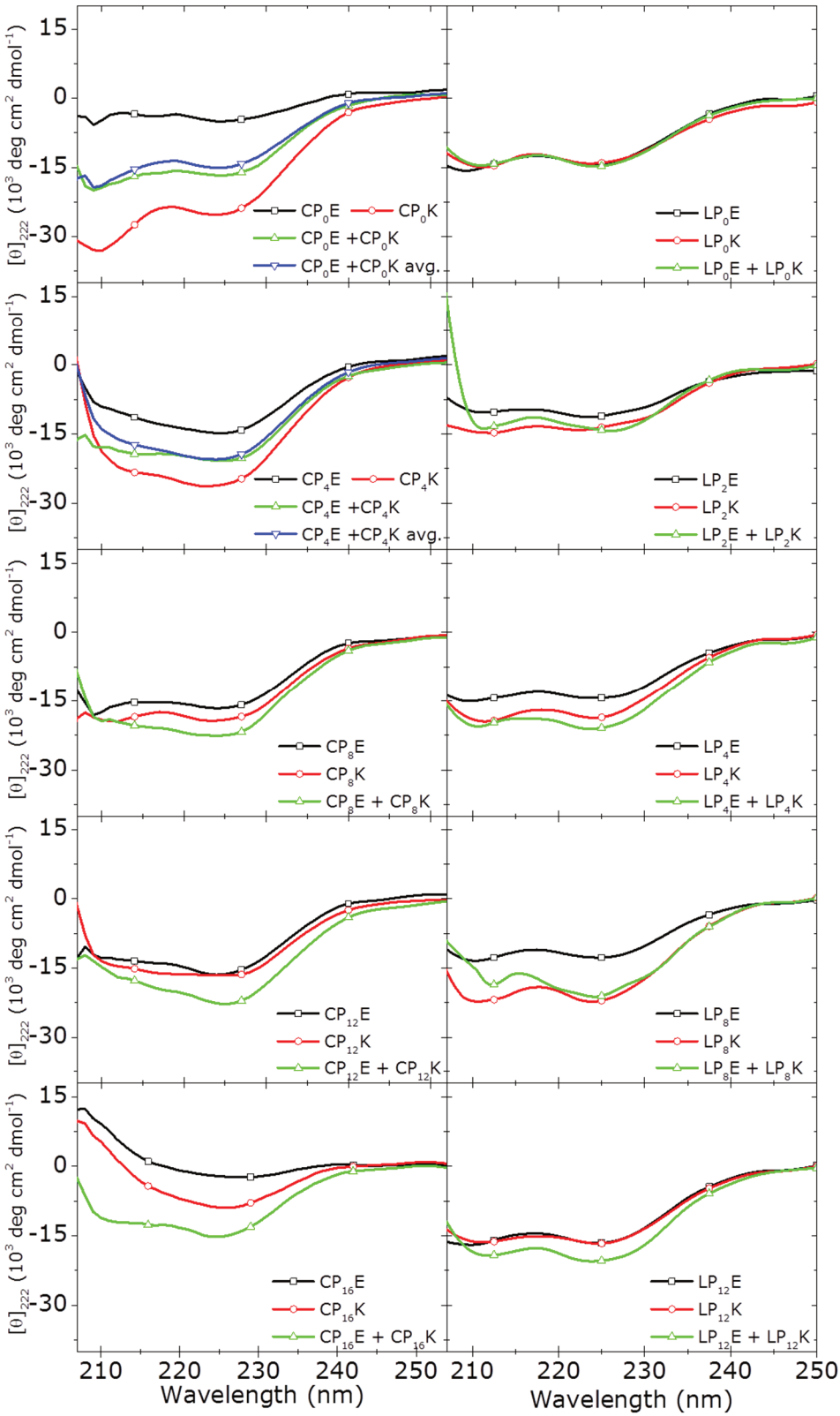


**Figure S1.** *Peptide secondary structure of E (black) and K (red)- decorated liposomes before and after mixing (green), measured by Circular Dichroism. Left series is with cholesterol anchor, right series contain a DOPE anchor. Only symmetric pairs (m = n) are used in this study. With $CP_0$ and $CP_4$ anchor coiled-coil formation is not evident, so the calculated average of the individual E and K spectra is added (blue). [Total lipid] = 0.5 mM with 1mol% lipopeptide, PBS pH 7.4.*

## FULL DATA OF 30MIN CONTENT MIXING ASSAY

Content mixing experiments were followed for 30 minutes, error bars and absolute values after 4 and 30 minutes were obtained by at least 3 individual experiments and are shown in Figure S2. Fluorescence increase was measured as a function of *m, n.* in a continuous fashion and showed characteristic 1st order kinetics in the initial minutes (*Figure S3*). Therefore, fluorescence increase after 4 minutes is used to estimate the relationship of $L_{PEG}$ and the fusion efficiency. In negative control experiments, peptide bearing liposomes (m, n = 4 or 8) were mixed with plain liposomes and the fluorescence increase was recorded for 30 minutes. Left out peptides *E* or *K*, *(X)*, are denoted with *X, n* or *m, X*.

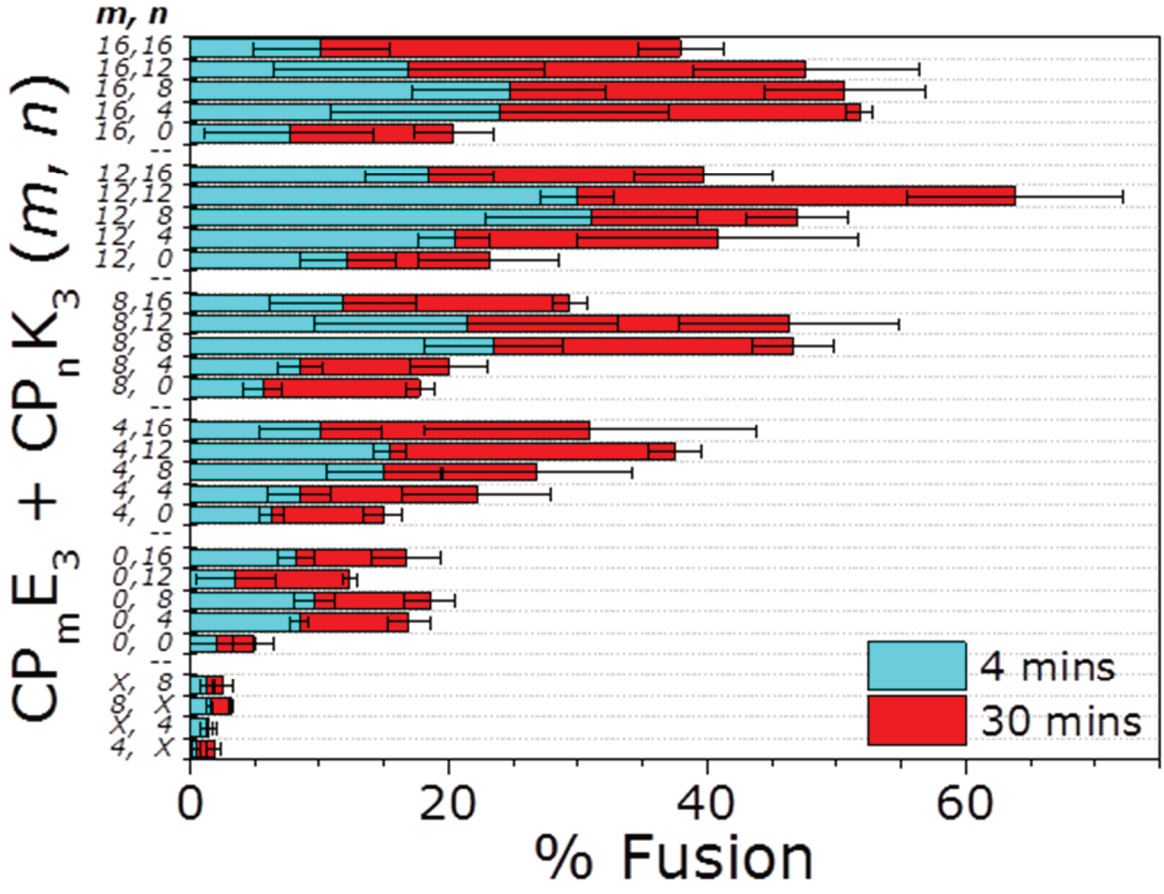


**Figure S2.** *Time resolved rate of fusion (Content mixing) with lipopeptide CPmE or CPnK decorated liposomes as a function of m, n, indicated by an increase in sulforhodamine B emission after 4 and 30minutes. Left out peptides E or K, (X), in negative control experiments are denoted with X, n or m, X. [Total lipid] = 0.1 mM with 1 mol% lipopeptide, in PBS pH 7.4.*

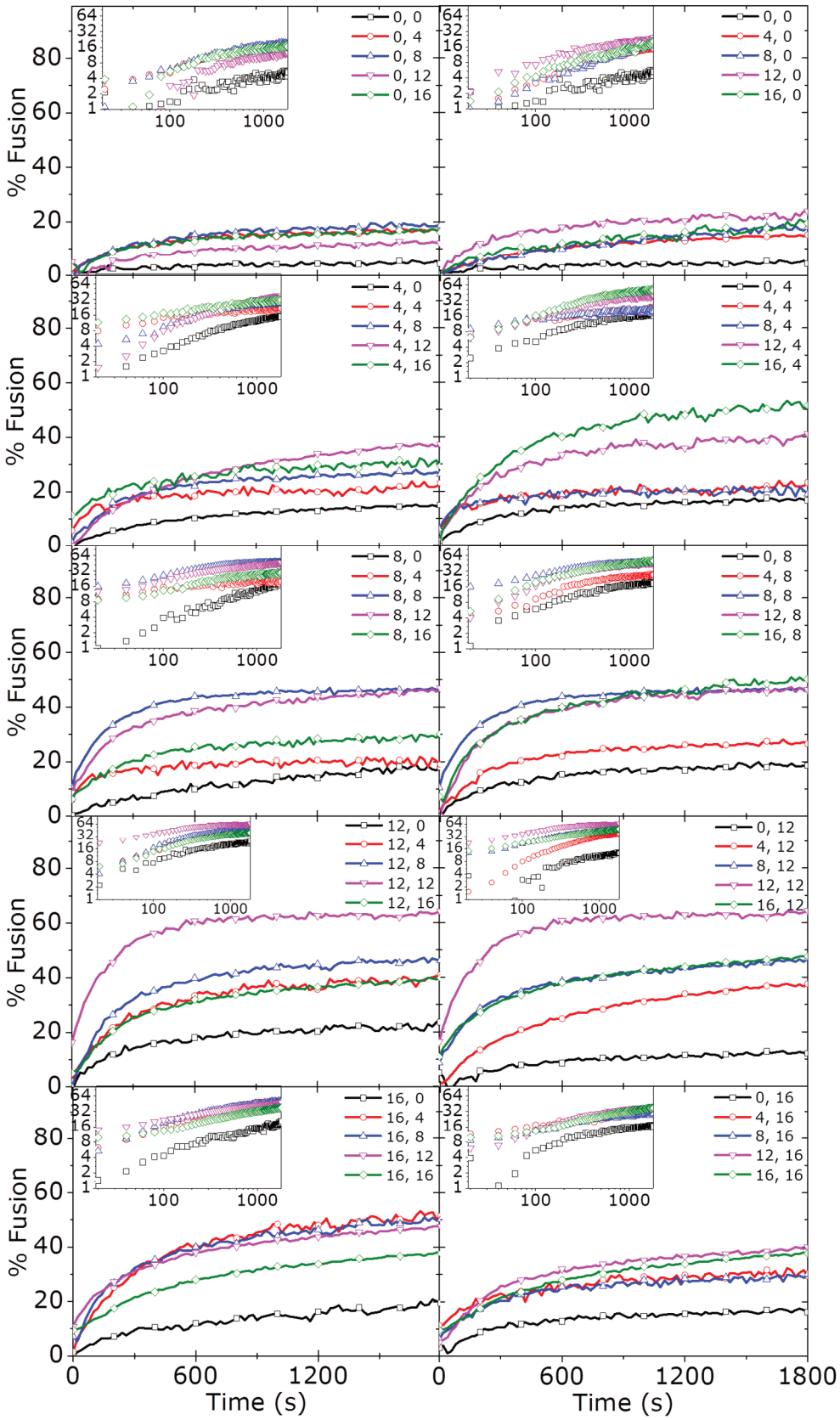


**Figure S3.** *Content mixing of $CP_mE$ and $CP_nK$ decorated liposomes as a function of m, n. Insets with log scale illustrate 1st order kinetics until at least the 4th minute. [Total lipid] = 0.1 mM with 1 mol% lipopeptide, PBS pH 7.4.*

## INFLUENCE OF CPE / CPK RATIO ON FUSION EFFICIENCY

A change in peptide functionalization ratio revealed the influence of peptide equilibria on the fusion process. Again, results are shown as a function of *m, n*. (*Figure S4*)

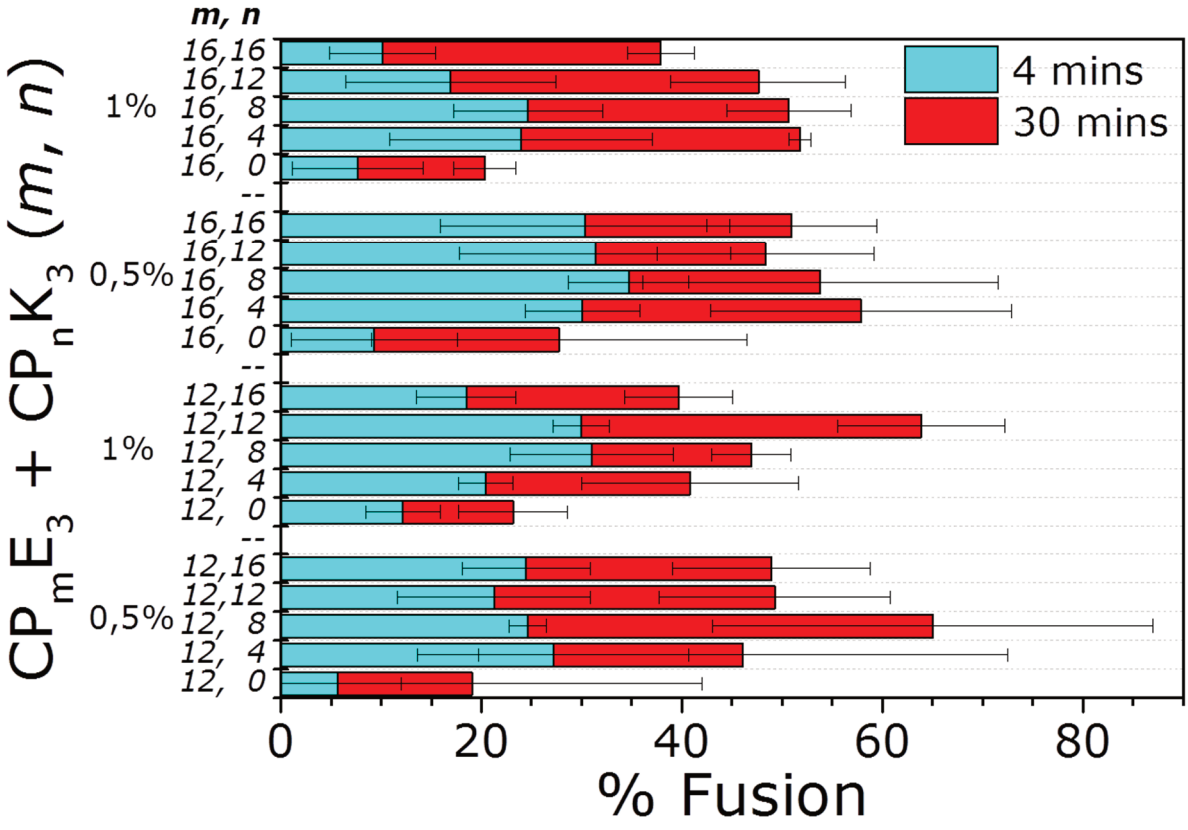


**Figure S4.** *Time resolved rate of fusion (Content mixing) with peptide $CP_mE$ and $CP_nK$ decorated liposomes as a function of m,n, and [$CP_mE$], as indicated by an increase in sulforhodamine B emission after 4 and 30 minutes. [Total lipid] = 0.1 mM with 1 mol% $CP_nK$ and 1 mol% or 0.5 mol% $CP_mE$, PBS pH 7.4.*

## REFERENCES


1. Hu, C.; Ahmed, M.; Melia, T. J.; Sollner, T. H.; Mayer, T.; Rothman, J. E., Fusion of cells by flipped SNAREs. *Science* **2003,** *300* (5626), 1745-1749.
2. Maximov, A.; Tang, J.; Yang, X. F.; Pang, Z. P. P.; Sudhof, T. C., Complexin Controls the Force Transfer from SNARE Complexes to Membranes in Fusion. *Science* **2009,** *323* (5913), 516-521.
3. Sudhof, T. C.; Rothman, J. E., Membrane Fusion: Grappling with SNARE and SM Proteins. *Science* **2009,** *323* (5913), 474-477.
4. Jahn, R.; Lang, T.; Sudhof, T. C., Membrane fusion. *Cell* **2003,** *112* (4), 519-533.
5. Chernomordik, L. V.; Kozlov, M. M., Mechanics of membrane fusion. *Nat. Struct. Mol. Biol.* **2008,** *15* (7), 675-683.
6. Weber, T.; Zemelman, B. V.; McNew, J. A.; Westermann, B.; Gmachl, M.; Parlati, F.; Sollner, T. H.; Rothman, J. E., SNAREpins: Minimal machinery for membrane fusion. *Cell* **1998,** *92* (6), 759-772.
7. Chen, Y. A.; Scales, S. J.; Scheller, R. H., Sequential SNARE assembly underlies priming and triggering of exocytosis. *Neuron* **2001,** *30* (1), 161-170.
8. Rizo, J.; Sudhof, T. C., Snares and Munc18 in synaptic vesicle fusion. *Nat. Rev. Neurosci.* **2002,** *3* (8), 641-653.
9. Jena, B. P., Role of SNAREs in membrane fusion. *Adv. Exp. Med. Biol.* **2011,** *713*, 13-32.
10. Han, J.; Pluhackova, K.; Bockmann, R. A., The Multifaceted Role of SNARE Proteins in Membrane Fusion. *Front. Membr. Physiol. Membr. Biophys.* **2017,** *8*, 5.
11. Stengel, G.; Simonsson, L.; Campbell, R. A.; Hook, F., Determinants for membrane fusion induced by cholesterol-modified DNA zippers. *J. Phys. Chem. B* **2008,** *112* (28), 8264-8274.
12. Chan, Y. H.; van Lengerich, B.; Boxer, S. G., Effects of linker sequences on vesicle fusion mediated by lipid-anchored DNA oligonucleotides. *Proc. Natl. Acad. Sci. U. S. A.* **2009,** *106* (4), 979-984.
13. Jakobsen, U.; Vogel, S., DNA-Controlled Assembly of Liposomes in Diagnostics. *Methods Enzymol.* **2009,** *464*, 233-248.
14. Ries, O.; Loffler, P. M. G.; Vogel, S., Convenient synthesis and application of versatile nucleic acid lipid membrane anchors in the assembly and fusion of liposomes. *Org. Biomol. Chem.* **2015,** *13* (37), 9673-9680.
15. Herrmann, A.; Meng, Z.; Yang, J.; Liu, Q.; de Vries, J. W.; Gruszka, A.; Rodriguez-Pulido, A.; Crielaard, B.; Kros, A., Efficient Fusion of Liposomes by Nucleobase Quadruple-Anchored DNA. *Chem. - Eur. J.* **2017**, DOI: 10.1002/chem.201701379.
16. Lygina, A. S.; Meyenberg, K.; Jahn, R.; Diederichsen, U., Transmembrane Domain Peptide/Peptide Nucleic Acid Hybrid as a Model of a SNARE Protein in Vesicle Fusion. *Angew. Chem., Int. Ed.* **2011,** *50* (37), 8597-8601.
17. Kashiwada, A.; Matsuda, K.; Mizuno, T.; Tanaka, T., Construction of a pH-responsive artificial membrane fusion system by using designed coiled-coil polypeptides. *Chem. - Eur. J.* **2008,** *14* (24), 7343-7350.
18. Meyenberg, K.; Lygina, A. S.; van den Bogaart, G.; Jahn, R.; Diederichsen, U., SNARE derived peptide mimic inducing membrane fusion. *Chem. Commun. (Cambridge, U. K.)* **2011,** *47* (33), 9405-9407.
19. Rauschenberg, M.; Bomke, S.; Karst, U.; Ravoo, B. J., Dynamic Peptides as Biomimetic Carbohydrate Receptors. *Angew. Chem., Int. Ed.* **2010,** *49* (40), 7340-7345.
20. Richard, A.; Marchi-Artzner, V.; Lalloz, M. N.; Brienne, M. J.; Artzner, F.; Gulik-Krzywicki, T.; Guedeau-Boudeville, M. A.; Lehn, J. M., Fusogenic supramolecular vesicle systems induced by metal ion binding to amphiphilic ligands. *Proc. Natl. Acad. Sci. U. S. A.* **2004,** *101* (43), 15279-15284.

21. Gong, Y.; Luo, Y.; Bong, D., Membrane activation: selective vesicle fusion via small molecule recognition. *J. Am. Chem. Soc.* **2006,** *128* (45), 14430-14431.
22. Kashiwada, A.; Tsuboi, M.; Takamura, N.; Brandenburg, E.; Matsuda, K.; Koksch, B., Design and Characterization of Endosomal-pH-Responsive Coiled Coils for Constructing an Artificial Membrane Fusion System. *Chem. - Eur. J.* **2011,** *17* (22), 6179-6186.
23. Marchi-Artzner, V.; Gulik-Krzywicki, T.; Guedeau-Boudeville, M. A.; Gosse, C.; Sanderson, J. M.; Dedieu, J. C.; Lehn, J. M., Selective adhesion, lipid exchange and membrane-fusion processes between vesicles of various sizes bearing complementary molecular recognition groups. *ChemPhysChem* **2001,** *2* (6), 367-376.
24. Ma, M. M.; Bong, D., Controlled Fusion of Synthetic Lipid Membrane Vesicles. *Acc. Chem. Res.* **2013,** *46* (12), 2988-2997.
25. Voskuhl, J.; Ravoo, B. J., Molecular recognition of bilayer vesicles. *Chem. Soc. Rev.* **2009,** *38* (2), 495-505.
26. Voskuhl, J.; Fenske, T.; Stuart, M. C.; Wibbeling, B.; Schmuck, C.; Ravoo, B. J., Molecular recognition of vesicles: host-guest interactions combined with specific dimerization of zwitterions. *Chemistry* **2010,** *16* (28), 8300-8306.
27. Nalluri, S. K. M.; Ravoo, B. J., Light-Responsive Molecular Recognition and Adhesion of Vesicles. *Angew. Chem., Int. Edit.* **2010,** *49* (31), 5371-5374.
28. Nalluri, S. K. M.; Bultema, J. B.; Boekema, E. J.; Ravoo, B. J., Photoresponsive Molecular Recognition and Adhesion of Vesicles in a Competitive Ternary Supramolecular System. *Chem. - Eur. J.* **2011,** *17* (37), 10297-10303.
29. Marsden, H. R.; Elbers, N. A.; Bomans, P. H. H.; Sommerdijk, N.; Kros, A., A Reduced SNARE Model for Membrane Fusion. *Angew. Chem., Int. Ed.* **2009,** *48* (13), 2330-2333.
30. Marsden, H. R.; Korobko, A. V.; Zheng, T. T.; Voskuhl, J.; Kros, A., Controlled liposome fusion mediated by SNARE protein mimics. *Biomater. Sci.* **2013,** *1* (10), 1046-1054.
31. Versluis, F.; Voskuhl, J.; van Kolck, B.; Zope, H.; Bremmer, M.; Albregtse, T.; Kros, A., In situ modification of plain liposomes with lipidated coiled coil forming peptides induces membrane fusion. *J. Am. Chem. Soc.* **2013,** *135* (21), 8057-8062.
32. Zheng, T.; Voskuhl, J.; Versluis, F.; Zope, H. R.; Tomatsu, I.; Marsden, H. R.; Kros, A., Controlling the rate of coiled coil driven membrane fusion. *Chem. Commun. (Cambridge, U. K.)* **2013,** *49* (35), 3649-3651.
33. Versluis, F.; Dominguez, J.; Voskuhl, J.; Kros, A., Coiled-coil driven membrane fusion: zipper-like vs. non-zipper-like peptide orientation. *Faraday Discuss.* **2013,** *166*, 349-359.
34. Zheng, T. T.; Bulacu, M.; Daudey, G.; Versluis, F.; Voskuhl, J.; Martelli, G.; Raap, J.; Sevink, G. J. A.; Kros, A.; Boyle, A. L., A non-zipper-like tetrameric coiled coil promotes membrane fusion. *Rsc Advances* **2016,** *6* (10), 7990-7998.
35. Rabe, M.; Aisenbrey, C.; Pluhackova, K.; de Wert, V.; Boyle, A. L.; Bruggeman, D. F.; Kirsch, S. A.; Bockmann, R. A.; Kros, A.; Raap, J.; Bechinger, B., A Coiled-Coil Peptide Shaping Lipid Bilayers upon Fusion. *Biophys. J.* **2016,** *111* (10), 2162-2175.
36. Strandberg, E.; Killian, J. A., Snorkeling of lysine side chains in transmembrane helices: how easy can it get? *FEBS Lett.* **2003,** *544* (1-3), 69-73.
37. McNew, J. A.; Weber, T.; Engelman, D. M.; Sollner, T. H.; Rothman, J. E., The length of the flexible SNAREpin juxtamembrane region is a critical determinant of SNARE-dependent fusion. *Mol. Cell* **1999,** *4* (3), 415-421.
38. Rabe, M.; Schwieger, C.; Zope, H. R.; Versluis, F.; Kros, A., Membrane Interactions of Fusogenic Coiled-Coil Peptides: Implications for Lipopeptide Mediated Vesicle Fusion. *Langmuir* **2014,** *30* (26), 7724-7735.

39. Hanwell, M. D.; Curtis, D. E.; Lonie, D. C.; Vandermeersch, T.; Zurek, E.; Hutchison, G. R., Avogadro: an advanced semantic chemical editor, visualization, and analysis platform. *J. Cheminf.* **2012,** *4*.
40. Kessel, A.; Ben-Tal, N.; May, S., Interactions of cholesterol with lipid bilayers: the preferred configuration and fluctuations. *Biophys. J.* **2001,** *81* (2), 643-658.
41. Zwang, T. J.; Fletcher, W. R.; Lane, T. J.; Johal, M. S., Quantification of the layer of hydration of a supported lipid bilayer. *Langmuir* **2010,** *26* (7), 4598-4601.
42. Tu, K.; Klein, M. L.; Tobias, D. J., Constant-pressure molecular dynamics investigation of cholesterol effects in a dipalmitoylphosphatidylcholine bilayer. *Biophys. J.* **1998,** *75* (5), 2147-2156.
43. Rabe, M.; Zope, H. R.; Kros, A., Interplay between Lipid Interaction and Homo-coiling of Membrane-Tethered Coiled-Coil Peptides. *Langmuir* **2015,** *31* (36), 9953-9964.
44. Sun, Q.; Cai, S.; Peterson, B. R., Practical Synthesis of 3 beta-Amino-5-cholestene and Related 3 beta-Halides Involving i-Steroid and Retro-i-Steroid Rearrangements. *Org. Lett.* **2009,** *11* (3), 567-570.
45. Yang, J.; Bahreman, A.; Daudey, G.; Bussmann, J.; Olsthoorn, R. C.; Kros, A., Drug Delivery via Cell Membrane Fusion Using Lipopeptide Modified Liposomes. *ACS Cent. Sci.* **2016,** *2* (9), 621-630.
46. Kyoung, M.; Srivastava, A.; Zhang, Y. X.; Diao, J. J.; Vrljic, M.; Grob, P.; Nogales, E.; Chu, S.; Brunger, A. T., In vitro system capable of differentiating fast Ca2+-triggered content mixing from lipid exchange for mechanistic studies of neurotransmitter release. *Proc. Natl. Acad. Sci. U. S. A.* **2011,** *108* (29), E304-E313.
47. Diao, J.; Grob, P.; Cipriano, D. J.; Kyoung, M.; Zhang, Y.; Shah, S.; Nguyen, A.; Padolina, M.; Srivastava, A.; Vrljic, M.; Shah, A.; Nogales, E.; Chu, S.; Brunger, A. T., Synaptic proteins promote calcium-triggered fast transition from point contact to full fusion. *Elife* **2012,** *1*, e00109.
48. Kyoung, M.; Zhang, Y.; Diao, J.; Chu, S.; Brunger, A. T., Studying calcium-triggered vesicle fusion in a single vesicle-vesicle content and lipid-mixing system. *Nat. Protoc.* **2013,** *8* (1), 1-16.
49. Lai, Y.; Zhao, L.; Bu, B.; Lou, X.; Li, D.; Ji, B.; Liu, J.; Diao, J.; Shin, Y. K., Lipid molecules influence early stages of yeast SNARE-mediated membrane fusion. *Phys. Biol.* **2015,** *12* (2), 025003.
50. Stratton, B. S.; Warner, J. M.; Wu, Z. Y.; Nikolaus, J.; Wei, G.; Wagnon, E.; Baddeley, D.; Karatekin, E.; O'Shaughnessy, B., Cholesterol Increases the Openness of SNARE-Mediated Flickering Fusion Pores. *Biophys. J.* **2016,** *110* (7), 1538-1550.
51. Yang, S. T.; Kreutzberger, A. J. B.; Lee, J.; Kiessling, V.; Tamm, L. K., The role of cholesterol in membrane fusion. *Chem. Phys. Lipids* **2016,** *199*, 136-143.
52. Abe, K.; Higashi, K.; Watabe, K.; Kobayashi, A.; Limwikrant, W.; Yamamoto, K.; Moribe, K., Effects of the PEG molecular weight of a PEG-lipid and cholesterol on PEG chain flexibility on liposome surfaces. *Colloids Surf., A* **2015,** *474*, 63-70.
53. Kusumoto, K.; Akita, H.; El-Sayed, A.; Harashima, H., Effect of the Anchor in Polyethylene Glycol-Lipids on the Transfection Activity of PEGylated Cationic Liposomes Encapsulating DNA. *Biol. Pharm. Bull.* **2012,** *35* (4), 445-448.
54. Pluhackova, K.; Wassenaar, T. A.; Kirsch, S.; Bockmann, R. A., Spontaneous Adsorption of Coiled-Coil Model Peptides K and E to a Mixed Lipid Bilayer. *J. Phys. Chem. B* **2015,** *119* (12), 4396-4408.
55. Woo, S. Y.; Lee, H., All-atom simulations and free-energy calculations of coiled-coil peptides with lipid bilayers: binding strength, structural transition, and effect on lipid dynamics. *Sci. Rep.* **2016,** *6*, 22299.

56. Garcia, R. A.; Pantazatos, S. P.; Pantazatos, D. P.; MacDonald, R. C., Cholesterol stabilizes hemifused phospholipid bilayer vesicles. *Biochim. Biophys. Acta, Biomembr.* **2001,** *1511* (2), 264-270.
57. Klok, H. A.; Vandermeulen, G. W.; Nuhn, H.; Rosler, A.; Hamley, I. W.; Castelletto, V.; Xu, H.; Sheiko, S. S., Peptide mediated formation of hierarchically organized solution and solid state polymer nanostructures. *Faraday Discuss.* **2005,** *128*, 29-41.
58. Chen, Y. H.; Yang, J. T.; Chau, K. H., Determination of the helix and beta form of proteins in aqueous solution by circular dichroism. *Biochemistry* **1974,** *13* (16), 3350-3359.
59. Cubberley, M. S.; Iverson, B. L., (1)H NMR investigation of solvent effects in aromatic stacking interactions. *J. Am. Chem. Soc.* **2001,** *123* (31), 7560-7563.
60. Shirude, P. S.; Kumar, V. A.; Ganesh, K. N., BisPNA targeting to DNA: Effect of neutral loop on DNA duplex strand invasion by aepPNA-N7G/aepPNA-C substituted peptide nucleic acids. *Eur. J. Org. Chem.* **2005,** (24), 5207-5215.
61. Sardan, M.; Kilinc, M.; Genc, R.; Tekinay, A. B.; Guler, M. O., Cell penetrating peptide amphiphile integrated liposomal systems for enhanced delivery of anticancer drugs to tumor cells. *Faraday Discuss* **2013,** *166*, 269-83.
62. Chen, Z.; Rand, R. P., The influence of cholesterol on phospholipid membrane curvature and bending elasticity. *Biophys. J.* **1997,** *73* (1), 267-76.

# CHAPTER III

## INFLUENCE OF MEMBRANE-FUSOGEN DISTANCE ON THE SECONDARY STRUCTURE OF COILED-COIL PEPTIDES

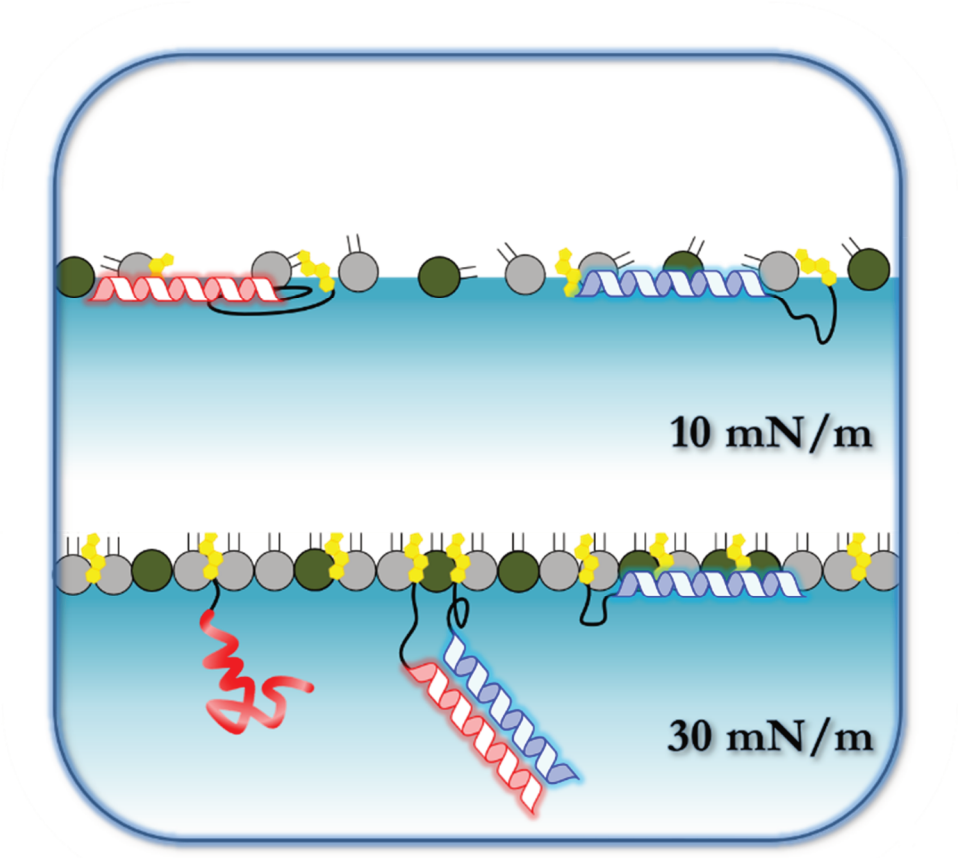

## ABSTRACT

Liposomal membrane fusion is an important tool to study complex biological fusion mechanisms. We use lipidated derivatives of the specific heterodimeric coiled-coil pair E: $(EIAALEK)_3$ and K: $(KIAALKE)_3$ to study and control the fusion of liposomes. In this model system peptides are tethered to their liposomes via a poly(ethylene glycol) (PEG) spacer and a lipid anchor. The efficiency of the fusion mechanism and function of the peptides is highly affected by the PEG-spacer length and the lipid anchor type. Here, the influence of membrane-fusogen distance on the peptide-membrane interactions and the peptide secondary structures is studied with Langmuir film balance and infrared reflection absorption spectroscopy (IRRAS). We found that the introduction of a spacer to monolayer tethered peptide E changes its conformation from solvated random coils to homo-oligomers. In contrast, the described peptide-monolayer interaction of peptide K is not affected by the PEG-spacer length. Furthermore, the co-existence of different conformations when both CPE and CPK are present at the membrane surface is demonstrated empirically, which has many implications for the design of effective fusogenic recognition units and the field of artificial membrane fusion.

# INTRODUCTION

Natural membrane fusion is a key process for cellular logistics and signaling. Thus, it has been extensively studied for decades. Whilst the overall process of membrane fusion is well understood,[1] mechanisms at the molecular level still are a matter of debate due to the intrinsic complexity of biological systems. To promote the understanding of the naturally occurring fusion machinery[2-3] and to identify important parameters in such mechanisms, a variety of functional mimics were developed recently.[4-8] In our group, we employed the lipidated heterodimeric coiled-coil pair E $(EIAALEK)_3$ and K $(KIAALKE)_3$ as a molecular recognition motif and fusogen. The peptides are held in lipid membranes by a lipid anchor, either cholesterol (*C*) or 1,2-dioleoyl-*sn*-glycero-3-phosphoethanol-amine (DOPE), (*L*) and this is conjugated to the peptide via a PEG-spacer of variable length *n* to yield C/L$P_n$E and C/L$P_n$K. The ability of these lipopeptides to effectively mediate liposomal fusion both *in vitro* and *in vivo* has been shown in several papers.[9-13]

In these studies, coiled-coil formation between E and K was thought to initiate the fusion of the bilayers. However, it was demonstrated recently that peptide K can insert into the lipid membrane because of the amphipathic nature of its α-helix. Peptide K orients its helical axis parallel to the monolayer surface with the hydrophobic moment of the α-helix pointing towards the hydrophobic part of the monolayer. It is anticipated that K interacts with the negatively charged phosphate moieties of the phospholipids via 'snorkeling' its positively charged Lys residues towards the polar region of the bilayer. The membrane insertion of peptide K may locally disrupt the uniformity of the membrane in its proximity, promoting the formation of protrusions. It is hypothesized that such protrusions are a fundamental step in the merging of the opposing membranes in the fusion process.[14]

Until now, the peptide conformation of peptides E and K on membrane surfaces was studied using $LP_{12}$ functionalized derivatives, because significant fusion efficiency was obtained when liposomes were functionalized with these peptides. However, liposome fusion mediated by cholesterol anchored peptides $CP_{12}E$ / $CP_{12}K$, is twice as efficient compared to DOPE anchored derivatives,[15] which raised interest in the influence of the anchor on the peptide dynamics. Furthermore, it was found recently that the membrane-

fusogen distance as defined by PEG spacer length is crucial for efficient fusion, and highest fusion efficiency was obtained with $CP_{12}E$ and $CP_8K$.[16] Measuring the dependency of the $CP_nE$ and $CP_nK$ fusion efficiency on *n* revealed the distinct asymmetric roles of both peptides in the fusion process (*Figure 10*). Liposome tethered peptide E is thought to act as a handle to enable docking of peptide K decorated liposomes, with the effectivity of this handle being enhanced by elongated spacers. After docking, fusion process is dictated by peptide K via incorporation into both opposing liposomal membranes, which destabilizes both lipid membranes and promotes the formation of fusion intermediates.[14] The results suggested that equilibria between these multiple peptide interactions in the docking state are affected by anchor type and PEG-spacer length of the utilized lipopeptides. Furthermore, it is anticipated that the incorporation of $CP_nK$ in the opposing liposomal membrane is crucial for efficient fusion. It is hypothesized that this highly dynamic docking state is rate-limiting the fusion cascade.

Here we study the influence of the membrane-fusogen distance on the peptide structure and the peptide-membrane interaction. A systematic variation of $CP_nE$ and $CP_nK$ was used by varying the length of the PEG-spacer from 0 to 16 monomers in steps of 4 monomers.[16] The ability of the peptide to immerse into a lipid monolayer was measured by Langmuir film balance, while IRRA spectroscopy was used to determine the peptide orientation with respect to the monolayer, and the solvent exposure of the peptide bonds. The results found for $CP_{12}E/CP_{12}K$ are compared with the results reported for $LP_{12}E/LP_{12}K$ derivatives to assess the influence of the anchor on the peptide structure.

## DESIGN AND SYNTHESIS

For peptide detection and quantitation, peptide E was functionalized at the C-terminus with a glycine and a tyrosine residue, while peptide K was equipped with a C-terminal glycine and a tryptophan residue. A PEG series P*n* was used with 0, 4, 8, 12, and 16 units of ethylene glycol, and cholesterol was used as the anchor moiety.[12] The molecular structures and used peptide sequences are shown in Figure 10. Peptides were synthesized with automated solid phase peptide synthesis (SPPS) using Fmoc chemistry,

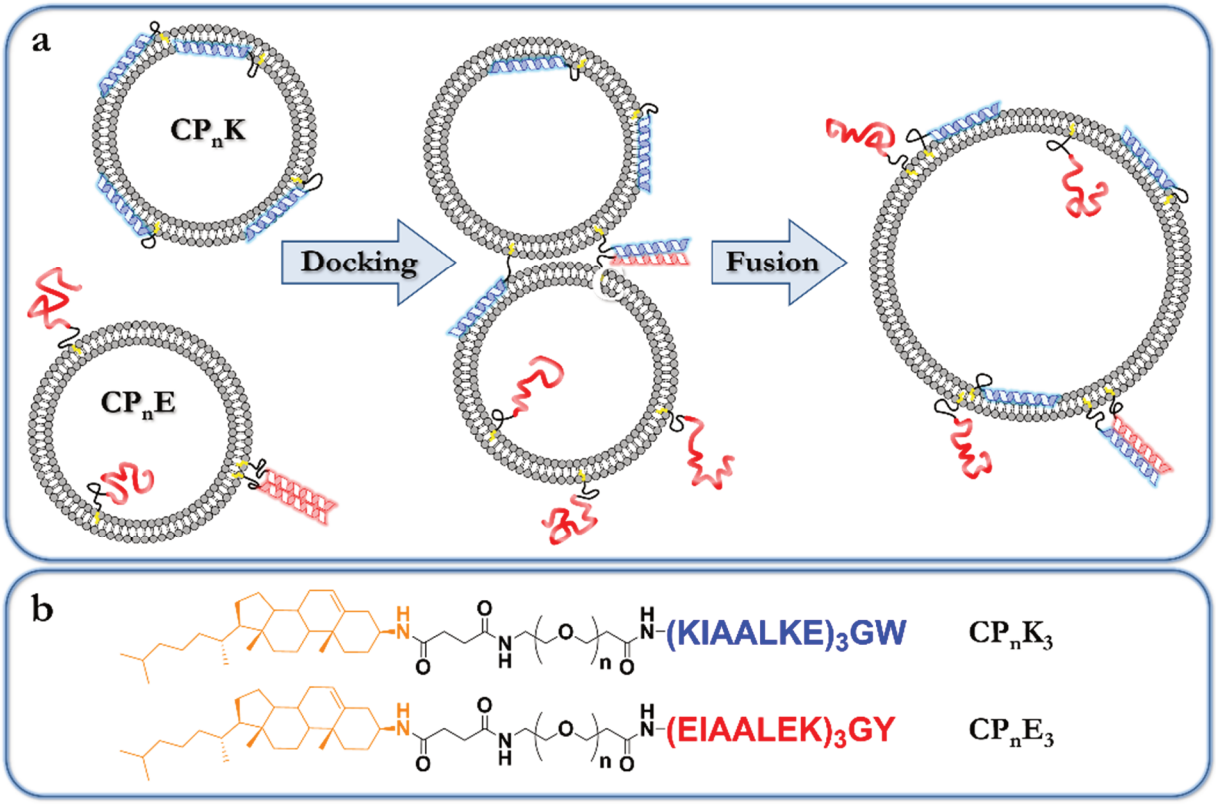


**Figure 10.** *Schematic representation of liposomal fusion process with fusogenic lipopeptides $CP_nK$ and $CP_nE$. a) Coiled-coil formation of complementary lipopeptides forces individual liposomes in close proximity and concomitant fusion. b) PEG-spacers were comprised of n repeating units of ethyleneglycol, with n = 0, 4, 8, 12, and 16. A succinic acid moiety was used to conjugate cholesterol-anchor and PEG-spacer.*

and after coupling of the final amino acid, the PEG component and the anchor moiety were coupled manually. The lipopeptides were cleaved from the resin and subsequently purified using reverse phase chromatography yielding purities >95%. Details of the synthetic procedures are described in Chapter II.[16]

## RESULTS AND DISCUSSION

### PEPTIDE-MEMBRANE INTERACTION BY LANGMUIR FILM BALANCE

The interactions of the various $CP_nE$ and $CP_nK$ derivatives with membranes were investigated by compression isotherms of lipid monolayers functionalized with peptides. (*Figure 11, Figure 12, Figure 13*) Monolayers with 4% lipopeptide were prepared on PBS pH 7.4 and the surface pressure ($\pi$) was measured as a function of molecular area ($A$) during compression and expansion of the monolayer. The $\pi$/A isotherm of the pure lipid mixture (DOPC : DOPE : Cholesterol (2 : 1 : 1)) showed no irregularities such as plateaus or break points, which is consistent with monolayers in a liquid expanded state

without phase transitions. With lipopeptides tethered to the monolayer, all π/A isotherms showed higher molecular areas at low pressures (0 – 15 mN/m) compared to the isotherm of the pure lipid film.

The absorption of peptides to lipid monolayers can be analyzed by calculation of lateral compressibility of the lipid film, $C_S = -1/A\ (\delta A/\delta\pi)_T$. The observed plateaus in π/A isotherms of $CP_nE$ are converted to peaks in $C_S/\pi$ isotherms. We interpret these plateaus or peaks to be caused by a squeeze-out of peptide material from the monolayer into the subphase, as was found previously with untethered peptides E and K.[17]

## MONOLAYERS FUNCTIONALIZED WITH $CP_NK$

Upon compression of $CP_nK$ functionalized monolayers a uniform surface pressure increase was observed until the membrane collapsed around ~35 mN/m. (*Figure 11*). The isotherms were shifted to higher molecular areas with respect to the pure lipid mixture, indicating the incorporation of K into the monolayer. Similar results were found for $LP_{12}K$ functionalized monolayers.[17]

These results showed that the anchor and various spacers did not inhibit the peptide-membrane interaction, regardless of their type and length. The compressibility of the lipopeptide decorated monolayers were found to be slightly increased compared to the pure monolayer. The increase in molecular area is similar for all spacer variants and no squeeze out was observed for any variant. Although, slightly higher values for A were observed for $CP_{16}K$ at low surface pressures, and slightly lower values for A were observed for $CP_0K$ above a surface pressure of 20 mN/m.

## MONOLAYERS FUNCTIONALIZED WITH $CP_NE$

Upon compression of $CP_nE$ functionalized monolayers, plateaus were observed at intermediate surface pressures (15-20 mN/m). Further compression above these plateaus led to isotherms comparable to those of the pure lipid film, as shown in Figure 12. The observed plateaus indicate the squeeze out of $CP_nE$ upon increasing surface pressure. The reversibility of the squeeze out of $CP_nE$ is demonstrated by the occurrence of plateaus at pressures around $\pi_{SO}$ during both stages of compression/expansion cycles. (*Figure S5*) ΔA calculation of the π/A graphs at 10 mN/m reveal that with increasing

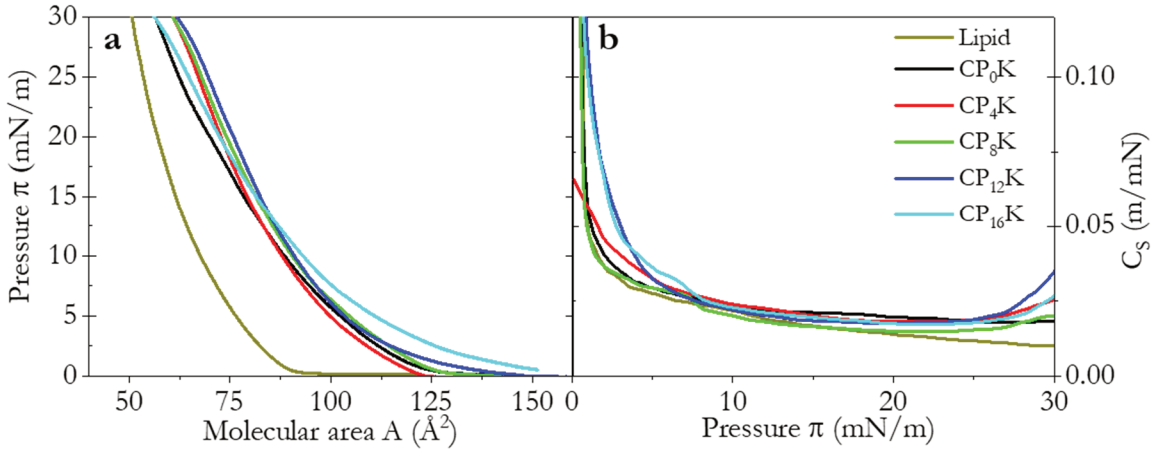


**Figure 11.** *Results of compression experiments with monolayers (lipid composition DOPC : DOPE : Cholesterol 2 : 1 : 1), functionalized with 4 mol% CPnK. a) surface pressure (π) against molecular area (A), b) lateral compressibility $C_S = -1/A\ (\delta A/\delta\pi)_T$ of the lipid film against π. PBS, pH 7.4, 20 °C.*

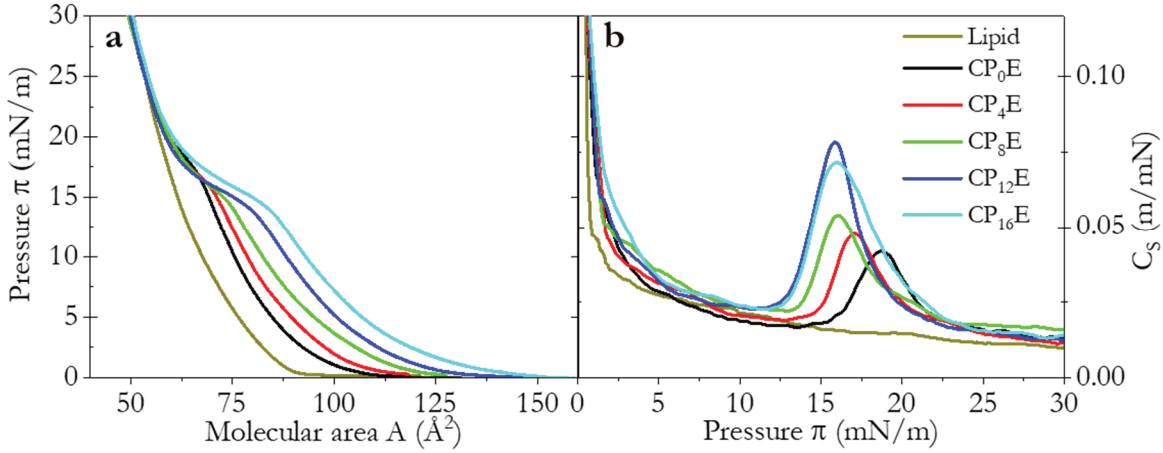


**Figure 12.** *Results of compression experiments with monolayers (lipid composition DOPC : DOPE : Cholesterol 2 : 1 : 1), functionalized with 4 mol% CPnE. a) surface pressure (π) against molecular area (A), b) lateral compressibility (Cs) against π. PBS, pH 7.4, 20 °C.*

**Table 4.** *Characteristics of monolayer experiments, with standard lipid composition and 4 mol% CPnE.*

| Peptide | $\pi_{SO}$[a] (mN/m) | $A_{SO}$[b] (Å²) | $A_{SO}$-$A_E$[c] (Å²) | $A_{PEG}$[c] (Å²) | %E incorporated |
|---|---|---|---|---|---|
| $CP_0E$ | 18.8 | 8.1 | -5.7 | 0.6 | 59 |
| $CP_4E$ | 17.1 | 10.7 | -3.1 | 3.0 | 78 |
| $CP_8E$ | 16.1 | 14.1 | 0.3 | 5.4 | 100 |
| $CP_{12}E$ | 16.0 | 20.9 | 7.1 | 7.8 | 100 |
| $CP_{16}E$ | 16.0 | 24.3 | 10.5 | 10.1 | 100 |

[a] *Squeeze-out pressures ($\pi_{SO}$) are determined from peak position in $C_S/\pi$ graph.* [b] *Experimental squeeze-out surfaces ($A_{SO}$) were obtained via ⊥A calculation of π/A graphs between 10 mN/m and 23 mN/m with pure lipid isotherm as baseline.* [c] *Theoretical occupied surface areas of lipopeptides ($A_E$, 13.8 Å²) and PEG-spacers ($A_{PEG}$, 0.598(n+1) Å²) were obtained via assumption of stiff rod models with appropriate molecular dimensions.*

PEG-spacer length *n* an increasing amount of molecular area is lost. (*Table 4*) To estimate the occupied surface area of peptide E we assumed a simple model for its helix of a stiff rod (diameter 10 Å, length 34.5 Å, see SI), and the expected loss of molecular area if all helices are squeezed out is 13.8 Å$^2$ for 4 mol% of lipopeptide. For $CP_0$ and $CP_4$ derivatives, ΔA is less than expected, implying respectively 59% and 78% or less of the helices are incorporated. Due to limited degrees of freedom for peptides equipped with a short spacer, a partial incorporation of all helices in the lipid monolayer is also reasonable.

On the other hand, monolayer tethered $CP_{12}E$ and $CP_{16}E$ show an extra contribution in molecular area ΔA. To estimate the theoretical molecular area occupied by a PEG-spacer of length *n* we assumed a simple molecular model of a stiff rod (diameter 4.15 Å, length 3.6(n+1) Å, see SI). The estimated surface area is in good agreement with the found extra contribution in lost molecular area. Although PEG is usually regarded as inert, it is known to interact with lipid monolayers at low π especially when conjugated to a membrane constituent.[18-21] The observed single peaks in the $C_S/\pi$ graph show the simultaneous squeeze-out of both spacer and peptide, which demonstrates the interdependent behavior of both peptide and PEG spacer during the squeeze-out process.

The loss in molecular area for $CP_8E$ containing monolayers is 14.1 Å. This could be explained in two ways: Peptides and spacers both insert partially in the monolayer, or the peptide is completely incorporated in the monolayer leaving no area for the PEG-spacer. Since there is an energy penalty on solvent exposed hydrophobic peptide residues, it is more likely that the peptide fully incorporates in the monolayer, with a solvent exposed PEG-spacer. Thus, we conclude that for $CP_nE$ peptides, elongated PEG-spacers incorporate in the membrane at low surface pressures, while the PEG-spacer of peptide $CP_nK$ stays solvated over the whole pressure-range as shown above.

Increasing the spacer length causes a decrease in squeeze-out pressure $\pi_{SO}$ to 16 mN/m implying an easier squeeze-out for those lipopeptides. This indicates a smaller energy-gap between low and high pressure monolayer states for E with elongated spacers, compared to lipopeptides with shorter spacers. A decreased energy-gap with increasing spacer length could be caused by a stabilization of the peptide conformation upon exclusion from the monolayer. Detailed study of the water accessibility of the peptide

bonds with IRRAS measurements supports the hypothesis that peptides with elongated PEG-spacers can form stabilized homo-oligomers after squeeze-out. *(vide infra)*

## MONOLAYERS FUNCTIONALIZED WITH $CP_NE$ AND $CP_NK$

As shown in Figure 13, monolayer films decorated with a mixture of 2 mol% $CP_nE$ and 2 mol% $CP_nK$ show a peak in compressibility at a pressure around 19 mN/m. ΔA calculation showed that a molecular area of 5.2 Å² is still occupied by peptides at a surface pressure of 25 mN/m. It was demonstrated previously that when both peptide E and peptide K are present in the proximity of vesicles, peptide K is in an equilibrium between coiled-coil formation with peptide E and membrane insertion.[14]

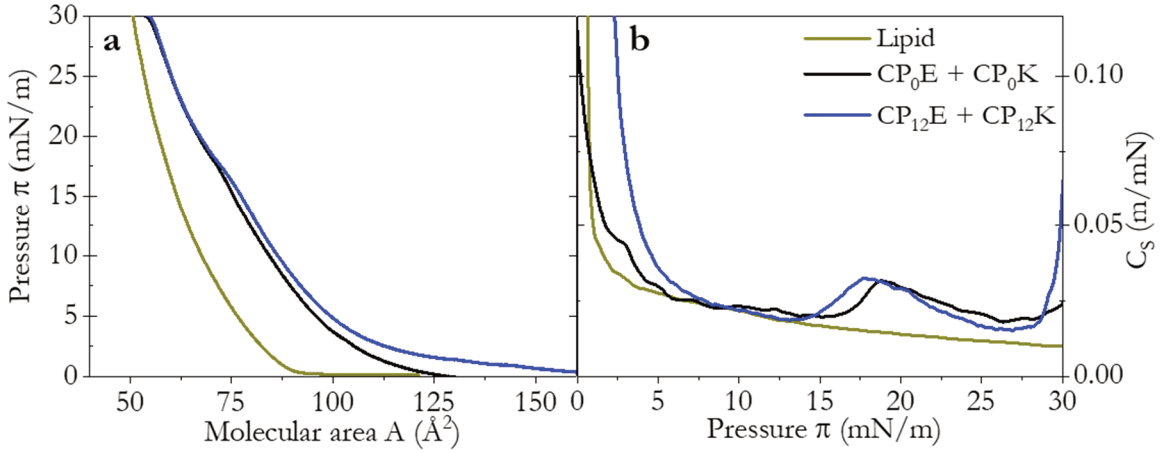


**Figure 13.** *Results of compression experiments with monolayers (lipid composition DOPC : DOPE : Cholesterol 2 : 1 : 1), functionalized with 4 mol% $CP_nE$ : $CP_nK$ (1:1, n = 0, 12). a) surface pressure (π) against molecular area (A), b) lateral compressibility ($C_S$) against π. PBS, pH 7.4, 20 °C.*

Because E-K coiled-coils lack the amphipathic nature needed for strong membrane interaction and E was found to squeeze out at moderate surface pressures, it can be assumed that the increased molecular area compared to pure lipid above the squeeze out pressure was solely caused by membrane-immersed peptide K.

Since peptides E and K were incorporated in equimolar amount in the monolayer, the dynamic equilibrium between the 3 hypothetical peptide conformations can be deduced. Assuming the occupied molecular area at high surface pressure, 5.2 Å², corresponds to 1.5 mol% of membrane embedded peptide K, 1.5 mol% of membrane tethered E is left in a solvated state. The remaining 1 mol% peptides can be assigned to the E-K coiled-coil complex. The dynamic equilibrium [EK] : ([E]+[K]) = 1 : 3, which supports the

previous finding that membrane immersion of K happens concomitant to E/K coiled-coil formation.[16-17]

## IRRAS MEASUREMENTS

To further study the conformation and the alignment of the peptides with respect to the supporting monolayer, we performed angle and polarization dependent infrared reflection absorption spectroscopy (IRRAS) measurements of the described monolayers at the air-water interface. Lipid monolayers containing 4 mol% $CP_nE$ and/or $CP_nK$ were prepared on *d*-PBS buffer pD 7.4 (prepared with pure $D_2O$). $D_2O$ was used to avoid overlapping water vapor contributions of $H_2O$ in the amide I spectral region. An important spectral region to study lipid and peptide properties is between 1600 and 1800 $cm^{-1}$. In this region the peptide amide I' band and the lipid C=O stretching vibrational band can be found, centered around ~1640 and ~1735 $cm^{-1}$, respectively. In all experiments the intensity of the C=O band increases upon monolayer compression due to the increasing lipid density in the IR-spot, and the relative intensity of the amide I' band, $A_{Amide\ I'}/A_{C=O}$ (short: AI/CO) is determined to quantify the amount of peptide in the IR-spot.

IRRA spectra with varying angle of incidence and polarization were recorded at constant surface pressures below and above the observed pressures $\pi_{SO}$, at 10 mN/m and 30 mN/m respectively. The peptide secondary structure was assumed to be on average in an α-helical conformation, as shown with circular dichroism.[16] Since peptide bonds in α-helices have comparable orientations, the band intensities of s-polarized spectra are sensitive to surface concentration provided that the helix orientation does not change. Thus, the recorded spectra were averaged over all angles of incidence to compare the results qualitatively. Also, fitting of angle and polarization dependent spectra yields the order parameter *S* of the peptide bonds. The comparable orientations of amide bonds in an α-helical conformation allows the determination of the angle of the helix axis with respect to the membrane normal, i.e. the peptide angle $\theta$. *S* can have values between -0.5 and 1, parallel or perpendicular to the monolayer plane respectively, and when *S* is close to 0 it is most likely that the peptides have a random orientation or no defined secondary structure. Detailed procedures and resulting spectra are available in Experimental section, Figure S6 -Figure S14.

Previous studies demonstrated that squeezed-out peptides readily leave the measurement spot by dissociation from the air-water interface into the subphase. However, monolayer tethered lipopeptides are confined close to the air-water interface and are still (partially) detected by the IR-beam, even after a peptide squeeze-out.[17] The obtained θ ≈ 90° at low surface pressure (10 mN/m), show that all peptides are aligned parallel to the monolayer plane. (*Table 5, Table 6*) Taken together with the results of the compression isotherms it is evident that the peptides are located in between the phospholipids at the air-water interface, most likely with the hydrophobic moment pointing to the hydrophobic region of the monolayer.

**Table 5.** *Results of IRRAS measurements of monolayers with unbound peptide and monolayer tethered peptide K.*

| Monolayer + | $\pi_{SO}$[a] | π | AI/CO[b] | S[c] | θ[d] |
|---|---|---|---|---|---|
| AcK[e] | 20.5 | 5 | 1.5 | -0.5 | 89 |
| | | 30 | 0.46 | -0.45 | 80 |
| $LP_{12}K$[e] | 29.5 | 15 | 0.77 | -0.47 | 83 |
| | | 30 | 0.76 | -0.49 | 85 |
| $CP_0K$ | n.a. | 10 | 0.53 | -0.5 | 90 |
| | | 30 | 0.46 | -0.5 | 89 |
| $CP_{12}K$ | n.a. | 10 | 0.44 | -0.5 | 90 |
| | | 30 | 0.48 | -0.5 | 90 |

[a] *Squeeze-out pressure obtained by monolayer compression cycles.* [b] *Ratio between observed peptide Amide I' band and lipid carbonyl band.* [c] *Order parameter S, calculated by fitting of angle and polarization dependent IR spectra.* [d] *Angle of peptide helix with respect to the membrane normal, derived from S.* [e] *Experiments conducted with monolayers and AcK/$LP_{12}K$ are taken from Rabe et al, 2014.*

For monolayers functionalized with $CP_0K$ and $CP_{12}K$, AI/CO is more or less equal at both low and high pressure, supporting the incorporation of K in the monolayer at all pressures. Peptide incorporation at higher surface pressure (30 mN/m) is further demonstrated by a parallel orientation of $CP_0K$ and $CP_{12}K$ with respect to the monolayer ($S$ = -0.5, Table 5). These results are in agreement with the characteristics of $LP_{12}K$ decorated monolayers, and no anchor induced effect on the peptide structure or the peptide membrane interaction was found.

For $CP_nE$, AI/CO decreases significantly upon pressure increase, while it stays rather constant for $CP_nK$ (*Table 6*). This observation supports once more the hypothesis that the plateaus in the π-A isotherms come along with a significant change in the peptide structure and/or orientation with respect to the incident IR-beam. The change in *S* to values around 0 at π = 30 mN/m supports the squeeze-out of all $CP_nE$ derivatives and indicates that excluded peptides probably have a random orientation of their helix or have no defined structure at all.

**Table 6.** *Results of IRRAS measurements of monolayers with unbound peptide and monolayer tethered peptide E and E + K.*

| Monolayer + | $\pi_{SO}$[a] | π | AI/CO[b] | S[c] | θ[d] |
|---|---|---|---|---|---|
| AcE[e] | 7 | 5 | 1.4 | -0.5 | 89 |
| | | 30 | 0 | - | - |
| $LP_{12}E$[e] | 17.9 | 15 | 0.7 | -0.47 | 82 |
| | | 30 | 0.52 | 0.05 | 53 |
| $CP_0E$ | 18.8 | 10 | 0.74 | -0.48 | 84 |
| | | 30 | 0.24 | -0.13 | 60 |
| $CP_4E$ | 17.1 | 10 | 0.52 | -0.45 | 80 |
| | | 30 | 0.26 | 0.30 | 43 |
| $CP_8E$ | 16.1 | 10 | 0.52 | -0.50 | 90 |
| | | 30 | 0.39 | 0.12 | 50 |
| $CP_{12}E$ | 16.0 | 10 | 0.67 | -0.50 | 90 |
| | | 30 | 0.3 | -0.15 | 61 |
| $CP_{16}E$ | 16.0 | 10 | 0.84 | -0.49 | 86 |
| | | 30 | 0.7 | -0.08 | 58 |
| E + K[e] | 9.7<br>22.5 | 5 | 2.68 | -0.5 | 88 |
| | | 15 | 1.71 | -0.5 | 89 |
| | | 30 | 0.96 | -0.45 | 80 |
| $LP_{12}E$ + $LP_{12}K$[e] | 18.4 | 15 | 0.87 | -0.47 | 82 |
| | | 30 | 0.62 | -0.15 | 61 |
| $CP_0E$ + $CP_0K$ | 18.6 | 10 | 0.43 | -0.5 | 90 |
| | | 30 | 0.31 | -0.23 | 65 |
| $CP_{12}E$ + $CP_{12}K$ | 17.8 | 10 | 0.78 | -0.5 | 90 |
| | | 30 | 0.57 | 0.02 | 54 |

[a] *Squeeze-out pressure obtained by monolayer compression cycles.* [b] *Ratio between observed peptide amide I' band and lipid carbonyl band.* [c] *Order parameter S, calculated by fitting of angle and polarization dependent IR spectra.* [d] *angle of amide I' moiety with respect to the membrane normal, derived from S.* [e] *Experiments conducted with monolayers and AcE/$LP_{12}K$/ $LP_{12}E$ + $LP_{12}K$ are taken from Rabe et al, 2014.*

The equimolar mixture of $CP_nE$ and $CP_nK$ (m = n) shows ordered peptide structures below the squeeze out pressure. Thus both peptides E and K independently incorporate into the monolayer, since the coiled-coil complex lacks an amphipathic nature. The exclusion of peptide E upon monolayer compression is supported here, by a decrease in AI/CO and an increase in S. Due to the occurrence of multiple different peptide conformations at high surface pressures, S is an average value that is difficult to interpret.

## AMIDE I' BAND FITTING

The position of the amide I' band is highly dependent on the peptide secondary structure and the solvent accessibility of its amide bonds, and is thus an important parameter for structure elucidation.[22-24] For E-K coiled-coil peptides, it is known that the amide I' bands observed by IRRAS at intermediate surface pressures (15 mN/m) consist of a maximum around 1634 $cm^{-1}$ and a shoulder around 1651 $cm^{-1}$.[17] Band shape analysis revealed two underlying main contributions that are often found in coiled-coil forming peptides. The two different band positions are caused by differences in hydrogen bonding of carbonyls buried in the hydrophobic core and solvent accessible carbonyls.[23-29] Water inaccessible amide bonds absorb at higher wavenumbers (1651 $cm^{-1}$) then the water accessible ones (1631 $cm^{-1}$). For membrane incorporated peptides, these differences in water-accessibility of the carbonyls is caused by the alignment of the peptides at the hydrophobic/hydrophilic interface and a partial insertion of hydrophobic side-chains into the hydrophobic part of the monolayer.[14]

Normalized S-polarized IRRAS spectra, averaged over all angles of incidence, were fitted with 3 gauss peaks at positions around 1631 $cm^{-1}$, 1651 $cm^{-1}$ and 1672 $cm^{-1}$ (*Figure 14*, *Figure S15 -Figure S23*). The nature of the third minor contribution around 1672 $cm^{-1}$ is unclear; it was assumed previously to be caused by residual TFA from HPLC purification of the lipopeptides,[30] but can also be assigned to C-terminal $CONH_2$ since the absorption occurs consistently in all spectra. However, most useful information is conserved in the intensities of the peaks at 1631 $cm^{-1}$ and 1651 $cm^{-1}$. The relative intensity of the peak at 1631 $cm^{-1}$ (hydrophilic fraction, as percentage of total amide I' band intensity) indicates the relative hydrophilicity of the environment of monolayer-tethered peptides, provided that the secondary structures are similar.

Monolayer incorporated peptides at low pressure show a hydrophilic fraction of 40 - 50%, which was found for all peptides consistently throughout the compression experiments. (*Figure 15, Figure 16*) At high pressure however, spacer and peptide-dependent trends are visible in the relative hydrophilicity of peptide helices.

For $CP_nK$ the hydrophilic fraction is still around 50% at high pressure, suggesting only minor differences in water accessibility. Also, the overall peptide orientations remain parallel to the membrane upon compression.

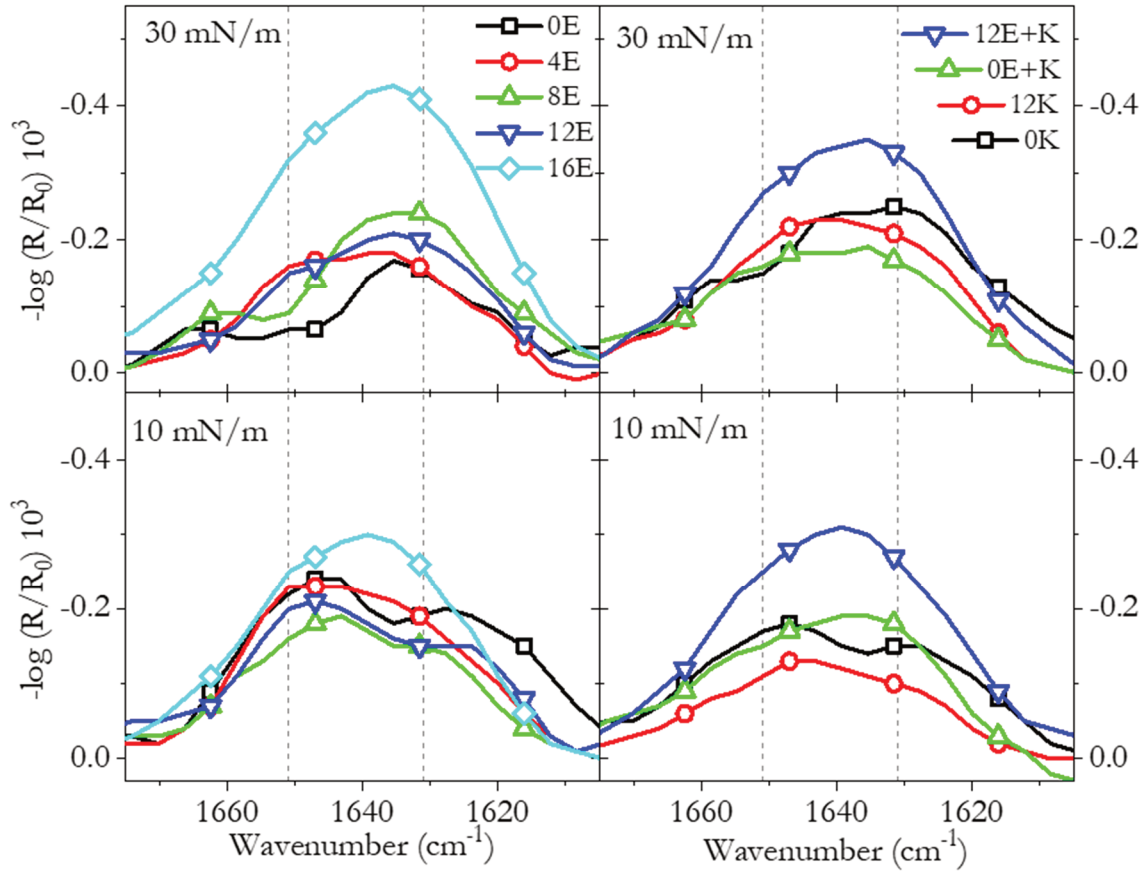


**Figure 14.** *Observed peptide amide I' bands of lipopeptide decorated monolayers at surface pressure of 10 mN/m and 30 mN/m. Peak positions at 1631 and 1651 cm$^{-1}$ are marked with dotted lines. Monolayers consists of 4 mol% lipopeptide, $D_2O$ PBS pD 7.4, with angle-averaged spectra of s-polarized light.*

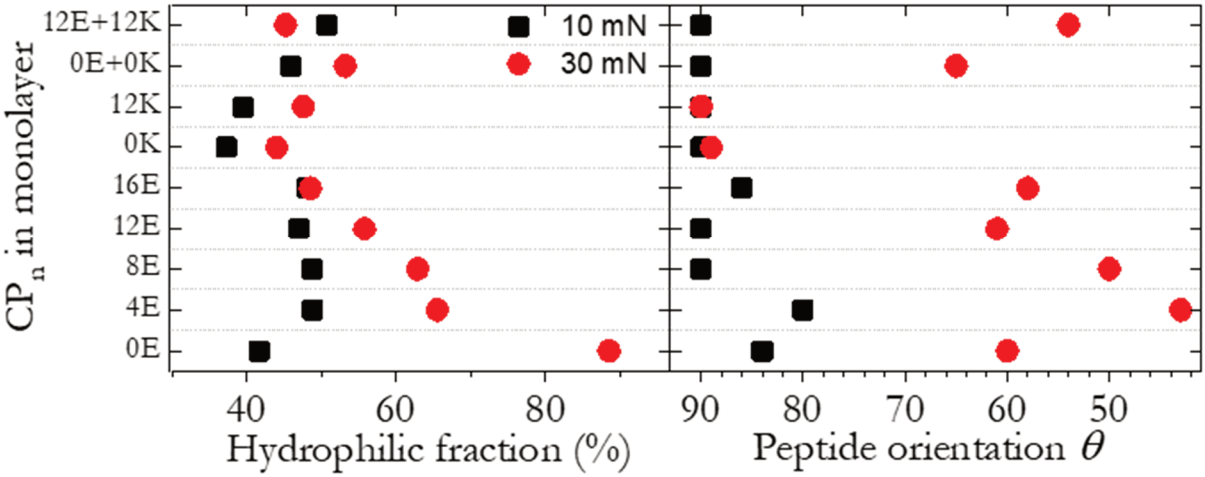


**Figure 15.** *Left: Shape-analysis of amide I' band (1610-1680 cm$^{-1}$) of lipopeptide decorated monolayers at surface pressure of 10 mN/m (black) and 30 mN/m (red). The amide I' band is fitted with three Gaussian peaks (1631, 1651 and 1671 cm$^{-1}$) and the hydrophilic fraction is defined as: (surface area of Gaussian peak at 1631 cm$^{-1}$)/(total surface area of amide I' band). Right: Calculated peptide orientation θ of monolayer tethered peptides at surface pressure of 10 mN/m (black) and 30 mN/m (red). Monolayers consists of 4 mol% lipopeptide, $D_2O$ PBS pD 7.4.*

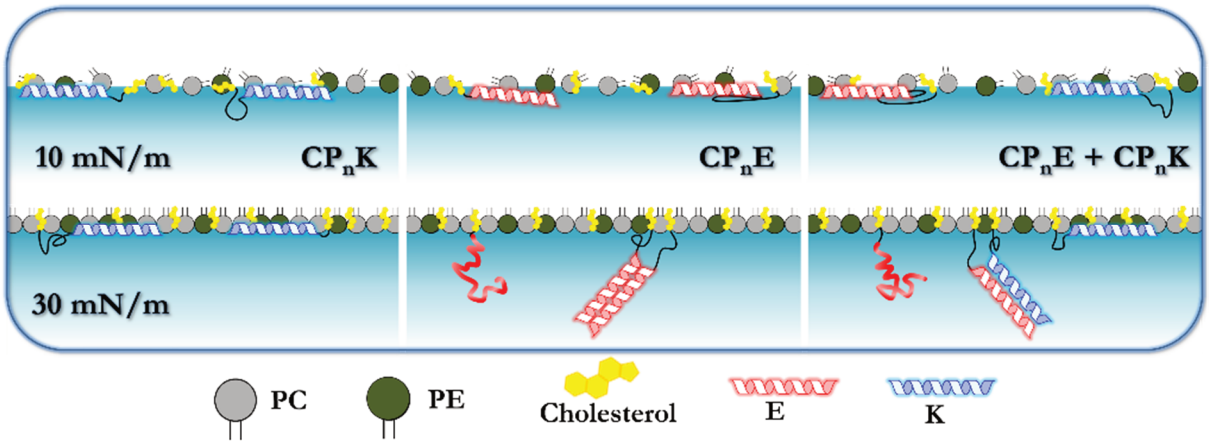


**Figure 16.** *Conformations of lipidated peptides in monolayers. $CP_nK$ is immersed in the monolayer at both low and high surface pressure while peptide $CP_nE$ is expelled upon compression of the lipid monolayer. Compressed monolayers containing a mixture of $CP_nE$ and $CP_nK$ suggest the simultaneous presence of hetero dimeric coiled-coil (EK), individual solvated (E), and membrane-bound (K) peptides. Lipid composition is DOPC : DOPE : Cholesterol 2 : 1 : 1.*

These findings are further evidence for membrane immersed helices of peptide K, with no apparent influence of spacer length *n*.For E-peptides the hydrophilic fraction increases which points to a more hydrophilic environment at high pressure. High solvent exposure of peptides is suggested by a significant decrease of the 1651 $cm^{-1}$ absorption band, and this is most pronounced for $CP_0E$ containing monolayers.

Remarkably, the hydrophilic fraction at high surface pressure decreases with increasing spacer length, and for $CP_{16}E$, the value is similar at both high and low pressure. Since all $CP_nE$ derivatives are excluded from the monolayer and show order parameters close to 0 at high pressure, we attribute the increasing 1651 $cm^{-1}$ absorption in the Amide I' band to the formation of less water accessible hydrophobic pockets of $CP_nE$ homo-oligomers,[28, 31] which thus becomes more pronounced for elongated spacers. So for this lipopeptide, two trends are observed with increasing PEG-spacer length. A decrease in squeeze-out pressure was measured with increasing spacer length. Secondly, at high surface pressure, peptide bonds were found to experience a partial hydrophobic environment, and the effect became more pronounced with increasing spacer length. These two observations suggest the increasing presence of homo-oligomer formation of monolayer tethered peptide E with increasing PEG-spacer length, at room temperature. When these results are compared with the reported characteristics of $LP_{12}E$, similar values of $\pi_{SO}$ and AI/CO are found for $CP_0E$ rather than for $CP_{12}E$.

For mixtures of $CP_0E$ + $CP_0K$ and $CP_{12}E$ + $CP_{12}K$ in the lipid monolayer, the hydrophilic fraction at low and high pressures are close to 50%. This demonstrates that peptide bonds in monolayer-excluded peptides still experience a combined hydrophilic/hydrophobic environment, which is in agreement with the formation of solvated hetero-oligomers. At high surface pressure, orientation changes were found for $CP_0E/K$ and $CP_{12}E/K$, which supports a random orientation of solvated heterodimeric coiled-coils of E/K peptides.

## CONCLUSIONS

In this study, we showed that the peptide-monolayer interaction of the E/K fusion model system is affected by the lipid anchor and the length of the conjugated PEG-spacer. Monolayer-tethered peptide K incorporates in the monolayer up to surface pressures of 30 mN/m. These peptides are known to incorporate in phospholipid bilayers, due to their amphipathic α-helical structure. Slight differences were found between the derivatives; the absence of a spacer hinders full monolayer incorporation, as $CP_0K$ endured a partial squeeze-out at high surface pressure, although the peptide orientation remained parallel to the monolayer. Remarkably, PEG-spacers did not incorporate in the membrane at any given surface pressure, although a slightly increased molecular area was found for $CP_{16}K$ at $\pi < 10$ mN/m. No squeeze out was measured for $CP_nK$ up to surface pressures of 30 mN/m, in contrast to $LP_{12}K$, which partially squeezed out at this pressure.

All monolayers functionalized with $CP_nE$ showed a plateau during compression-expansion cycles, which evidenced the squeeze-out of peptide material at high surface pressure. Furthermore, elongated PEG-spacers were found to immerse together with the conjugated peptide in the phospholipid monolayer at low surface pressures and were found to promote the formation of homo-oligomers at high surface pressure.

Compression experiments on monolayers consisting a mixture of $CP_nE$ and $CP_nK$ supports the simultaneous existence of coiled-coil structures and membrane bound peptides.

The length of the PEG spacer of peptide $CP_nK$ was found to be the major factor influencing the fusion efficiency of $CP_nE/CP_nK$ decorated liposomes.[16] We hypothesized

that the PEG-spacer length *n* of peptide K is crucial for efficient fusion by defining the distance between opposing, coiled-coil connected liposomes. Another possible explanation – the membrane interaction of peptide K is affected by *n*, thereby influencing the fusion efficiency – could not be supported here. Peptide $CP_nE$ exhibits a minor enhancement of the fusion process with increasing spacer length. This can be attributed to an increased accessibility of peptides with elongated spacers and/or to the increased tendency of homo-oligomer formation for peptides with elongated spacers.

# EXPERIMENTAL SECTION

## MATERIALS

DOPC, DOPE and cholesterol were purchased from Avanti Polar Lipids. Chloroform, methanol (both HPLC grade), $D_2O$ (99.9 % deuterium content), buffer salts and HCl and DCl (99% deuterium content) for pH/pD adjustment, were purchased from Sigma-Aldrich. All water was ultrapure with resistance ≥ 18 MΩ and TOC ≤ 2 ppm produced from a MilliQ Reference A+ purification system. All monolayer and IR experiments were carried out in phosphate buffered saline of the following composition: 150 mM NaCl, 20 mM $PO_4^{3-}$ in $H_2O$ (PBS) or $D_2O$ (d-PBS) at pH / pD 7.4, respectively.

# METHODS

## CALCULATION OF LIPOPEPTIDE DIMENSIONS

To estimate the dimensions of the used lipopeptides we assumed stiff rod models for both peptide and PEG components. Since the movements of lipopeptides at monolayers is regarded predominantly 2-dimensional, bending of the linear molecule will not alter occupied surface area significantly.

Peptide helices have a diameter of 10 Å, 3.6 residues per turn and a pitch of 5.1 Å. This gives a peptide length of 34.5 Å for 23 residues.

The PEG length is estimated via calculation of stretched end-to-end distance of the PEG-chain in ChemDraw, which yielded an average length of 3.6 Å per ethyleneglycol unit. The length of the succinimide moiety is comparable to one unit of ethyleneglycol and covered by factor n+1. A diameter of 4.15 Å is found for any primary alkylchain and a good approximation of the diameter of a polyethyleneglycol chain.

## MONOLAYER PREPARATION

Lipid solutions of DOPC : DOPE : Cholesterol 2 : 1 : 1 ([total lipid] = 1 mM) with 0 or 4 mol% lipopeptides were prepared in $CHCl_3/CH_3OH$ 3:1 vol%. For the preparation of a lipid monolayer a distinct volume of these solutions was spread on PBS buffer at 25 °C by means of a microliter syringe, the solvent was allowed to evaporate and the film to equilibrate for at least 15 minutes. A microbalance was used for surface pressure measurements using a filter paper as pressure probe.

Initial cleaning of the troughs was achieved by means of diluted detergent solution (2% Hellmanex (Hellma Analytics, Müllheim, Germany) in $H_2O$), followed by extensive rinsing with ~50°C Milli-Q water, wiping with $CHCl_3$/MeOH and final multiple rinsing with Milli-Q water. All Langmuir trough setups were hold constant at 25 °C by means of a circulating water bath and were isolated from the environment by plastic covers.

## COMPRESSION-EXPANSION CYCLES

For compression-expansion cycles of lipid monolayers containing monolayer tethered peptides $CP_nE$ and/or $CP_nK$, monolayers on PBS were prepared. After equilibration, compression-expansion cycles of the monolayer were performed with a compression/expansion speed of 3 Å² / (molecule min), and experiments were repeated twice to ensure reproducibility of the isotherm shape. For determination of lateral compressibility, compression isotherms over a surface pressure of 0 to 30 mN/m were smoothed by means of a 60 point adjacent average method and the film compressibility was calculated as:

$$C_S = \frac{-1}{A} * \left(\frac{\delta A}{\delta \pi}\right)_T$$

with molecular area $A$ and surface pressure $\pi$.

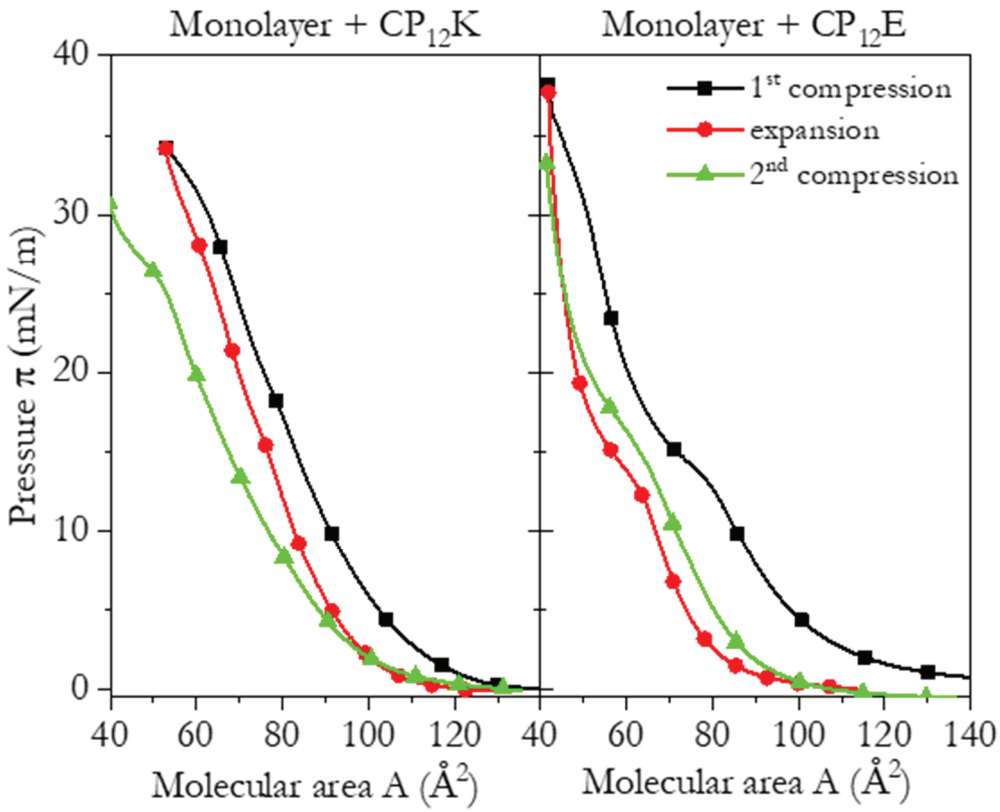


**Figure S5.** *Results of compression-expansion experiments with monolayers (lipid composition DOPC : DOPE : Cholesterol 2 : 1 : 1) functionalized with 4% lipopeptide $CP_{12}K$ or $CP_{12}E$. Surface pressure (π) against molecular area (A) of compression-expansion cycles show reversible squeeze-out of E peptides, and a loss of monolayer material over the course of the experiment. PBS, pH 7.4, 20 °C.*

## IRRAS MEASUREMENTS

IRRAS measurements were performed on a BRUKER Vector 70 FT–IR spectrometer equipped with a nitrogen cooled MCT detector and an A511 reflection unit (Bruker Optics, Germany), placed over the Langmuir trough setup (Riegler & Kierstein, Germany). The sample trough (30 x 6 $cm^2$) was equipped with a Wilhelmy balance using a filter paper as pressure probe. A circular reference trough (r = 3 cm) placed next to the sample trough can be brought into the focus of the IR beam by means of a shuttle. The filling levels of both troughs were kept equal and constant by means of an automated, laser reflection controlled, pumping system connected to reservoirs of $D_2O$.

Lipid monolayers containing the lipopeptides were prepared as described above, on a subphase of d-PBS. The pD was set to 7.4 by adding 0.4 to the read-out of a standard pH-meter.[32] IRRA spectra were recorded at constant surface pressures below (10 mN/m) and above (30 mN/m) the expected squeeze out pressure of the peptides.

## DETAILS OF IRRA SPECTRA MEASUREMENTS

At each pressure at least 2 cycles of angle dependent IRRA spectra were recorded. For each spectral cycle s- and p-polarized spectra were recorded at incident angles varying from 25° to 70° with an increment of 3°, while spectra close to the Brewster angle (52°, 55° and 58°) were discarded. For each sample reflectance spectrum (R) a total number of 2000 scans at a resolution of 8 $cm^{-1}$ and a zero-filling factor of 2 were averaged. Reference reflectance spectra ($R_0$) were recorded at the same experimental conditions at an identical subphase without monolayer. The reflectance absorbance spectra were calculated as $RA = -log (R / R_0)$.

RA spectra recorded at identical polarization and angle of incidence were averaged and corrected with a *d*-PBS background spectrum prior to data evaluation to minimize spectral contributions of water vapor absorptions and to improve the signal to noise (S/N) ratio. Additional mathematical baseline corrections were avoided as much as possible. All spectra obtained in s-polarization were averaged for obtaining spectra with good S/N ratio being interpretable in terms of secondary structure and for quantification of the amount of peptide present.

## FITTING OF ANGLE DEPENDENT AMIDE I' IRRAS BANDS

The intensities of IRRAS bands strongly depend on the angle of incidence and the polarization (parallel (p) or perpendicular (s) to the plane of incidence) of the incident IR beam. These dependencies contain detailed information about the orientation of the transition dipole moment of the absorbing moieties with respect to the monolayer normal. Fitting of the angle dependent absorbance can be achieved and yields molecular order parameter *S*, and additionally the angle α between the molecular axis and the transition dipole moment can be estimated. The optical model of Kuzmin and Mikhailov[33-34] was extended to calculate and fit the reflectance absorbance bands consisting of multiple overlapping spectral components as reported by Schwieger *et al.*[35] Simulations and fitting of IRRA spectra was performed using MATLAB software (The MathWorks Inc., USA).

The IRRAS band intensities and shapes are simulated assuming lorentzian absorption bands with the vibrational frequency $n_0$, the full width at half height *fwhh* and the

absorption coefficient *k*. Depending on the orientation of the transition dipole moment within the molecule (*a*), the tilt angle of the molecule with respect to the layer normal ($\theta$), the intensity varies with experimental parameters angle of incidence (AoI) and polarization (p or s) of the IR beam. Furthermore, the refractive index of the film *n* and the film thickness as well as the polarizer quality $\Gamma$ have to be known to simulate complete reflectance-absorbance spectra. $\Gamma$ was determined from independent measurements and set to 0.007 for all simulations. The frequency dependent refractive indices and absorption coefficients of the $D_2O$ subphase are taken from Bertie *et al.*[36] Simulations were fitted to the experimental spectra by means of a non-linear least-square fit in the amide I' region (1620-1670 $cm^{-1}$).

The parameters *n* and *d* were determined for each measurement by a fit of the $D_2O$ absorption in the spectral range of 2300 - 2800 $cm^{-1}$. The spectra were then simulated with three bands: one C=O stretching vibrational band in the range of 1710 - 1770 $cm^{-1}$ and two amide I' components at $\upsilon 1$ = 1631 and $\upsilon 2$ = 1651 $cm^{-1}$, accounting for amide bonds in hydrophilic and hydrophobic environment, respectively. For both components $\alpha$ was set to 38°.[37]

The lipid C=O band intensity was fitted via adjustment of the respective *k* value. Finally, the amide I' band of s- and p-polarized spectra over all measured AoI were fitted by means of a global non-linear least square method using a Levenberg-Marquardt algorithm, in the wavenumber range of 1620 – 1670 $cm^{-1}$. The helix tilt angle $\theta$, as well as the absorption coefficients *k1* and *k2*, and *fwhh1* and *fwhh2* of both amide I' components were free fitting parameters. To yield reliable and reproducible fits different starting values for the fitting parameters were tested.

Within the applied model[34-35] the tilt angle $\theta$ is calculated from the order parameter *S* under the assumption of a unimodal and small tilt angle distribution, according to:

$$S = \frac{3\langle cos^2\theta \rangle - 1}{2}$$

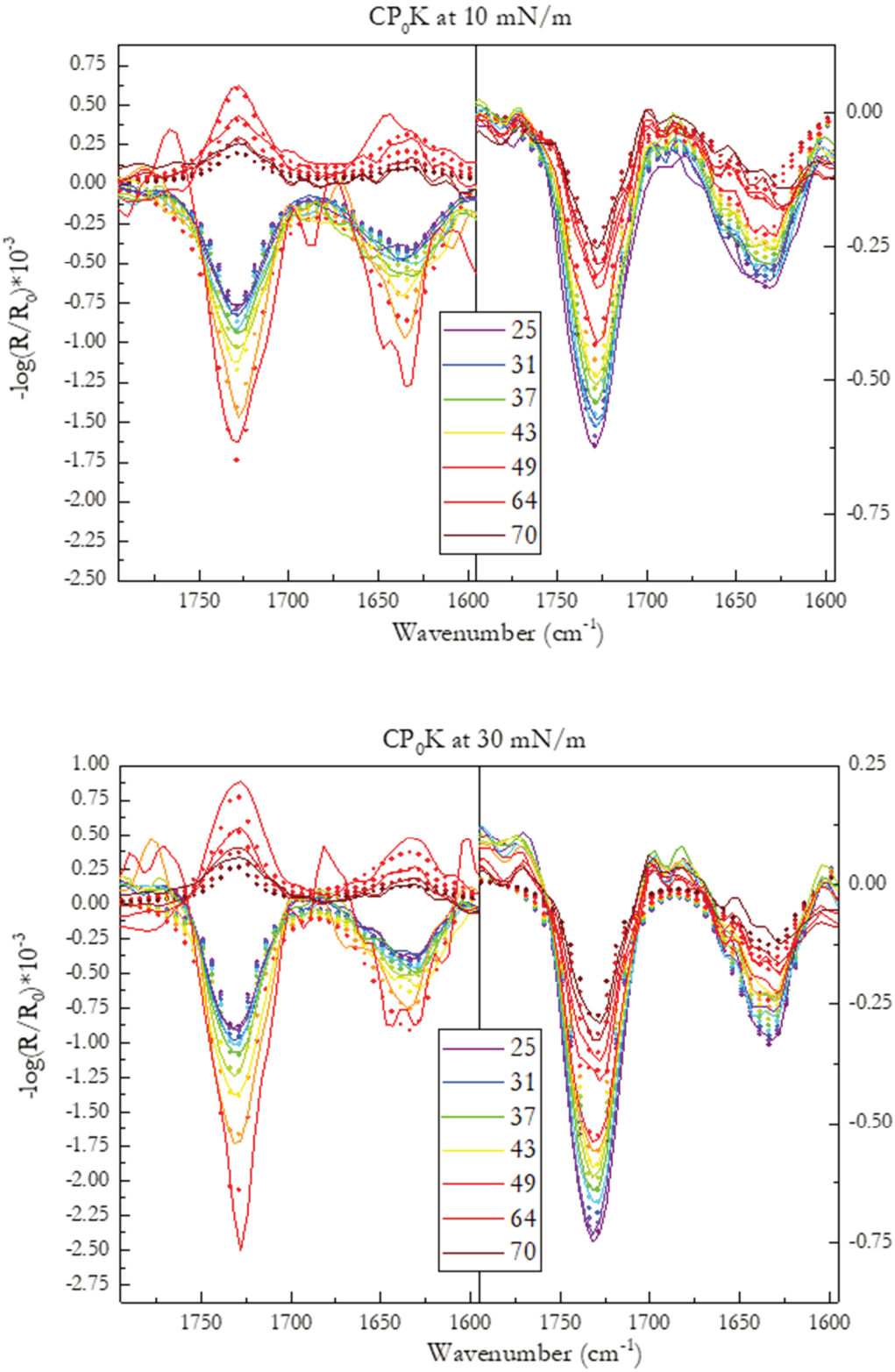


**Figure S6.** *Experimental data of Amide I' absorption bands (1600-1800 cm$^{-1}$, lines), and best fits obtained with Matlab (dots) of CP$_0$K decorated monolayers at a surface pressure of 10 mN/m and 30 mN/m. Left graphs are angle dependent P-polarized spectra, right graphs are angle dependent S-polarized spectra. Monolayers consists of 4 mol% lipopeptide, D2O PBS pD 7.4.*

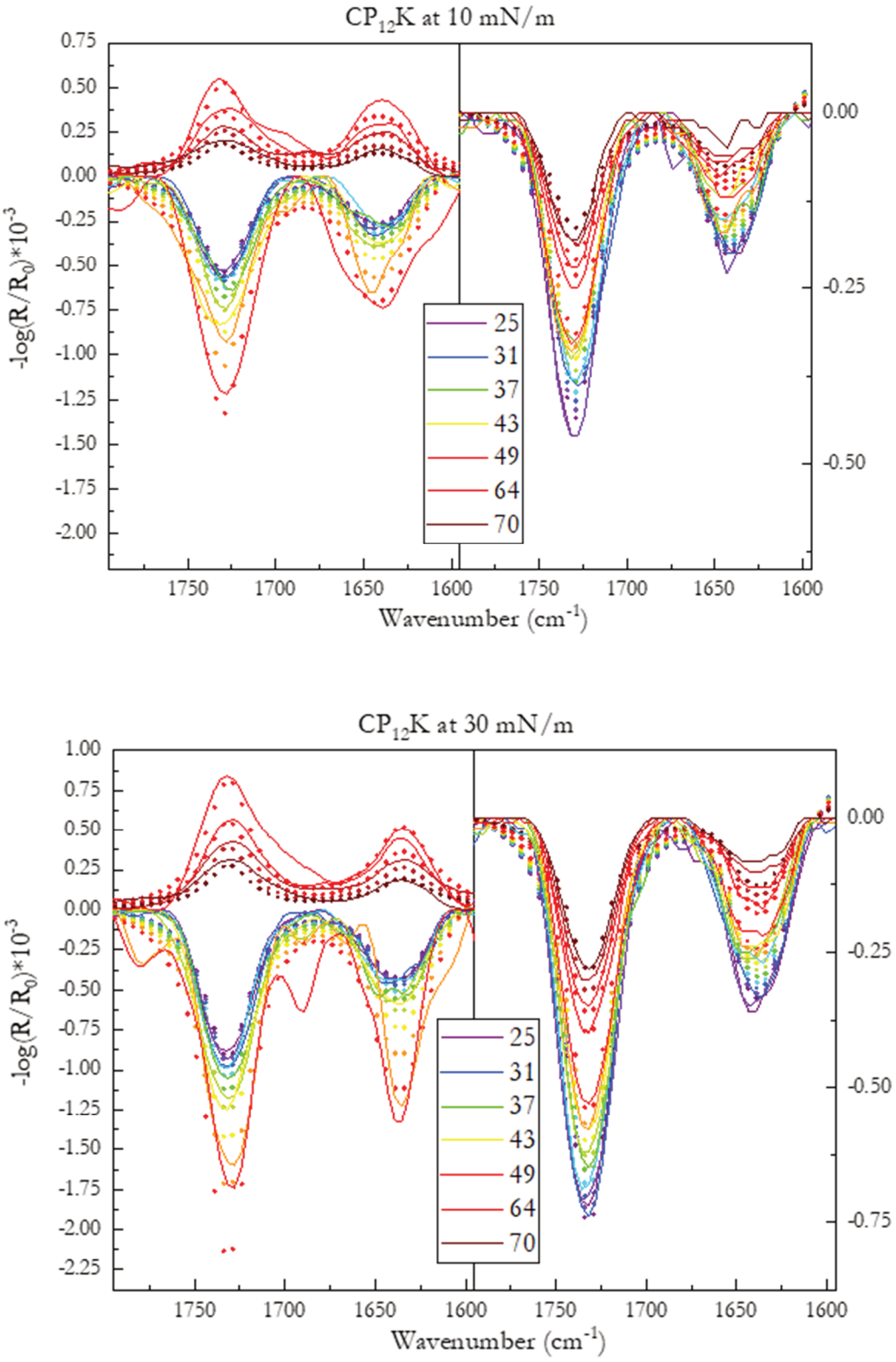


**Figure S7.** *Experimental data of Amide I' absorption bands (1600-1800 cm$^{-1}$, lines), and best fits obtained with Matlab (dots) of CP$_{12}$K decorated monolayers at a surface pressure of 10 mN/m and 30 mN/m. Left graphs are angle dependent P-polarized spectra, right graphs are angle dependent S-polarized spectra. Monolayers consists of 4 mol% lipopeptide, D2O PBS pD 7.4.*

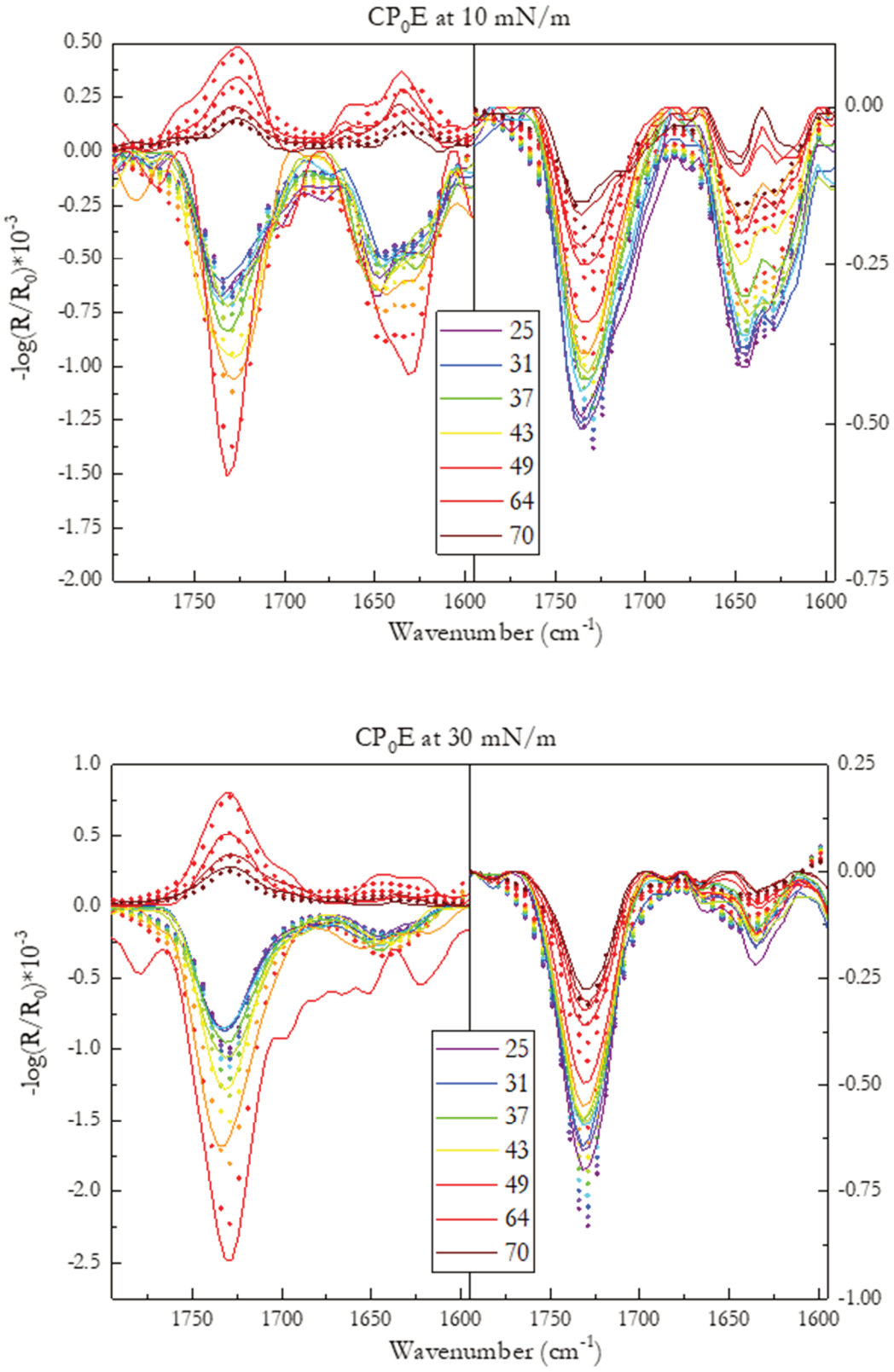


**Figure S8.** *Experimental data of Amide I' absorption bands (1600-1800 cm$^{-1}$, lines), and best fits obtained with Matlab (dots) of CP$_0$E decorated monolayers at a surface pressure of 10 mN/m and 30 mN/m. Left graphs are angle dependent P-polarized spectra, right graphs are angle dependent S-polarized spectra. Monolayers consists of 4 mol% lipopeptide, D2O PBS pD 7.4.*

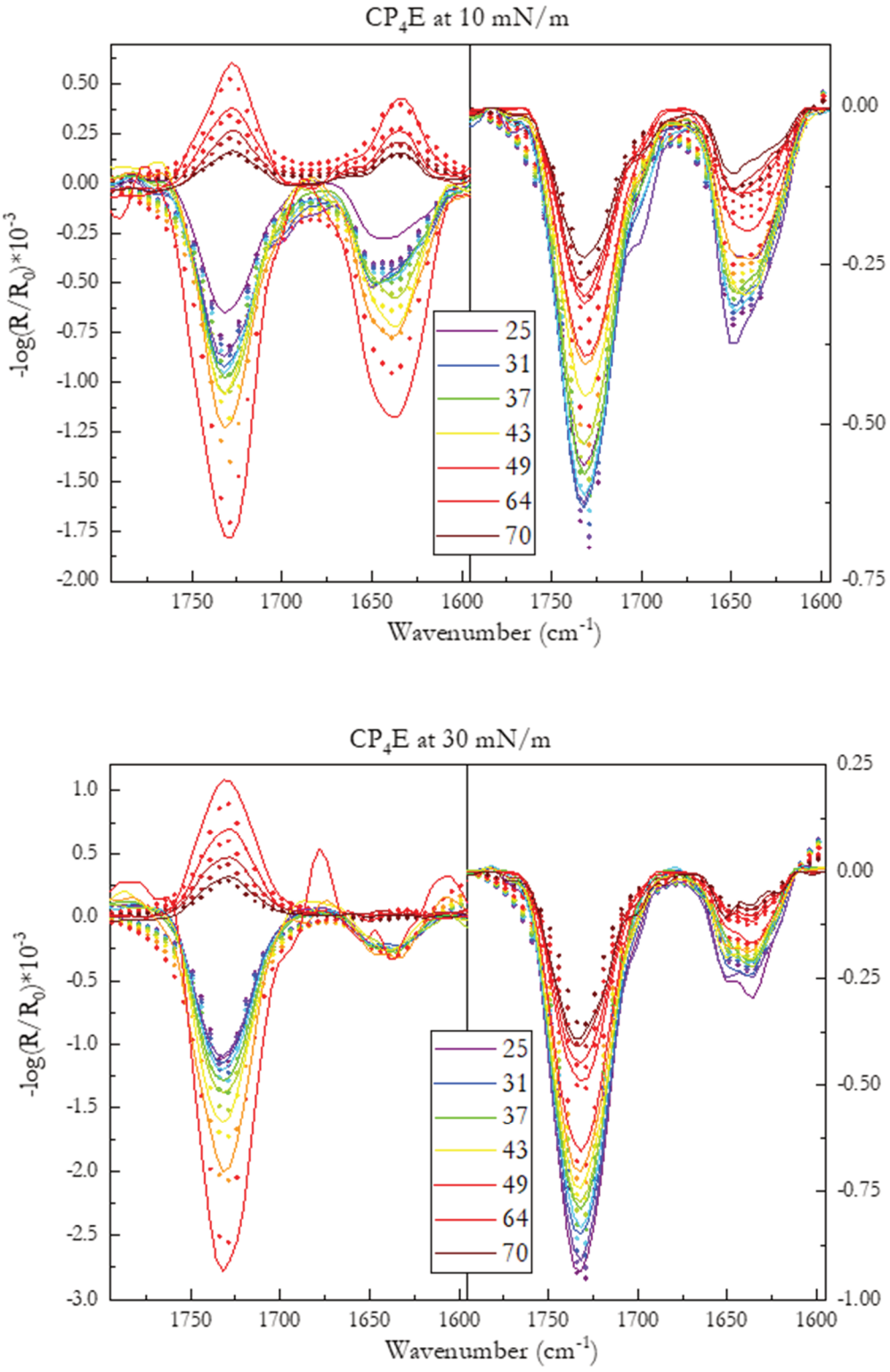


**Figure S9.** *Experimental data of Amide I' absorption bands (1600-1800 cm$^{-1}$, lines), and best fits obtained with Matlab (dots) of CP$_4$E decorated monolayers at a surface pressure of 10 mN/m and 30 mN/m. Left graphs are angle dependent P-polarized spectra, right graphs are angle dependent S-polarized spectra. Monolayers consists of 4 mol% lipopeptide, D2O PBS pD 7.4.*

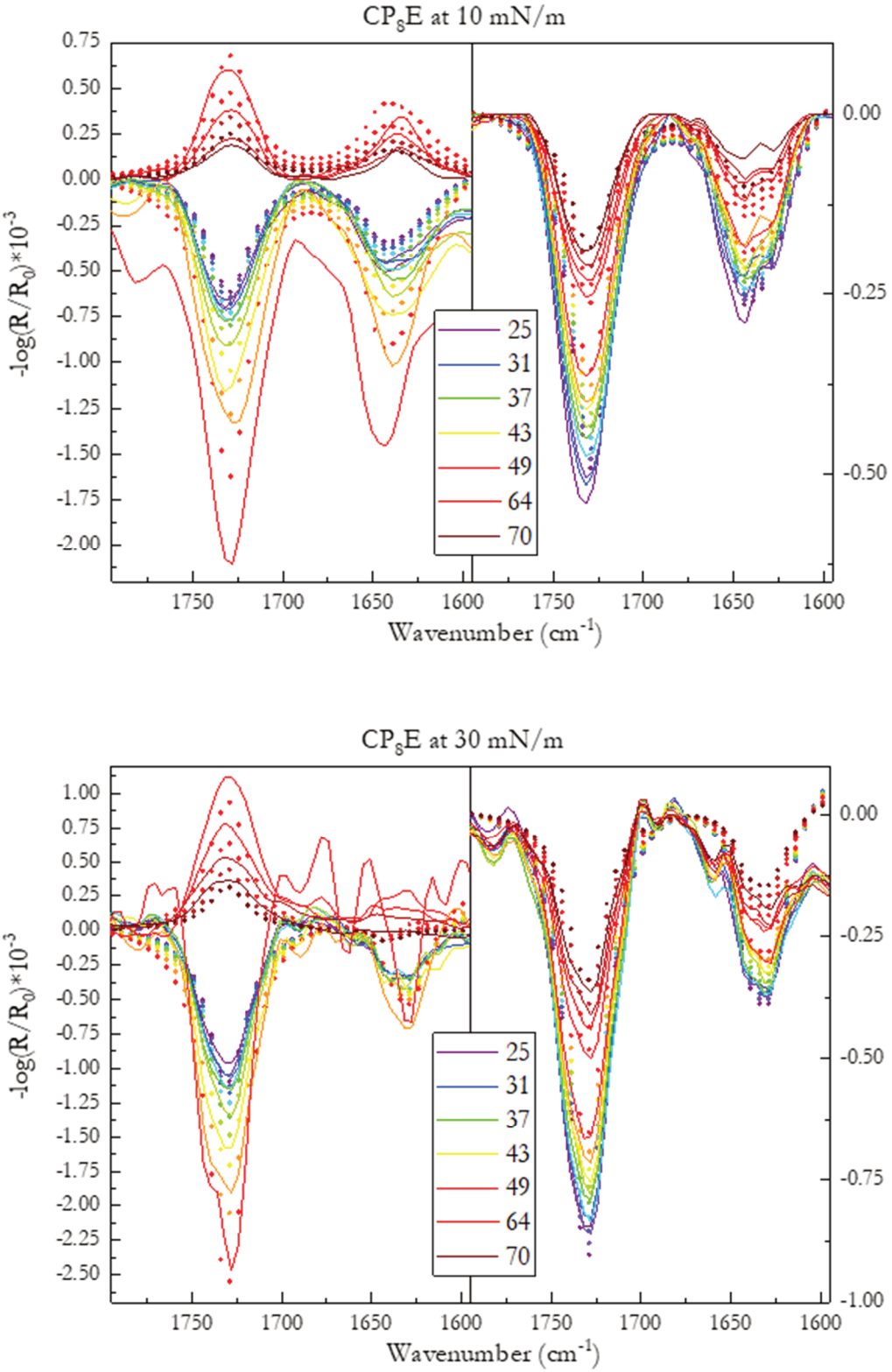


**Figure S10.** *Experimental data of Amide I' absorption bands (1600-1800 cm$^{-1}$, lines), and best fits obtained with Matlab (dots) of CP$_8$E decorated monolayers at a surface pressure of 10 mN/m and 30 mN/m. Left graphs are angle dependent P-polarized spectra, right graphs are angle dependent S-polarized spectra. Monolayers consists of 4 mol% lipopeptide, D2O PBS pD 7.4.*

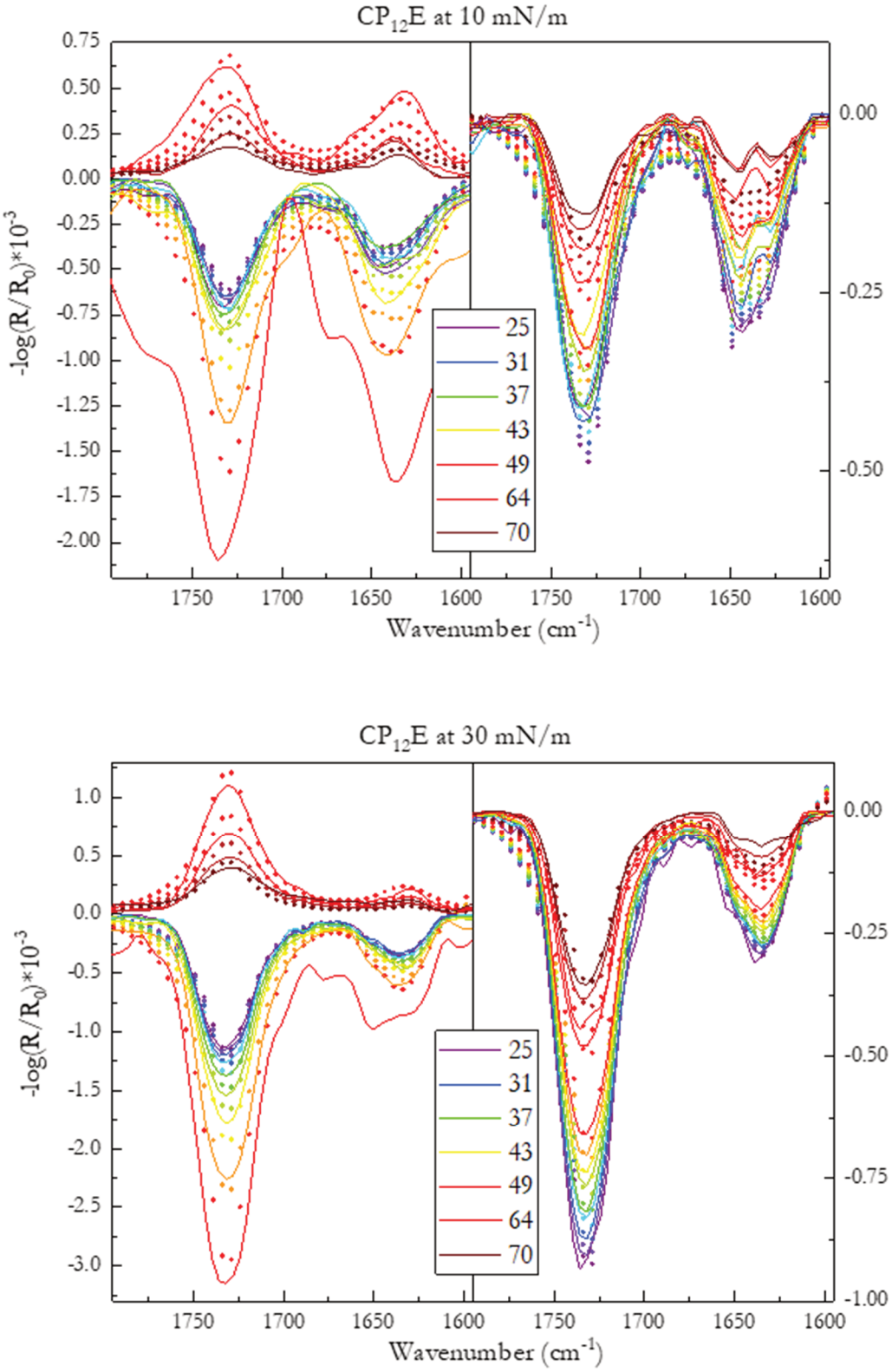


**Figure S11.** *Experimental data of Amide I' absorption bands (1600-1800 cm$^{-1}$, lines), and best fits obtained with Matlab (dots) of CP$_{12}$E decorated monolayers at a surface pressure of 10 mN/m and 30 mN/m. Left graphs are angle dependent P-polarized spectra, right graphs are angle dependent S-polarized spectra. Monolayers consists of 4 mol% lipopeptide, D2O PBS pD 7.4.*

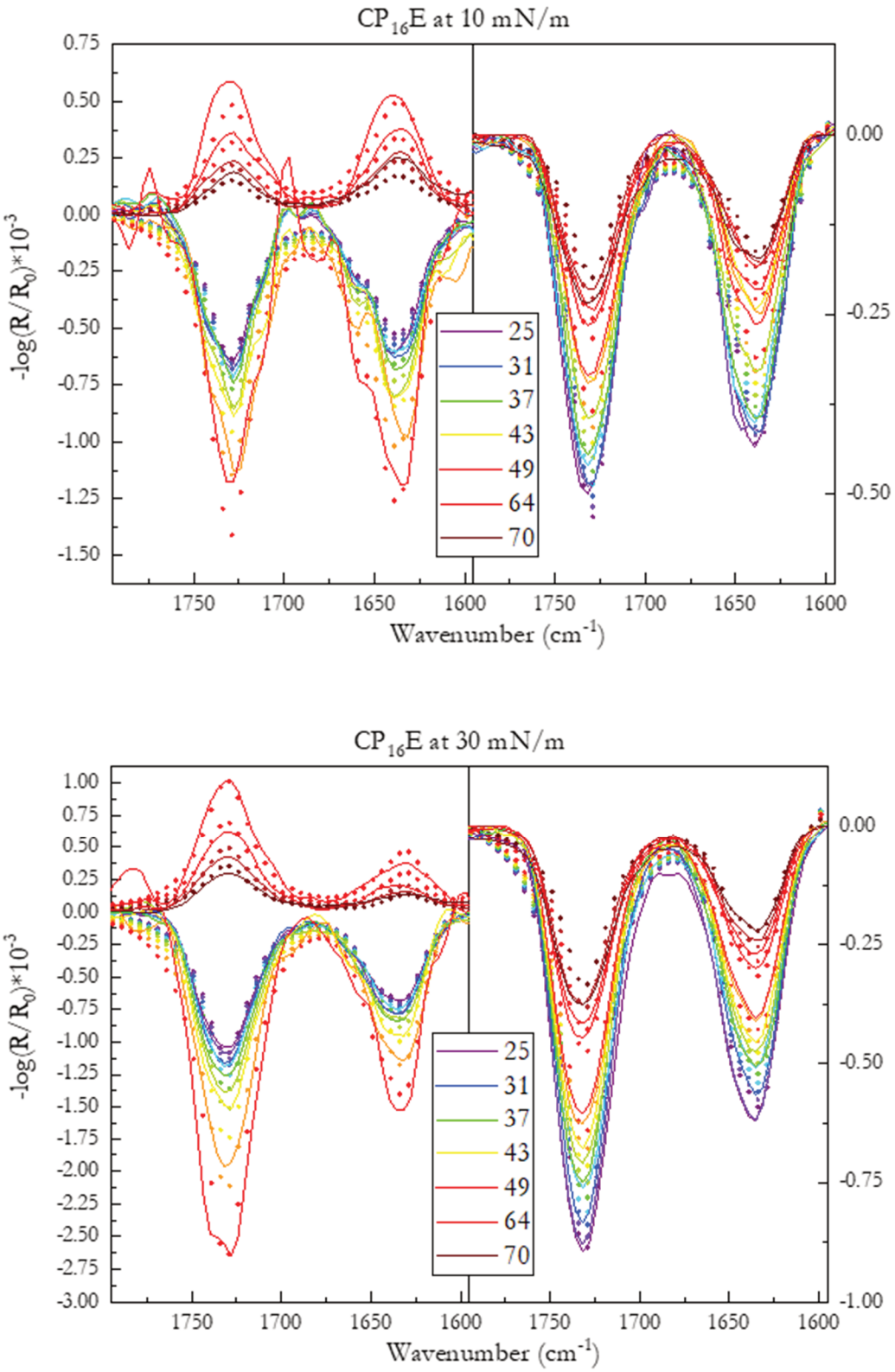


**Figure S12.** *Experimental data of Amide I' absorption bands (1600-1800 cm$^{-1}$, lines), and best fits obtained with Matlab (dots) of $CP_{16}E$ decorated monolayers at a surface pressure of 10 mN/m and 30 mN/m. Left graphs are angle dependent P-polarized spectra, right graphs are angle dependent S-polarized spectra. Monolayers consists of 4 mol% lipopeptide, D2O PBS pD 7.4.*

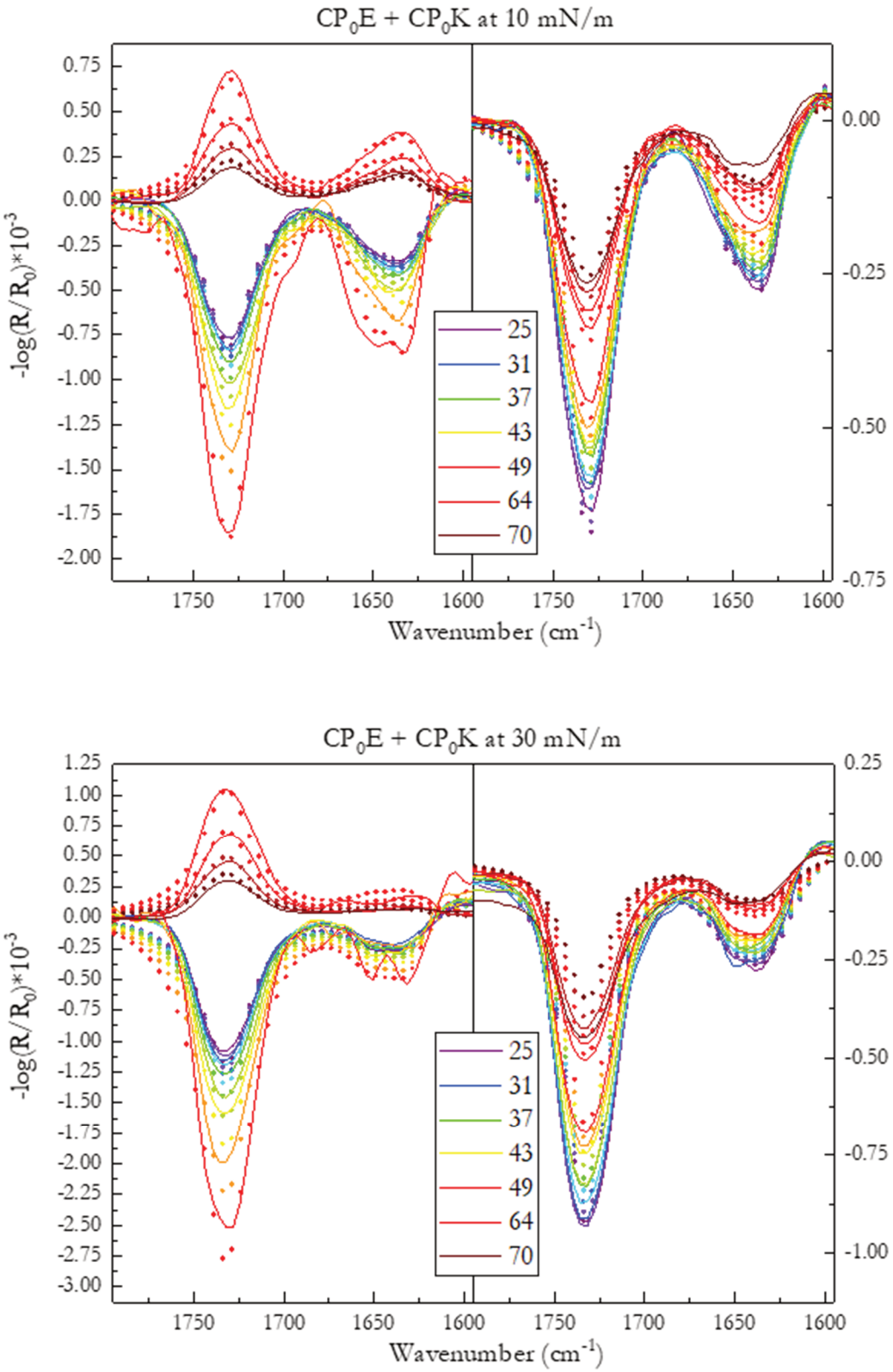


**Figure S13.** *Experimental data of Amide I' absorption bands (1600-1800 cm$^{-1}$, lines), and best fits obtained with Matlab (dots) of CP$_0$E and CP$_0$K decorated monolayers at a surface pressure of 10 mN/m and 30 mN/m. Left graphs are angle dependent P-polarized spectra, right graphs are angle dependent S-polarized spectra. Monolayers consists of 4 mol% lipopeptide, D2O PBS pD 7.4.*

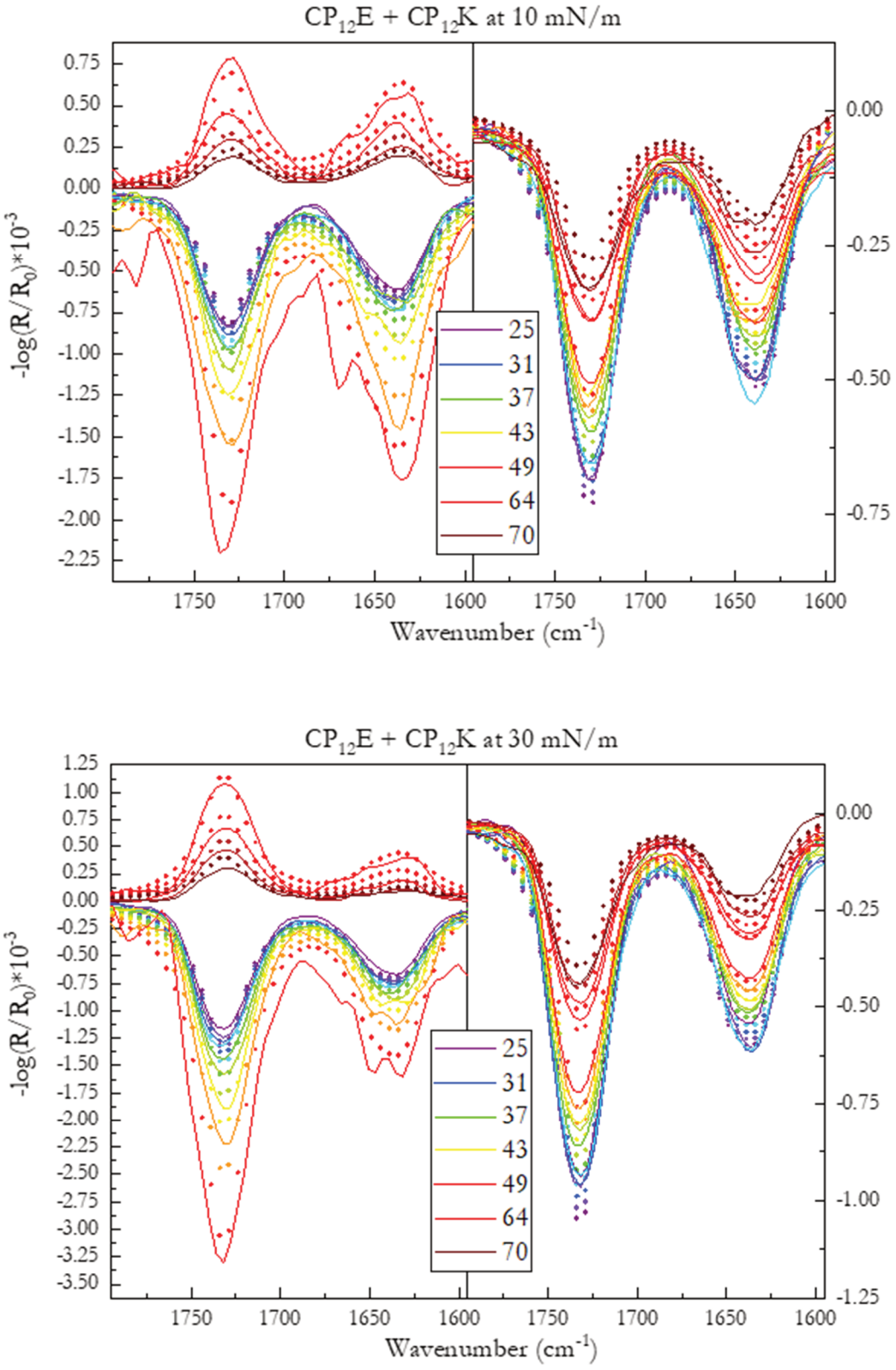


**Figure S14.** *Experimental data of Amide I' absorption bands (1600-1800 cm$^{-1}$, lines), and best fits obtained with Matlab (dots) of $CP_{12}E$ and $CP_{12}K$ decorated monolayers at a surface pressure of 10 mN/m and 30 mN/m. Left graphs are angle dependent P-polarized spectra, right graphs are angle dependent S-polarized spectra. Monolayers consists of 4 mol% lipopeptide, D2O PBS pD 7.4.*

## FITTING PROCEDURE OF S-POLARIZED AMIDE I' IRRAS BANDS

Amide I' absorption bands were evaluated by a Gaussian band fitting procedure by OriginPro 9.1 (OriginLab Corp., USA). S-polarized spectra in the range of 1600–1680 $cm^{-1}$ were averaged over all AoI. Peak positions were fixed at 1631, 1651 and 1671 (± 4) $cm^{-1}$. Free fitting parameters were restricted to sensible boundaries and in some cases fixed to obtain reasonable and comparable results for all spectra. The integrated surface areas of the Gaussian peaks were used to calculate the surface-ratio and hydrophilic fraction of the absorption bands at 1631 and 1651 $cm^{-1}$, for each peptide derivative at both applied surface pressures. The relative change in peak shape as a function of surface pressure may indicate the relative hydrophilicity of the environment of monolayer-tethered peptides, upon assumption of similar secondary structures (α-helices) at both surface pressures.

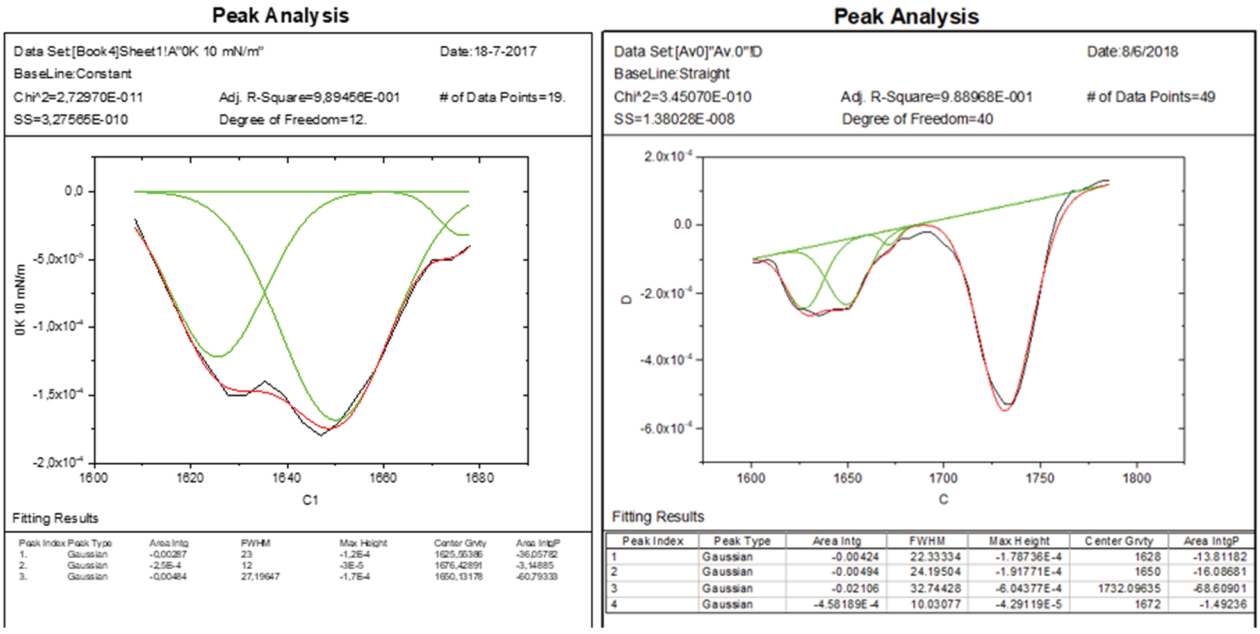


**Figure S15.** *Averaged S-polarized spectra over all AoI of a CP₀K decorated monolayer at a surface pressure of 10 mN/m (left, range of 1600–1680 $cm^{-1}$) and 30 mN/m (right, range of 1600–1780 $cm^{-1}$). Peak positions for the gaussian fitting procedure were fixed at 1631, 1651 and 1671 (± 4) $cm^{-1}$. Monolayers consists of 4 mol% lipopeptide, D2O PBS pD 7.4.*

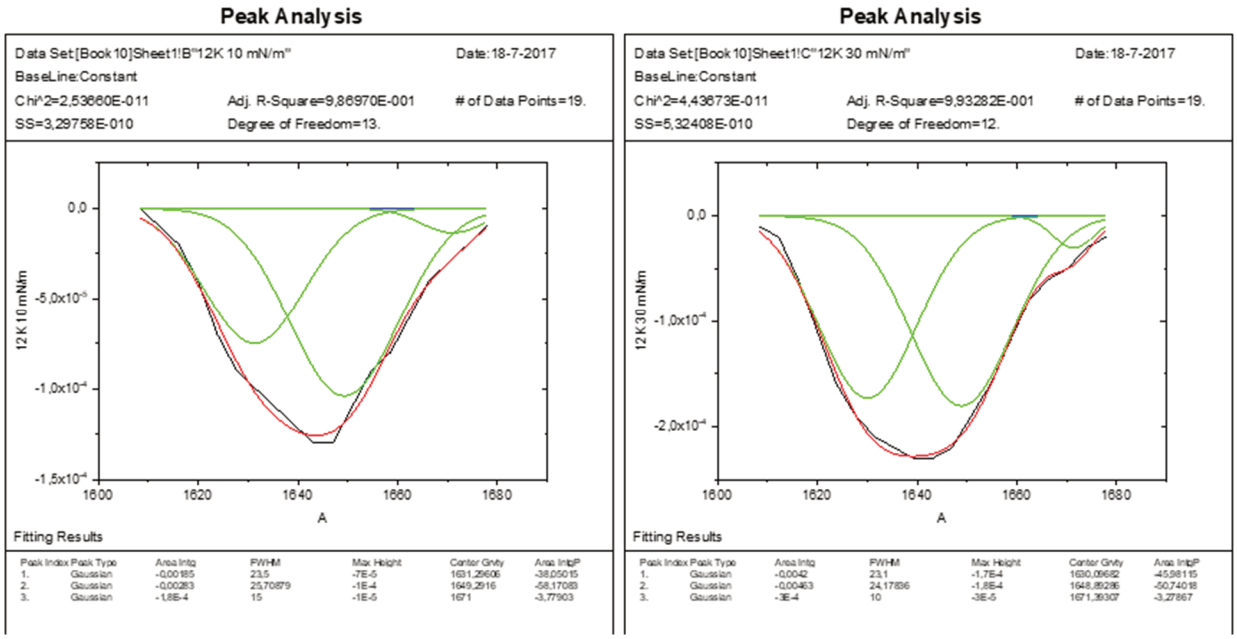


**Figure S16.** *Averaged S-polarized spectra over all AoI in the range of 1600–1680 $cm^{-1}$ of a $CP_{12}K$ decorated monolayer at a surface pressure of 10 mN/m (left) and 30 mN/m (right). Peak positions for the gaussian fitting procedure were fixed at 1631, 1651 and 1671 (± 4) $cm^{-1}$. Monolayers consists of 4 mol% lipopeptide, D2O PBS pD 7.4.*

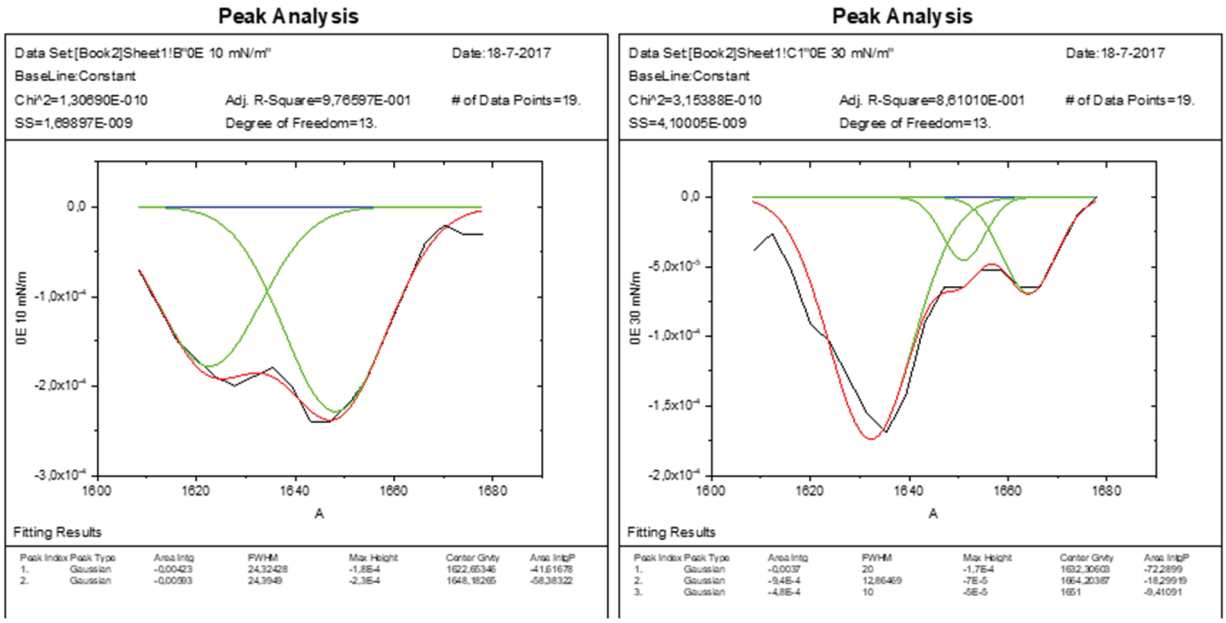


**Figure S17.** *Averaged S-polarized spectra over all AoI in the range of 1600–1680 $cm^{-1}$ of a $CP_0E$ decorated monolayer at a surface pressure of 10 mN/m (left) and 30 mN/m (right). Peak positions for the gaussian fitting procedure were fixed at 1631, 1651 and 1671 (± 4) $cm^{-1}$. Monolayers consists of 4 mol% lipopeptide, D2O PBS pD 7.4.*

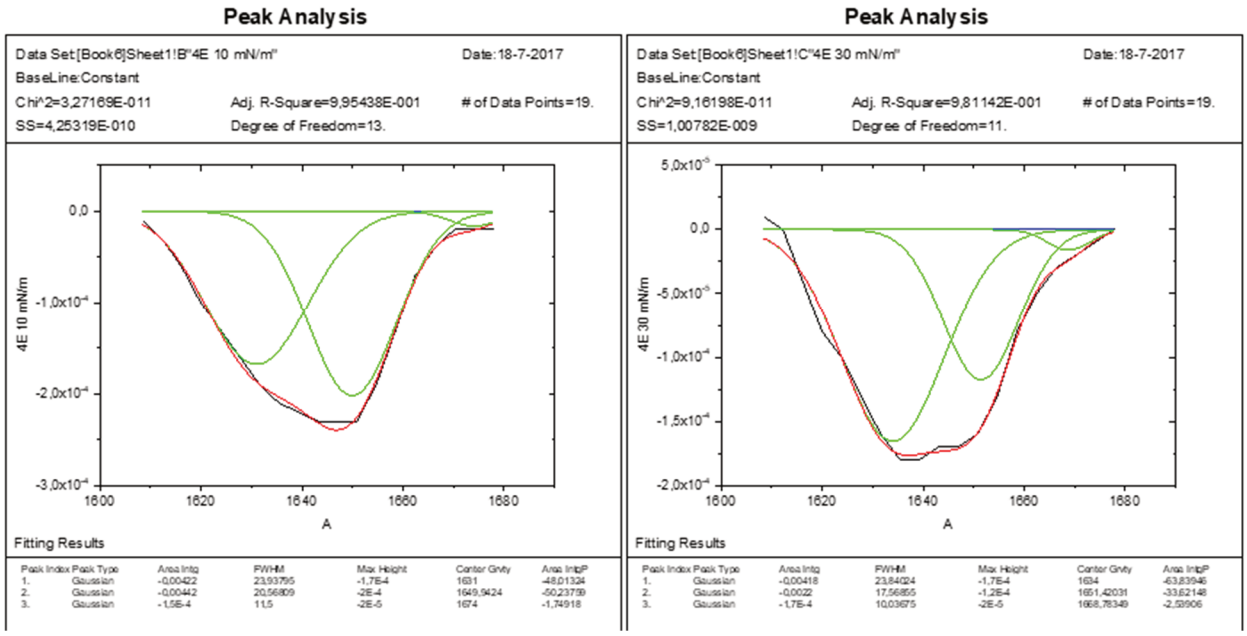


**Figure S18.** *Averaged S-polarized spectra over all AoI in the range of 1600–1680 cm$^{-1}$ of a CP$_4$E decorated monolayer at a surface pressure of 10 mN/m (left) and 30 mN/m (right). Peak positions for the gaussian fitting procedure were fixed at 1631, 1651 and 1671 (± 4) cm$^{-1}$. Monolayers consists of 4 mol% lipopeptide, D2O PBS pD 7.4.*

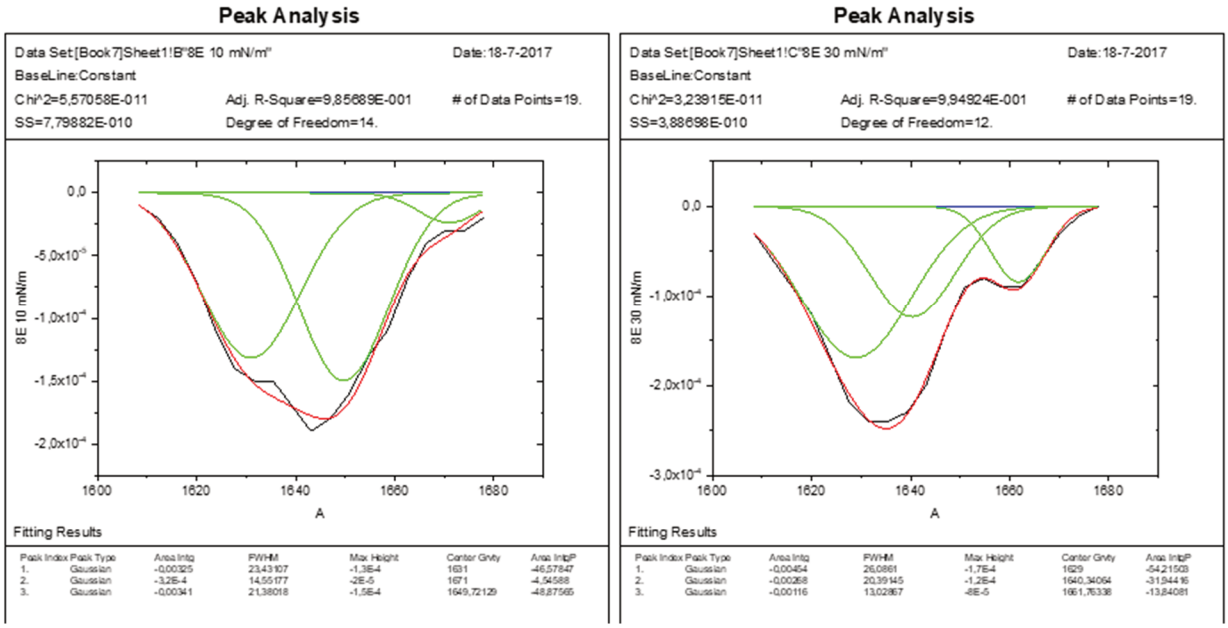


**Figure S19.** *Averaged S-polarized spectra over all AoI in the range of 1600–1680 cm$^{-1}$ of a CP$_8$E decorated monolayer at a surface pressure of 10 mN/m (left) and 30 mN/m (right). Peak positions for the gaussian fitting procedure were fixed at 1631, 1651 and 1671 (± 4) cm$^{-1}$. Monolayers consists of 4 mol% lipopeptide, D2O PBS pD 7.4.*

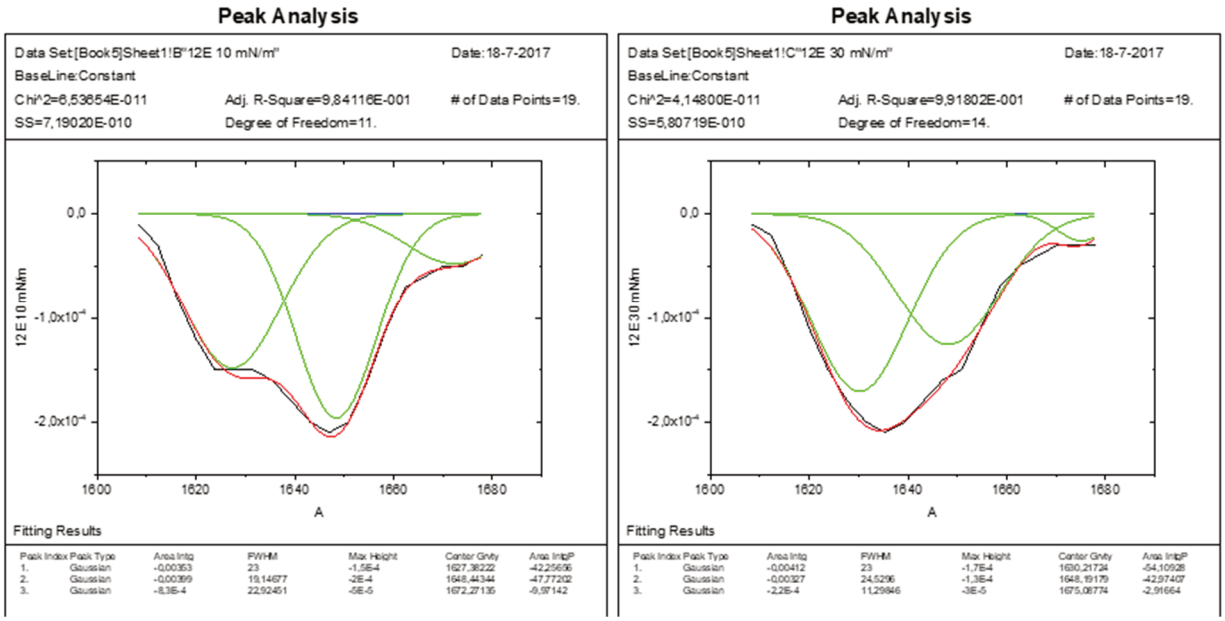


**Figure S20.** *Averaged S-polarized spectra over all AoI in the range of 1600–1680 $cm^{-1}$ of a $CP_{12}E$ decorated monolayer at a surface pressure of 10 mN/m (left) and 30 mN/m (right). Peak positions for the gaussian fitting procedure were fixed at 1631, 1651 and 1671 (± 4) $cm^{-1}$. Monolayers consists of 4 mol% lipopeptide, D2O PBS pD 7.4.*

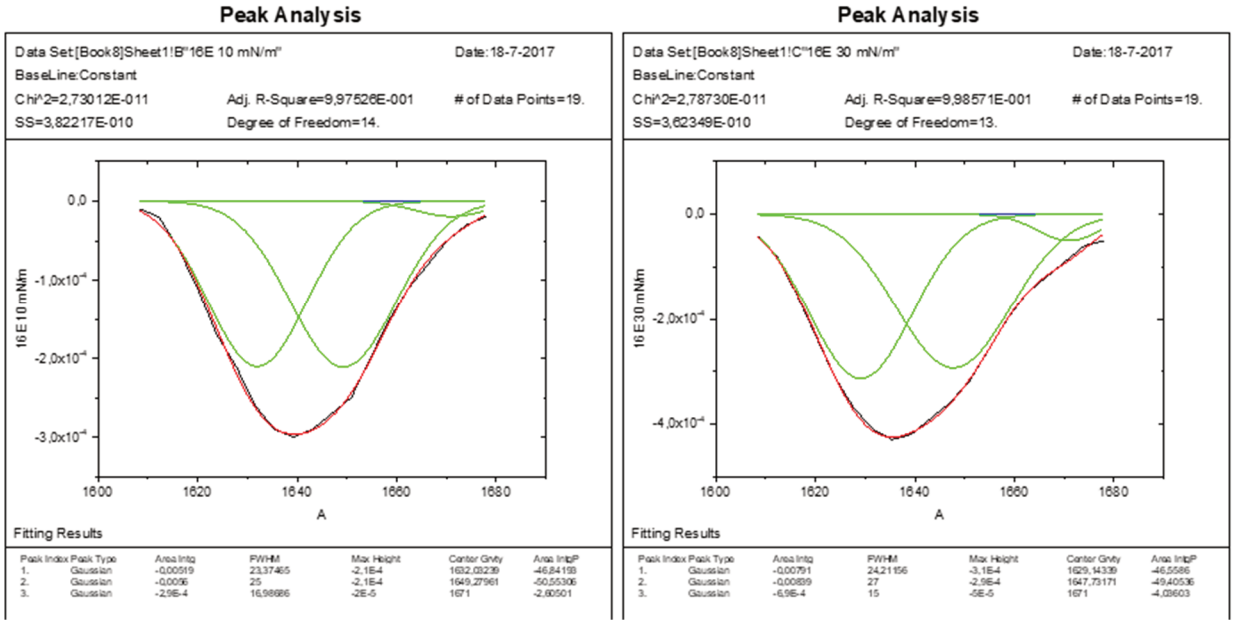


**Figure S21.** *Averaged S-polarized spectra over all AoI in the range of 1600–1680 $cm^{-1}$ of a $CP_{16}E$ decorated monolayer at a surface pressure of 10 mN/m (left) and 30 mN/m (right). Peak positions for the gaussian fitting procedure were fixed at 1631, 1651 and 1671 (± 4) $cm^{-1}$. Monolayers consists of 4 mol% lipopeptide, D2O PBS pD 7.4.*

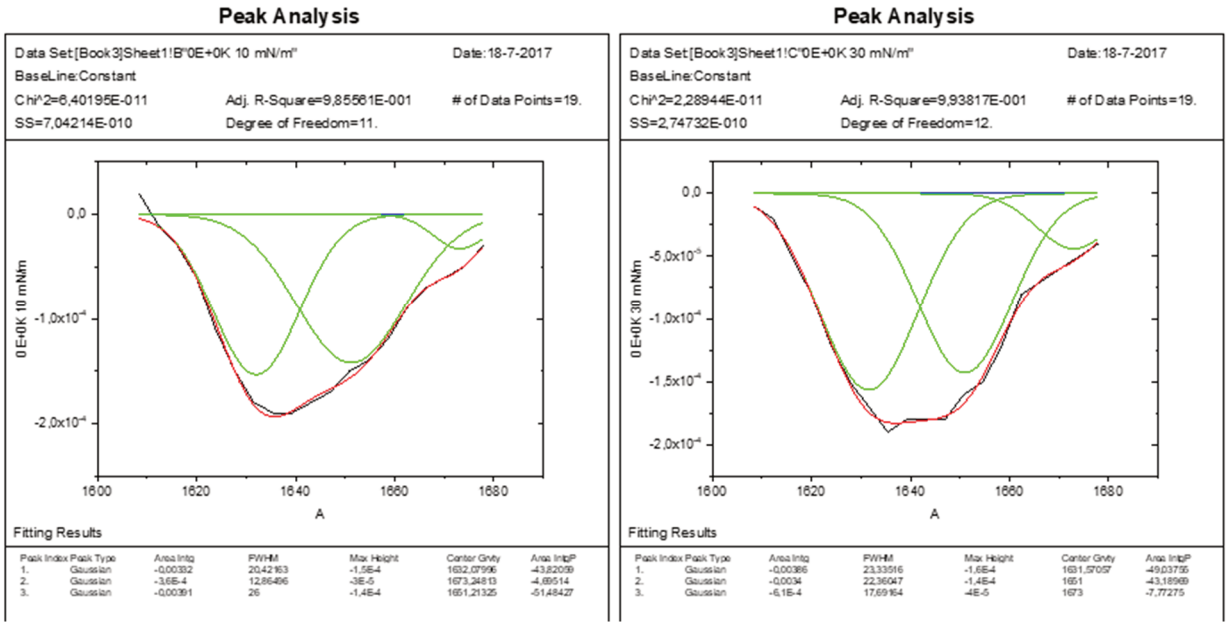


**Figure S22.** *Averaged S-polarized spectra over all AoI in the range of 1600–1680 cm$^{-1}$ of a CP$_0$E and CP$_0$K decorated monolayer at a surface pressure of 10 mN/m (left) and 30 mN/m (right). Peak positions for the gaussian fitting procedure were fixed at 1631, 1651 and 1671 (± 4) cm$^{-1}$. Monolayers consists of 4 mol% lipopeptide, D2O PBS pD 7.4.*

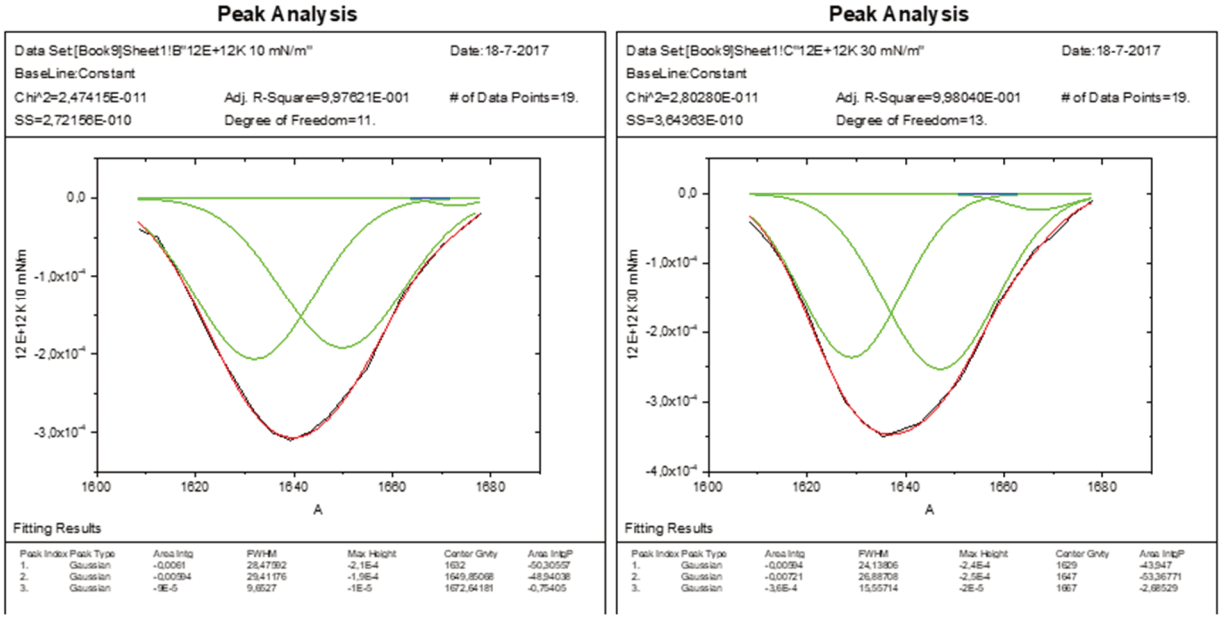


**Figure S23.** *Averaged S-polarized spectra over all AoI in the range of 1600–1680 cm$^{-1}$ of a CP$_{12}$E and CP$_{12}$K decorated monolayer at a surface pressure of 10 mN/m (left) and 30 mN/m (right). Peak positions for the gaussian fitting procedure were fixed at 1631, 1651 and 1671 (± 4) cm$^{-1}$. Monolayers consists of 4 mol% lipopeptide, D2O PBS pD 7.4.*

# REFERENCES


1. Chernomordik, L. V.; Kozlov, M. M., Mechanics of membrane fusion. *Nat. Struct. Mol. Biol.* **2008,** *15* (7), 675-683.
2. Chen, Y. A.; Scheller, R. H., SNARE-mediated membrane fusion. *Nat. Rev. Mol. Cell Biol.* **2001,** *2* (2), 98-106.
3. Jahn, R.; Scheller, R. H., SNAREs--engines for membrane fusion. *Nat. Rev. Mol. Cell Biol.* **2006,** *7* (9), 631-43.
4. Chan, Y. H.; van Lengerich, B.; Boxer, S. G., Lipid-anchored DNA mediates vesicle fusion as observed by lipid and content mixing. *Biointerphases* **2008,** *3* (2), FA17.
5. Marsden, H. R.; Tomatsu, I.; Kros, A., Model systems for membrane fusion. *Chem. Soc. Rev.* **2011,** *40* (3), 1572-1585.
6. Ries, O.; Loffler, P. M. G.; Rabe, A.; Malavan, J. J.; Vogel, S., Efficient liposome fusion mediated by lipid-nucleic acid conjugates. *Org. Biomol. Chem.* **2017,** *15* (42), 8936-8945.
7. Loffler, P. M. G.; Ries, O.; Rabe, A.; Okholm, A. H.; Thomsen, R. P.; Kjems, J.; Vogel, S., A DNA-Programmed Liposome Fusion Cascade. *Angew. Chem., Int. Ed.* **2017,** *56* (43), 13228-13231.
8. Herrmann, A.; Meng, Z.; Yang, J.; Liu, Q.; de Vries, J. W.; Gruszka, A.; Rodriguez-Pulido, A.; Crielaard, B.; Kros, A., Efficient Fusion of Liposomes by Nucleobase Quadruple-Anchored DNA. *Chem. - Eur. J.* **2017**, DOI: 10.1002/chem.201701379.
9. Marsden, H. R.; Elbers, N. A.; Bomans, P. H. H.; Sommerdijk, N.; Kros, A., A Reduced SNARE Model for Membrane Fusion. *Angew. Chem., Int. Ed.* **2009,** *48* (13), 2330-2333.
10. Marsden, H. R.; Korobko, A. V.; Zheng, T. T.; Voskuhl, J.; Kros, A., Controlled liposome fusion mediated by SNARE protein mimics. *Biomater. Sci.* **2013,** *1* (10), 1046-1054.
11. Zheng, T.; Voskuhl, J.; Versluis, F.; Zope, H. R.; Tomatsu, I.; Marsden, H. R.; Kros, A., Controlling the rate of coiled coil driven membrane fusion. *Chem. Commun. (Cambridge, U. K.)* **2013,** *49* (35), 3649-3651.
12. Yang, J.; Bahreman, A.; Daudey, G.; Bussmann, J.; Olsthoorn, R. C.; Kros, A., Drug Delivery via Cell Membrane Fusion Using Lipopeptide Modified Liposomes. *ACS Cent. Sci.* **2016,** *2* (9), 621-630.
13. Yang, J.; Tu, J.; Lamers, G. E. M.; Olsthoorn, R. C. L.; Kros, A., Membrane Fusion Mediated Intracellular Delivery of Lipid Bilayer Coated Mesoporous Silica Nanoparticles. *Adv. Healthc. Mater.* **2017,** *6* (20).
14. Rabe, M.; Aisenbrey, C.; Pluhackova, K.; de Wert, V.; Boyle, A. L.; Bruggeman, D. F.; Kirsch, S. A.; Bockmann, R. A.; Kros, A.; Raap, J.; Bechinger, B., A Coiled-Coil Peptide Shaping Lipid Bilayers upon Fusion. *Biophys. J.* **2016,** *111* (10), 2162-2175.
15. Versluis, F.; Voskuhl, J.; van Kolck, B.; Zope, H.; Bremmer, M.; Albregtse, T.; Kros, A., In situ modification of plain liposomes with lipidated coiled coil forming peptides induces membrane fusion. *J. Am. Chem. Soc.* **2013,** *135* (21), 8057-8062.
16. Daudey, G. A.; Zope, H. R.; Voskuhl, J.; Kros, A.; Boyle, A. L., Membrane-Fusogen Distance Is Critical for Efficient Coiled-Coil-Peptide-Mediated Liposome Fusion. *Langmuir* **2017,** *33* (43), 12443-12452.
17. Rabe, M.; Schwieger, C.; Zope, H. R.; Versluis, F.; Kros, A., Membrane Interactions of Fusogenic Coiled-Coil Peptides: Implications for Lipopeptide Mediated Vesicle Fusion. *Langmuir* **2014,** *30* (26), 7724-7735.
18. Winterhalter, H.; Burner, H.; Marzinka, S.; Benz, R.; Kasianowicz, J. J., Interaction of Poly(Ethylene-Glycols) with Air-Water Interfaces and Lipid Monolayers - Investigations on Surface Pressure and Surface-Potential. *Biophys. J.* **1995,** *69* (4), 1372-1381.

19. Gew, L. T.; Misran, M., Interaction between C18 fatty acids and DOPE PEG2000 in Langmuir monolayers: effect of degree of unsaturation. *J. Biol. Phys.* **2017,** *43* (3), 397-414.
20. Macdonald, R. I., Membrane-Fusion Due to Dehydration by Polyethylene-Glycol, Dextran, or Sucrose. *Biochemistry* **1985,** *24* (15), 4058-4066.
21. Arnold, K.; Pratsch, L.; Gawrisch, K., Effect of Poly(Ethylene Glycol) on Phospholipid Hydration and Polarity of the External Phase. *Biochim. Biophys. Acta* **1983,** *728* (1), 121-128.
22. Barth, A., Infrared spectroscopy of proteins. *Biochim. Biophys. Acta, Bioenerg.* **2007,** *1767* (9), 1073-1101.
23. Manas, E. S.; Getahun, Z.; Wright, W. W.; DeGrado, W. F.; Vanderkooi, J. M., Infrared spectra of amide groups in alpha-helical proteins: Evidence for hydrogen bonding between helices and water. *J. Am. Chem. Soc.* **2000,** *122* (41), 9883-9890.
24. Walsh, S. T. R.; Cheng, R. P.; Wright, W. W.; Alonso, D. O. V.; Daggett, V.; Vanderkooi, J. M.; DeGrado, W. F., The hydration of amides in helices; a comprehensive picture from molecular dynamics, IR, and NMR. *Protein Sci.* **2003,** *12* (3), 520-531.
25. Brewer, S. H.; Tang, Y. F.; Vu, D. M.; Gnanakaran, S.; Raeigh, D. P.; Dyer, R. B., Temperature Dependence of Water Interactions with the Amide Carbonyls of alpha-Helices. *Biochemistry* **2012,** *51* (26), 5293-5299.
26. Wang, T.; Lau, W. L.; DeGrado, W. F.; Gai, F., T-jump infrared study of the folding mechanism of coiled-coil GCN4-p1. *Biophys. J.* **2005,** *89* (6), 4180-4187.
27. Heimburg, T.; Schunemann, J.; Weber, K.; Geisler, N., FTIR-spectroscopy of multistranded coiled coil proteins. *Biochemistry* **1999,** *38* (39), 12727-12734.
28. Rabe, M.; Zope, H. R.; Kros, A., Interplay between Lipid Interaction and Homo-coiling of Membrane-Tethered Coiled-Coil Peptides. *Langmuir* **2015,** *31* (36), 9953-9964.
29. Pahler, G.; Panse, C.; Diederichsen, U.; Janshoff, A., Coiled-Coil Formation on Lipid Bilayers-Implications for Docking and Fusion Efficiency. *Biophys. J.* **2012,** *103* (11), 2295-2303.
30. Andrushchenko, V. V.; Vogel, H. J.; Prenner, E. J., Optimization of the hydrochloric acid concentration used for trifluoroacetate removal from synthetic peptides. *J. Pept. Sci.* **2007,** *13* (1), 37-43.
31. Bulacu, M.; Sevink, G. J. A., Computational insight in the role of fusogenic lipopeptides at the onset of liposome fusion. *Biochim. Biophys. Acta, Biomembr.* **2015,** *1848* (3), 848-858.
32. Glasoe, P. K.; Long, F. A., Use of Glass Electrodes to Measure Acidities in Deuterium Oxide. *J. Phys. Chem.* **1960,** *64* (1), 188-190.
33. Kuzmin, V. L.; Mikhailov, A. V., Molecular Theory of Light-Reflection and the Applicability Limits of a Macroscopic Approach. *Opt. Spektrosk.* **1981,** *51* (4), 691-695.
34. Flach, C. R.; Gericke, A.; Mendelsohn, R., Quantitative determination of molecular chain tilt angles in monolayer films at the air/water interface: Infrared reflection/absorption spectroscopy of behenic acid methyl ester. *J. Phys. Chem. B* **1997,** *101* (1), 58-65.
35. Schwieger, C.; Chen, B.; Tschierske, C.; Kressler, J.; Blume, A., Organization of T-Shaped Facial Amphiphiles at the Air/Water Interface Studied by Infrared Reflection Absorption Spectroscopy. *J. Phys. Chem. B* **2012,** *116* (40), 12245-12256.
36. Bertie, J. E.; Ahmed, M. K.; Eysel, H. H., Infrared Intensities of Liquids .5. Optical and Dielectric-Constants, Integrated-Intensities, and Dipole-Moment Derivatives of H2o and D2o at 22-Degrees-C. *J. Phys. Chem.* **1989,** *93* (6), 2210-2218.
37. Marsh, D.; Muller, M.; Schmitt, F. J., Orientation of the infrared transition moments for an alpha-helix. *Biophys. J.* **2000,** *78* (5), 2499-2510.

# CHAPTER IV

## DIMERS OF PEPTIDE K: (SUPER)SECONDARY STRUCTURES AND FUSOGENIC ACTIVITY

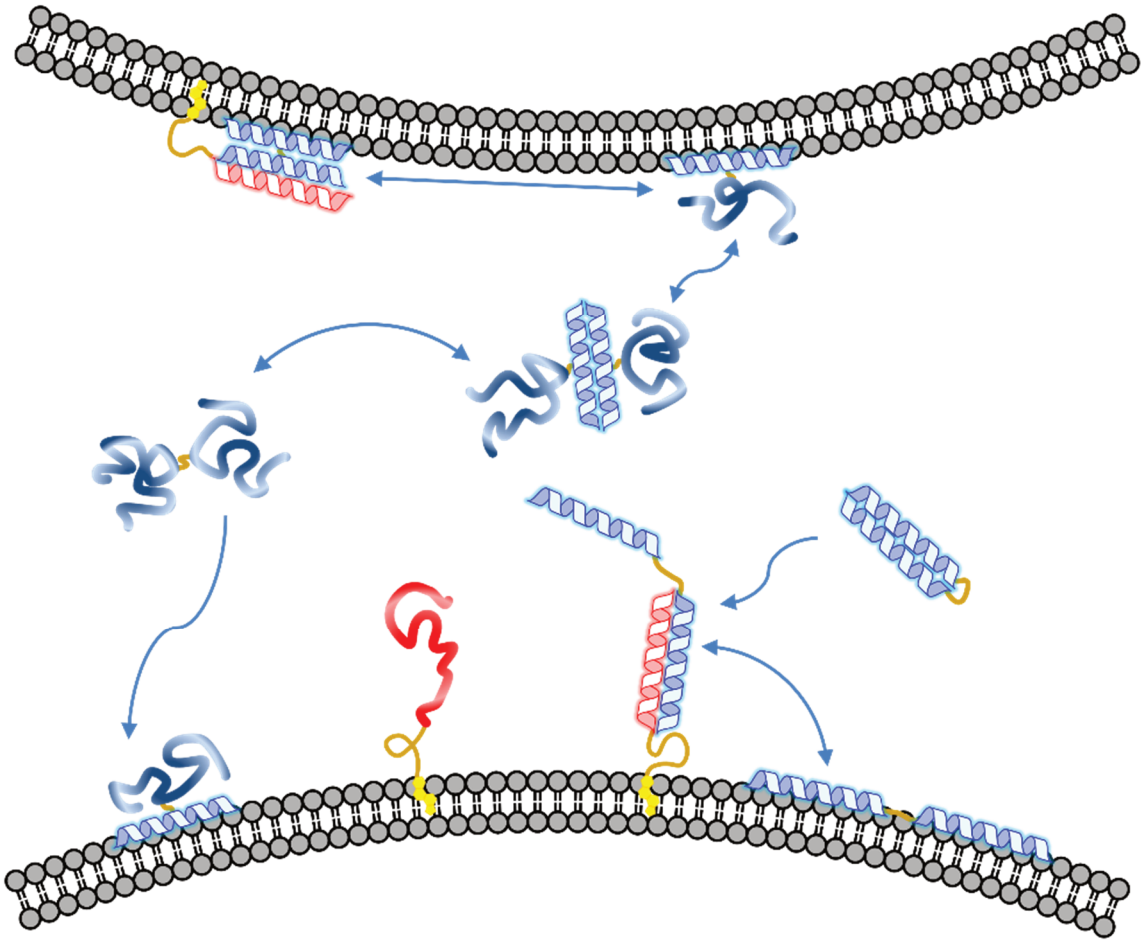

## ABSTRACT

In Chapter III, we demonstrated the asymmetric roleplay of membrane anchored coiled-coil lipopeptides CPE and CPK in the process of liposome fusion. The asymmetric behavior of these lipopeptides originates from the different affinities of the E and K peptides to phospholipid membranes. To further study the membrane affinity of peptide K, covalently linked K dimers were synthesized with disulfide bridges in the second heptad of the peptide backbone (f-K*c*K) or between the N-terminal ends (n-K*c*K). The effect of the linker region was investigated with N-terminal K dimers by using a rigid *p*-fluorobenzene (n-K*b*K) or a flexible $PEG_{600}$ (n-K*p*K) moiety as a spacer. We found that N-terminal modifications promoted intramolecular coiled-coil interactions accompanied with a Tm around 70 °C, but n-K*b*K showed both intra- and intermolecular coiled-coil interactions. Conversely, f-K*c*K showed only intermolecular interactions, and unfolded at 35 °C. Furthermore, f-K*c*K and n-K*c*K were found to trigger fusion of CPE functionalized liposomes, with N-terminally linked n-K*c*K being more efficient compared to Cys(14) linked f-K*c*K.

# INTRODUCTION

In the previous chapters, structure and fusogenic activity relationships of the heterodimeric coiled-coil peptides E $(EIAALEK)_3$ and K $(KIAALKE)_3$ were investigated. The secondary structure of the peptides changed significant upon membrane immobilization, and the resulting (super)-secondary structures were found to be highly important for the fusogenic efficiency of these peptides. Membrane tethering of these peptides is achieved via lipidation, but the position of the membrane anchor at the peptide sequence was found to influence the peptide structure and the related fusogenic efficiency.[1-2] Besides the designed E-K heterodimeric coiled-coil formation, it has been demonstrated that peptide K interacts strongly with phospholipid membranes, while membrane tethered peptide E was mainly found as homomeric coiled-coils, thereby both enhancing the fusion efficiency.[3-4]

Recently, an intramolecular homomeric coiled-coil formation was found for polymers with two covalent peptide K strands.[5] This non-favorable coiled-coil interaction depends on the distance between the 2 peptide K strands and was stronger at a shorter distance, but only minor effort was put in the understanding of this forced homodimer formation. Furthermore, by connecting two or more peptides using short linkers, fairly complex assembled structures can be formed as a result of the well-defined folding pattern of each single peptide folding motif.[6-10] Peptides have also been conjugated to larger synthetic polymeric backbones, such as poly(ethylene glycol) (PEG),[11-12] in order to create a wider range of supramolecular hybrid materials and nanostructures, including peptide-polymer hybrid hydrogels,[13-15] fibrils,[16] and micelles.[17]

Therefore, conjugated homodimers of peptide K can be used to further probe the peptide behavior. A high local peptide concentration will influence the secondary structures and equilibria between various interactions of these peptide dimers. Secondly, the type and position of the linker could have an additional influence on the peptide structure by favoring or disabling intramolecular coiled-coil formation of the covalent peptide dimer. Also, the various peptide derivatives will exhibit differences in binding affinities and peptide-membrane interactions, which would allow for an in-depth study of peptide homodimer formation. Furthermore, strong K-K homodimer formation could

interfere with the formation of the E-K heterodimer, which can be used to influence equilibria between various peptide-peptide interactions.

Since the coiled-coil peptide pair E and K is highly fusogenic, it is envisaged that these K dimers could trigger fusion of liposomes bearing peptide E. Usually, fusion of liposomes is initiated via heterodimeric coiled-coil formation between liposomes functionalized with lipopeptide derivatives of E and K.[18] However, here two liposomes functionalized with lipopeptide E will be brought into close proximity and concomitant fusion via the sequential binding to one K dimer present in solution. The influence of the used K dimer derivative on the fusion efficiency will reveal the structure-activity relationships of these peptide fusogens. This approach will allow the study of peptide fusogens with both membrane-bound and solvated peptides.

## DESIGN OF THE STUDY

A versatile peptide modification is the incorporation of a cysteine residue into the primary sequence, which is frequently used for intramolecular peptide stapling.[19] To control intramolecular peptide-peptide interactions, two different linking positions were introduced in the peptidic backbone; a N-terminal Cys functionalization, or a Cys incorporation at the **f** position in the second heptad, which yield peptides n-K and f-K respectively. Intramolecular homodimer formation is disabled by the latter modification via steric hindrance, while the N-terminal modification could enhance homodimer formation. To investigate the influence of the length and the nature of the linker region on homodimer formation, we introduced various linkers: a short disulfide bridge, a rigid *p*-fluorobenzene spacer,[20] and a PEG-based linker with an average mass of 600 Da (±13 repeating ethylene glycol units based on NMR measurements). (*Figure 17*)

Binding affinities of the different homomers are quantified via concentration- and temperature-dependent CD measurements, and analyzed using *FitDis!*.[21] The peptide secondary/tertiary structure was also evaluated in the presence of plain liposomes and CPE functionalized liposomes, to investigate whether K-dimers interact with lipid membranes in the absence or presence of membrane anchored CPE. Furthermore, lipid mixing assays were used to determine the fusion efficiency of f-K*c*K and n-K*c*K with CPE functionalized liposomes.

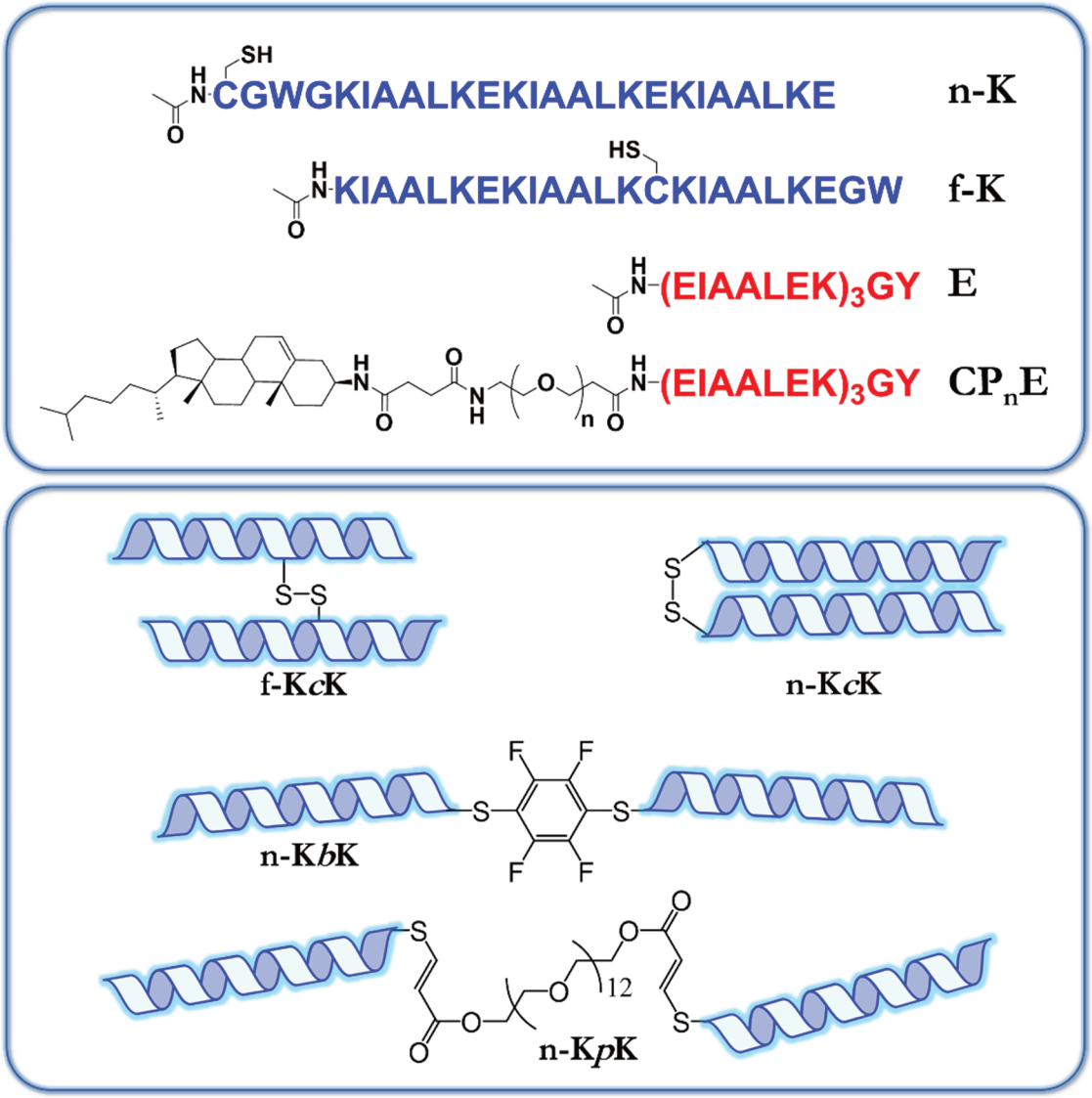


**Figure 17.** *Overview of peptide sequences of K and its cognate partner E, and structure of cholesterol-anchored E peptides (n = 8, 12). The lower box depicts the four K dimers used in this study.*

## RESULTS AND DISCUSSION

### DISULFIDE DIMERS

The (super)secondary structure of K*c*K dimers is affected by the position of the linker at the peptide backbone, as illustrated in Figure 18. For f-K*c*K, the extend of helicity is highly dependent on peptide concentration and shows a $T_m$ of 35 °C at 150 mM. The peptide structure of the N-terminal linked n-K*c*K is independent of peptide concentration and shows a relatively high $T_m$ of 70 °C. These observations suggest an intermolecular interaction for the sterically hindered f-K*c*K dimer, and a more stable intramolecular interaction for the N-terminal linked n-K*c*K dimer.

## N-TERMINAL K DIMERS WITH LINKER

The type of the linker highly affected the peptide structure of N-terminally dimerized K peptides, as shown in Figure 19. The rigid *p*-fluorobenzene linker of n-K*b*K induced structural characteristics of both intra- and intermolecular interactions, as shown by a high melting temperature and a concentration dependent peptide helicity. The flexible $PEG_{600}$ linker of n-K*p*K showed only a slight dependency on peptide concentration and dimerized predominantly via intramolecular interactions.

## ANALYSIS OF K-HOMODIMER MELTING CURVES

Analysis of concentration dependent thermal unfolding curves by FitDis![21] revealed the oligomeric state of the peptide K dimers and provided the binding characteristics of the coiled-coil peptide interactions. (*Table 7, Figure 20*) The exclusive intramolecular interaction of n-K*c*K is supported by a best fit with an oligomer state (*n*) of 1. On the other hand, similar values for $K_F$ and Tm of f-K*c*K and monomeric K demonstrate the intermolecular coiled-coil interaction of f-K*c*K, which is further supported by a best fit with $n = 2$. The high RMSE values obtained for n-K*b*K show that these peptide interactions are less defined, and do not form a solely intra- or intermolecular coiled-coil structure.

**Table 7.** *FitDis analysis of CD melting curves.*

| Peptide | K monomer [a] | f-K*c*K | n-K*c*K | n-K*b*K | n-K*p*K |
|---|---|---|---|---|---|
| $P_{Tmin} - P_{Tmax}$ / µM [b] | 22 – 178 | 73 - 300 | 40 - 360 | 50 - 400 | 40 – 300 |
| Found $\upsilon_1, \upsilon_2, \upsilon_3$, [c] | 2 | 2 | 1 | 2 | 2 |
| Tm / °C (50uM) | 23 | 23 | 70 | 65 | 70 |
| ΔH° / kJ mol$^{-1}$ | 163 | 189 | 121 | 212 | 333 |
| T° / °C | 92 | 93 | 78 | 131 | 103 |
| $\Delta C_P$ / kJ mol$^{-1}$ K$^{-1}$ | 1.5 | 1.9 | 1.8 | 1.9 | 4.2 |
| $\theta_{F0}$ / $10^3$ | -27.8 | -17.9 | -17.2 | -19.4 | -14.5 |
| $m_{F0}$ | (0) | 65.4 | 64.5 | 80.0 | 78.2 |
| $\theta_{U0}$ / $10^3$ | -3.9 | -3.9 | -4.0 | -3.8 | -4.0 |
| $m_{U0}$ | -10 | (0) | (0) | (0) | (0) |
| $\Delta S_{25}$ / J mol$^{-1}$ K$^{-1}$ | 150 | 119 | 44 | -46 | -101 |
| $\Delta G_{25}$ / kJ mol$^{-1}$ | 20.2 | 22.0 | 10.6 | 26.9 | 32.2 |
| $\Delta H_{25}$ / kJ mol$^{-1}$ | 65.0 | 57.6 | 23.6 | 13.1 | 1.97 |
| $K_{F\,25}$ / M$^{-1}$ | $3.4 \times 10^3$ | $7.2 \times 10^3$ | $7.1 \times 10^1$ | $5.1 \times 10^4$ | $4.4 \times 10^5$ |
| $K_{U\,25}$ / M$^{-1}$ | $2.9 \times 10^{-4}$ | $1.4 \times 10^{-4}$ | $1.4 \times 10^{-2}$ | $1.9 \times 10^{-5}$ | $2.3 \times 10^{-6}$ |

*[a] Data taken from Rabe et al.[22] [b] Range of total peptide complex concentration used in experiment. [c] Stoichiometric factors of best fitting model. Values in parenthesis were fixed during all fitting procedures.*

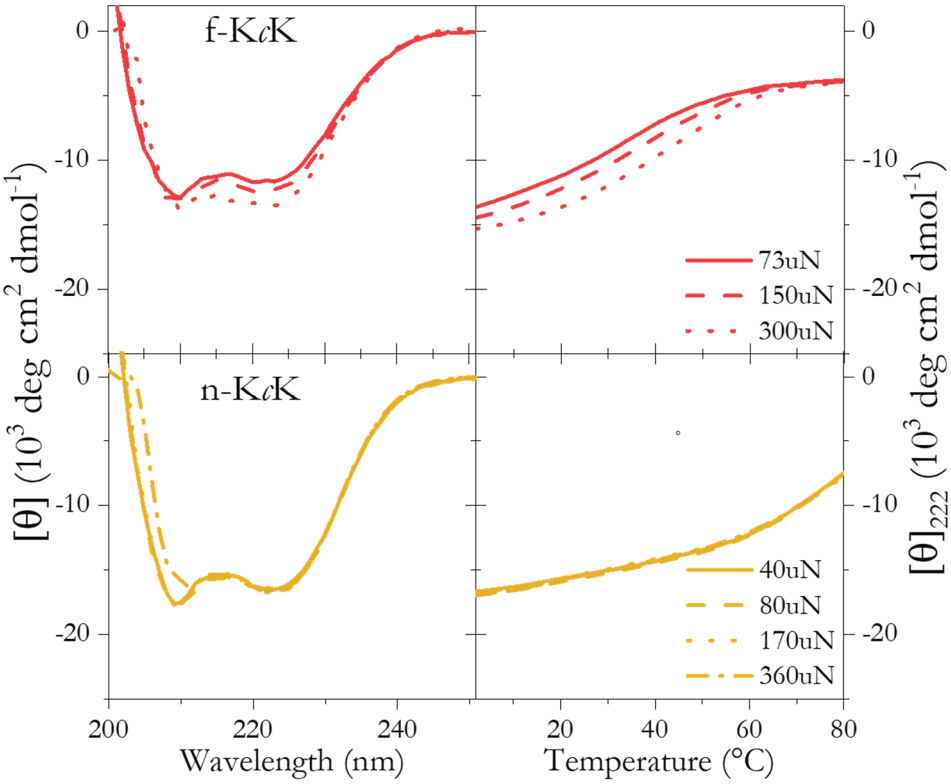


**Figure 18.** *Left: CD spectra of f-KcK and n-KcK at various concentrations, recorded at 20 °C. Right: Concentration dependent thermal unfolding curves of f-KcK and n-KcK. PBS, pH 7.4.*

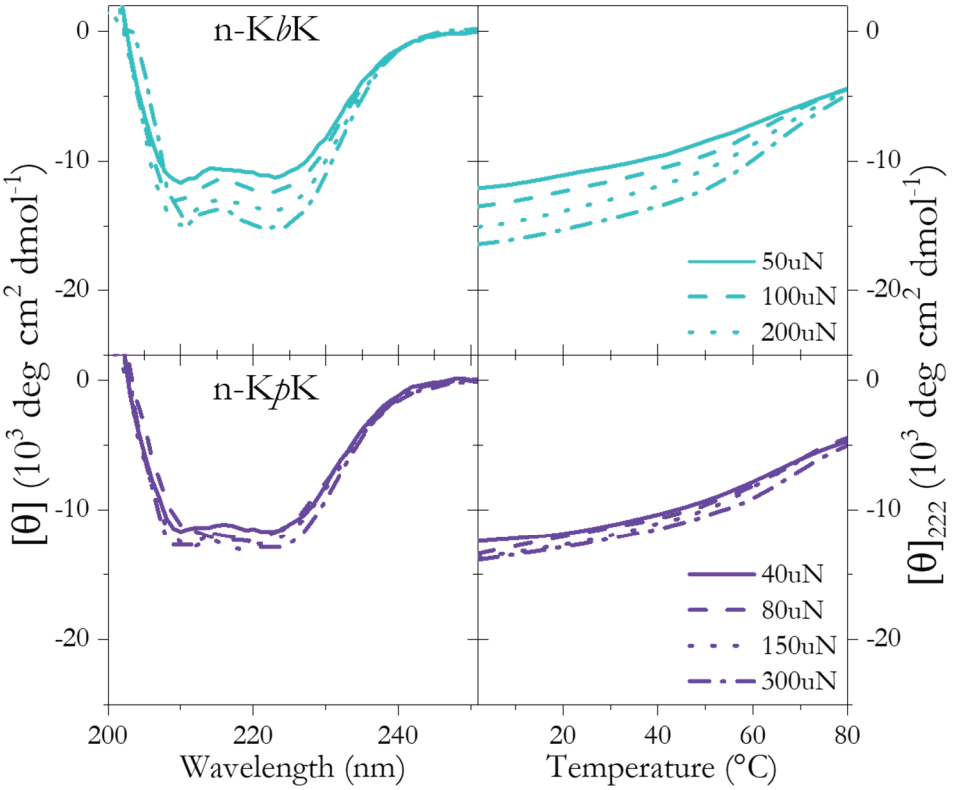


**Figure 19.** *Left: CD spectra of n-KbK and n-KpK at various concentrations, recorded at 20 °C. Right: Concentration dependent thermal unfolding curves of n-K dimers. PBS, pH 7.4.*

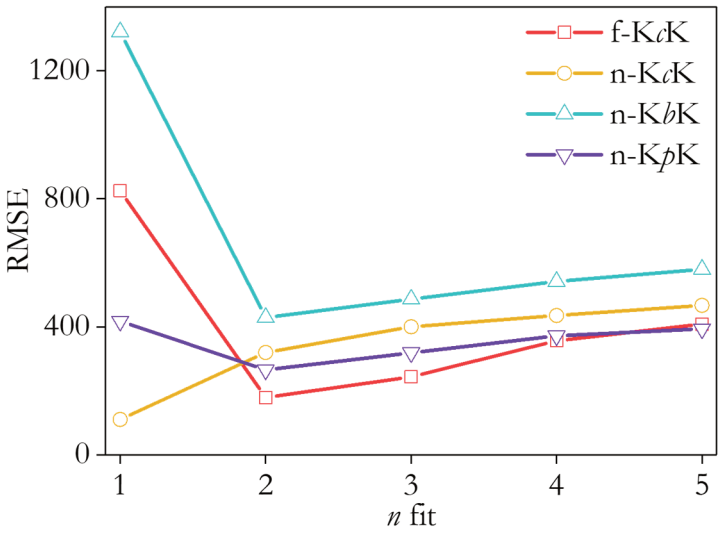


**Figure 20.** *Root mean square error (RMSE) of the fitting of concentration dependent thermal unfolding curves, indicative for coiled-coil oligomer state (n).*

The small differences in RMSE values obtained for n-K*p*K with different oligomer state *n* shows that the data can be described by various parameters, which indicates that both intra- and intermolecular interactions contribute to the coiled-coil formation.

## E + K COILED-COIL INTERACTION

Next, we probed the interaction of the K-dimers with its cognate partner E at room temperature (*Figure 21*). The K-peptides were analyzed with CD-spectroscopy before and after mixing with equimolar amounts of peptide E, and the results are shown in Figure 22 and Table 8.

The N-terminal disulfide dimer n-K*c*K showed an increased helicity and stability over the K monomer and the other dimeric derivatives, which supports the intramolecular stabilization of the homomeric peptide interaction. The slight decrease in helicity with respect to the K monomer observed for all other K-dimers is accompanied by a slight increase in $\theta_{222}/\theta_{208}$ ratio, which points towards slightly distorted helices with a higher degree of coiled-coil formation for dimeric peptides.

Upon mixing dimeric K and peptide E in equal normality, a heterodimeric coiled-coil formation is evidenced in all cases by an increase in helicity. However, coiled-coil formation between E and K dimers is less pronounced compared to coiled-coils involving monomeric K. The covalent linker could very well interfere with heteromeric

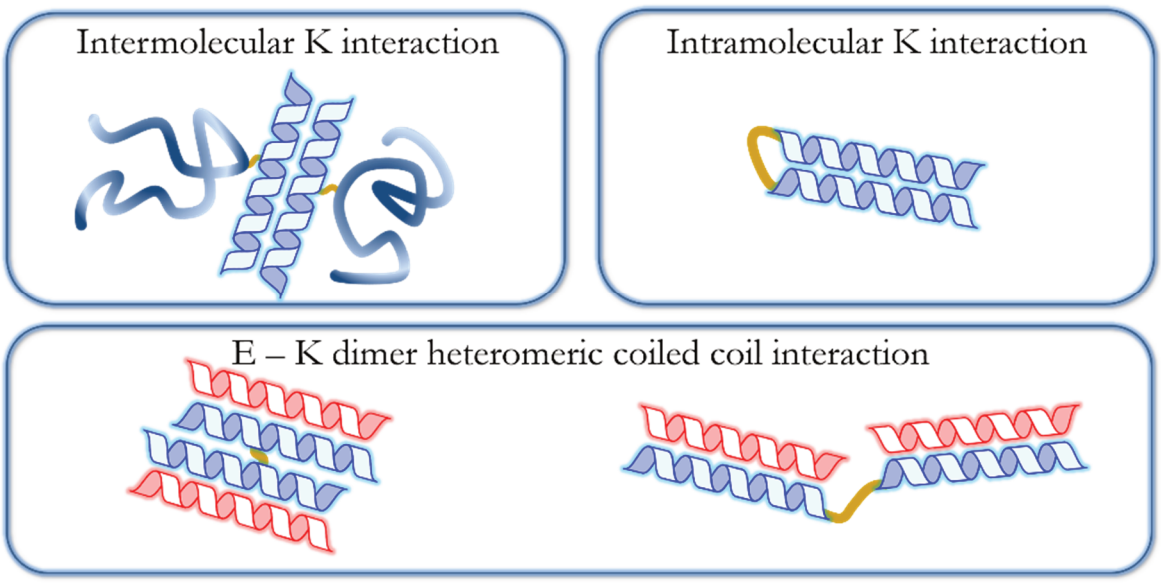


**Figure 21.** *Overview of inter- and intramolecular homodimeric interactions in K dimers, and the heterodimeric coiled-coil formation between E and K dimers.*

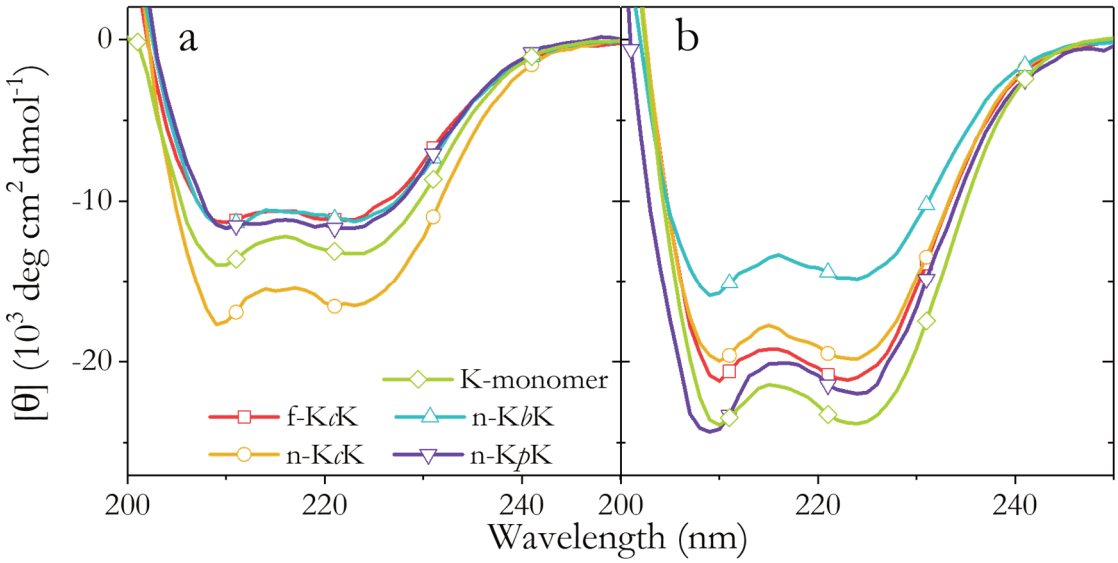


**Figure 22.** *CD spectra of K dimers (a), and an equimolar mixture of K dimers with peptide E (b). [Total peptide] = 40uN, in PBS pH 7.4, 20 °C.*

**Table 8.** *Degree of peptide helicity of K – E heterodimeric coiled-coil formation.*

| | | K-monomer | f-K*c*K | n-K*c*K | n-K*b*K | n-K*p*K |
|---|---|---|---|---|---|---|
| PBS | %H | 41 | 35 | 52 | 35 | 36 |
| | $\theta_{222}/\theta_{208}$ | 0.9 | 1 | 0.9 | 1 | 1 |
| K + E | %H | 74 | 66 | 62 | 46 | 69 |
| | $\theta_{222}/\theta_{208}$ | 1 | 1 | 1 | 0.9 | 0.9 |
| Helicity increase (%) | | 100 | 79 | 45 | 29 | 85 |

coiled-coil formation via steric effects, causing an equilibrium between K-K homodimers and E-K heterodimers.The influence of the linker on this equilibrium can be estimated via the relative helicity increase, compared to native E and K. To calculate the relative increase in helicity for the K dimers upon mixing with E, the helicity of the coiled-coil formation of monomeric K and E was taken as 100%. (*Table 8*) The data shows that heterodimeric coiled-coil formation of E with f-K*c*K and n-K*p*K closely match with the hetero coiled-coil structure of E and monomeric K, with 80% relative helicities at $\theta_{222}$. Minor differences in absorbance at $\theta_{208}$ could indicate small linker-induced structural differences for these two K-dimers. Conversely, for n-K*c*K a relative helicity around 45% was found. Combined with the relatively high association constant of this homodimer formation, this data suggests a competition between intramolecular homodimeric and intermolecular heterodimeric coiled-coil formation. For n-K*b*K, the relative helicity of only 30% indicates that heteromeric coiled-coil formation is inhibited. Since the homodimer interaction and the coiled-coil melting temperature are similar to n-K*c*K, an additional factor should be accounted for, next to homodimer stability. This is most likely an electrostatic π – peptide or π – π interaction of the rigid tetrafluoro-biscysteine spacer moiety which could be further investigated by UV spectroscopy but is not performed in the scope of this study.

## PEPTIDE MEMBRANE INTERACTION

As demonstrated in Chapters II and III, peptide K interacts spontaneously with lipid membranes, and this behavior becomes more pronounced with elongated peptides sequences resulting in more efficient membrane fusion[23] or when peptides are tethered to a membrane.[3] It was anticipated that the K dimers also interact with membranes, but differences between the various derivatives are clearly visible, as shown in Figure 23 and Table 9.

For n-K*c*K and n-K*p*K, peptide helicities increase only slightly in the presence of plain vesicles, supporting the very stable intramolecular interaction shown for these peptide dimers; these interactions are not disrupted in the presence of vesicles. When the membrane surface is functionalized with $CP_{12}E$ however, the helicity of the resulting peptide structures is increased, via disruption of the homodimeric intramolecular K – K coiled-coil formation and formation of the heterodimeric $CP_{12}E$ – K coiled-coil

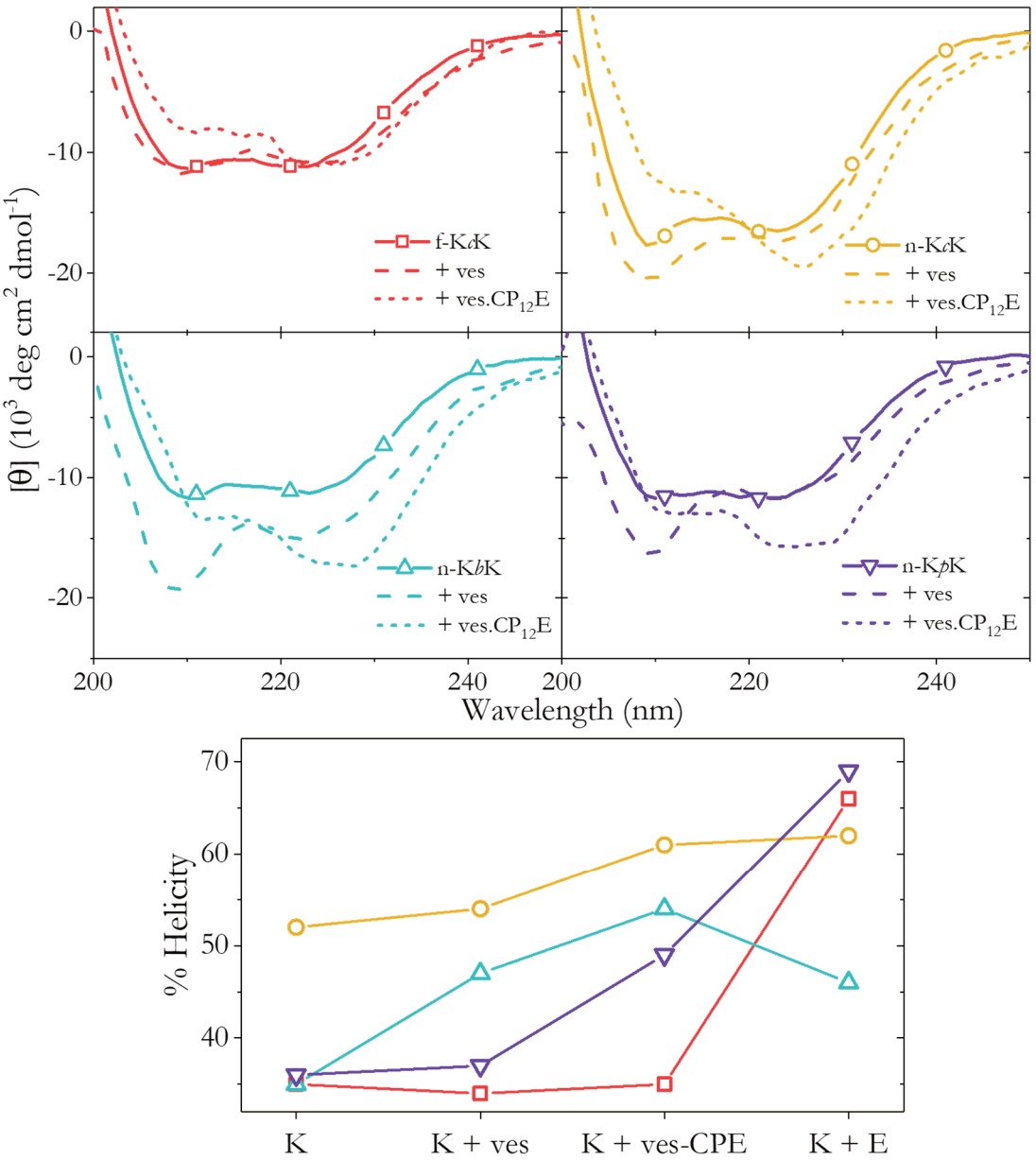


**Figure 23.** *CD spectra of solvated K dimers, a mixture of K dimers and vesicles and a mixture of K dimers and $CP_{12}E$ decorated vesicles. Lower graph shows degree of peptide helicity as determined from CD. [Total lipid] = 0.5mM, [total peptide] = 10 uN, in PBS pH 7.4. Functionalized vesicles contained 2% $CP_{12}E$.*

**Table 9.** *Degree of peptide helicity of K – vesicle interactions.*

| K-dimer + | | f-K*c*K | n-K*c*K | n-K*b*K | n-K*p*K |
|---|---|---|---|---|---|
| PBS | %H | 35 | 52 | 35 | 36 |
| | $\Theta_{222}/\theta_{208}$ | 1.0 | 0.9 | 1.0 | 1.0 |
| Vesicles (0.5 mM) | %H | 34 | 54 | 47 | 37 |
| | $\Theta_{222}/\theta_{208}$ | 0.9 | 0.8 | 0.8 | 0.7 |
| Vesicles + $CP_{12}E$ [a] | %H | 35 | 61 | 54 | 49 |
| | $\Theta_{222}/\theta_{208}$ | 1.3 | 1.5 | 1.3 | 1.2 |

[a] *2 mol% lipopeptide functionalization, [K] / [E] = 1.*

formation. It has been shown that this structural motif is an intermediate stage for the K – membrane interaction, since the membrane interaction occurs concomitant to heteromeric coiled-coil formation of lipopeptides.[24] Therefore, the K-dimer is expected to fully immerse in the membrane, but an equilibrium could be established between heteromeric coiled-coil formation and K-dimer – membrane interaction, as is reported for similar peptide systems in Chapter III.

In the presence of plain vesicles, an increase in helicity is only observed for the n-K*b*K dimer. This shows that the membrane interaction is favored over the coiled-coil interaction, and that the transition between these two conformations occurs spontaneously. Therefore, the coiled-coil interaction of this derivative is mostly intermolecular, since intramolecular coiled-coil forming dimers (n-K*c*K, n-K*p*K) did not show this spontaneous incorporation in plain membranes.

Remarkably, f-K*c*K shows similar helicities in both the absence and presence of vesicles. Since this derivative is sterically constrained by the linking site at the backbone, peptide – membrane interactions are accompanied by an energy penalty because one peptide of the peptide dimer is forced into the aqueous phase. This also reduces the number of peptides available for membrane incorporation by at least 50%. Consequently, most of the peptide interactions are intermolecular peptide – peptide interactions, and the presence of vesicles does not influence the overall peptide structures significantly.

## LIPOSOME FUSION

One of the important stages in the fusion cascade, besides full fusion, is hemifusion, when the outer membranes of opposing liposomes are merged. This mixing of phospholipids is measured via the incorporation of a lipidated FRET pair (DOPE-NBD and DOPE-LR) in the membrane of one population of liposomes. Fusion events with non-functionalized liposomes increases the average distance between the FRET components, which increases the donor emission. The standard liposomal fusion model system, as discussed in Chapter II, uses $CP_{12}E$ and $CP_{12}K$ functionalized liposomes to mediate the fusion process. Here, K-dimers are used as solvated fusogens (without a cholesterol anchor) bringing two $CP_nE$ functionalized liposomes in close proximity and concomitant fusion. Therefore, the standard fusion assay was slightly altered: one batch of liposomes bearing peptide $CP_nE$ was decorated with the FRET pair and was mixed

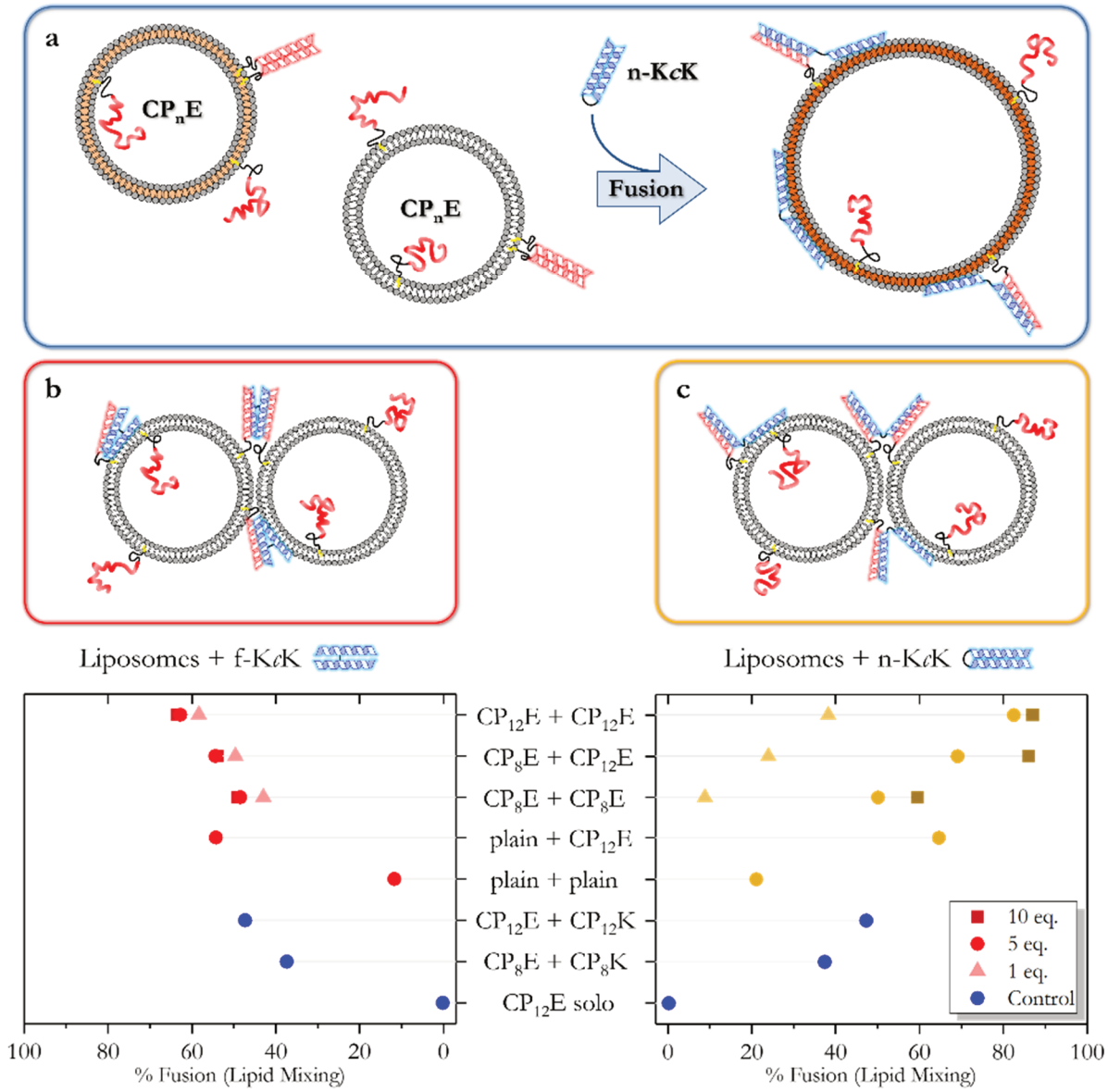


**Figure 24.** *(a) For a successful fusion event, a KcK dimer should form a (simultaneous or sequential) coiled-coil interaction with 2 CPnE peptides, tethered to opposing liposomes. This will force both liposomes in close proximity and concomitant fusion. Relative emission of DOPE-NBD before and after fusion is shown with pale and bright orange colored membranes. Lipid mixing fusion efficiency of CPnE decorated vesicles (n = 8, 12), in the presence of f-KcK (b, red) or n-KcK (c, yellow) at various concentrations (square, 5uN; circle, 2.5 uN; triangle, 0.5 uN; with appropriate color gradient). Control experiments of liposomes lacking E-lipopeptides in the presence of KcK dimer are denoted 'plain'. The fusion efficiency of liposomes functionalized with CPnE and CPnK is added for comparison (blue). [Total lipid] = 0.1 mM, with 1 mol% CPnE, in PBS pH 7.4 20 °C. [KcK] = 5 μN, 2.5 μN, 0.5 μN.*

with non-fluorescent, peptide CP$_n$E bearing liposomes. The K dimer (aq) was added and the NBD emission was measured for 20 minutes. (*Figure 24, Table S3*) The structurally very different dimers f-K*c*K and n-K*c*K were used in this fusion assay as proof of principle. Also, these K-dimers have a high affinity for membrane incorporation, and highly dynamic intermediate stages are expected prior to fusion with several peptides

involved, both K dimers as multiple E peptides, tethered to opposing liposomes. Since it was also shown that the fusion efficiency is influenced by the PEG spacer length of both $CP_nE$ and $CP_nK$,[24] here $CP_8E$ and $CP_{12}E$ are used to determine this effect on the fusion process. The results show that fusion efficiency depends on the K-dimer and on the spacer length of the employed $CP_nE$ derivative.

First of all, with the intermolecular interaction promoting f-K*c*K, fusion between $CP_{12}E$ functionalized liposomes is even more efficient as fusion between $CP_{12}E$ and $CP_{12}K$ decorated liposomes (Chapter II),[24] and did not depend significantly on the peptide dimer concentration in the range of 0.5 μN to 5 μN ([K]:[E] = 1:1 to 10:1). For n-K*c*K however, fusion does depend on peptide dimer concentration. At [n-K*c*K] = 0.5uN, fusion is less efficient compared to f-K*c*K, while at higher concentrations fusion becomes more efficient, reaching fusion efficiencies around 90% at 10-fold peptide excess.

The increasing fusion efficiency for liposomes functionalized with E lipopeptides with increasing spacer length, is illustrated here by a linear correlation between cumulative spacer lengths ($n + n$) and fusion efficiency, and this trend was observed with both K*c*K-dimers at all measured concentrations. Furthermore, control experiments showed that efficient fusion already occurred between non-functionalized liposomes and $CP_{12}E$ functionalized liposomes (plain + $CP_{12}E$), for both K*c*K-dimers. This shows that peptide K first interacts with $CP_{12}E$ decorated liposomes, which then proceed to interact and fuse with non-functionalized liposomes. This supports the findings of Chapters II and III that the fusion mechanism involves both E and K peptides and the K – membrane interaction. It further demonstrates the main role of peptide E in the fusion mechanism: trigger the dissociation of the stable homodimer of n-K*c*K and facilitate docking of the liposomes.

## CONCLUSIONS

Conjugation of two K peptides increases the stability of the homodimer formation, but the site and nature of the linker moiety highly influences the equilibrium between intra- and intermolecular interactions. A linking site at the second heptad and opposed to the hydrophobic core prohibited the intramolecular peptide interaction via steric hindrance, and yielded a $T_m$ similar to single K, around 35 °C. Furthermore, we found no significant peptide stabilization by lipid membranes. Since massive peptide induced liposomal aggregation was found at high lipid concentrations (indicative for significant peptide – membrane interactions), we strongly think that the peptide structure is similar in peptide – peptide interactions and peptide – membrane interactions.

With a N-terminal linking site and a flexible spacer, n-K*p*K showed a $T_m \approx 70$ °C, while a spontaneous peptide – membrane interaction was not observed. Therefore, n-K*p*K forms highly stable intramolecular coiled-coil homodimers. In the presence of membrane tethered $CP_{12}E$ however, peptide helicities increased sharply, indicative for disruption of the homodimer structure, and the formation of heteromeric coiled-coil structures and/or membrane immersion.

A rigid *p*-fluorobenzene linker affected the heteromeric coiled-coil formation between E and n-K*b*K, as only 30% helicity increase was observed in the presence of E. Remarkably, a spontaneous peptide-membrane interaction was only measured with this derivative.

Solvated K dimers are very efficient in mediating fusion between $CP_{12}E$ functionalized liposomes, as measured by lipid mixing, with efficiencies reaching 90%, even higher than the reported values of fusion mediated by membrane-tethered $CP_{12}E$ and $CP_{12}K$. No significant influence of [f-K*c*K] was found in the range of 1 eq. to 10 eq. with respect to the peptide decoration at the liposomes, while [n-K*c*K] highly enhanced the fusion efficiency with increasing concentration. Fusion efficiencies depended linearly on the cumulative spacer lengths of the E lipopeptides. Also, the fusion mechanisms involve both E and K lipopeptides and the K – membrane interaction as $CP_{12}E$ decorated liposomes were found to fuse with non-functionalized liposomes in the presence of K*c*K dimers. Finally, the main role of peptide E is to cause the dissociation of the stable homodimer formation of n-K*c*K, and to facilitate docking of the liposomes.

## FUTURE WORK

In this work, the fundamental characteristics of K dimers are explored, and compared to the native K structure and behavior. The understanding of structure and function relationships opens ways to the rational design of coiled-coil peptide dimers and multimers, with tunable binding strengths and defined equilibria between intra- and intermolecular interactions. Investigations could start with the evaluation of f-K dimers with a rigid hexafluorobenzene linker or a flexible $PEG_{600}$ linker. Also, a C-terminal Cys handle can be introduced in the peptides, and the effect of this modification can be correlated to the behavior of N-terminal linked dimers. The linker series can be extended with a well-defined tetraethyleneglycol spacer, in combination with Cysteine containing peptides n-K and f-K. Furthermore, a $PEG_{2000}$-dialkyne, and $PEG_{5000}$-tetraalkyne are available and azide-functionalized peptides can be conjugated to these linkers via the CuAAC click reaction. These multimeric peptide-dimers with elongated spacers can also be useful to trigger aggregation of peptide functionalized particles.

Next, K*c*K and K*b*K dimers can be used to determine the effect of the linker type and linker position on their fusogenic activity via lipid and content mixing assays. The understanding of the fusion mechanism with non-anchored peptides will allow the development of fusion systems with an external and site-specific trigger, which could have broad implications for drug delivery systems, and would increase the understanding of naturally occurring multicomponent coiled-coil interactions. Furthermore, the f-K*c*K dimer can be functionalized with a single or double N-terminal Chol-$PEG_4$ anchor. The resulting constructs can be tethered to liposomes, which could yield very high fusion efficiencies with $CP_{12}E$ decorated liposomes. Furthermore, surprising peptide conformations and membrane interactions could be obtained, due to the intrinsic steric hindrance of these peptide dimers and the tight membrane immobilization via the double cholesterol anchor. Finally, various E dimers can be synthesized like the different K dimers. Since membrane tethered E shows a tendency to form homodimers, and even homotetramers *in silico*,[25] surprisingly stable binding affinities could be found. Mixing of E dimers with K dimers could result in many different interlocked coiled-coil structures, depending on concentration and peptide ratio, and would allow the study of multivalent coiled-coil peptide aggregates.

# EXPERIMENTAL SECTION

## MATERIALS

See Chapter II. Fmoc-Cys was purchased from NovaBioChem. PEG(600)-OH and propiolic acid were obtained from Sigma Aldrich. PBS buffer contains 20 mM $PO_4^{3-}$, 150 mM NaCl, pH 7.4. Peptide concentrations are calculated in Normality, to compensate for dimerization (2 uN = 1 uM).

## METHODS

**Liposome preparation.** A 1 mM stock solution containing DOPC : DOPE : cholesterol (50 : 25 : 25 mol%) lipids in 1 : 1 (v/ v) methanol : chloroform was prepared for all fusion experiments. Lipopeptides were dissolved in 1 : 1 (v/v) chloroform : methanol at 50 μM concentration.

Lipid mixing experiments: liposomes bearing 1 mol% of a FRET pair are required besides plain liposomes, and an additional 1 mM stock solution of DOPC : DOPE : cholesterol : DOPE-LR : DOPE-NBD (49.5 : 24.75 : 24.75 : 0.5 : 0.5mol%) in 1 : 1 (v:v) methanol : chloroform was made. 1 mol% of the lipopeptide solution was mixed with the appropriate liposome solution and the solvent was removed under a stream of air. The dry lipid/peptide layer was rehydrated with PBS. These solutions were subsequently sonicated for 5-10 minutes at 55 °C to yield ~100 nm diameter liposomes,[27] and used without further purification.

**Fluorescence spectroscopy.** Lipid-mixing experiments were performed on a TECAN Infinite M1000 PRO fluorimeter using a 96-well plate at 25 °C. The percentage of fluorescence increase %F was calculated as:

$$\%F = \frac{F(t) - F_0}{F_{max} - F_0} * 100$$

For lipid-mixing experiments the fluorescence intensity F(t) was monitored, by measuring NBD emission at 530 nm in a continuous fashion for 20 min upon addition of K*d*K dimer solution to a equimolar mixture of fluorescent liposomes and non-fluorescent

liposomes. $F_0$ was determined by measuring NBD emission of fluorescent liposomes to which an equal amount of PBS was added. $F_{max}$ was determined by using plain liposomes which contained half the concentration of fluorescent lipids. [Total lipid] = 0.1mM, in PBS pH 7.4.

**Circular dichroism spectroscopy.** CD spectra were obtained using a Jasco J-815 spectropolarimeter equipped with a peltier temperature controller. The ellipticity, given as mean residue molar ellipticity, [θ] (deg $cm^2$ $dmol^{-1}$), is calculated using the following equation

$$[\theta] = \frac{100 * \theta_{obs}}{nlc}$$

where $\theta_{obs}$ is the observed ellipticity (mdeg), *n* is the number of peptide residues, *l* is the path length of the cuvette (cm) and *c* is the peptide concentration (mM). Spectra were recorded from 260 nm to 200 nm at 20 °C. Data points were collected with a 1 nm bandwidth at 1 nm intervals, using a scan speed of 1 nm $s^{-1}$. Each spectrum was an average of 5 scans. For analysis, each spectrum had the proper background spectrum (PBS, or plain liposomes in PBS) subtracted. Percentage α-helicity was calculated using the predicted value $[\theta]_{222}$=-39500*(1-2.57/n) as 100% value for an α-helical peptide of *n* residues.[26] For temperature dependent measurements $[\theta]_{222}$ was recorded as a function of temperature, with a range of 2 - 80°C and ΔT = 40°C/h. For experiments involving liposomes, [Total lipid] = 0.5mM, with 1mol% lipopeptide, in PBS pH 7.4.

**Dynamic light scattering.** Particle size distributions were measured by dynamic light scattering using a Malvern Zetasizer Nano ZS ZEN3500 equipped with a peltier thermostatic cell holder. The laser wavelength was 633nm and the scattering angle was 173°. The Stokes Einstein relationship

$$D = \frac{k_B T}{3\pi\eta D_h}$$

was used to estimate the hydrodynamic diameter $D_h$. Here, $k_B$ is the Boltzmann constant, η is the solvent viscosity, and measurements were carried out at room temperature.

## SYNTHESIS

**PEG(600)-dialkyne:** PEG(600)-OH (6 grams, 10 mmol) was dissolved in toluene (50 mL) and conc. $H_2SO_4$ (0.1 mL, cat.) was added. The obtained solution was stirred and heated to 80 °C to obtain a clear homogenous solution. Propiolic acid (2,8 grams, 40 mmol, 4 eq.) was added, and the solution was heated to reflux under Dean Stark conditions (± 140 °C). After no more water was collected (± 20 hours), the solution was allowed to cool to rt. Toluene was evaporated *in vacuo* and the residue was dissolved in 20 mL DCM. The obtained solution was washed with saturated $NaHCO_3$ (10 mL) and Brine (10 mL). The organic phase was dried with $Na_2SO_4$, and 0,1 g of activated carbon was added. The activated carbon was removed through vacuum filtration over Celite®545. Vacuum filtration was performed twice for effective removal of the activated coal. The solvent was removed *in vacuo* and the product (5.9g, 96%) was obtained as a clear oil, and was stored in a glass vial in the dark at -20 °C. $^1$H NMR (400MHz, $CDCl_3$) $\delta$ = 4.37 (m, 4H), 3.76 (m, 4H), 3.68 (m, 44H) 2.98 (s, 2H). IR (film) $\nu$ 3213, 2870, 2112, 1713, 1452, 1349, 1225, 1095 cm$^{-1}$; MALDI/TOF $m/z$ 761.211 ($[M+Na]^+$ $C_{34}H_{58}O_{17}Na$ cald. 761.36).

## PEPTIDE SYNTHESIS

**SPPS:** Peptide synthesis was performed on a CEM Liberty I on a 100 μmol scale using Rink amide resin of 0.73 mmol/g substitution. Amino acid activation was achieved using HCTU/DIPEA in DMF. Fmoc deprotection was carried out using 2 cycles of 20% piperidine in DMF. All automated reactions were carried out at 70-80 °C with the use of a microwave. The N-terminal free amine was acylated using a mixture of $Ac_2O$ (50 mM) and DIPEA (12.5 mM) in NMP.

**Cleavage:** The peptides were cleaved from the resin and side-chain deprotected using a mixture of TFA/Thioanisole/EDT/Anisole (90:5:3:2 v/v) for 2h. The peptides were precipitated in cold diethyl ether followed by centrifugation and dried under vacuum.

**Purification:** RP-HPLC was performed with a Shimadzu HPLC system with two LC-8A pumps, and a SPD-10AVP UV-VIS detector. Sample elution was monitored by UV detection at 214 nm and 278 nm. Samples were eluted with a linear gradient from 10% to 50% (v/v) B in A, A being $H_2O$, 0.1% (v/v) TFA, and B being MeCN, 0.1% (v/v) TFA. A Phenomenex C18 reversed phase column (21.2 mm diameter, 150 mm length, 5.00 μM

particle size) was used with a flow rate of 15 mL $min^{-1}$. Collected fractions were tested for >95% purity using LC-MS with Gemini C18 column, pooled and freeze dried.

**K*c*K dimer formation:** Purified K peptides were dissolved in PBS (pH 8.5) and cysteine oxidation was achieved with bubbling of air through the solution for 30 min. The reaction mixture was subjected to RP-HPLC with a linear gradient from 10% to 50% (v/v) B in A, A being $H_2O$, 0.1% (v/v) TFA, and B being MeCN, 0.1% (v/v) TFA. Collected fractions were tested for >95% purity using MALDI/TOF, pooled and freeze dried.

**K*b*K dimer formation:** A stock solution was prepared of hexafluorobenzene in DMSO:$H_2O$ (1:1 v/v). Of this solution, 0.48 eq. were added to a solution of peptide n-K (1 mM) in PBS (0.5 mL, pH 8.5) and the mixture was shaken for 2h at room temperature. The reaction mixture was subjected to RP-HPLC with a linear gradient from 10% to 50% (v/v) B in A, A being $H_2O$, 0.1% (v/v) TFA, and B being MeCN, 0.1% (v/v) TFA. Collected fractions were tested for >95% purity using MALDI/TOF, pooled and freeze dried.

**K*p*K dimer formation:** A stock solution was prepared of PEG(600)-dialkyne in DMSO:$H_2O$ (1:1 v/v). Of this solution, 0.48 eq. were added to a solution of peptide n-K (1 mM) in PBS (0.5 mL, pH 8.5) and the mixture was shaken for 2h at room temperature. The reaction mixture was subjected to RP-HPLC with a linear gradient from 10% to 50% (v/v) B in A, A being $H_2O$, 0.1% (v/v) TFA, and B being MeCN, 0.1% (v/v) TFA. Collected fractions were tested for >95% purity using LC-MS with Gemini C18 column, pooled and freeze dried.

## PEPTIDE ANALYSIS

**Table S2.** *Analysis of synthesized peptides.*

| Peptide | Formula | Calc mass | Observed mass | RT (min) | isoelectric point [a] | Charge [a] |
|---|---|---|---|---|---|---|
| f-K | $C_{118}H_{205}N_{31}O_{28}S$ | 2538.16 | 1269.53 $[M+2H]^{2+}$ | 5.1 | 8.94 | 3.4 |
| n-K | $C_{125}H_{215}N_{33}O_{32}S$ | 2724.33 | 908.87 $[M+3H]^{3+}$ | 5.1 | 8.68 | 2.4 |
| f-K*c*K | $C_{236}H_{408}N_{62}O_{56}S_2$ | 5074.28 | MALDI/TOF | n.d. | | |
| n-K*c*K | $C_{250}H_{428}N_{66}O_{64}S_2$ | 5446.61 | MALDI/TOF | n.d. | | |
| n-K*b*K | $C_{256}H_{428}N_{66}O_{64}S_2F_4$ | 5594.66 | MALDI/TOF | n.d. | | |
| n-K*p*K | $C_{282}H_{484}N_{66}O_{80}S_2$ | 6143.38 | 1536.60 $[M+4H]^{4+}$ | 7.7 | | |

[a] *Calculated with Isoelectric Point Calculator and peptide charge is calculated at pH 7.4.*[28]

## LIPID MIXING FUSION EFFICIENCY

**Table S3.** *Fusion efficiency of $CP_nE$ decorated vesicles in the presence of f-KcK and n-KcK*

| functionalized liposomes 0.1 mM | f-K*c*K 10 uN | f-K*c*K 5 uN | f-K*c*K 1 uN | n-K*c*K 10 uN | n-K*c*K 5 uN | n-K*c*K 1 uN |
|---|---|---|---|---|---|---|
| $CP_8E$ + $CP_8E$ | 49 | 48 | 43 | 60 | 61 | 9 |
| $CP_8E$ + $CP_{12}E$ | 54 | 54 | 50 | 86 | 69 | 24 |
| $CP_{12}E$ + $CP_{12}E$ | 64 | 63 | 58 | 87 | 82 | 38 |
| Plain + $CP_{12}E$ | | 54 | | | 65 | |
| Plain + Plain | | 12 | | | 21 | |

## REFERENCES


1. Crone, N. S. A.; Minnee, D.; Kros, A.; Boyle, A. L., Peptide-Mediated Liposome Fusion: The Effect of Anchor Positioning. *International Journal of Molecular Sciences* **2018,** *19* (1).
2. Versluis, F.; Dominguez, J.; Voskuhl, J.; Kros, A., Coiled-coil driven membrane fusion: zipper-like vs. non-zipper-like peptide orientation. *Faraday Discuss.* **2013,** *166*, 349-359.
3. Rabe, M.; Zope, H. R.; Kros, A., Interplay between Lipid Interaction and Homo-coiling of Membrane-Tethered Coiled-Coil Peptides. *Langmuir* **2015,** *31* (36), 9953-9964.
4. Rabe, M.; Aisenbrey, C.; Pluhackova, K.; de Wert, V.; Boyle, A. L.; Bruggeman, D. F.; Kirsch, S. A.; Bockmann, R. A.; Kros, A.; Raap, J.; Bechinger, B., A Coiled-Coil Peptide Shaping Lipid Bilayers upon Fusion. *Biophys. J.* **2016,** *111* (10), 2162-2175.
5. Gerling-Driessen, U. I. M.; Mujkic-Ninnemann, N.; Ponader, D.; Schone, D.; Hartmann, L.; Koksch, B., Exploiting Oligo(amido amine) Backbones for the Multivalent Presentation of Coiled-Coil Peptides. *Biomacromolecules* **2015,** *16* (8), 2394-2402.
6. Gradisar, H.; Bozic, S.; Doles, T.; Vengust, D.; Hafner-Bratkovic, I.; Mertelj, A.; Webb, B.; Sali, A.; Klavzar, S.; Jerala, R., Design of a single-chain polypeptide tetrahedron assembled from coiled-coil segments. *Nature Chemical Biology* **2013,** *9* (6), 362-+.
7. Boyle, A. L.; Bromley, E. H. C.; Bartlett, G. J.; Sessions, R. B.; Sharp, T. H.; Williams, C. L.; Curmi, P. M. G.; Forde, N. R.; Linke, H.; Woolfson, D. N., Squaring the Circle in Peptide Assembly: From Fibers to Discrete Nanostructures by de Novo Design. *Journal of the American Chemical Society* **2012,** *134* (37), 15457-15467.
8. Larsen, A. N.; Sorensen, K. K.; Johansen, N. T.; Martel, A.; Kirkensgaard, J. J. K.; Jensen, K. J.; Arleth, L.; Midtgaard, S. R., Dimeric peptides with three different linkers self-assemble with phospholipids to form peptide nanodiscs that stabilize membrane proteins. *Soft Matter* **2016,** *12* (27), 5937-5949.
9. Ljubetic, A.; Lapenta, F.; Gradisar, H.; Drobnak, I.; Aupic, J.; Strmsek, Z.; Lainscek, D.; Hafner-Bratkovic, I.; Majerle, A.; Krivec, N.; Bencina, M.; Pisanski, T.; Velickovic, T. C.; Round, A.; Carazo, J. M.; Melero, R.; Jerala, R., Design of coiled-coil protein-origami cages that self-assemble in vitro and in vivo. *Nature Biotechnology* **2017,** *35* (11), 1094-+.
10. Fletcher, J. M.; Harniman, R. L.; Barnes, F. R. H.; Boyle, A. L.; Collins, A.; Mantell, J.; Sharp, T. H.; Antognozzi, M.; Booth, P. J.; Linden, N.; Miles, M. J.; Sessions, R. B.; Verkade, P.; Woolfson, D. N., Self-Assembling Cages from Coiled-Coil Peptide Modules. *Science* **2013,** *340* (6132), 595-599.
11. Klok, H. A.; Vandermeulen, G. W.; Nuhn, H.; Rosler, A.; Hamley, I. W.; Castelletto, V.; Xu, H.; Sheiko, S. S., Peptide mediated formation of hierarchically organized solution and solid state polymer nanostructures. *Faraday Discuss.* **2005,** *128*, 29-41.
12. Hamley, I. W., PEG-Peptide Conjugates. *Biomacromolecules* **2014,** *15* (5), 1543-1559.
13. Maslovskis, A.; Guilbaud, J. B.; Grillo, I.; Hodson, N.; Miller, A. F.; Saiani, A., Self-Assembling Peptide/Thermoresponsive Polymer Composite Hydrogels: Effect of Peptide-Polymer Interactions on Hydrogel Properties. *Langmuir* **2014,** *30* (34), 10471-10480.
14. Versluis, F.; van Elsland, D. M.; Mytnyk, S.; Perrier, D. L.; Trausel, F.; Poolman, J. M.; Maity, C.; le Sage, V. A.; van Kasteren, S. I.; van Esch, J. H.; Eelkema, R., Negatively Charged Lipid Membranes Catalyze Supramolecular Hydrogel Formation. *J. Am. Chem. Soc.* **2016,** *138* (28), 8670-3.
15. Staples, J. K.; Oshaben, K. M.; Horne, W. S., A modular synthetic platform for the construction of protein-based supramolecular polymers via coiled-coil self-assembly. *Chemical Science* **2012,** *3* (12), 3387-3392.
16. Zhou, M.; Bentley, D.; Ghosh, I., Helical supramolecules and fibers utilizing leucine zipper-displaying dendrimers. *Journal of the American Chemical Society* **2004,** *126* (3), 734-735.

17. Versluis, F.; Marsden, H. R.; Kros, A., Power struggles in peptide-amphiphile nanostructures. *Chem. Soc. Rev.* **2010,** *39* (9), 3434-44.
18. Marsden, H. R.; Korobko, A. V.; Zheng, T. T.; Voskuhl, J.; Kros, A., Controlled liposome fusion mediated by SNARE protein mimics. *Biomater. Sci.* **2013,** *1* (10), 1046-1054.
19. Fairlie, D. P.; de Araujo, A. D., Stapling Peptides Using Cysteine Crosslinking. *Biopolymers* **2016,** *106* (6), 843-852.
20. Spokoyny, A. M.; Zou, Y. K.; Ling, J. J.; Yu, H. T.; Lin, Y. S.; Pentelute, B. L., A Perfluoroaryl-Cysteine SNAr Chemistry Approach to Unprotected Peptide Stapling. *Journal of the American Chemical Society* **2013,** *135* (16), 5946-5949.
21. Rabe, M.; Boyle, A.; Zope, H. R.; Versluis, F.; Kros, A., Determination of Oligomeric States of Peptide Complexes Using Thermal Unfolding Curves. *Biopolymers* **2015,** *104* (2), 65-72.
22. Rabe, M.; Schwieger, C.; Zope, H. R.; Versluis, F.; Kros, A., Membrane Interactions of Fusogenic Coiled-Coil Peptides: Implications for Lipopeptide Mediated Vesicle Fusion. *Langmuir* **2014,** *30* (26), 7724-7735.
23. Zheng, T.; Voskuhl, J.; Versluis, F.; Zope, H. R.; Tomatsu, I.; Marsden, H. R.; Kros, A., Controlling the rate of coiled coil driven membrane fusion. *Chem. Commun. (Cambridge, U. K.)* **2013,** *49* (35), 3649-3651.
24. Daudey, G. A.; Zope, H. R.; Voskuhl, J.; Kros, A.; Boyle, A. L., Membrane-Fusogen Distance Is Critical for Efficient Coiled-Coil-Peptide-Mediated Liposome Fusion. *Langmuir* **2017,** *33* (43), 12443-12452.
25. Bulacu, M.; Sevink, G. J. A., Computational insight in the role of fusogenic lipopeptides at the onset of liposome fusion. *Biochim. Biophys. Acta, Biomembr.* **2015,** *1848* (3), 848-858.
26. Lacroix, E.; Viguera, A. R.; Serrano, L., Elucidating the folding problem of alpha-helices: Local motifs, long-range electrostatics, ionic-strength dependence and prediction of NMR parameters. *Journal of Molecular Biology* **1998,** *284* (1), 173-191.
27. Marsden, H. R.; Elbers, N. A.; Bomans, P. H. H.; Sommerdijk, N.; Kros, A., A Reduced SNARE Model for Membrane Fusion. *Angew. Chem., Int. Ed.* **2009,** *48* (13), 2330-2333.
28. Kozlowski, L. P., IPC - Isoelectric Point Calculator. *Biology Direct* **2016,** *11*.

# CHAPTER V

## LIPOSOME FUSION WITH ORTHOGONAL COILED-COIL PEPTIDES AS FUSOGENS: PEPTIDE ROLEPLAY IS CRITICAL FOR EFFICIENT FUSION

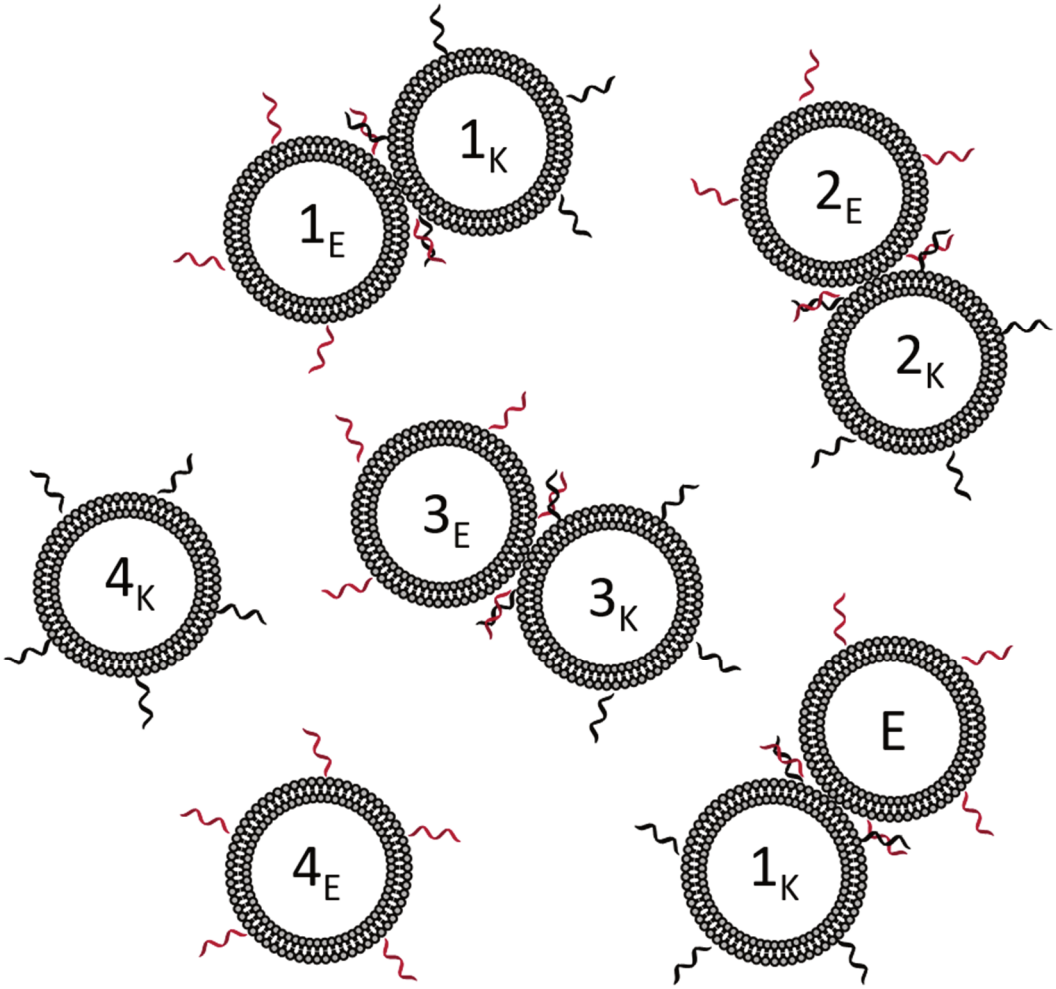

## ABSTRACT

Biological membrane fusion is a highly specific and coordinated process, with multiple different vesicular fusion events proceeding simultaneously in the complex environment of a cell. Specific molecular recognition between transport vesicles and target membranes is established by various proteins, mostly belonging to the SNARE family of proteins, with minimal recognition between non-complementary proteins to avoid non-targeted fusion events. Here, specific recognition is introduced to a liposomal fusion model system by using lipidated derivatives of a set of four *de novo* designed heterodimeric coiled-coil peptide pairs. Content mixing of liposomes was only obtained between liposomes functionalized with complementary peptides, demonstrating the fusogenic activity of various coiled-coil peptides in general. The used peptide fusogens differ in coiled-coil binding affinities and peptide-membrane interactions which allowed us to study the relationship of the peptide characteristics and the efficiency of the fusion process. It was found that peptide-membrane interactions enhanced the fusion process, especially when the affinity between complementary peptides was relatively low. Furthermore, a new coiled-coil pair ($E/1_K$) was discovered, which was demonstrated to be an efficient fusogen together with coiled-coil pairs $2_E/2_K$ and $3_E/3_K$. These results will have broad implications for drug delivery systems by enabling targeted delivery of different carrier vesicles at various peptide-functionalized locations.

# INTRODUCTION

Artificial membrane fusion is a steadily expanding field which allows the exploration of drug delivery systems and the study of cellular transport. In the last two decades, a variety of model systems were developed using phospho-lipid mimics of biological membranes with DNA,[1-9] peptides,[10-13] or small molecules[14-20] acting as fusogens. Most model systems are based on single complementary recognition units,[21] and thus are a limited mimic of the specific fusion events occurring in nature.[22-23] In cells, multiple different 'cargo vesicles' are transported to and delivered at precise locations in a complex environment, mainly mediated by the well-conserved class of SNARE-proteins.[24-25] Therefore, the ability to mimic the specificity of biological membrane fusion is the next challenge in the field of artificial membrane fusion. This would enable future drug delivery applications by enabling the development of simultaneous and/or site-specific fusion events.

Recently, the Vogel group achieved specific recognition with DNA based fusogens in a three-step liposomal fusion cascade.[8] However, their model system showed only efficient fusion at 50 °C, making their approach unsuitable for biological application. Our efforts in liposome fusion with the lipidated heterodimeric coiled-coil pair E and K (amino acid sequence $(EIAALEK)_3$ and $(KIAALKE)_3$ showed that lipidated coiled-coil peptides can mediate the fusion of liposomes in biological environments. Lipidation of peptides enables the insertion of these conjugates in liposomal membranes. Therefore, specific recognition in a liposomal fusion model system at biologically relevant temperatures could be achieved by using lipidated derivatives of orthogonal coiled-coil peptides. In recent years sets of orthogonal heterodimeric coiled-coil peptides became available via *de novo* peptide design.[26-31] These peptide pairs are able to form coiled-coils exclusively with their cognate partner while interactions with other (coiled-coil) peptides and homo-interactions are negligible.

Several orthogonal sets of heterodimeric coiled-coil peptides have been designed to date.[32-37] Although selective coiled-coil binding was demonstrated for all these sets of complementary peptides, they have to meet additional requirements to be useful candidates for peptide mediated fusion systems. Firstly, the coiled-coil peptides should interact at temperatures up to at least 30 °C to be applicable as fusogens at biologically

relevant temperatures, which is not the case for several sets of peptides developed by de groups of Aili and Woolfson.[32, 36-37] Also, the candidate peptides should not bind to biological targets to avoid unintended interactions, as could be the case with the set of coiled-coil peptides derived from Leucine peptide zipper DNA binding peptides.[35] The maximum number of potential pairs developed by Kennan was limited to 3 pairs due to a minimalistic approach using 3 heptad repeat peptides only.[33] Recently, this issue was solved by using 4 heptad repeat peptides (dubbed here $P_E/P_K$ with P = 1 - 4). Elongation of the peptide sequence increased the coiled-coil stability (Tm > 40 °C) and the number of orthogonal pairs of coiled-coil peptides to four,[34] making these peptides useful candidates to be considered as fusogens in a partner specific liposomal fusion system.

Membrane conjugation of coiled-coil peptides can result in a change in the adopted conformation, oligomerization state or membrane interaction resulting in stabilized α-helical structures depending on their amphipathicity.[38-39] For the lipidated heterodimeric coiled-coil pair E and K it was demonstrated that both peptides have a distinct role in the fusion process and that the peptide-membrane interaction of K is crucial for efficient fusion. Here it's important to note that peptide K is an Amphipathic class A peptide.[40] Amphipathic class A peptides in an α-helical conformation have positive charges adjacent to a hydrophobic surface. This leads to stable membrane immersion of folded helices in phospholipid membranes via an electrostatic interaction between upward bended 'snorkeling' Lys sidechains and phosphate headgroups.[41-42] The peptides designed by Jerala can be regarded as analogs of E and K, but have varying electrostatic charges in positions **e** and **g**, and polar Asn residues in the hydrophobic core resulting in varying degree of class A amphipathicity for individual peptide helices.[43-44] Also, (super)secondary structures and membrane interactions of peptide fusogens are thought to be influential on the fusion efficiency and even the fusogen-membrane distance was found to be crucial for efficient fusion.[40, 45-46] Therefore, using this set of membrane anchored $P_E/P_K$ peptides as fusogens in a liposomal fusion assay the influence of the roleplay of the peptide fusogens on the fusion mechanism and the fusion efficiency will be revealed.

## DESIGN OF THE STUDY

Functional membrane tethered complementary recognition motifs as well as soluble N-acetylated peptides were synthesized (*Figure 25*) and the secondary structures of the peptides were measured both in solution and conjugated to phospholipid liposomes. Next, peptide-peptide and peptide-membrane interactions of acylated and lipidated peptides were characterized by temperature and concentration dependent Circular Dichroism (CD) spectroscopy. The ability of the complementary lipidated peptide pairs to mediate fusion was investigated using a content mixing assay. The interactions between the $P_E/P_K$ peptides and the heterodimeric E/K peptide pair were also determined, resulting in the discovery of a new highly fusogenic peptide pair $E/1_K$. Peptide $1_K$ is the only P-peptide with Lys residues at all **e** and **g** positions, enabling a stable membrane immersion with help of the 'snorkeling' mechanism as was found for peptide K. The interplay of peptide amphipathicity and (super)secondary structures, peptide-membrane interactions and fusogenic efficiency of complementary peptides provides further insight as to the mechanism of peptide mediated fusion of liposomes. Remarkably, very efficient fusion with multiple rounds of fusion was only found for fusogens with moderate stability, showing that significant coiled-coil dissociation after a fusion event is crucial for initiating a next fusion event. This study demonstrates the first step toward orthogonal fusion of peptide functionalized liposomes, revealing a significant and distinct influence of coiled-coil binding strength and peptide-membrane interactions on the fusion efficiency.

## PEPTIDE DESIGN AND SYNTHESIS

In this study, 5 heterodimeric coiled-coil peptides and their lipidated derivatives were synthesized. The $P_E/P_K$ four-heptad repeat sequences were taken from Jerala,[34] and the E/K sequences were used previously in membrane fusion studies (Chapter II, *Figure S24*). When folded as helices all peptides possess a small hydrophobic moment. Peptides were synthesized on a Rink Amide resin using automated Solid Phase Peptide Synthesis (SPPS) protocols and Fmoc chemistry. For solution studies the N-termini of the peptides were acylated before cleavage from the resin. For lipopeptide derivatives, the N-termini were functionalized with a PEG spacer of length n (n = 4 or 8 ethylene glycol units) and a

cholesterol anchor.[47] The resulting acylated or lipidated peptides were cleaved from the resin and purified using reverse phase chromatography (RP-HPLC). Details of the peptide design and synthetic protocols are described in the supporting information.

## RESULTS AND DISCUSSION

### ORTHOGONALITY STUDIES

In the original design by Jerala and coworkers, peptides contained helix-stabilizing N-terminal (SPED) and C-terminal (G) modifications creating flexible, helix-disrupting G-SP tripeptide segments between coiled-coil regions in C-N linked polypeptides. These modifications were omitted in this study because lipidated peptides are used instead of polypeptides. The orthogonality of the coiled-coil pairs and the (super)secondary structure of peptides in solution was studied using CD spectroscopy.[48-49] (*Figure 26, Table 10*) The obtained spectra agree with the orthogonal coiled-coil interactions reported by Jerala, showing that the modifications at the peptide termini did not influence the coiled-coil interactions significantly. All possible peptide-peptide combinations were mixed in an equimolar ratio in PBS to study the orthogonality of this set of 10 coiled-coil peptides.

**Table 10.** *$\theta_{222}/\theta_{208}$ ratio of all peptide combinations.*

| | $1_E$ | $1_K$ | $2_E$ | $2_K$ | $3_E$ | $3_K$ | $4_E$ | $4_K$ | E | K |
|---|---|---|---|---|---|---|---|---|---|---|
| K | 0.64 | 0.85 | 0.72 | 0.39 | 0.77 | 0.69 | 0.66 | 0.45 | 1.00 | 0.63 |
| E | 0.42 | 0.99 | 0.53 | 0.43 | 0.50 | 0.96 | 0.62 | 0.41 | 0.48 | |
| $4_K$ | 0.24 | 0.34 | 0.46 | 0.27 | 0.41 | 0.65 | 1.01 | 0.32 | | |
| $4_E$ | 0.39 | 0.54 | 0.74 | 0.47 | 0.78 | 0.77 | 0.71 | | | |
| $3_K$ | 0.41 | 0.49 | 0.55 | 0.63 | 1.01 | 0.82 | | | | |
| $3_E$ | 0.30 | 0.76 | 0.56 | 0.49 | 0.62 | | | | | |
| $2_K$ | 0.25 | 0.33 | 1.06 | 0.34 | | | | | | |
| $2_E$ | 0.38 | 0.55 | 0.80 | | | | | | | |
| $1_K$ | 1.10 | 0.39 | | | | | | | | |
| $1_E$ | 0.20 | | | | | | | | | |

*Measured $\theta_{222}/\theta_{208}$ ratio of all possible combinations of N-acylated peptides $P_E$, $P_K$, E and K. Values >1 are characteristic for coiled-coil formation. [Total peptide] = 200 μM, PBS pH 7.4.*

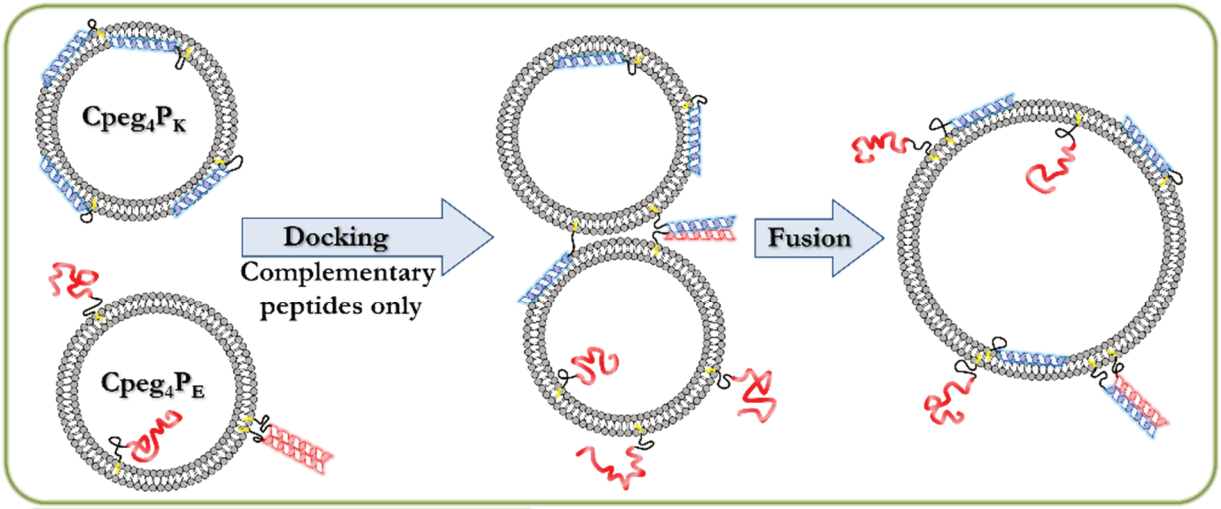


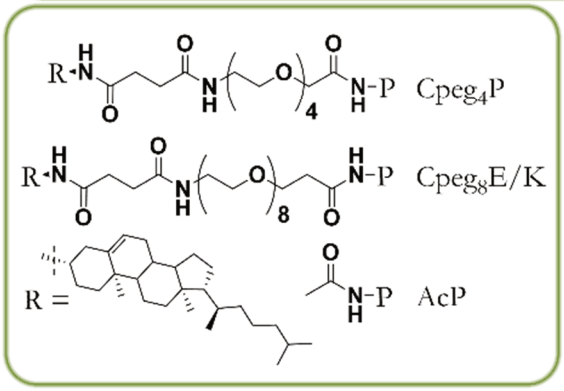


| Name (P) | Sequence (gabcdef) [1] |
|---|---|
| $1_E$ | EIQALEE E**N**AQLEQ E**N**AALEE EIAQLEY |
| $1_K$ | KIAQLKE K**N**AALKE K**N**QQLKE KIQALKY |
| $2_E$ | EIQQLEE EIAQLEQ K**N**AALKE K**N**QALKY |
| $2_K$ | KIAQLKQ KIQALKQ E**N**QQLEE E**N**AALEY |
| $3_E$ | K**N**AALKE EIQALEE E**N**QALEE KIAQLKY |
| $3_K$ | E**N**AALEE KIAQLKQ K**N**AALKE EIQALEY |
| $4_E$ | EIQALEE K**N**AQLKQ EIAALEE K**N**QALKY |
| $4_K$ | KIAQLKE E**N**QQLEQ KIQALKE E**N**AALEY |
| **E** | EIAALEK EIAALEK EIAALEK GY |
| **K** | KIAALKE KIAALKE KIAALKE GW |

**Figure 25.** *Schematic overview of orthogonal liposomal recognition and lipopeptide structures. Peptide functionalized liposomes are initially separated, and liposomes dock and fuse due to coiled-coil formation of complementary peptides. The sequences of the used peptides are shown in the table, with highlighted Ile-Asn mutations. The peptide N-terminus was either acetylated or conjugated with the spacer-anchor moieties (Cpeg4 for P-peptides, Cpeg8 for E/K peptides) depicted in the boxed region next to the table.*

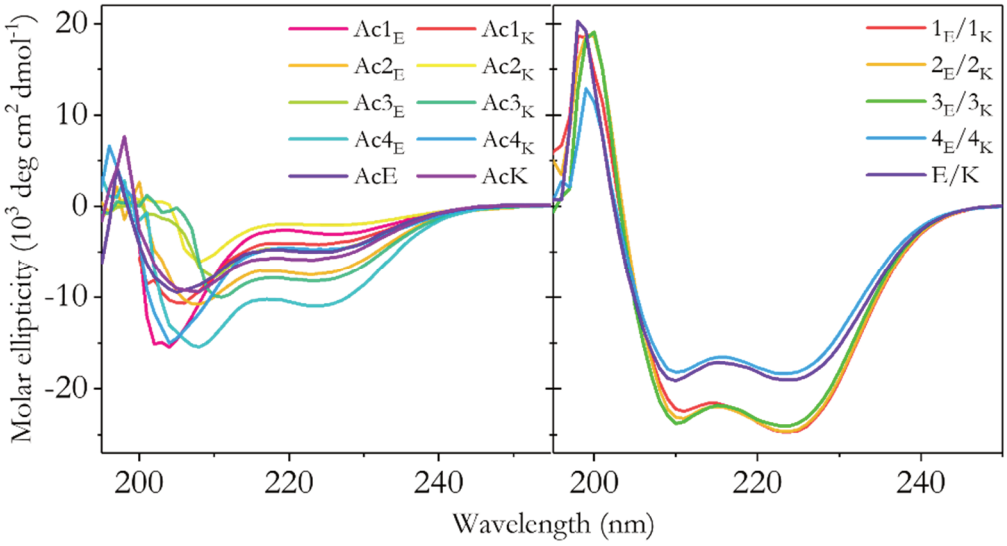


**Figure 26.** *Left: CD spectra of individual peptides, showing a-helical structures. Right: CD spectra of designed heterodimers, showing typical coiled-coil structures. [Total peptide] = 200 μM, PBS pH 7.4, at 20 °C.*

Intermolecular interaction between different peptides is observed when the $\theta_{222}$ value and $\theta_{222}/\theta_{208}$ ratio of the peptide combination has a higher value compared to the averaged value of both single peptides. The CD spectra revealed that peptides do not self-interact significantly and adopt α-helical structures with various degree of helicity. Typical coiled-coil spectra with 2 strong minima at wavelengths of 222 nm and 208 nm and a $\theta_{222}/\theta_{208}$ ratio ≥ 1 were only found for the designed peptide pairs. However, a $\theta_{222}/\theta_{208}$ ratio close to 1 was found for mixtures of E/$1_K$ and E/$3_K$, indicating a high degree of folding for these hybrid peptide combinations (peptide lengths of 23 and 28 residues respectively). Calculation of their α-helicity values at $\theta_{222}$ indicated that only the peptide pair E/$1_K$ formed a significant coiled-coil formation with a relatively high helicity of 42% (*Table S7*). This super secondary structure was rationalized by the helical wheel diagram of the assumed coiled-coil interaction. Coiled-coil formation between P-peptides and E or K is penalized via unfavorable Asn – Ile pairing in the hydrophobic core. However, all **e** and **g** positions of peptide $1_K$ are occupied by positively charged Lys residues, closely mimicking the charged distribution of peptide K. Since peptide E has Glu residues at complementary **e** and **g** positions, numerous electrostatic interactions are possible. These interactions overcome the polar-apolar Asn – Ile repulsion in the hydrophobic core of a coiled-coil complex.

## COILED-COIL BINDING STRENGTH AND OLIGOMER STATE

Next, the binding strength and oligomer state of the found coiled-coil complexes were evaluated using *FitDis!*.[50] This program yields information about oligomeric peptide interactions by fitting both oligomer state and thermodynamics of folding to thermal unfolding curves of the coiled-coil peptide complexes obtained by CD. Thermal unfolding curves were conducted at 25 μM, 50 μM, 100 μM and 200 μM (*Figure 27, Figure S26*). All peptide complexes unfolded between 20 °C and 80 °C but their melting temperatures were lower compared to the values reported by Jerala and coworkers. Therefore, omission of helix stabilizing modifications at peptide termini lowered the strength of the coiled-coil interactions significantly. The strongest interaction at 200 μM was measured in the $1_E/1_K$ peptide pair, with a Tm of 63 °C, while the $4_E/4_K$ pair showed the weakest coiled-coil interaction and unfolded at 37 °C. The other coiled-coil pairs, $2_E/2_K$ and $3_E/3_K$ have a moderate interaction with Tm around 50 °C. For the

interaction of the peptide pair E/$1_K$ a Tm of 30 °C was found. (*Figure 28*) Analysis of the data with *FitDis!* yielded the parameters shown in Table S8. The fitting procedure demonstrated the heterodimeric nature of all coiled-coil peptide pairs, since the root mean square error (RMSE) of the fitted unfolding curves showed a minimum at $\upsilon_1 + \upsilon_2 = 2$ in all cases. Although all used peptides share similar designs and bind in heterodimeric fashion, coiled-coil interactions differ vastly in terms of thermodynamic parameters as quantified with *FitDis!*. (*Table 11*) The peptide pair $1_E/1_K$ shows indeed a strong intramolecular interaction, with a $K_F$ of $5.3 \times 10^7$ $M^{-1}$. Coiled-coil complexes $2_E/2_K$ and $3_E/3_K$ have comparable binding strengths ($K_F$ of ~$1.5 \times 10^6$ $M^{-1}$) and are an order of magnitude weaker compared to $1_E/1_K$. The interaction in the coiled-coil complex $4_E/4_K$ is, with a $K_F$ of $2.3 \times 10^5$ $M^{-1}$, two orders of magnitude weaker than $1_E/1_K$ and E/K.

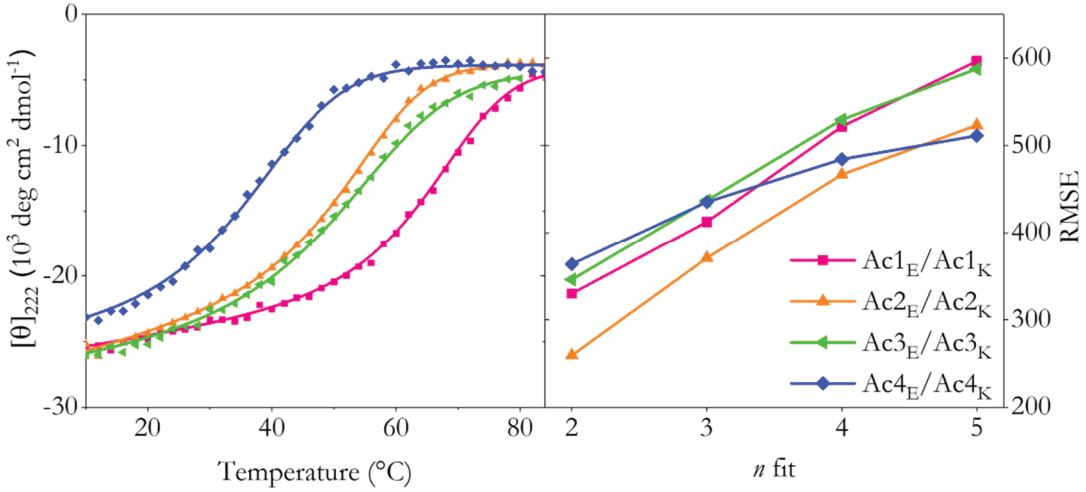


**Figure 27.** *Thermal unfolding of designed heterodimers $1_E/1_K$ (black), $2_E/2_K$ (red), $3_E/3_K$ (green), and $4_E/4_K$ (blue). Best fits (lines) of experimental data (dots) are obtained using FitDis!. Right graph: RMSE of best fits using different stoichiometric variables shows that the unfolding is best described by a heterodimeric coiled-coil interaction for all peptide sets. [Total peptide] = 200 μM, PBS pH 7.4 at 20 °C.*

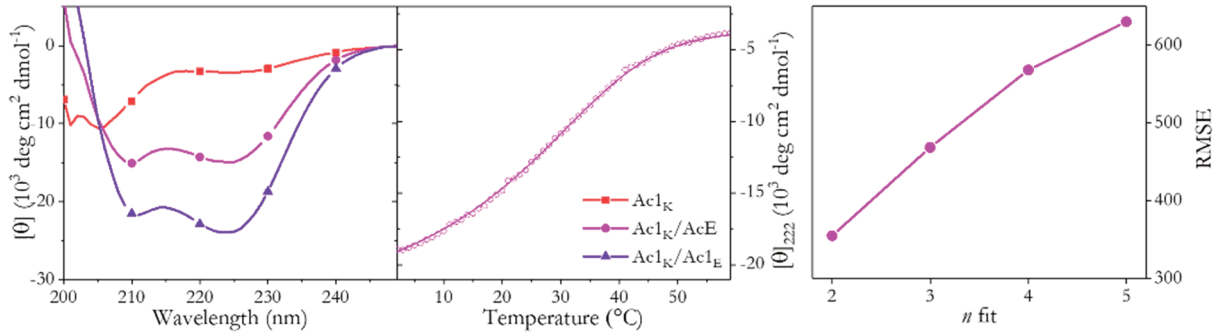


**Figure 28.** *Analysis of $Ac1_K/AcE$ interaction. Left: characteristic CD spectra of $Ac1_K$, $Ac1_K/AcE$, and $Ac1_K/Ac1_E$ reveal the structural differences between different peptide (super)structures. Middle: thermal unfolding curve of $Ac1_K/AcE$ at 200 μM, and best fit of the experimental data by FitDis!. Right: root mean square error of best fits as a function of stoichiometrics n fit = $\upsilon_1 + \upsilon_2$.*

**Table 11.** *Thermodynamic parameters at 25°C for $P_E/P_K$ and E/K coiled-coil pairs.*

| Coiled-coil | $1_E/1_K$ | $2_E/2_K$ | $3_E/3_K$ | $4_E/4_K$ | E/K | $E/1_K$ |
|---|---|---|---|---|---|---|
| $\Delta S_{25}$ / J mol$^{-1}$ K$^{-1}$ | 305 | 282 | 248 | 453 | 162 | 291 |
| $\Delta G_{25}$ / kJ mol$^{-1}$ | 44.1 | 35.7 | 34.9 | 30.6 | 41.4 | 24.9 |
| $\Delta H_{25}$ / kJ mol$^{-1}$ | 135 | 120 | 109 | 166 | 89.7 | 112 |
| $K_{F\,25}$ / M$^{-1}$ | $5.3 \times 10^7$ | $1.8 \times 10^6$ | $1.3 \times 10^6$ | $2.3 \times 10^5$ | $1.8 \times 10^7$ | $2.3 \times 10^4$ |
| $K_{U\,25}$ / M$^{-1}$ | $1.9 \times 10^{-8}$ | $5.5 \times 10^{-7}$ | $7.7 \times 10^{-7}$ | $4.4 \times 10^{-6}$ | $5.9 \times 10^{-8}$ | $4.4 \times 10^{-5}$ |

The folding constant of $E/1_K$ is even lower compared to the interactions of the designed coiled-coil pairs with a value of $2.3 \times 10^4$ M$^{-1}$. Comparison of these peptide pairs with E/K shows a similar melting temperature for $1_E/1_K$ and E/K ($K_F = 1.8 \times 10^7$ M$^{-1}$). Destabilization of the hydrophobic core by two **a**-positional asparagine residues in the $1_E/1_K$ pair is thus balanced by a more stable 4 heptad repeat, compared to the 3 heptad repeat of the E/K peptide pair.

## STRUCTURE OF MEMBRANE TETHERED PEPTIDES

To investigate the effect of membrane immobilization on peptide secondary structure, CD spectra were measured for peptide functionalized liposomes, prepared with $Cpeg_4P$ (1-4 mol%), and compared to CD-spectra of solvated peptides. (*Figure S27, Figure S28, Table* S9) Membrane tethered peptides showed an increased helicity compared to N-acetylated peptides; and all peptides adopt partially folded α-helices at 1 mol% decoration except for $Cpeg_41_E$. With increasing [$Cpeg_4P$] at the liposomal membrane, the observed helicity increased, indicative of homo-oligomerization or stabilization of the peptide helix at the membrane surface.[51] Surprisingly, for three lipopeptides β-sheet like structures were found at distinct concentrations: [$Cpeg_42_E$] = 2 mol%, [$Cpeg_42_K$] ≥ 2 mol%, and [$Cpeg_44_K$] ≥ 3 mol% peptide functionalization of the liposomal membrane.

Next, the temperature dependency of the peptides was probed using CD spectroscopy to gain further insight as to the secondary structures and possible membrane interactions of the membrane tethered peptides. Acylated peptides were analyzed in both the absence and presence of liposomes. Secondly, liposomes were decorated with $Cpeg_4$ functionalized lipopeptides and subsequently analyzed, as shown in Figure 29. Because peptide-membrane interactions and homodimer formation of lipopeptides show different concentration dependent unfolding behavior, unfolding curves of $Cpeg_4P$ decorated

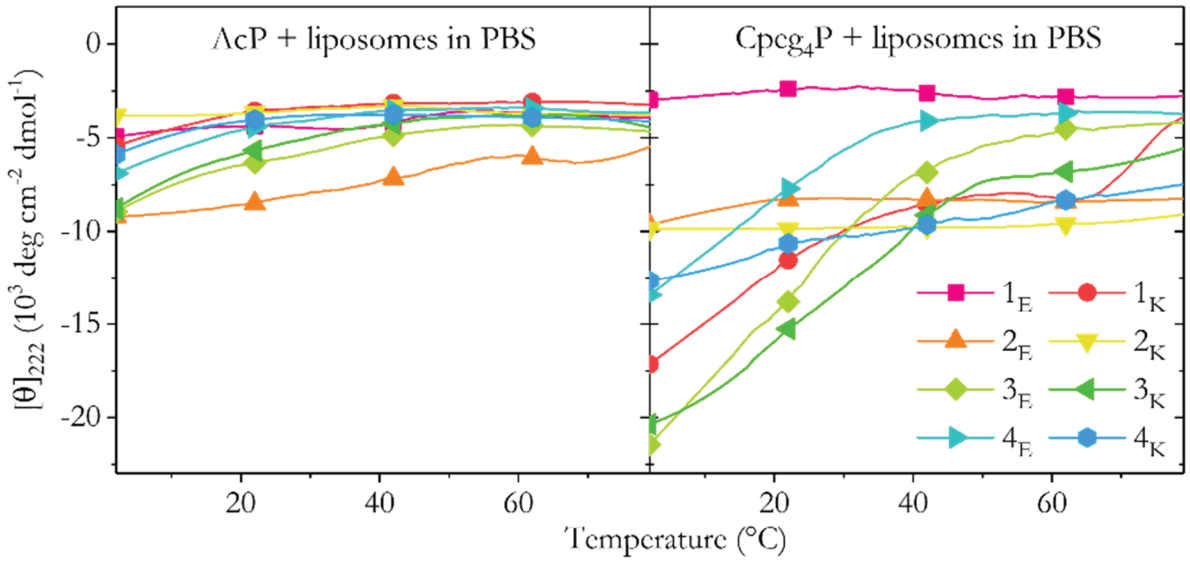


**Figure 29.** *Left: Temperature dependent unfolding curves of AcP-peptides in the presence of liposomes as determined by $\theta_{222}$ absorption. [Total lipid] = 1 mM, [peptide] = 20 μM, in PBS pH 7.4. Right: Temperature dependent unfolding curves of Cpeg4P peptides tethered to liposomes as determined by $\theta_{222}$ absorption. [Total lipid] = 0.5 mM, [lipopoptide] = 10 μM (2 mol%), in PBS pH 7.4.*

liposomes were recorded as a function of [Cpeg4P] (2, 3, 4 mol%, Figure S29 - Figure S32). The helical content of N-acetylated peptides, as determined by $\theta_{222}$, did not change significant in the presence of liposomal membranes. In contrast, tethering the peptides to liposomes with Cpeg4 spacers induced structural changes for all derivatives except Cpeg4$1_E$. This shows that Asn incorporation in the hydrophobic core of the P-peptides inhibits a membrane interaction for N-acetylated peptides, since AcK (with a Leu – Ile hydrophobic core) interacts with liposomal membranes. Conversely, the limited degree of freedom of the peg4 spacer forces all peptides (except $1_E$) in distinct secondary structures, but differences in supramolecular interactions were observed between the different lipopeptides. The thermal unfolding curves suggest that Cpeg4$1_K$ and Cpeg4$3_K$ have interactions with their membranes according to the increased helicity still occurring at 60 °C, but homodimer formation is also possible.[51] Interestingly, peptide $1_K$ is the only P-peptide with Lys residues at all **e** and **g** positions, which could enable a stable membrane immersion with help of the 'snorkeling' mechanism as was found for peptide K.[40] Cpeg4$3_E$ and Cpeg4$4_E$ show increased helicities at room temperature but similar helicities at 60 °C compared to their N-acetylated derivatives, indicative of homodimer formation. Conversely, the melting curves of membrane tethered Cpeg4$2_E$, -$2_K$ and -$4_K$ support the observed β-sheet formation with an increased $\theta_{222}$ and a low or absent temperature dependency.

## LIPOSOME DOCKING

Docking of liposomes is facilitated via coiled-coil formation between complementary peptides tethered to liposomes. The change in peptide structure was measured using CD spectroscopy; liposomes functionalized with complementary peptides were mixed and the resulting CD spectra before and after mixing are shown in Figure 30 and Table 12.

Significant differences in coiled-coil binding between all above described coiled-coil peptide pairs was observed upon mixing of peptide functionalized liposomes. The increase in %H and a $\theta_{222}/\theta_{208}$ closer to 1 indicates coiled-coil formation for mixtures of liposomes decorated with lipopeptide fusogens $2_E/2_K$, $3_E/3_K$, E/K and $E/1_K$ with respect to the obtained values of liposomes prior to mixing. In contrast, the observed low values for %H and $\theta_{222}/\theta_{208}$ for mixtures of liposomes decorated with lipopeptides $1_E/1_K$ and $4_E/4_K$ are illustrative for the absence of coiled-coil superstructures.

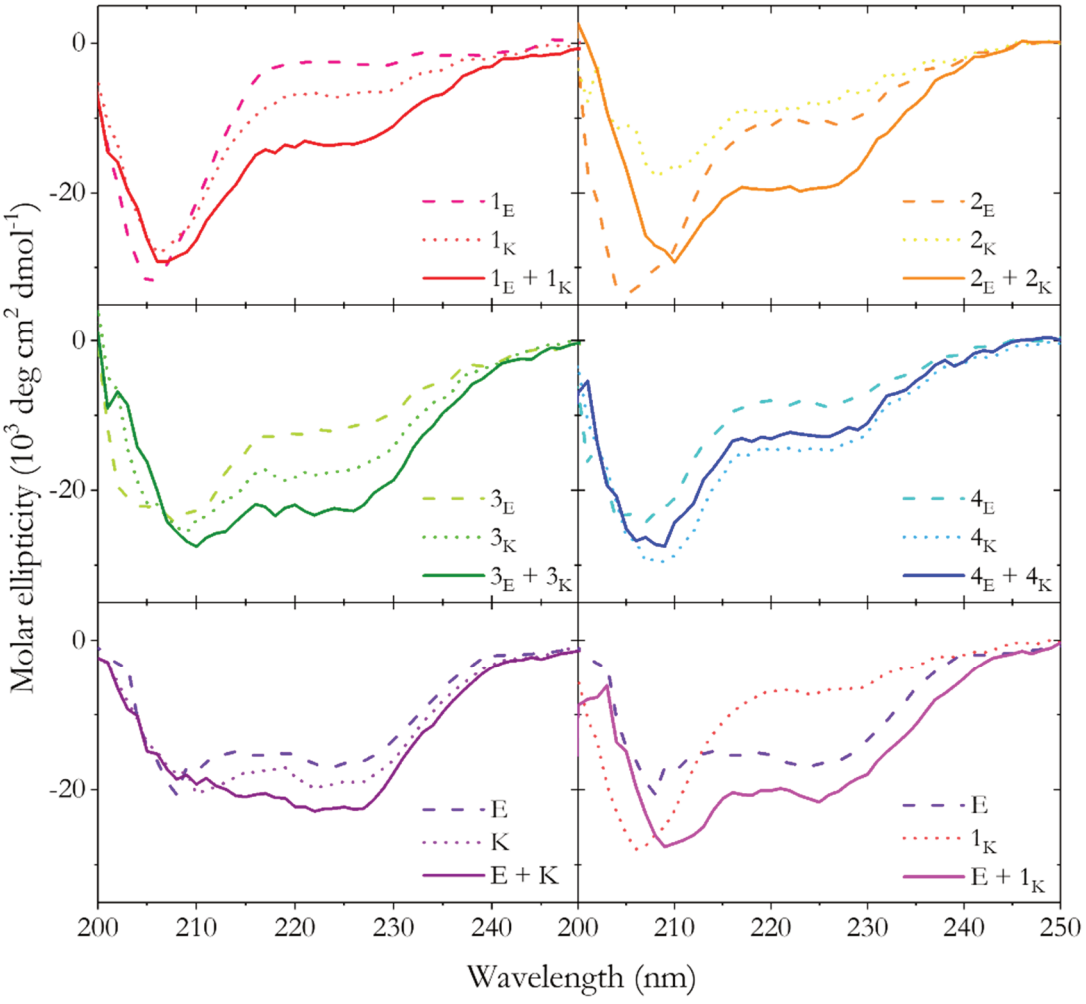


**Figure 30.** *CD spectra of liposomes decorated with $Cpeg_4P$ or $Cpeg_8E/K$, and the equimolar mixture of liposomes bearing complementary peptides. [Total lipid] = 0.5 mM, with 1 %mol lipopeptide, PBS pH 7.4, 20 °C.*

**Table 12.** *Degree of peptide helicity before and after mixing of peptide functionalized liposomes.*

| Peptide | | $1_E$ | $1_K$ | $2_E$ | $2_K$ | $3_E$ | $3_K$ | $4_E$ | $4_K$ | E | K | $1_K$ | E |
|---|---|---|---|---|---|---|---|---|---|---|---|---|---|
| $Cpeg_4$ | %H | 8 | 20 | 30 | 26 | 36 | 53 | 25 | 44 | 52 | 60 | 20 | 52 |
| | $\theta_{222}/\theta_{208}$ | 0,1 | 0,2 | 0,3 | 0,5 | 0,5 | 0,7 | 0,4 | 0,5 | 0,9 | 1,0 | 0,2 | 0,9 |
| $Cpeg_4P_E$+ $Cpeg_4P_K$ | %H | 40 | | 58 | | 69 | | 37 | | 71 | | 61 | |
| | $\theta_{222}/\theta_{208}$ | 0,5 | | 0,7 | | 0,9 | | 0,5 | | 1,2 | | 0,8 | |

*[Lipopeptide] = 5 μM, and [total lipid] = 0.5 mM. Recorded in PBS pH 7.4, 20 °C.*

## CONTENT MIXING ASSAY

Content mixing in the absence of leakage is regarded as a completed fusion event between two liposomes. We use a quantitative content mixing model for populations of small liposomes by encapsulating the water-soluble dye Sulphorhodamine B.[47, 52-53] The dye is self-quenched at high concentrations, which upon dilution results in relief of self-quenching and concomitant fluorescence increase. In these experiments $Cpeg_4$ functionalized P-peptides and $Cpeg_8$ functionalized E/K peptides were used to account for the shorter peptide length of E/K compared to P-peptides; also, $Cpeg_8E/K$ is more fusogenic than $Cpeg_4E/K$.[46] Therefore, one batch of liposomes bearing peptide $Cpeg_4P$ was loaded with 20mM sulphorhodamine B in PBS, and mixed with peptide $Cpeg_4P$-, $Cpeg_8E$- or $Cpeg_8K$-functionalized buffer-containing liposomes. The fluorescence increase was followed for 30 minutes. (*Figure 31, Figure S33*)

Fluorescence increase was only observed with a few coiled-coil pairs: Efficient fusion of liposomes (>40% content mixing) was obtained when cholesterol anchored $2_E/2_K$, $3_E/3_K$ or $E/1_K$ were used as fusogens. Liposomes functionalized with cholesterol anchored $1_E/1_K$ or combinations of lipopeptides P and K yielded only <25% content mixing. The $Cpeg_41_K/Cpeg_8E$ peptide pair was even more efficient in mediating fusion than the designed $Cpeg_8E/Cpeg_8K$ fusogen (±50% content mixing), which again demonstrated the influence of both peptides on the efficiency of the fusion process. Conversely, liposome fusion was not initiated by the complementary peptides $Cpeg_44_E/Cpeg_44_K$ and by all other non-complementary peptide combinations. It is evident that fusion only occurs when coiled-coil formation is established between complementary peptides tethered to opposing liposomes. The absence of fusion for

liposomes functionalized with $Cpeg_4 4_E$/$Cpeg_4 4_K$ agrees with the absence of coiled-coil formation observed for liposomes functionalized with these peptides. The high selectivity of the orthogonal fusion system is further illustrated by the absence of fusion when non-complementary $Cpeg_4P$ peptides are used. On the other hand, fusion efficiencies of ±20% were found with almost all liposomal mixtures involving $Cpeg_8K$ decorated liposomes, demonstrating the high fusion activity of the amphipathic K peptide.

## STRUCTURE-ACTIVITY RELATIONSHIP OF FUSOGENS

Analysis of the peptide structure could shed light on the required peptide characteristics for fusion. As shown in Figure 32, some correlation is found between CC binding strength, helicity of the peptide structures and fusion efficiency. Efficient fusogens are characterized by relatively high peptide helicities and low fusion efficiencies are accompanied with relatively low helicities of the involved fusogens.

Comparison of the fusogens $1_E/1_K$, $2_E/2_K$, $3_E/3_K$, $4_E/4_K$ and E/K showed that peptides with higher helicities before fusion reach higher fusion efficiencies, suggesting that fusion is enhanced by pre-formed helices. But we also hypothesized previously that CpegE/CpegK peptide mediated liposome fusion is mainly driven by the characteristic membrane destabilization of peptide CpegK.[40] For the $Cpeg_4P$ peptides, CD measurements suggest peptide-membrane interactions for only $1_K$ and $3_K$, which correlates very well with the high fusion efficiency of $Cpeg_4 1_K$/$Cpeg_8E$ and $Cpeg_4 3_E$/$Cpeg_4 3_K$, supporting this hypothesis. The importance of a peptide-membrane interaction in agreement with SNARE-mediated membrane fusion, in which the proteins not only bring opposing membranes in close proximity, but also play an active role in overcoming subsequent fusion barriers by applying mechanical stress to the membranes of fusion intermediates.[54-55] Also, $1_K$ and $3_K$ are the only P-peptides having lysine residues occupying positions **e** and **g** of the 2nd and 3th heptad, indicating some correlation between positive charges at these positions and a higher fusogenic activity and/or a more profound membrane interaction. Interestingly, the membrane-interacting fusogens $E/1_K$, $3_E/3_K$ and E/K exhibit a reverse relationship between fusion efficiency and CC binding strength, whereas lipopeptides $1_E/1_K$, $2_E/2_K$ and $4_E/4_K$ show no apparent influence of the CC binding strength of the fusion efficiency. Therefore, binding strength of the fusogens is not the main driving force of coiled-coil peptide mediated fusion, as was

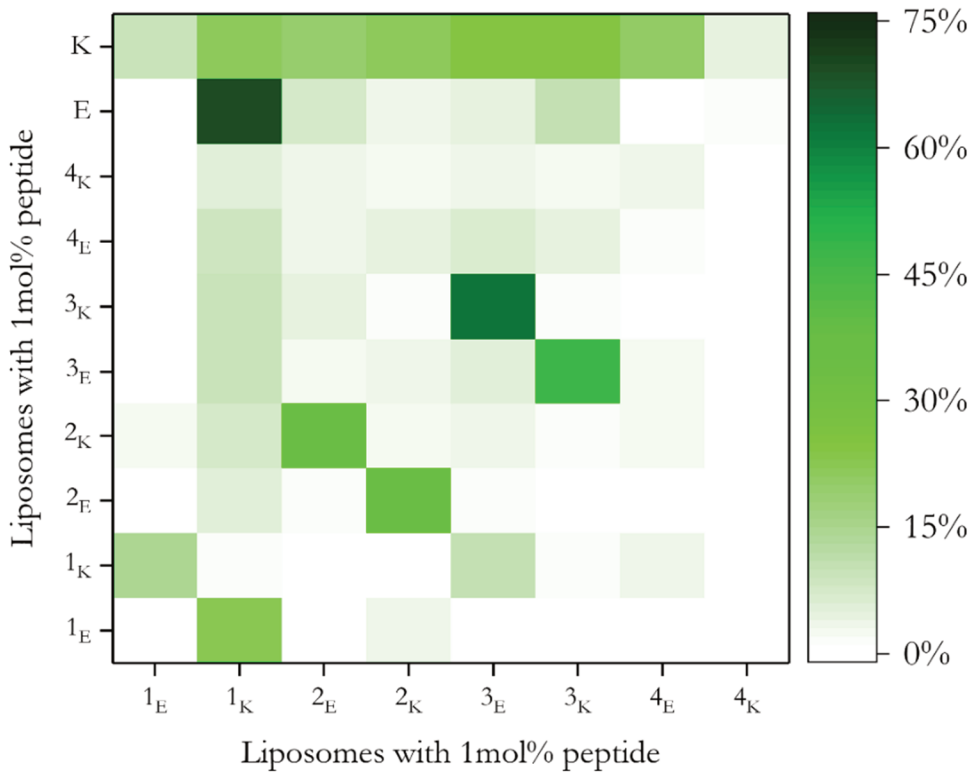


**Figure 31.** *Membrane fusion assay. Content mixing between vesicles loaded with Sulphorhodamine B (x-axis) and plain vesicles (y-axis), as a function of peptide derivative, after 30 minutes. [Total lipid] = 0.1 mM, with 1mol% lipopeptide in PBS pH 7.4 at 20 °C.*

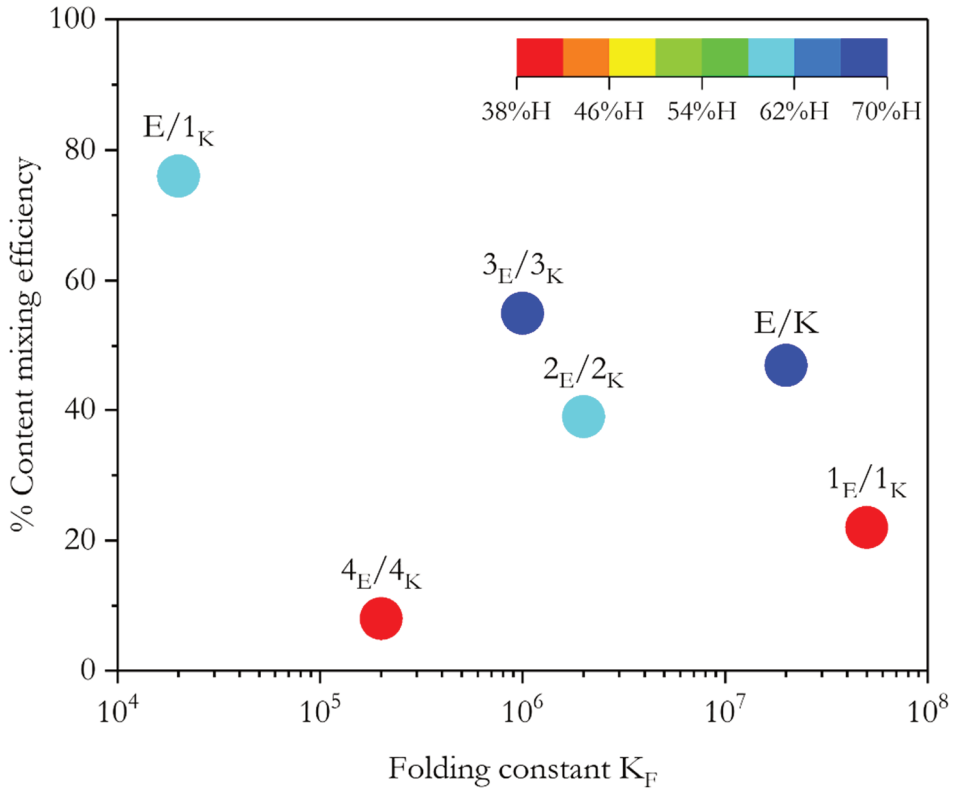


**Figure 32.** *Content mixing efficiency as a function of KF of the heteromeric peptide pair. Colors correspond to helicities of peptide functionalized liposomes.*

hypothesized for other fusion model systems.[21] Fusogens used in those model systems do not interact with liposomal membranes, and solely facilitate docking of liposomes. The very close apposition of both liposomes itself causes the fusion process to proceed, without further influence of the fusogen.

Here, a similar behavior was observed for the fusogen $2_E/2_K$.Both lipopeptides do not interact with their supportive membranes, as shown with CD measurements, and are most likely only facilitating liposomal docking. The obtained moderate fusion efficiency with this fusogen (40%) further supports our hypothesis that fusogen-membrane interactions are crucial for efficient fusion.

Comparison of the $Cpeg_41_K/Cpeg_41_E$ and $Cpeg_41_K/Cpeg_8E$ fusogens reveal the remarkable influence of the counter-peptide on the efficiency of the fusion process. $Cpeg_41_E$ and $Cpeg_8E$ are both negatively charged peptides, but their secondary structures differ vastly. CD spectra of $Cpeg_41_E$ indicate a random coil conformation, while $Cpeg_8E$ was found to be mainly in a homodimeric coiled-coil conformation at room temperature. Also, peptide helicity increased to 61% upon mixing of $Cpeg_41_K$ and $Cpeg_8E$ functionalized liposomes while a mixture of $Cpeg_41_K/Cpeg_41_E$ functionalized liposomes only showed 40% helicity although the binding strength of $Ac1_K/Ac1_E$ is 3 orders of magnitude larger compared to Ac1K/AcE.

The higher local peptide concentration and the highly ordered structure of $Cpeg_8E$ over $Cpeg_41_E$ could enhance the peptide availability to bind with $Cpeg_41_K$, as indicated by the relatively high helicity of $Cpeg_41_K/Cpeg_8E$, thereby enhancing the fusion efficiency. Secondly, visible aggregates of liposomes were only observed when $Cpeg_41_K/Cpeg_8E$ were used as fusogens, as was found for $Cpeg_{12}E$/ $Cpeg_{12}K$ fusogens also.[46] However, aggregation of liposomes was not observed when $Cpeg_42_E/Cpeg_42_K$ and $Cpeg_43_E/Cpeg_43_K$ were used as fusogens. These observations suggest that formation of micron sized assemblies is due to the occurrence of multiple rounds of fusion, because the affinity of $Cpeg_41_K/Cpeg_8E$ is too low to trigger aggregation of liposomes specifically. Furthermore, multiple rounds of fusion are only possible when a considerable amount of the involved fusogens disassociate after the fusion process, which is enhanced by the low binding strength of $Cpeg_41_K/Cpeg_8E$. Therefore, the high fusion efficiency of this specific peptide pair is likely due to the combination of the enhanced availability of the

homodimer $Cpeg_8E$, the presumable membrane interaction of $Cpeg_41_K$ and the very transient heterodimeric coiled-coil interaction.

## CONCLUSIONS

This study demonstrated the orthogonal interactions of a library of lipidated coiled-coil peptides. The interactions of these peptides with the coiled-coil peptide pair E/K were investigated also, and a minor interaction was found between $1_K$ and E. Coiled-coil stability and oligomeric state were determined with concentration and temperature dependent CD spectroscopy. Also, the observed secondary structure of almost all $Cpeg_4P$ peptides was affected by membrane tethering due to increased local concentration.

It was shown that various coiled-coil peptides can mediate membrane fusion, and efficient orthogonal content mixing was obtained between liposomes decorated with the lipopeptide pairs $2_E/2_K$, $3_E/3_K$, and $E/1_K$. Examination of peptide structure and fusogenic efficiency revealed that transient coiled-coil interactions enhance the fusion process. Furthermore, fusogens with clear asymmetric roles were found to be highly fusogenic. Two roles could be identified: An active role with a membrane interacting peptide, and a passive role with a highly accessible peptide homodimer. This active – passive roleplay was found for the efficient fusogens $3_K/3_E$ and $E/1_K$ (and the well described E/K pair), respectively. The fusogen $2_E/2_K$ lacked this distinct roleplay and mediated fusion by forcing liposomes just in close proximity, thereby reaching only moderate fusion efficiencies.

The high efficiency of the $Cpeg_41_K/Cpeg_8E$ fusogen makes these peptides useful candidates for liposome – cell fusion assays.[47, 56-57] Other favorable characteristics of this fusogen are the very transient coiled-coil interaction which increases peptide availability after a successful fusion event and the absence of nonspecific fusion events. Above all, this research lays the foundations for the development of partner specific liposome – cell fusion models and supramolecular self-assembly of peptide functionalized building blocks.

# EXPERIMENTAL SECTION

## MATERIALS

Fmoc-protected amino acids, rink amide resin, and O-(1H-6-Chlorobenzotriazole-1-yl)-1,1,3,3-tetramethyluronium hexafluorophosphate (HCTU) were purchased from NovaBioChem. Diisopropylethylamine (DIPEA), piperidine, acetic anhydride, N-methylpyrrolidine (NMP), dimethylformamide (DMF), acetonitrile, and trifluoroacetic acid (TFA) were obtained from Biosolve. Dichloromethane (DCM), diethyl ether, triisopropylsilane (TIS), trimethylamine (TEA), trifluoroethanol (TFE), cholesterol, trimethylphosphine (1M in toluene), (1H-benzotriazol-1-yloxy) tripyrrolidinophosphonium hexafluorophosphate (PyBOP), succinic anhydride, and sulforhodamine B were obtained from Sigma Aldrich. 1,2-dioleoyl-sn-glycero-3-phosphatidylcholine (DOPC), and 1,2-dioleoyl-sn-glycero-3-phosphatidylethanolamine (DOPE) were purchased from Avanti polar lipids. The $N_3$–$(PEG)_4$–COOH spacer[58-59] and Cholesteryl-4-amino-4-oxobutanoic acid[60] were synthesized according to literature procedures. PBS buffer contains 5 mM $KH_2PO_4$, 15 mM $K_2HPO_4$, 150 mM NaCl, pH 7.4. Data analysis and visualization was performed using OriginPro 9.1.

## METHODS

**Liposome preparation.** A 1 mM stock solution containing DOPC/DOPE/cholesterol (50:25:25 mol%) in 1:1 (v/v) chloroform/methanol was prepared for all fusion experiments. Lipopeptides (50 μM) were dissolved in 1:1 (v/v) chloroform/methanol. In general, 1 mol% of the lipopeptide solution was mixed with the liposome solution and the solvent was removed under a stream of $N_2$. One lipid/lipopeptide film was rehydrated with PBS (1 mL). A second lipid/lipopeptide film was rehydrated with PBS buffer containing 20 mM sulforhodamine B (1 mL). The solutions were briefly vortexed and subsequently sonicated for 5-10 minutes at 55 °C to yield ~100 nm diameter liposomes, verified with dynamic light scattering (DLS).[61] Solutions of plain liposomes were used without further purification, whereas sulforhodamine B containing liposomes were purified using a Sephadex G25 column to remove any non-encapsulated sulphorhodamine B. The purification dilution factor was 1:5.

**Fluorescence spectroscopy.** Content-mixing experiments were performed on a TECAN Infinite M1000 PRO fluorimeter using a 96-well plate at 25 °C. The percentage of fluorescence increase, *%F*, was calculated as

$$\%F = \frac{F(t) - F_0}{F_{max} - F_0} * 100$$

**Content mixing experiments:** The sulphorhodamine B fluorescence intensity, *F(t)*, at 580 nm was monitored in a continuous fashion for 30 min after mixing non-fluorescent liposomes with sulphorhodamine B loaded liposomes. $F_0$ was obtained by measuring the emission of sulphorhodamine B-loaded liposomes to which an equal amount of PBS was added, and $F_{max}$ was obtained by measuring the emission of plain liposomes loaded with 10 mM sulphorhodamine B. [Total lipid] = 0.1mM, in PBS pH 7.4, 25 °C.

**Dynamic Light Scattering.** Particle size distributions were measured by dynamic light scattering using a Malvern Zetasizer Nano ZS ZEN3500 equipped with a peltier thermostatic cell holder. The laser wavelength was 633nm and the scattering angle was 173°. The Stokes Einstein relationship

$$D = \frac{k_B T}{3\pi\eta D_h}$$

was used to estimate the hydrodynamic diameter $D_h$. Here, $k_B$ is the Boltzmann constant, $\eta$ is the solvent viscosity, and measurements were carried out at room temperature. For size increase experiments, 0.5mM liposomes functionalized with 1 mol% lipopeptide were prepared. Upon mixing of lipopeptide bearing liposomes, size distribution was followed for 30 min.

**Circular Dichroism Spectroscopy.** CD spectra were obtained using a Jasco J-815 spectropolarimeter equipped with a peltier temperature controller. The ellipticity, given as mean residue molar ellipticity, [$\theta$] (deg cm$^2$ dmol$^{-1}$), is calculated using the following equation

$$[\theta] = \frac{100 * \theta_{obs}}{nlc}$$

where $\theta_{obs}$ is the observed ellipticity (mdeg), *n* is the number of peptide residues, *l* is the path length of the cuvette (cm) and *c* is the peptide concentration (mM). Spectra were recorded from 260 nm to 200 nm at 20 °C. Data points were collected with a 1 nm bandwidth at 1 nm intervals, using a scan speed of 1 nm s-1. Each spectrum was an average of five scans. For analysis, each spectrum had the background spectrum (plain liposomes in PBS) subtracted. The percentage α-helicity was calculated using the predicted value $[\theta]_{222}$ = -39500*(1-2.57/n) as 100% value for an α-helical peptide of n residues.[62] For temperature dependent measurements $[\theta]_{222}$ was recorded as a function of temperature, with a range of 2 - 80°C and ΔT = 40°C/h. Cuvette path length = 2mm, [total lipid] = 0.5 or 1mM, with 1, 2, 3 or 4 mol% lipopeptide, in PBS at pH 7.4.

## PEPTIDE SYNTHESIS

**Peptide Synthesis:** Peptide synthesis was performed on a CEM Liberty I peptide synthesizer on a 100 μM scale using Rink amide resin (0.55-0.73 mmol/g). Amino acid activation was achieved using HCTU/DIPEA (4eq/6eq) in DMF. Fmoc-deprotection was carried out using two cycles of 20% piperidine in DMF. All reactions were carried out at 70-80 °C using microwave irradiation for three minutes.

**Acylated peptides:** The N-terminal free amine was acylated using a mixture of $Ac_2O$ (50 mM) and DIPEA (12.5 mM) in NMP for 1h. The resin was washed thoroughly with DMF and DCM to remove excess reactants.

**Lipopeptides:** The $N_3$-$Peg_4$-COOH spacer was conjugated to the peptide free N-terminus using PyBOP/DIPEA activation (3eq/5eq) in DMF containing LiCl (1mg/mL) for 2h. $N_3$-$PEG_4$-COOH-containing peptides were reduced using two cycles of PME in dioxane/water (4:1). Cholesteryl-4-amino-4-oxobutanoic acid was activated with PyBOP/DIPEA (3eq/5eq) in DCM/DMF 1:1, added to the resin-bound peptides and the reaction was shaked for two days at rt. The resin was washed thoroughly with DMF and DCM to remove excess reactants.

**Cleavage:** The (lipo)peptides were cleaved from the resin and side-chain deprotected using a mixture of TFA/TIS/$H_2O$ (95:2.5:2.5 v/v) for 2h. The (lipo)peptides were precipitated in cold diethyl ether followed by centrifugation and dried under vacuum.

**Purification:** RP-HPLC was performed with a Shimadzu HPLC system with two LC-8A pumps, and a SPD-10AVP UV-VIS detector. Sample elution was monitored by UV detection at 214 nm and 278 nm. Samples were eluted with a linear gradient from 10% to 90% (v/v) B in A, A being $H_2O$, 0.1% (v/v) TFA, and B being MeCN, 0.1% (v/v) TFA. Purification of (lipo)peptides was performed on a Phenomenex C18 reversed phase column (21.2 mm diameter, 150 mm length, 5.00 μM particle size) with a flow rate of 15 mL $min^{-1}$. Collected fractions were tested for >95% purity using LC-MS with Gemini C18 column and freeze dried.

## PEPTIDE SEQUENCES AND HELICAL WHEEL OF P-PEPTIDES

Asn-Asn (N) and Ile-Ile (I) are both inserted twice in the hydrophobic core of each coiled-coil pair at position **a**, with different positions for the individual orthogonal pairs and thereby enhancing pairing specificity. For electrostatic interactions at positions **e** and **g**, Glu (E) and Lys (K) were used as charged residues,[63] with opposite charges at complementary heptads within the paired heterodimer. Again, the electrostatic pattern along the coiled-coil complex differs for all orthogonal pairs, contributing to partner specificity. E $(EIAALEK)_3$ and K $(KIAALKE)_3$ are also shown for comparison.

**Table S4.** *The used sequences of peptides $P_E$ / $P_K$, and E / K.*

| Name | Sequence $(gabcdef)_4$ [1] | Hydrophobic pattern [2] | Electrostatic pattern [2] |
|---|---|---|---|
| $1_E$ | EIQALEE ENAQLEQ ENAALEE EIAQLEY | I N N I | E E E E |
| $1_K$ | KIAQLKE KNAALKE KNQQLKE KIQALKY | I N N I | K K K K |
| $2_E$ | EIQQLEE EIAQLEQ KNAALKE KNQALKY | I I N N | E E K K |
| $2_K$ | KIAQLKQ KIQALKQ ENQQLEE ENAALEY | I I N N | K K E E |
| $3_E$ | KNAALKE EIQALEE ENQALEE KIAQLKY | N I N I | K E E K |
| $3_K$ | ENAALEE KIAQLKQ KNAALKE EIQALEY | N I N I | E K K E |
| $4_E$ | EIQALEE KNAQLKQ EIAALEE KNQALKY | I N I N | E K E K |
| $4_K$ | KIAQLKE ENQQLEQ KIQALKE ENAALEY | I N I N | K E K E |
| E | EIAALEK EIAALEK EIAALEK GY | I I I | E E E |
| K | KIAALKE KIAALKE KIAALKE GW | I I I | K K K |

*[1] All peptides contain a N-terminal acyl and C-terminal amide. [2] The designed orthogonal interactions are illustrated by differences in hydrophobic (position a) and electrostatic patterns (positions e and g) between the peptide pairs.*

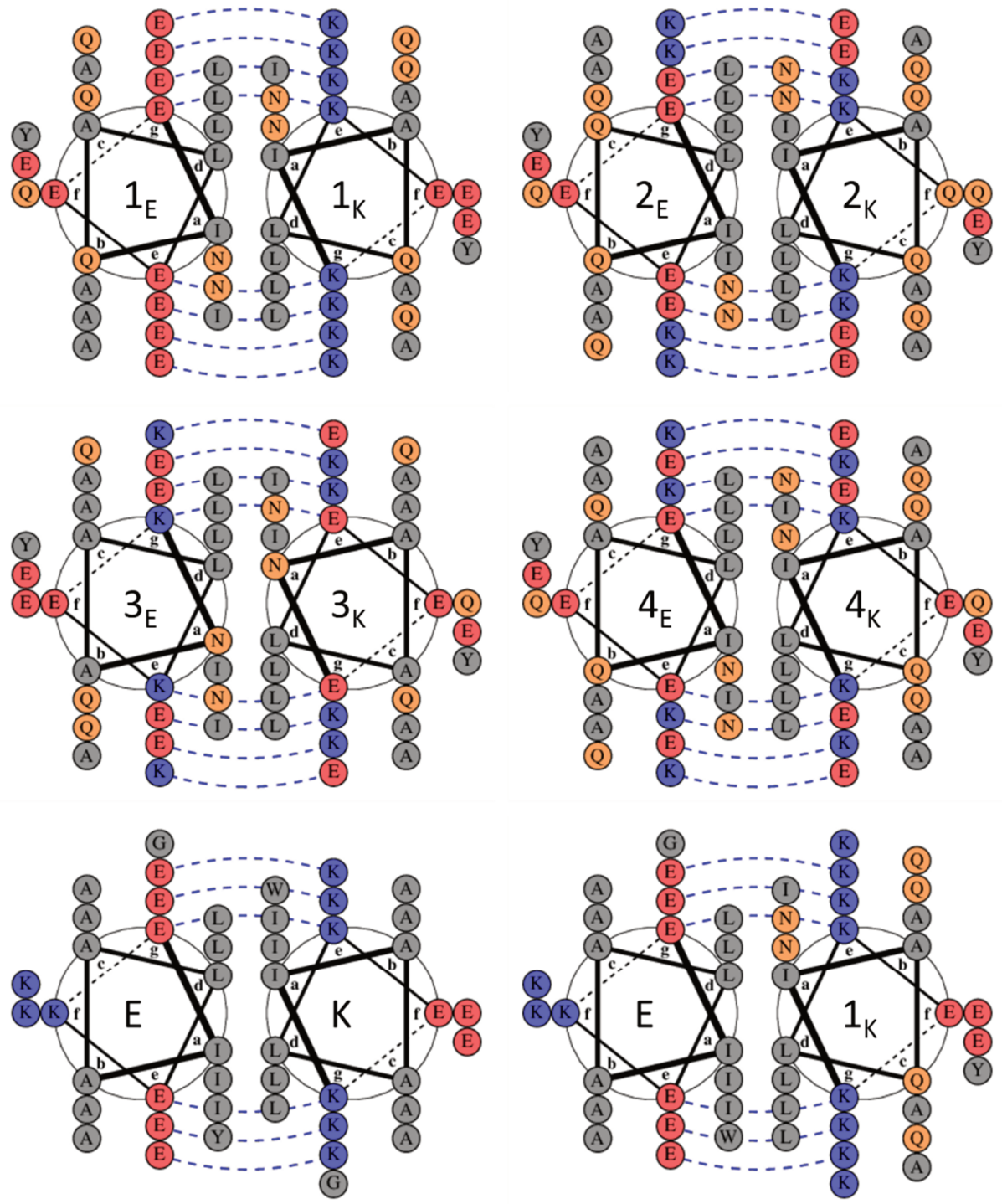


**Figure S24.** *Helical wheel projection of the coiled-coil pairs, illustrating the designed electrostatic and hydrophobic interactions stabilizing the coiled-coil formation. Helical wheels were made using Drawcoil 1.0.*

## PEPTIDE ANALYSIS

Peptide purity was confirmed using LC-MS analysis equipped with Gemini 3µ C18 column coupled with Finningan LCQ advantage max (Thermo) ESI-MS analyzer and the results are summarized in Table S5. LCMS eluents were A) H2O + 0.1% v/v TFA, B) MeCN + 0.1% v/v TFA, with a flow rate of 1 mL $min^{-1}$. Gradient for acylated peptides was applied from 2 to 30 min, from 10% B in A to 90% B in A, while the same gradient was applied for lipopeptides from 1 to 12 min. Retention time RT is rounded to 2 significant numbers.

**Table S5.** *Analysis of AcP Peptides*

| Peptide | Formula | Calc. mass | Observed mass | RT (min) | Isoelectric point[a] | Charge[a] |
|---|---|---|---|---|---|---|
| $Ac1_E$ | $C_{140}H_{219}N_{35}O_{56}$ | 3288.458 | 3312.325 $[M+Na]^+$ | 22 | 2.78 | -10.0 |
| $Ac1_K$ | $C_{150}H_{261}N_{43}O_{42}$ | 3338.963 | 3340.463 $[M+H]^+$ | 12 | 10.40 | +4.8 |
| $Ac2_E$ | $C_{146}H_{242}N_{40}O_{49}$ | 3341.744 | 3343.847 $[M+H]^+$ | 19 | 4.62 | -2.1 |
| $Ac2_K$ | $C_{146}H_{243}N_{41}O_{48}$ | 3340.759 | 3342.646 $[M+H]^+$ | 16 | 4.92 | -1.1 |
| $Ac3_E$ | $C_{144}H_{238}N_{38}O_{49}$ | 3285.677 | 3287.231 $[M+H]^+$ | 20 | 4.44 | -3.1 |
| $Ac3_K$ | $C_{142}H_{236}N_{38}O_{47}$ | 3227.641 | 3229.010 $[M+H]^+$ | 18 | 4.62 | -2.1 |
| $Ac4_E$ | $C_{144}H_{239}N_{39}O_{48}$ | 3284.692 | 3287.046 $[M+H]^+$ | 17 | 4.62 | -2.1 |
| $Ac4_K$ | $C_{146}H_{242}N_{40}O_{49}$ | 3341.744 | 3344.621 $[M+H]^+$ | 16 | 4.62 | -2.1 |

[a] *Calculated with Isoelectric Point Calculator and peptide charge is calculated at pH 7.4.*[64]

**Table S6.** *Analysis of synthesized lipopeptides*

| Peptide | Formula | Calc mass | Observed mass | RT (min) |
|---|---|---|---|---|
| $Cpeg41_E$ | $C_{179}H_{284}N_{36}O_{63}$ | 3948.36 | 1974.80 $[M+2H]^{2+}$ | 11 |
| $Cpeg41_K$ | $C_{189}H_{326}N_{44}O_{49}$ | 3998.86 | 1357.73 $[M+3Na]^{3+}$ | 7.4 |
| $Cpeg42_E$ | $C_{185}H_{307}N_{41}O_{56}$ | 4001.65 | 1335.00 $[M+3H]^{3+}$ | 9.2 |
| $Cpeg42_K$ | $C_{185}H_{308}N_{42}O_{55}$ | 4000.66 | 1334.60 $[M+3H]^{3+}$ | 8.6 |
| $Cpeg43_E$ | $C_{183}H_{303}N_{39}O_{56}$ | 3945.58 | 1973.47 $[M+2H]^{2+}$ | 8.7 |
| $Cpeg43_K$ | $C_{181}H_{301}N_{39}O_{54}$ | 3887.54 | 1944.27 $[M+2H]^{2+}$ | 9.0 |
| $Cpeg44_E$ | $C_{183}H_{304}N_{40}O_{55}$ | 3944.59 | 1973.53 $[M+2H]^{2+}$ | 9.6 |
| $Cpeg44_K$ | $C_{185}H_{307}N_{41}O_{56}$ | 4001.65 | 1334.93 $[M+3H]^{3+}$ | 9.3 |

## CD SPECTRA OF PEPTIDE-PEPTIDE INTERACTION

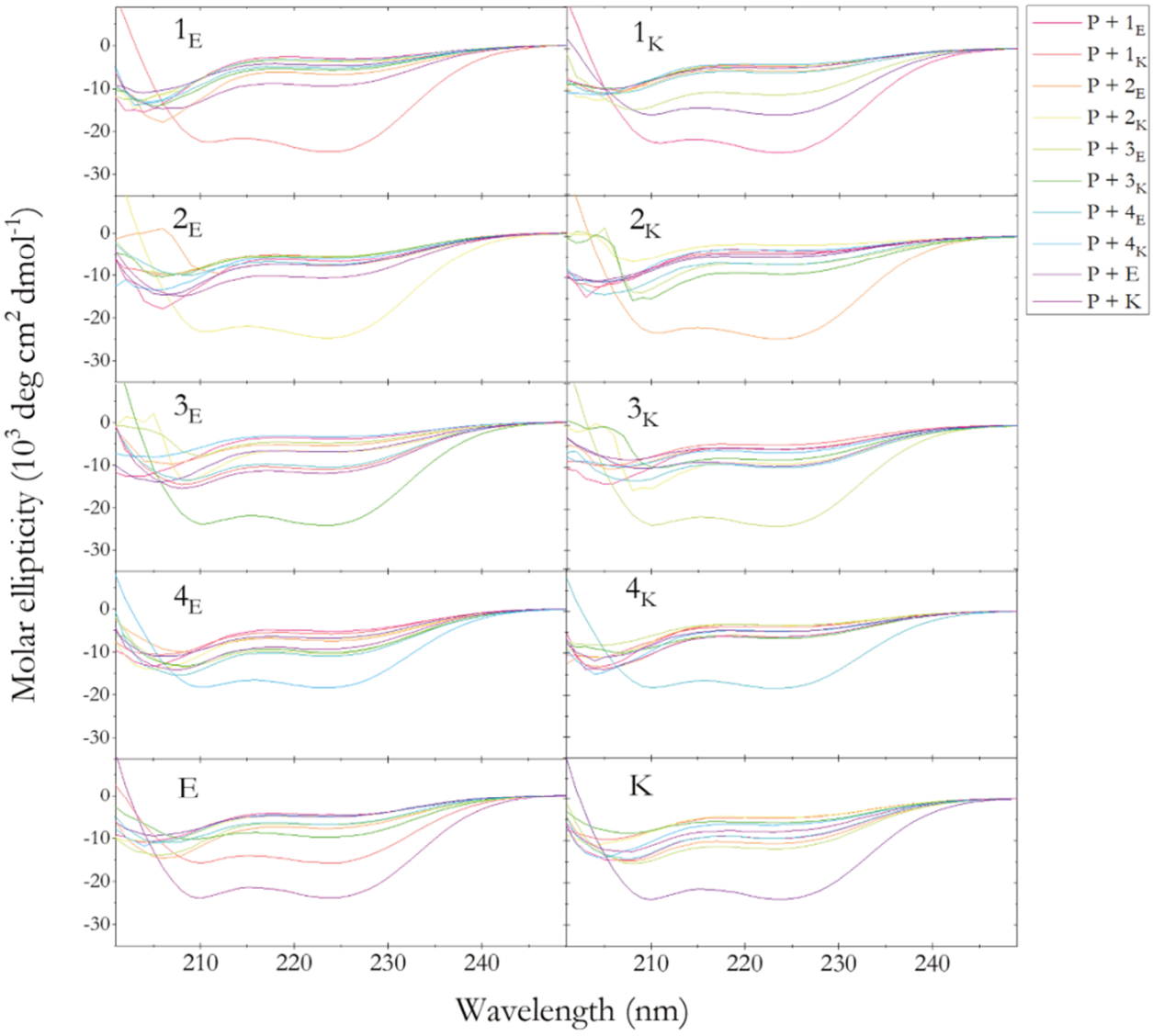


**Figure S25.** *CD spectra of P-peptide combinations. [Total peptide] = 200 μM, in PBS pH 7.4*

**Table S7.** *Helicity of equimolar peptide combinations*

| Peptide | $1_E$ | $1_K$ | $2_E$ | $2_K$ | $3_E$ | $3_K$ | $4_E$ | $4_K$ | E | K |
|---|---|---|---|---|---|---|---|---|---|---|
| K | 24 | 10 | 27 | 10 | 31 | 14 | 24 | 15 | 52 | 15 |
| E | 11 | 42 | 19 | 12 | 17 | 25 | 17 | 11 | 9 | |
| $4_K$ | 7 | 9 | 15 | 8 | 8 | 16 | 49 | 11 | | |
| $4_E$ | 13 | 14 | 19 | 17 | 27 | 26 | 29 | | | |
| $3_K$ | 14 | 11 | 11 | 19 | 65 | 22 | | | | |
| $3_E$ | 9 | 29 | 10 | 14 | 13 | | | | | |
| $2_K$ | 8 | 9 | 67 | 5 | | | | | | |
| $2_E$ | 17 | 13 | 21 | | | | | | | |
| $1_K$ | 67 | 10 | | | | | | | | |
| $1_E$ | 7 | | | | | | | | | |

*Percentage α-helicity was calculated using the formula $[\theta]_{222} = -39500*(1-2.57/n)$ to obtain a 100% helicity value for an α-helical peptide of n residues.[62] For E/K, n = 23; For $P_{E/K}$, n = 28; For mixtures of E/K and P-peptides, n = 25.5. [Total peptide] = 200 μM, PBS pH 7.4 at 20 °C.*

## CONCENTRATION DEPENDENT THERMAL UNFOLDING CURVES

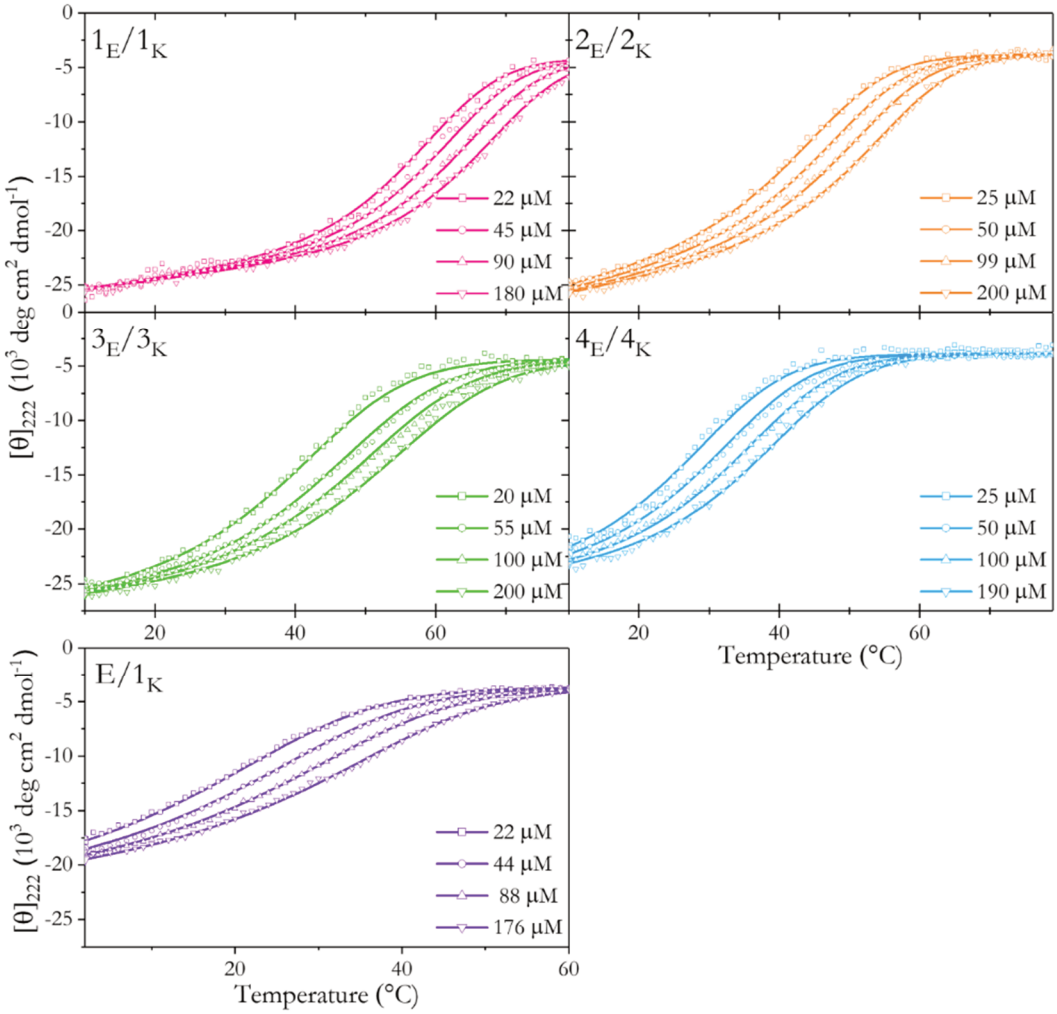


**Figure S26.** *Concentration dependent thermal unfolding of designed heterodimers $1_E/1_K$, $2_E/2_K$, $3_E/3_K$, $4_E/4_K$ and $E/1_K$. Best fits (lines) of experimental data (dots) are obtained using FitDis!.[50] In PBS, pH 7.4.*

**Table S8.** *Parameters for formal description of P-peptide complexes and the E-K complex.*

| Coiled-coil | $1_E/1_K$ | $2_E/2_K$ | $3_E/3_K$ | $4_E/4_K$ | E/K [c] | $E/1_K$ |
|---|---|---|---|---|---|---|
| $P_{Tmin} - P_{Tmax}$ / μM [a] | 22 – 180 | 25 – 200 | 20 – 200 | 25 – 190 | 3 – 25 | 44 – 380 |
| Found $\upsilon_1$, $\upsilon_2$, $\upsilon_3$,. [b] | 1,1 | 1,1 | 1,1 | 1,1 | 1,1 | 1,1 |
| Tm / °C (200 μM) | 63 | 50 | 51 | 37 | 67 | 32 |
| ΔH° / kJ mol$^{-1}$ [d] | 282 | 281 | 171 | 194 | 215 | 163 |
| T° / °C [d] | 107 | 92 | 114 | 88 | 144 | 92 |
| $\Delta C_P$ / kJ mol$^{-1}$ K$^{-1}$ [d] | 1.6 | 2.5 | 0.3 | 0.8 | 1.1 | 0.8 |
| $\theta_{F0}$ / $10^3$ | -26.2 | -27.3 | -27.0 | -24.7 | -29.9 | -20.7 |
| $m_{F0}$ | 78.2 | 113.4 | 84.8 | 60.4 | 94.5 | 76.4 |
| $\theta_{U0}$ / $10^3$ | -4.1 | -3.8 | -4.4 | -3.9 | -5.8 | -3.7 |
| $m_{U0}$ | (0) | (0) | (0) | (0) | 4 | (0) |

*[a] Range of total peptide complex concentration used in experiment. [b] Stoichiometric factors of best fitting model. [c] Taken from M. Rabe et al.[50] [d] Calculated at 25 °C*

**Table S9.** *Peptide helicity as determined by circular dichroism spectroscopy.*

| Peptide | | $1_E$ | $1_K$ | $2_E$ | $2_K$ | $3_E$ | $3_K$ | $4_E$ | $4_K$ |
|---|---|---|---|---|---|---|---|---|---|
| Acetyl[b] | %H[a] | 7 | 10 | 21 | 13 | 5 | 22 | 29 | 11 |
| | $\theta_{222}$ / $\theta_{208}$ | 0.2 | 0.4 | 0.8 | 0.6 | 0.3 | 0.8 | 0.7 | 0.3 |
| 1% $Cpeg_4$ | %H[a] | 7 | 19 | 28 | 34 | 24 | 50 | 23 | 41 |
| | $\theta_{222}$ / $\theta_{208}$ | 0.1 | 0.3 | 0.3 | 0.5 | 0.5 | 0.7 | 0.4 | 0.5 |
| 2% $Cpeg_4$ | %H[a] | 5 | 16 | 16 | 37 | 24 | 39 | 20 | 28 |
| | $\theta_{222}$ / $\theta_{208}$ | 0.1 | 0.4 | -0.4 | 0.6 | -0.3 | 0.7 | 0.4 | 0.5 |
| 3% $Cpeg_4$ | %H[a] | 7 | 22 | 35 | 37 | 36 | 46 | 27 | 62 |
| | $\theta_{222}$ / $\theta_{208}$ | 0.2 | 0.5 | 2.1 | 0.7 | -0.3 | 0.8 | 0.6 | -18.2 |
| 4% $Cpeg_4$ | %H[a] | 7 | 21 | 34 | 50 | 42 | 53 | 33 | 63 |
| | $\theta_{222}$ / $\theta_{208}$ | 0.1 | 0.5 | 1.0 | 0.7 | -0.5 | 1.0 | 0.5 | -12.3 |

*[a] Percentage a-helicity was calculated using the formula $[\theta]_{222}$=-39500*(1-2.57/n) to obtain a 100% helicity value for an a-helical peptide of n residues.[62] [b] Measurements with N-acylated peptides, in PBS pH 7.4, without vesicles. [Total lipid] = 0.5 mM, PBS pH 7.4.*

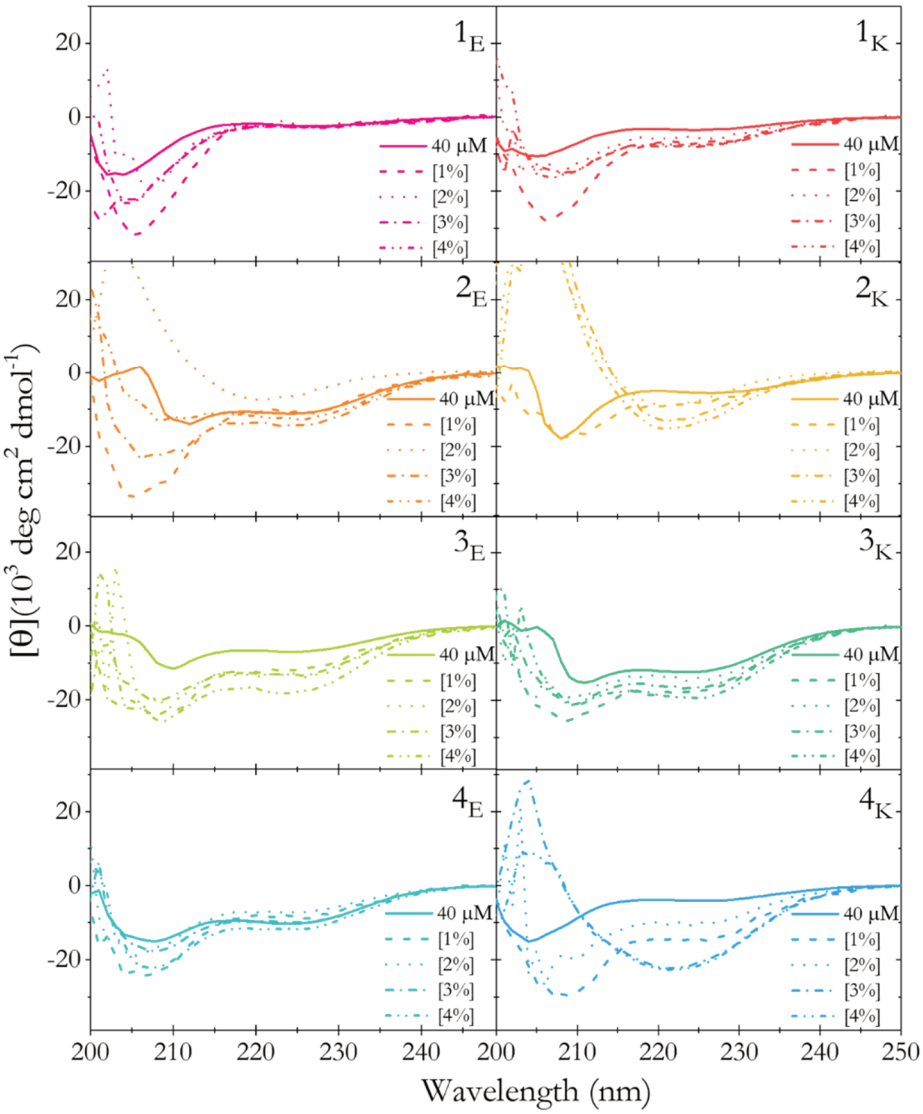


**Figure S27.** *CD spectra of peptides tethered to liposomes with increasing [Cpeg$_4$P]. [Total lipid] = 0.5 mM, in PBS pH 7.4 at 20 °C.*

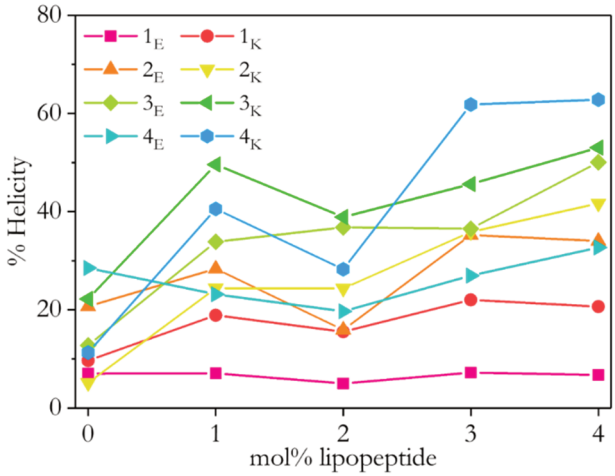


**Figure S28.** *Helicity of peptides tethered to liposomes with increasing [Cpeg$_4$P]. The first entry contains helicity of AcP-peptides. [AcP] = 200 µM; [total lipid] = 0.5 mM; with [Cpeg$_4$P] = 5, 10, 15, or 20 µM, in PBS pH 7.4 at 20 °C.*

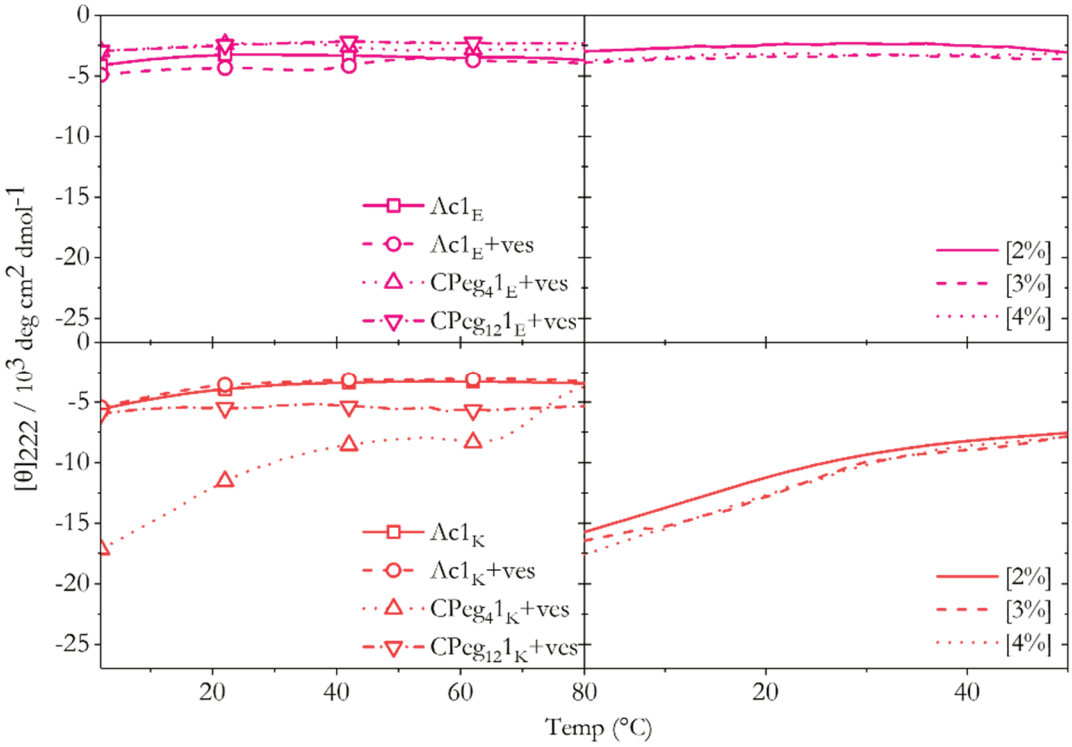


**Figure S29.** *Melting curves of $1_E$ and $1_K$ peptides. Left: with acylated peptides in the absence and presence of vesicles, and with lipopeptide decorated liposomes. Right: with increasing [Cpeg4P]. [Total lipid]+[AcP] = 1 mM+20 μM. [Total lipid]+[ Cpeg4P] = 0.5 mM+ 5, 10, 15, or 20 μM, in PBS pH 7.4 at 20 °C.*

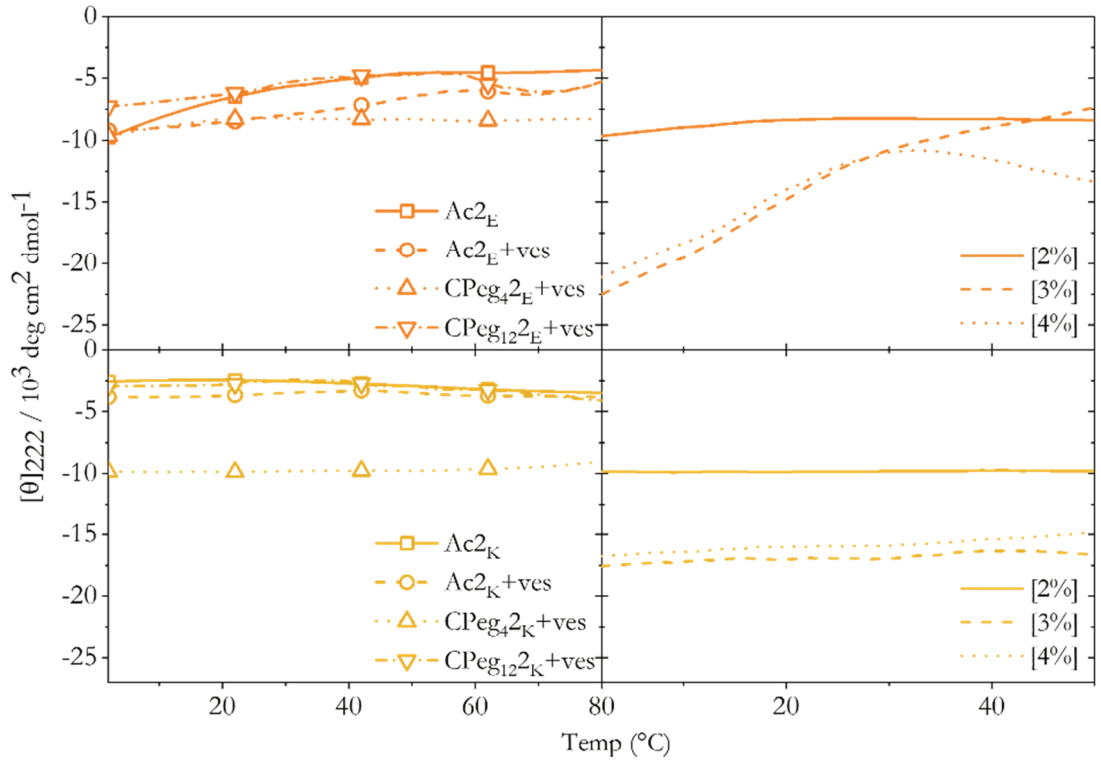


**Figure S30.** *Melting curves of $2_E$ and $2_K$ peptides. Left: with acylated peptides in the absence and presence of vesicles, and with lipopeptide decorated liposomes. Right: with increasing [Cpeg4P]. [Total lipid]+[AcP] = 1 mM+20 μM. [Total lipid]+[ Cpeg4P] = 0.5 mM+ 5, 10, 15, or 20 μM, in PBS pH 7.4 at 20 °C.*

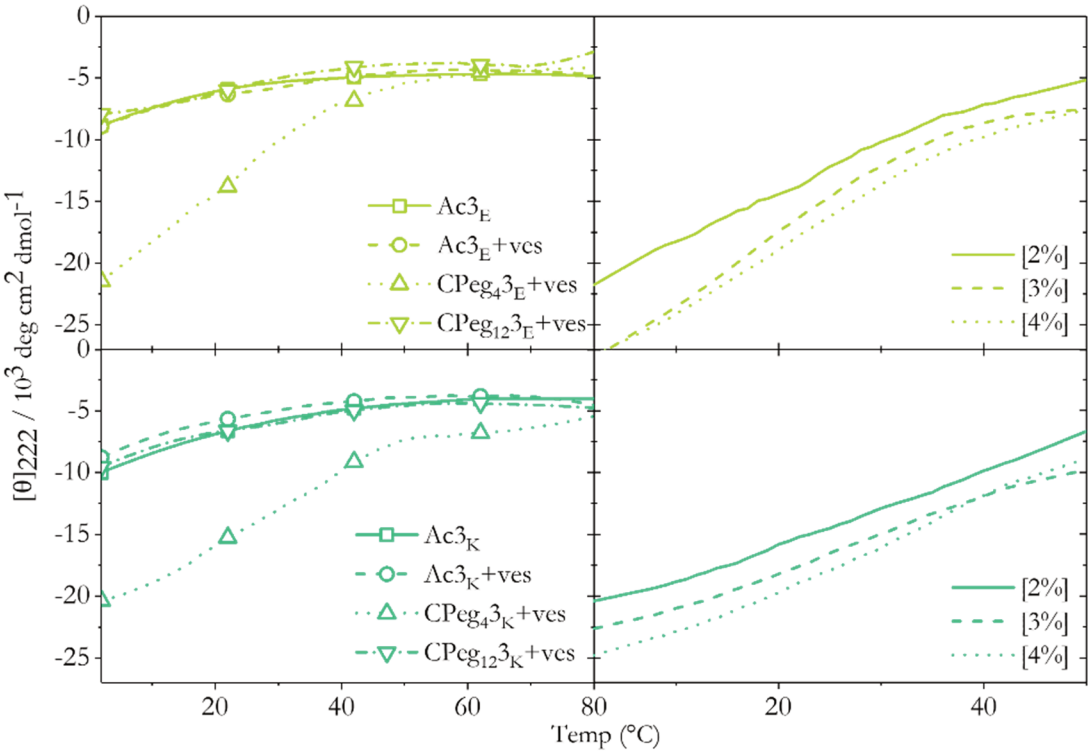


**Figure S31.** *Melting curves of $3_E$ and $3_K$ peptides. Left: with acylated peptides in the absence and presence of vesicles, and with lipopeptide decorated liposomes. Right: with increasing [Cpeg$_4$P]. [Total lipid]+[AcP] = 1 mM+20 μM. [Total lipid]+[Cpeg$_4$P] = 0.5 mM+ 5, 10, 15, or 20 μM, in PBS pH 7.4 at 20 °C.*

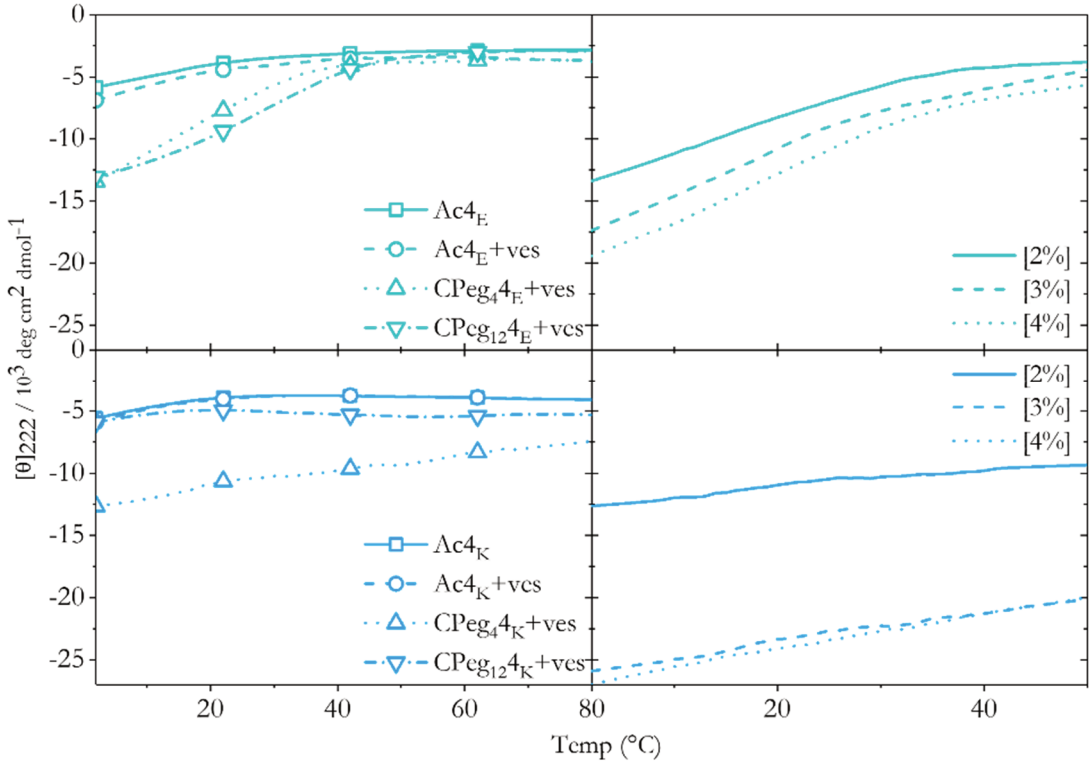


**Figure S32.** *Melting curves of $4_E$ and $4_K$ peptides. Left: with acylated peptides in the absence and presence of vesicles, and with lipopeptide decorated liposomes. Right: with increasing [Cpeg$_4$P]. [Total lipid]+[AcP] = 1 mM+20 μM. [Total lipid]+[Cpeg$_4$P] = 0.5 mM+ 5, 10, 15, or 20 μM, in PBS pH 7.4 at 20 °C.*

## CONTENT MIXING

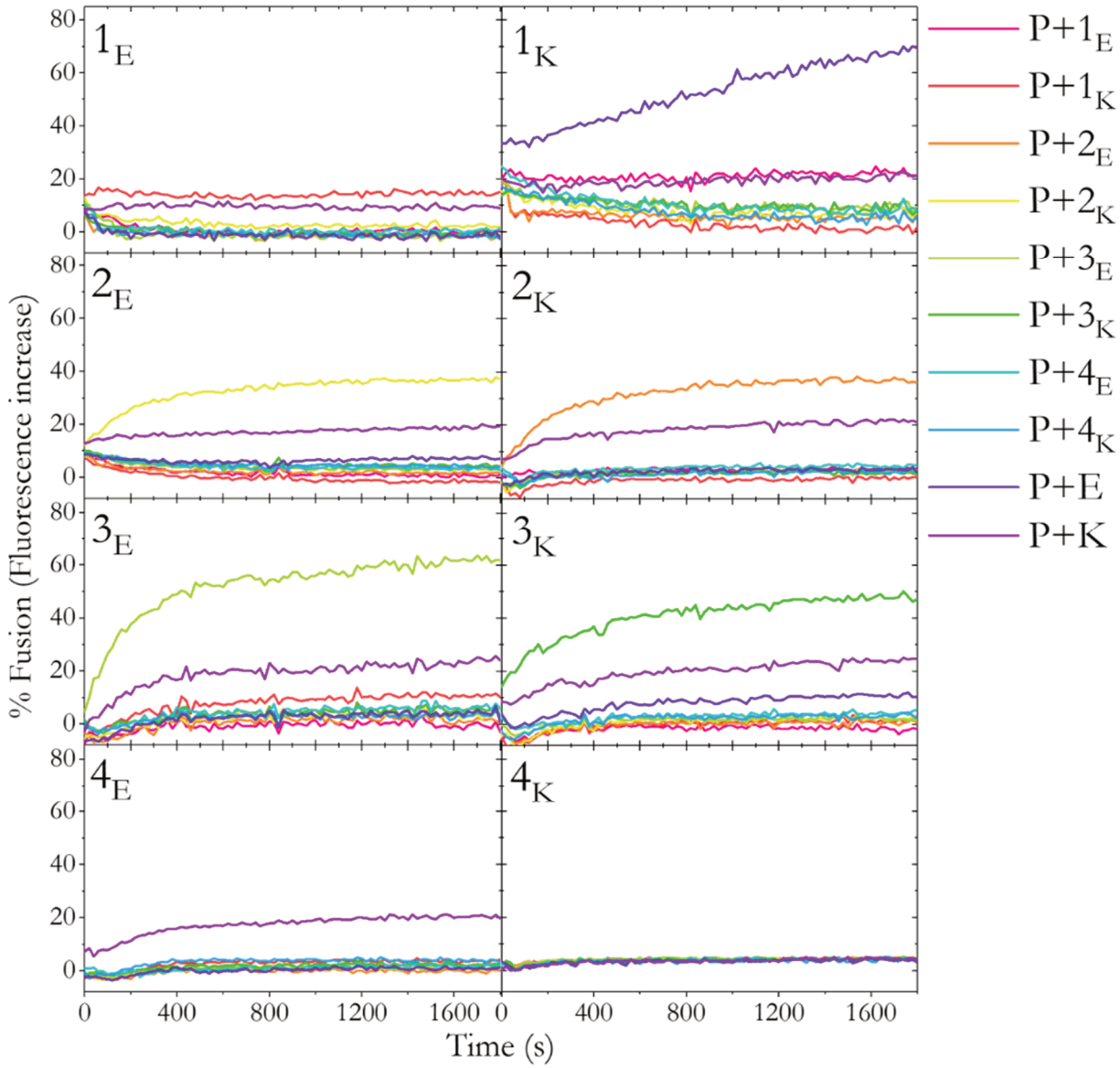


**Figure S33.** *Content mixing assay of liposomes functionalized with Cpeg$_4$P or Cpeg$_8$E/Cpeg$_8$K.. Results are ordered for liposomes functionalized with Cpeg$_4$P and loaded with Sulphorhodamine B, and all possible combinations of peptide functionalized liposomes were tested. [Total lipid] = 0.1 mM with 1 mol% lipopeptide in PBS pH 7.4 at 25 °C.*

# REFERENCES


1. Stengel, G.; Zahn, R.; Hook, F., DNA-induced programmable fusion of phospholipid vesicles. *J. Am. Chem. Soc.* **2007,** *129* (31), 9584-9585.
2. Stengel, G.; Simonsson, L.; Campbell, R. A.; Hook, F., Determinants for membrane fusion induced by cholesterol-modified DNA zippers. *J. Phys. Chem. B* **2008,** *112* (28), 8264-8274.
3. Chan, Y. H.; van Lengerich, B.; Boxer, S. G., Lipid-anchored DNA mediates vesicle fusion as observed by lipid and content mixing. *Biointerphases* **2008,** *3* (2), FA17.
4. Chan, Y. H.; van Lengerich, B.; Boxer, S. G., Effects of linker sequences on vesicle fusion mediated by lipid-anchored DNA oligonucleotides. *Proc. Natl. Acad. Sci. U. S. A.* **2009,** *106* (4), 979-984.
5. Jakobsen, U.; Vogel, S., DNA-Controlled Assembly of Liposomes in Diagnostics. *Methods Enzymol.* **2009,** *464*, 233-248.
6. Ries, O.; Loffler, P. M. G.; Vogel, S., Convenient synthesis and application of versatile nucleic acid lipid membrane anchors in the assembly and fusion of liposomes. *Org. Biomol. Chem.* **2015,** *13* (37), 9673-9680.
7. Herrmann, A.; Meng, Z.; Yang, J.; Liu, Q.; de Vries, J. W.; Gruszka, A.; Rodriguez-Pulido, A.; Crielaard, B.; Kros, A., Efficient Fusion of Liposomes by Nucleobase Quadruple-Anchored DNA. *Chem. - Eur. J.* **2017**, DOI: 10.1002/chem.201701379.
8. Loffler, P. M. G.; Ries, O.; Rabe, A.; Okholm, A. H.; Thomsen, R. P.; Kjems, J.; Vogel, S., A DNA-Programmed Liposome Fusion Cascade. *Angewandte Chemie-International Edition* **2017,** *56* (43), 13228-13231.
9. Ries, O.; Loffler, P. M. G.; Rabe, A.; Malavan, J. J.; Vogel, S., Efficient liposome fusion mediated by lipid-nucleic acid conjugates. *Organic & Biomolecular Chemistry* **2017,** *15* (42), 8936-8945.
10. Lygina, A. S.; Meyenberg, K.; Jahn, R.; Diederichsen, U., Transmembrane Domain Peptide/Peptide Nucleic Acid Hybrid as a Model of a SNARE Protein in Vesicle Fusion. *Angew. Chem., Int. Ed.* **2011,** *50* (37), 8597-8601.
11. Kashiwada, A.; Matsuda, K.; Mizuno, T.; Tanaka, T., Construction of a pH-responsive artificial membrane fusion system by using designed coiled-coil polypeptides. *Chem. - Eur. J.* **2008,** *14* (24), 7343-7350.
12. Meyenberg, K.; Lygina, A. S.; van den Bogaart, G.; Jahn, R.; Diederichsen, U., SNARE derived peptide mimic inducing membrane fusion. *Chem. Commun. (Cambridge, U. K.)* **2011,** *47* (33), 9405-9407.
13. Rauschenberg, M.; Bomke, S.; Karst, U.; Ravoo, B. J., Dynamic Peptides as Biomimetic Carbohydrate Receptors. *Angew. Chem., Int. Ed.* **2010,** *49* (40), 7340-7345.
14. Richard, A.; Marchi-Artzner, V.; Lalloz, M. N.; Brienne, M. J.; Artzner, F.; Gulik-Krzywicki, T.; Guedeau-Boudeville, M. A.; Lehn, J. M., Fusogenic supramolecular vesicle systems induced by metal ion binding to amphiphilic ligands. *Proc. Natl. Acad. Sci. U. S. A.* **2004,** *101* (43), 15279-15284.
15. Gong, Y.; Luo, Y.; Bong, D., Membrane activation: selective vesicle fusion via small molecule recognition. *J. Am. Chem. Soc.* **2006,** *128* (45), 14430-14431.
16. Kashiwada, A.; Tsuboi, M.; Matsuda, K., Target-selective vesicle fusion induced by molecular recognition on lipid bilayers. *Chem. Commun.* **2009,** (6), 695-697.
17. Kashiwada, A.; Tsuboi, M.; Mizuno, T.; Nagasaki, T.; Matsuda, K., Target-selective vesicle fusion system with pH-selectivity and responsiveness. *Soft Matter* **2009,** *5* (23), 4719-4725.
18. Kashiwada, A.; Tsuboi, M.; Takamura, N.; Brandenburg, E.; Matsuda, K.; Koksch, B., Design and Characterization of Endosomal-pH-Responsive Coiled-coils for

Constructing an Artificial Membrane Fusion System. *Chem. - Eur. J.* **2011,** *17* (22), 6179-6186.
19. Marchi-Artzner, V.; Gulik-Krzywicki, T.; Guedeau-Boudeville, M. A.; Gosse, C.; Sanderson, J. M.; Dedieu, J. C.; Lehn, J. M., Selective adhesion, lipid exchange and membrane-fusion processes between vesicles of various sizes bearing complementary molecular recognition groups. *ChemPhysChem* **2001,** *2* (6), 367-376.
20. Ma, M. M.; Bong, D., Controlled Fusion of Synthetic Lipid Membrane Vesicles. *Acc. Chem. Res.* **2013,** *46* (12), 2988-2997.
21. Marsden, H. R.; Tomatsu, I.; Kros, A., Model systems for membrane fusion. *Chem. Soc. Rev.* **2011,** *40* (3), 1572-85.
22. Chen, Y. A.; Scheller, R. H., SNARE-mediated membrane fusion. *Nat. Rev. Mol. Cell Biol.* **2001,** *2* (2), 98-106.
23. Jahn, R.; Scheller, R. H., SNAREs--engines for membrane fusion. *Nat. Rev. Mol. Cell Biol.* **2006,** *7* (9), 631-43.
24. Jena, B. P., Membrane fusion: role of SNAREs and calcium. *Protein Pept. Lett.* **2009,** *16* (7), 712-7.
25. Sudhof, T. C.; Rothman, J. E., Membrane Fusion: Grappling with SNARE and SM Proteins. *Science* **2009,** *323* (5913), 474-477.
26. Woolfson, D. N., The design of coiled-coil structures and assemblies. *Fibrous Proteins: Coiled-Coils, Collagen and Elastomers* **2005,** *70*, 79-+.
27. Ogihara, N. L.; Weiss, M. S.; Degrado, W. F.; Eisenberg, D., The crystal structure of the designed trimeric coiled-coil coil-V(a)L(d): Implications for engineering crystals and supramolecular assemblies. *Protein Sci.* **1997,** *6* (1), 80-88.
28. Fletcher, J. M.; Boyle, A. L.; Bruning, M.; Bartlett, G. J.; Vincent, T. L.; Zaccai, N. R.; Armstrong, C. T.; Bromley, E. H. C.; Booth, P. J.; Brady, R. L.; Thomson, A. R.; Woolfson, D. N., A Basis Set of de Novo Coiled-Coil Peptide Oligomers for Rational Protein Design and Synthetic Biology. *ACS Synth. Biol.* **2012,** *1* (6), 240-250.
29. Mende-Thomas, F.; Boyle, A. L.; Armstrong, C. T.; Woolfson, D. N., De novo designed heterodimeric coiled-coils - Useful tools for the development of new biomaterials. *J. Pept. Sci.* **2012,** *18*, S27-S28.
30. Thomas, F.; Boyle, A. L.; Burton, A. J.; Woolfson, D. N., A Set of de Novo Designed Parallel Heterodimeric Coiled-coils with Quantified Dissociation Constants in the Micromolar to Sub-nanomolar Regime. *J. Am. Chem. Soc.* **2013,** *135* (13), 5161-5166.
31. Wood, C. W.; Bruning, M.; Ibarra, A. A.; Bartlett, G. J.; Thomson, A. R.; Sessions, R. B.; Brady, R. L.; Woolfson, D. N., CCBuilder: an interactive web-based tool for building, designing and assessing coiled-coil protein assemblies. *Bioinformatics* **2014,** *30* (21), 3029-3035.
32. Gradisar, H.; Jerala, R., De novo design of orthogonal peptide pairs forming parallel coiled-coil heterodimers. *J. Pept. Sci.* **2011,** *17* (2), 100-106.
33. Bromley, E. H. C.; Sessions, R. B.; Thomson, A. R.; Woolfson, D. N., Designed alpha-Helical Tectons for Constructing Multicomponent Synthetic Biological Systems. *J. Am. Chem. Soc.* **2009,** *131* (3), 928-+.
34. Diss, M. L.; Kennan, A. J., Orthogonal recognition in dimeric coiled-coils via buried polar-group modulation. *J. Am. Chem. Soc.* **2008,** *130* (4), 1321-1327.
35. Reinke, A. W.; Grant, R. A.; Keating, A. E., A Synthetic Coiled-Coil Interactome Provides Heterospecific Modules for Molecular Engineering. *J. Am. Chem. Soc.* **2010,** *132* (17), 6025-6031.
36. Skyttner, C.; Enander, K.; Aronsson, C.; Aili, D., Tuning Liposome Membrane Permeability by Competitive Coiled-coil Heterodimerization and Heterodimer Exchange. *Langmuir* **2018,** *34* (22), 6529-6537.

37. Aronsson, C.; Danmark, S.; Zhou, F.; Oberg, P.; Enander, K.; Su, H. B.; Aili, D., Self-sorting heterodimeric coiled-coil peptides with defined and tuneable self-assembly properties. *Scientific Reports* **2015,** *5*.
38. Ladokhin, A. S.; White, S. H., Folding of amphipathic alpha-helices on membranes: Energetics of helix formation by melittin. *J. Mol. Biol.* **1999,** *285* (4), 1363-1369.
39. Almeida, P. F.; Ladokhin, A. S.; White, S. H., Hydrogen-bond energetics drive helix formation in membrane interfaces. *Biochim. Biophys. Acta, Biomembr.* **2012,** *1818* (2), 178-182.
40. Rabe, M.; Aisenbrey, C.; Pluhackova, K.; de Wert, V.; Boyle, A. L.; Bruggeman, D. F.; Kirsch, S. A.; Bockmann, R. A.; Kros, A.; Raap, J.; Bechinger, B., A Coiled-Coil Peptide Shaping Lipid Bilayers upon Fusion. *Biophys. J.* **2016,** *111* (10), 2162-2175.
41. Strandberg, E.; Killian, J. A., Snorkeling of lysine side chains in transmembrane helices: how easy can it get? *FEBS Lett.* **2003,** *544* (1-3), 69-73.
42. Mishra, V. K.; Palgunachari, M. N., Interaction of model class A(1), class A(2) and class Y amphipathic helical peptides with membranes. *Biochemistry* **1996,** *35* (34), 11210-11220.
43. Segrest, J. P.; Deloof, H.; Dohlman, J. G.; Brouillette, C. G.; Anantharamaiah, G. M., Amphipathic Helix Motif - Classes and Properties. *Proteins: Struct., Funct., Genet.* **1990,** *8* (2), 103-117.
44. Drin, G.; Antonny, B., Amphipathic helices and membrane curvature. *Febs Lett.* **2010,** *584* (9), 1840-1847.
45. Rabe, M.; Schwieger, C.; Zope, H. R.; Versluis, F.; Kros, A., Membrane Interactions of Fusogenic Coiled-Coil Peptides: Implications for Lipopeptide Mediated Vesicle Fusion. *Langmuir* **2014,** *30* (26), 7724-7735.
46. Daudey, G. A.; Zope, H. R.; Voskuhl, J.; Kros, A.; Boyle, A. L., Membrane-Fusogen Distance Is Critical for Efficient Coiled-Coil-Peptide-Mediated Liposome Fusion. *Langmuir* **2017,** *33* (43), 12443-12452.
47. Yang, J.; Bahreman, A.; Daudey, G.; Bussmann, J.; Olsthoorn, R. C.; Kros, A., Drug Delivery via Cell Membrane Fusion Using Lipopeptide Modified Liposomes. *ACS Cent. Sci.* **2016,** *2* (9), 621-630.
48. Greenfield, N. J., Using circular dichroism spectra to estimate protein secondary structure. *Nat. Protoc.* **2006,** *1* (6), 2876-2890.
49. Greenfield, N. J., Methods to estimate the conformation of proteins and polypeptides from circular dichroism data. *Anal. Biochem.* **1996,** *235* (1), 1-10.
50. Rabe, M.; Boyle, A.; Zope, H. R.; Versluis, F.; Kros, A., Determination of Oligomeric States of Peptide Complexes Using Thermal Unfolding Curves. *Biopolymers* **2015,** *104* (2), 65-72.
51. Rabe, M.; Zope, H. R.; Kros, A., Interplay between Lipid Interaction and Homo-coiling of Membrane-Tethered Coiled-Coil Peptides. *Langmuir* **2015,** *31* (36), 9953-9964.
52. Kyoung, M.; Srivastava, A.; Zhang, Y. X.; Diao, J. J.; Vrljic, M.; Grob, P.; Nogales, E.; Chu, S.; Brunger, A. T., In vitro system capable of differentiating fast Ca2+-triggered content mixing from lipid exchange for mechanistic studies of neurotransmitter release. *Proc. Natl. Acad. Sci. U. S. A.* **2011,** *108* (29), E04-E13.
53. Stratton, B. S.; Warner, J. M.; Wu, Z. Y.; Nikolaus, J.; Wei, G.; Wagnon, E.; Baddeley, D.; Karatekin, E.; O'Shaughnessy, B., Cholesterol Increases the Openness of SNARE-Mediated Flickering Fusion Pores. *Biophys. J.* **2016,** *110* (7), 1538-1550.
54. Han, J.; Pluhackova, K.; Bockmann, R. A., The Multifaceted Role of SNARE Proteins in Membrane Fusion. *Front. Membr. Physiol. Membr. Biophys.* **2017,** *8*, 5.
55. Rizo, J.; Xu, J., The Synaptic Vesicle Release Machinery. *Annu. Rev. Biophys.* **2015,** *44*, 339-67.

56. Yang, J.; Shimada, Y.; Olsthoorn, R. C. L.; Snaar-Jagalska, B. E.; Spaink, H. P.; Kros, A., Application of Coiled-coil Peptides in Liposomal Anticancer Drug Delivery Using a Zebrafish Xenograft Model. *ACS Nano* **2016,** *10* (8), 7428-7435.
57. Zope, H. R.; Versluis, F.; Ordas, A.; Voskuhl, J.; Spaink, H. P.; Kros, A., In vitro and in vivo supramolecular modification of biomembranes using a lipidated coiled-coil motif. *Angew. Chem., Int. Ed.* **2013,** *52* (52), 14247-51.
58. Cubberley, M. S.; Iverson, B. L., (1)H NMR investigation of solvent effects in aromatic stacking interactions. *J. Am. Chem. Soc.* **2001,** *123* (31), 7560-7563.
59. Shirude, P. S.; Kumar, V. A.; Ganesh, K. N., BisPNA targeting to DNA: Effect of neutral loop on DNA duplex strand invasion by aepPNA-N7G/aepPNA-C substituted peptide nucleic acids. *Eur. J. Org. Chem.* **2005,** (24), 5207-5215.
60. Sun, Q.; Cai, S.; Peterson, B. R., Practical Synthesis of 3 beta-Amino-5-cholestene and Related 3 beta-Halides Involving i-Steroid and Retro-i-Steroid Rearrangements. *Org. Lett.* **2009,** *11* (3), 567-570.
61. Marsden, H. R.; Elbers, N. A.; Bomans, P. H. H.; Sommerdijk, N.; Kros, A., A Reduced SNARE Model for Membrane Fusion. *Angew. Chem., Int. Ed.* **2009,** *48* (13), 2330-2333.
62. Lacroix, E.; Viguera, A. R.; Serrano, L., Elucidating the folding problem of alpha-helices: local motifs, long-range electrostatics, ionic-strength dependence and prediction of NMR parameters. *J Mol Biol* **1998,** *284* (1), 173-91.
63. Oshea, E. K.; Lumb, K. J.; Kim, P. S., Peptide Velcro - Design of a Heterodimeric Coiled-Coil. *Curr. Biol.* **1993,** *3* (10), 658-667.
64. Kozlowski, L. P., IPC - Isoelectric Point Calculator. *Biology Direct* **2016,** *11*.

# CHAPTER VI

## SUMMARY AND PERSPECTIVES

# SUMMARY

In daily life, the accurate logistics of nutrients is very important for keeping our communities in order. The American writer Alfred H. Lewis illustrated this relationship 100 years ago by stating "There are only nine meals between mankind and anarchy". Within our bodies and even in every cell, this principle also applies. When necessary nutrients are not available, or are delivered at wrong places, cells or organs will die a sudden death. Therefore, biological life has massive and extremely fast logistic systems with highly specific molecular zip codes: folded proteins named SNARE proteins. The study of these coiled-coil forming proteins, and the art of constructing synthetic coiled-coil mimics of those SNARE proteins, is of high value for many different scientific fields of research. In biological studies, researchers seek to understand the molecular mechanisms of targeted delivery. Understanding of these processes and the roles of the involved proteins leads to the construction of functional mimics of SNARE proteins. This lays the foundation for chemists to develop drug delivery systems or repair occurring faults. In materials sciences, these SNARE mimics can be used as a bottom-up approach to construct new materials with control over the ordering of the building blocks.

In this thesis five different complementary coiled-coil peptide pairs are used as functional mimics of SNARE proteins to study molecular recognition processes between small liposomes. Peptides are tethered to these particles via a poly(ethylene glycol) (i.e. PEG) spacer with variable length and a conjugated cholesterol anchor. Molecular recognition of the peptides leads with liposomes to immediate fusion. Studying the efficiency of fusion and aggregation processes provides insight as to the underlying molecular mechanism of the involved peptides.

In **Chapter I**, SNARE mediated membrane fusion is explained, and the use of our coiled-coil peptides E and K as an *in vivo* drug delivery system is described. The influence of the PEG-spacer length and an in-depth study of the fusion mechanism of E and K mediated liposomal fusion were the focus of **Chapter II**. We observed a significant influence of the PEG-spacer length and the anchor type on the fusion efficiency. For peptide E, more elongated spacers yielded higher fusion efficiencies, while for peptide K

an optimal $PEG_8$/$PEG_{12}$ spacer length was found. The combination of these findings with the knowledge that peptide K can immerse in the membrane, unraveled the dynamics of the peptide roleplay in the intial stages of the process of merging membranes. The following mechanism for the initial stages of E-K mediated liposomal fusion is proposed: Lipopeptide K is fully immersed in the liposomal membrane, while lipopeptide E adopts a largely unfolded state and does not interact with the membrane. Interliposomal coiled-coil formation occurs when liposomes interact and lipopeptide E binds with lipopeptide K to form a transient heterodimeric coiled-coil. Since the peptide K-membrane interaction is favored over coiled-coil formation, peptides are in an equilibrium, switching between the different states. Upon initial coiled-coil formation, K is in close proximity to both membranes and hence can interact with either. Immersing itself in the opposite membrane will force both membranes into even closer proximity, destabilizing both membranes by forming protrusions with concomitant dehydration of the opposing membranes providing the necessary initial conditions for the membrane fusion.

In **Chapter III**, the conformation of membrane tethered peptides is studied with infrared spectroscopy at the air-water interface, and we found an unexpected and significant influence of the PEG-spacer length on the conformation of the peptides. Peptide E doesn't interact with its supporting membrane, but differences in squeeze-out pressure and peptide orientation with altering spacer length revealed that elongated spacers somehow stabilize weak peptide-peptide interactions, only occurring when peptides are immobilized at a surface. For peptide K, a strong peptide-membrane interaction was found for both short and elongated spacers. A minor squeeze-out upon compression of monolayers containing both E and K demonstrated the simultaneous occurrence of both membrane immersed K and coiled-coil bound K, which wasn't observed before.

Since peptide K tends to homo-associate in a concentration dependent manner, covalent peptide dimers were synthesized to study and exploit this behavior, as described in **Chapter IV**. It was found that the position and the spacer-type influences the equilibrium of the peptide-peptide interaction between inter- and intramolecular interactions, and binding strengths could be obtained by CD spectroscopy. Dimers with a short linker were found to trigger and mediate fusion of lipopeptide $CP_{12}E$ decorated

liposomes efficiently, which shows the suitability of a recognition motif with both membrane tethered and non-anchored fusogens for liposomal fusion.

The possibility of liposomal fusion based on orthogonal recognition of a set of coiled-coil peptide pairs was examined in **Chapter V**. This study showed the significant influence of peptide conformations, peptide – membrane interactions, and coiled-coil binding strengths on fusion efficiency. When one of the peptides in a pair show some degree of membrane interaction, fusion of liposomes functionalized with these peptides is highly efficient. Also, more helical peptides were more efficient in mediating fusion than weakly helical peptides, but coiled-coil binding strength did not have an pronounced effect on peptide helicities. Furthermore, a weak interaction between the positively charged peptide $1_K$ and the negatively charged peptide E was measured. This non-designed coiled-coil peptide pair was even more efficient in mediating fusion compared to the designed E - K peptide pair. These results revealed that peptide mediated fusion highly depends on the helicity and on the peptide membrane interactions of the involved peptides and shed new light on the mechanisms of membrane fusion.

# PERSPECTIVES

This research has deepened our insight in the mechanism of membrane fusion induced by complementary pairs of lipopeptides able to form coiled-coil assemblies, and provides directions for future investigations. The finding that the anchor and spacer-length of the lipopeptides dramatically influence their fusogenic activity revealed the peptide – roleplay in the fusion mechanism, but also changed the view on lipopeptide design. Large molecules with distinct conjugated moieties display molecular dynamics that differ from the sum of the individual parts, and intramolecular effects have to be addressed. These intramolecular effects on molecular dynamics are also applicable for other conjugated molecules, and not limited to lipopeptides.

The increased fusion efficiency of peptides showing a peptide-membrane interaction provides evidence for the importance of membrane destabilization in the fusion process. The important question here is how these different peptides ($1_K$, $3_K$ and K) incorporate in the membrane, and what the effect is of the involved peptide association constants on peptide conformations and fusion efficiency. Membrane fusion is a highly dynamic process, and understanding of the dynamic parameters of the used lipopeptides is vital for designing artificial fusion systems with high fusion efficiencies, which is essential for developing successful drug delivery systems.

The demonstrated orthogonal fusion assay enables the development of multicomponent targeted fusion *in vitro* and *in vivo*. Many issues have to be addressed in this journey, such as peptide compatibility with live cells, peptide accessibility on cellular membranes and selective peptide functionalization of target membranes. The accomplishment of targeted orthogonal fusion of different drug loaded liposomes with live tissues will redefine currently used treatments and circumvent most of the known side effects of today's drugs.

# SAMENVATTING

Voor een ordelijke gang van zaken in onze samenleving is een accurate logistiek voor voedingsmiddelen zeer belangrijk. Met de woorden "De grens tussen menswaardigheid en wetteloosheid is maar 9 maaltijden" beschreef de Amerikaanse schrijver Alfred H. Lewis 100 jaar geleden al deze relatie tussen de beschikbaarheid van voedsel en een waardige samenleving. In ons lichaam, en zelfs in iedere cel gaat dit principe ook op. Wanneer essentiële voedingsmiddelen ontbreken, of zintuiglijke signalen op een verkeerde plaats worden afgeleverd, zullen cellen en organen afsterven en is het hele lichaam in gevaar. Biologisch leven heeft daarom uitgebreide en uitermate snelle bezorgdiensten voor zowel voedingsmiddelen als zintuiglijke informatie met zeer specifieke adressering: speciale eiwitten aangeduid als SNARE-eiwitten. Deze eiwitten zorgen ervoor dat de pakketjes met voedingsmiddelen / afvalstoffen / chemische zintuiglijke informatie bij de juiste cellen herkend en opgenomen worden via zogenoemde fusie mechanismen. De studie van deze fusie mechanismen, en de kunst van het begrijpen en namaken van de moleculaire herkenning van SNARE eiwitten, is van onschatbare waarde voor verschillende academische onderzoeksrichtingen; van biologen die lichamelijke ziekten willen begrijpen en genezen, en biochemici die medicijnen gericht willen afleveren bij ziekteverwekkers, tot materiaalkundigen die nieuwe materialen met bijvoorbeeld zelfhelende eigenschappen willen ontwerpen.

Dit proefschrift beschrijft de studie naar moleculaire herkenning tussen kleine deeltjes met gebruikmaking van 5 verschillende coiled-coil peptide paren. De gebruikte deeltjes zijn stevige 'zeepbelletjes', liposomen, met een diameter van 0.1 micrometer. De peptiden zelf hebben een lengte van ongeveer 0.004 micrometer (4 nanometer), en zijn door middel van een flexibele polymeerketen en een cholesterol molecuul verankerd in het liposoommembraan. Interactie tussen verschillende peptiden leidt bij liposomen tot fusie van de liposomen. De efficientie van de fusieprocessen geeft inzicht in de onderliggende moleculaire herkenning van de gebruikte peptiden.

In **Hoofdstuk I** wordt de werking uitgelegd van de SNARE-eiwitten in het proces van membraanfusie, en wordt het gebruik beschreven van het coiled-coil peptidepaar E en K als modelsysteem voor het gericht afleveren van medicijnen in cellen.

**Hoofdstuk II** focust op de invloed van de lengte van de poly(ethylene glycol) (PEG)-keten en het anker waarmee de peptiden E en K aan het liposoom zijn gebonden, op het fusiemechanisme. De invloed van de PEG-keten op de rol van beide peptiden in het mechanisme werd onderzocht. Liposoom fusie wordt efficiënter met langere PEG ketens voor peptide E, terwijl peptide K een $PEG_8$ / $PEG_{12}$ keten prefereert. Gecombineerd met de kennis dat peptide K interactie vertoont met het membraan, kan de dynamiek verklaart worden van de peptiden in de voorstadia van het fusieproces, en het volgende mechanisme wordt voorgesteld: Peptide K is volledig geïncorporeerd in het liposoommembraan, terwijl peptide E zich in de waterige omgeving in de nabijheid van het membraan bevindt. Als twee liposomen elkaar naderen kan peptide E een tijdelijke coiled-coil formatie vormen met peptide K, maar omdat de membraan geïncorporeerde toestand van K energetisch iets gunstiger is dan coiled-coil vorming met peptide E, is er een dynamisch evenwicht tussen de verschillende toestanden. Omdat door de coiled-coil formatie beide membranen dicht tegen elkaar aan worden geforceerd, kan peptide K na initiële coiled-coil vorming een interactie aangaan met beide membranen. Incorporatie van peptide K in het tegenoverliggende membraan brengt beide liposomen nog dichter bij elkaar, destabiliseert beide membranen en verdringt de aanwezige watermoleculen tussen beide membranen, welke de noodzakelijke voorwaarden zijn voor het fuseren van de membranen met elkaar.

In **Hoofdstuk III** wordt de structuur bestudeerd van membraan gebonden peptiden met infrarood spectroscopie, en een onverwachte en significante invloed van lengte van de PEG-keten op de peptidestructuur van peptide E werd waargenomen. Dit peptide heeft weinig interactie met het membraan waarin het verankerd is, maar de invloed van de ketenlengte op de peptide oriëntatie en op de membraandruk waarbij het peptide geen interactie meer heeft met het membraan wijzen op een extra stabilisatie van peptide-interacties bij langere ketenlengte. Bij peptide K werd een sterke interactie met het membraan gemeten die niet afhankelijk is van lengte van de PEG-keten. Wanneer beide peptiden in hetzelfde membraan zijn verankerd, vormt zich een evenwicht tussen E – K coiled-coil interacties en de membraan geïncorporeerde toestand van K. Omdat de laatstgenoemde interactie energetisch iets gunstiger is dan de coiled-coil vorming, is het dynamische evenwicht zichtbaar tussen beide conformaties, welke tot nu toe nooit direct was waargenomen.

Omdat peptide K ook met zichzelf kan associëren resulterend in een zogenaamde homocoil zijn er covalent gebonden peptide dimeren gesynthetiseerd om dit gedrag beter te bestuderen in **Hoofdstuk IV**. De positie en de chemische structuur van deze covalente verbinding tussen twee K peptiden heeft een grote invloed op de homocoil bindingsenergie. Ook het evenwicht tussen inter- en intramoleculaire interacties wordt beïnvloed, d.w.z. interacties van peptiden binnen een dimeer of tussen peptiden behorend tot verschillende dimeren. Deze K – K dimeren zijn ook in staat om fusie te initiëren tussen liposomen die gefunctionaliseerd zijn met peptide E, wat laat zien dat het mogelijk is om een herkenningssysteem te ontwikkelen voor liposoomfusie met zowel verankerde peptiden als niet-verankerde peptiden.

In **Hoofdstuk V** wordt een orthogonale set van coiled-coil peptiden geïntroduceerd. Deze set bevat 8 peptiden, die 4 onafhankelijke coiled-coil peptide paren vormen. Dit geeft de mogelijkheid om het mechanisme van liposoomfusie verder te onderzoeken aan de hand van de verschillen tussen de 4 peptideparen. Deze studie laat een grote invloed zien van de peptidestructuur, de peptide – membraan interactie en de coiled-coil bindingssterkte op de efficiëntie van het fusieproces. Zodra één van de peptiden een interactie vertoont met het membraan, wordt de fusie-efficiëntie drastisch verhoogd. Ook werd er een verband gevonden tussen de heliciteit van de peptiden en fusie-efficiëntie; peptiden met een hogere heliciteit zorgen voor een hogere fusie-efficientie. Opvallend is dat de coiled-coil bindingssterkte voor zover dat kon worden nagegaan geen enkele zichtbare invloed heeft op de fusie-efficientie. Een onverwachte en relatief zwakke interactie werd gemeten tussen het positief geladen peptide $1_K$ en het negatief geladen peptide E. Fusie tussen liposomen gefunctionaliseerd met deze peptiden is zelfs efficiënter dan de fusie tussen liposomen gedecoreerd met het originele coiled-coil paar E en K. Deze resultaten laten zien dat liposoomfusie gemedieerd door coiled-coil peptiden sterk afhangt van de karakteristieke eigenschappen van de peptiden, en geeft nieuwe inzichten in het mechanisme van membraanfusie.

# LIST OF ABBREVIATIONS

| | |
|---|---|
| CD | Circular dichroism |
| $CDCl_3$ | Deuterochloroform |
| CHOL | Cholesteryl-4-amino-4-oxobutanoic acid |
| $CP_n$ | Cholesteryl-4-amino-4-oxobutanoic acid-poly(ethylene glycol) with *n* repeating ethylene glycol units (only used for lipopeptides) |
| $D_2O$ | Deuterium oxide |
| DCM | Dichloromethane |
| DIC | N,N'-Diisopropylcarbodiimide |
| DIPEA | Diisopropylethylamine |
| DLS | Dynamic light scattering |
| DMF | N,N-dimethylformamide |
| DOPC | 1,2-Dioleoyl-*sn*-glycero-3-phosphatidylcholine |
| DOPE | 1,2-Dioleoyl-*sn*-glycero-3-phosphatidylethanolamine |
| DOPE-LR | 1,2-Dioleoyl-*sn*-glycero-3-phosphatidylethanolamine-lissamine-rhodamine B |
| DOPE-NBD | 1,2-Dioleoyl-sn-glycero-3-phosphatidylethanolamine -N- (7 nitro-2-1,3-benzoxadiazol-4-yl) (ammonium salt) |
| EDT | 1,2-Ethanedithiol |
| ESI | Electrospray Ionization |
| Fmoc | Fluorenylmethoxycarbonyl |
| FRET | Fluorescence resonance energy transfer |
| HCTU | O-(1H-6-Chlorobenzotriazole-1-yl)-1,1,3,3-tetramethyl-uronium hexafluorophosphate |
| IRRAS | Infrared Reflection Absorption Spectroscopy |
| LC-MS | Liquid chromatography-mass spectrometry |
| LiCl | Lithiumchloride |
| MALDI-TOF | Matrix assisted laser desorption/ionization time-of-flight detector |
| MeCN | Acetonitrile |
| MHz | Megahertz |
| $NaN_3$ | Sodium azide |

| | |
|---|---|
| NMP | N-methylpyrrolidine |
| NMR | Nuclear magnetic resonance |
| PBS | Phosphate buffered saline |
| PEG | Poly(ethylene glycol) |
| $PMe_3$ | trimethylphosphine |
| PyBOP | (1H-benzotriazol-1-yloxy)tripyrrolidinophosphonium hexafluorophosphate |
| RT | Retention time |
| rt | Room temperature |
| RP-HPLC | Reversed-phase high-pressure liquid chromatography |
| SNARE | Soluble NSF attachment protein receptor |
| SPPS | Solid phase peptide synthesis |
| TEA | Triethylamine |
| TFA | Trifluoroacetic acid |
| TFE | Trifluoroethanol |
| TIS | Triisopropylsilane |

Aminoacids

| | | | |
|---|---|---|---|
| A | Alanine | L | Leucine |
| C | Cysteine | N | Asparagine |
| E | Glutamic acid | Q | Glutamine |
| G | Glycine | W | Tryptophan |
| I | Isoleucine | Y | Tyrosine |
| K | Lysine | | |

# CURRICULUM VITAE

Geert Arend Daudey was born on October 4th, 1988 in Rijssen, the Netherlands. He obtained his Bachelor in Applied Sciences from Hogeschool Utrecht, specialized in 'Research and Development in Organic Chemistry'. He conducted his Bachelor internship at Radboud University Nijmegen and combined this internship with a premaster in theoretical chemistry. Next, Geert obtained his MSc degree in Synthetic Organic Chemistry under the guidance of Dr. Floris van Delft. During his MSc internship, he developed the total synthesis of the fluorescent dye Singapore Green, and became experienced in the use of the synthetic toolbox of Organic Chemists. In 2011, he obtained his MSc degree in Organic Chemistry.

In 2012, Geert joined the Supramolecular and Biomaterials Chemistry group of Prof.dr. Alexander Kros at the University of Leiden, the Netherlands, where he started his PhD research on a ChemThem grant from the Netherlands Organisation for Scientific Research. He explored the mechanisms and dynamics of molecular recognition of peptide decorated liposomes and particles, as described in this PhD thesis. He is currently working as a Peptide Chemist in the group of Dr. Javier Montenegro at the University of Santiago de Compostela, Spain, on the rational development of cell penetrating peptides.

# LIST OF PUBLICATIONS

Zheng, T. T.; Bulacu, M.; Daudey, G.A.; Versluis, F.; Voskuhl, J.; Martelli, G.; Raap, J.; Sevink, G. J. A.; Kros, A.; Boyle, A. L., A non-zipper-like tetrameric coiled-coil promotes membrane fusion. *RSC Advances* **2016**, *6* (10), 7990-7998.

Yang, J.; Bahreman, A.; Daudey, G.A.; Bussmann, J.; Olsthoorn, R. C.; Kros, A., Drug Delivery via Cell Membrane Fusion Using Lipopeptide Modified Liposomes. *ACS Central Science* **2016**, *2* (9), 621-630.

Daudey, G.A.; Zope, H.R.; Voskuhl, J.; Boyle, A.L.; Kros, A. Membrane-Fusogen Distance Is Critical for Efficient Coiled-Coil-Peptide-Mediated Liposome Fusion. *Langmuir* **2017**, *33* (43), 12443–12452.

Daudey, G.A.; Schwieger, C.; Rabe, M.; Kros, A.; Influence of Membrane-fusogen distance on the secondary structure of membrane-tethered coiled-coil peptides. *Manuscript in preparation.*

Daudey, G.A.; Kros, A.; Liposome fusion with orthogonal coiled-coil peptides as fusogens: Peptide roleplay is critical for efficient fusion. *Manuscript in preparation.*

Daudey, G.A.; Kros, A.; Dimers of peptide K: (Super)secondary structures and fusogenic activity. *Manuscript in preparation*